Pyridazinediones: Versatile Scaffolds for Site-Selective Protein Modification

Maximillian Lee

Department of Chemistry
UCL

Primary Supervisors: Dr Vijay Chudasama and Prof. Stephen Caddick
Secondary Supervisor: Dr Tom Sheppard

Declaration

I, Maximillian Taro William Lee confirm that the work presented in this thesis is my own. Where information has been derived from other sources, I confirm that this has been indicated in the thesis.

06/09/2017

For Christopher
dreaming about the lions

Acknowledgements

My PhD has been an incredible journey, over the course of which I've received support from many directions; some expected, some not, but all were welcome and all of which I am extremely grateful for.

First, I will thank my best friend and wife, Caoimhe, who both humbles and inspires me, for enduring three years of my complaining, for affording both *Triumph and Disaster* the same level-headed counsel and for believing in me even when I did not. Thank you, Squash.

I have enjoyed my time at UCL more than I would have thought possible, which is due, in no small part, to my supervisor, and good friend, Dr Vijay Chudasama. Vijay gives more of himself to his job than anyone I've ever worked with; this is reflected not just in the quality of his group's research but in the calibre and character of the people who work for him. Prof. Stephen Caddick has also been a great support over the years and I am especially grateful for him having trusted me to carry out a PhD in the first place. My thanks also go out to other UCL faculty, including Dr Jamie Baker and Dr Tom Sheppard, both of whom have provided guidance and support as well as Dr Abil Aliev, for his help with NMR work, and Dr Kersti Karu and Dr Xiaoping Yang for help with mass spectrometry.

I feel very privileged to have had the opportunity to work with so many exceptionally talented scientists, but even more privileged to count so many of them amongst my friends. First amongst them is Dr Antoine Maruani, who, despite being a jammy Argentinian (presumably – still can't figure out the accent) scoundrel, has been available to help, at the drop of a hat, day or night for three years. I've learnt a huge amount from Antoine, unfortunately all I've been able to offer in return is a stream of absolute nonsense and, possibly, a mild case of PTSD. Amongst my other colleagues, Dr Daniel Richards also deserves special mention for being an island of 'refreshing cynicism' to keep the egos of the junior members in check. The other Chuds; Calise, André, João, Marcos, Peter and Faiza have all made a big impact on my time here and I'm sure will all keep the great atmosphere of our group alive.

The extended KLB family, especially Marco, Brian and Nafsika, also deserve mention as you make our building a very special place to work; never a dull moment and a wonderfully supportive environment. I'm sure I speak for many KLB members, in thanking Ensemble Studios and Microsoft for creating Age of Empires II™, which has provided many hours of entertainment.

I could not have finished this work without the support of my family, especially from the 'original' Dr M Lee who fostered my scientific interest and inspired me to pursue this career. I am also grateful for the lessons I learnt from my father who, despite lacking supporting evidence, believed I could achieve whatever I desired. In spite of being told outright, by several of my school teachers, that I lacked the faculties necessary to pursue a meaningful career in science, and being actively encouraged to drop science and maths, my parents never showed a shred of doubt, something for which I am immensely grateful. My other incredibly supportive family members to whom I am very grateful, namely; Oli, Keira, Nan, Granny, Grandpa, Hamzah, Margot and Razay.

I extend my gratitude to my examiners, Dr Steven Cobb and Dr Stephen Hilton, who have taken the time to read through this work with due care and carry out my *viva* examination.

Finally, I would like to thank my funding body, the EPSRC, and my host institution, UCL, for enabling me to do a PhD in the first place as such an opportunity is a tremendous privilege.

"It is more fun to talk with someone who doesn't use long, difficult words but rather short, easy words like, "*What about lunch*?""

– Winnie-the-Pooh

Abstract

Disulfide bonds represent an important target for site-selective protein modification, particularly *via* the strategy of functional re-bridging. Reduction of interchain disulfide bonds, followed by their re-bridging allows proteins to be functionalised in a site-selective manner whilst retaining the stability and integrity offered by the original bridge. This work describes the design and development of two distinct pyridazinedione-based technologies that, through the conduit of functional disulfide re-bridging, enable the synthesis of antibody – drug conjugates with hitherto unmet levels of control and homogeneity.

As proteins often contain multiple disulfide bonds that are critical to conformation and stability, reagents that allow functional disulfide re-bridging without disulfide scrambling (non-native disulfide re-bridging) in multiple disulfide containing systems are critical for the success of this method. The first presented technology is a molecule that is capable of both reducing and re-bridging disulfide bonds, enabling a rapid and efficient one-reagent protocol for the functionalisation of disulfide containing proteins, moreover, it does so in such a way that native disulfide configuration is retained *via* a high local concentration effect. This novel pyridazinedione scaffold has been shown to functionalise a variety of therapeutically relevant proteins, including the widely used mAb Herceptin™, enabling the synthesis of homogenous antibody – drug conjugates from a native mAb.

Shifting focus from homogeneity to control over drug loading, the second presented technology is a single pyridazinedione-based molecule that contains four cysteine reactive centres and only one bioorthogonal reactive handle, which enables the generation of antibody conjugates with a loading of two modules. A loading of two is desirable for many reasons, especially in the context of large, hydrophobic payloads, which are increasingly popular for use in antibody-drug conjugates. A loading of two drugs per antibody has been shown to provide an optimal balance between efficacy and biophysical properties in many cases. A reliable method based on a native antibody scaffold without the use of enzymes or harsh oxidative conditions has hitherto not been achieved. The use of native antibodies has several advantages in terms of cost, practicality, accessibility and time. Thus, a novel, reliable method of furnishing antibody conjugates with a loading of two modules starting from a native antibody scaffold was developed.

Contents

Abbreviations

AcOH	Acetic Acid
ADC	Antibody–Drug Conjugate
ADCC	Antibody-dependent Cell-mediated Cytotoxicity
aq.	Aqueous
BBS	Borate Buffered Saline
b.p.	Boiling point
Boc	*tert*-Butyloxycarbonyl
br.	Broad
calcd	Calculated
CDI	1,1'-Carbonyldiimidazole
CI	Chemical Ionisation
CuAAC	Copper(I)-catalyzed Alkyne–Azide Cycloaddition
Cys	Cysteine
DAR	Drug-to-antibody ratio
d	Doublet
DCC	*N,N*'-Dicyclohexylcarbodiimide
DCM	Dichloromethane
DIPEA	*N,N*-Diisopropylethylamine
DMF	Dimethylformamide
DNA	Deoxyribonucleic Acid
Dox	Doxorubicin
EDTA	Ethylenediaminetetraacetic acid
ELISA	Enzyme-Linked Immunosorbent Assay
EI	Electron Ionisation
eq.	Equivalents
ES	Electrospray
Fab	Fragment antigen-binding
FAR	Fluorophore-to-Antibody Ratio
FDA	U.S. Food and Drug Administration
HATU	1-[Bis(dimethylamino)methylene]-1*H*-1,2,3-triazolo[4,5-*b*]pyridinium-3-oxid hexafluorophosphate

HIC	Hydrophobic Interaction Chromatography
HIV	Human Immunodeficiency Virus
HRMS	High Resolution Mass Spectrometry
Ig	Immunoglobulin
IR	Infrared
J	Coupling constant
LCMS	Liquid Chromatography Mass Spectrometry
LRMS	Low Resolution Mass Spectrometry
m	Multiplet
m/z	Mass to charge ratio
mAb	Monoclonal Antibody
MALDI-TOF	Matrix Assisted Laser Disorption/Ionisation – Time of Flight
Me	Methyl
MeCN	Acetonitrile
MMAE	Monomethylauristatin E
MOPS	3-(*N*-morpholino)propanesulfonic acid
MS	Mass Spectroscopy
MWCO	Molecular Weight Cut Off
NAA	Natural Amino Acid
NHS	*N*-Hydroxysuccinimide
NMR	Nuclear Magnetic Resonance
p	Para
PB	Phosphate Buffer
PBS	Phosphate Buffered Saline
PD	Pyridazinedione
PDAR	PD-to-Antibody Ratio
PEG	Polyethylene Glycol
Ph	Phenyl
PK	Pharmacokinetic
ppm	Parts per million
PTM	Post-translational modifications
PBD	Pyrrolobenzodiazepines
Q	Quartet

rt	Room temperature
s	Singlet
sat.	Saturated
SDS-PAGE	Sodium Dodecyl Sulfate - Polyacrylamide Gel Electrophoresis
SPAAC	Strain-Promoted Alkyne–Azide Cycloadditions
t	Triplet
TG	Transglutaminase
TCEP	Tris(2-carboxyethyl)phosphine
TFA	Trifluoroacetic Acid
THPTA	Tris(3-hydroxypropyltriazolylmethyl)amine
TLC	Thin Layer Chromatography
Tris	Tris(hydroxymethyl)aminomethane
UAA	Unnatural Amino Acid
UCL	University College London
uPLC	Ultra Performance Liquid Chromatography
UV-Vis	Ultraviolet-Visible Spectrophotometry
wt	Weight

Chapter 1: Introduction

Proteins have some of the most dynamic and diverse roles of any macromolecule in biology. For instance, they facilitate complex biochemical pathways and reactions, transport molecules throughout systems and can act as receptors within a cell membrane.[1] The human genome consists of 25,000 – 30,000 genes, however, due to alternative splicing and post-translational modifications (PTMs) the human proteome is much more complex; consisting of over 1,000,000 proteins.[1-4] Whilst proteins already boast a huge array of functions, chemical biologists seek to understand their function in greater detail and/or increase their versatility, through the conduit of protein modification. Through manipulating proteins, powerful new tools can be created for a variety of different purposes.[5] For example, to probe biological systems with a previously unattainable level of detail, to construct tools for advanced biosynthesis and for designing novel therapies for use against diseases.[5, 6]

As proteins innately have, or are designed to have, unique and highly specific interactions with biological systems, they represent versatile platforms for creating novel therapeutics. To date, bioconjugates have been used successfully to treat many serious and life-threatening indications, including HIV,[7] malaria[8] and cancer.[9] Furthermore, bioconjugates have seen use as diagnostic tools.[10]

Protein modification, through various synthetic and biological strategies, is a well-established field of research.[11-14] However, selectively modifying proteins at a specific site remains a significant challenge. Proteins often consist of hundreds of amino acids, each of which potentially carry a reactive side chain. This means that any reactions required to achieve selective modification at a particular residue (this may be a natural or unnatural residue) must be capable of proceeding chemoselectively, *i.e.* in the presence of numerous other functional groups (*e.g.*

amines, carboxylic acids, thiols and alcohols), and regioselectively, *i.e.* in the presence of other competing residues of the same type.

The use of synthetic methodologies to achieve site-selective protein modification on amino acids within a protein's sequence has garnered much attention and the field has advanced rapidly over the years. A large number of distinct strategies have been developed, which can generally be categorised as (i) modification of unnatural amino acids; and (ii) modification of natural amino acids; each general category presents its own set of unique benefits and challenges.

1.1 Chemical modification of proteins

1.1.1 Unnatural amino acids

Unnatural amino acids (UAAs) are powerful tools in the field of site-selective protein modification owing to their ability to grant unique bioorthogonal reactive handles directly into a protein's peptidic backbone. The range of possible bioorthogonal handles available can include, but is not limited to, arylhalide, alkene, alkyne, tetrazene and azide functional groups (Figure 1). Furthermore, such handles can be installed with a high degree of accuracy at a specific point within a protein's sequence using site-directed mutagenesis.[15-17] The term bioorthogonal, initially coined by Bertozzi in 2004, denotes any kind of chemical reaction that can proceed within biological systems without interfering with native biochemical pathways.[18]

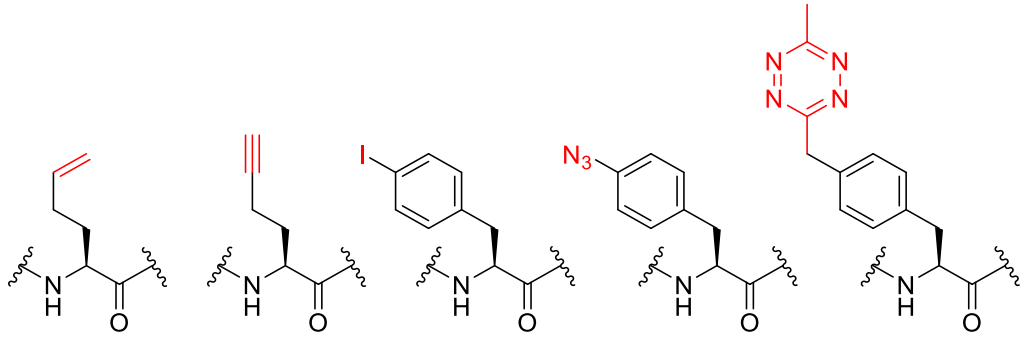

Figure 1 Examples of UAAs featuring a range of bioorthogonal reaction handles; (from left to right) alkene, alkyne, arylhalide, arylazide and tetrazene.

Once installed, UAAs can undergo further chemical modification in a regio- and chemoselective manner though various synthetic processes such as palladium catalysed cross couplings,[19] metatheses,[20] copper-catalysed and copper-free azide-alkyne Huisgen cycloadditions (Scheme 1).[21] Bernardes, Davis and co-workers have demonstrated that these techniques can work successfully on a diverse portfolio of proteins to create many different diagnostic and therapeutic bioconjugates. However, the production of UAA containing proteins can be prohibitively expensive and presently remains highly challenging for large scale production of bioconjugates. This is due, in part, to the required optimisation of cell culture conditions and intricate mutagenesis techniques; the processes are specific to given targets.[22, 23] These issues have been somewhat mitigated by Chin *et al.* in recent years by improving the efficiency and yields of mutagenesis techniques.[24, 25] Specifically, by improving response to the amber stop codon, UAA-bearing proteins were synthesised at previously unattainable yields.[26] However, these strategies are still protein specific and, therefore, lack broad applicability.

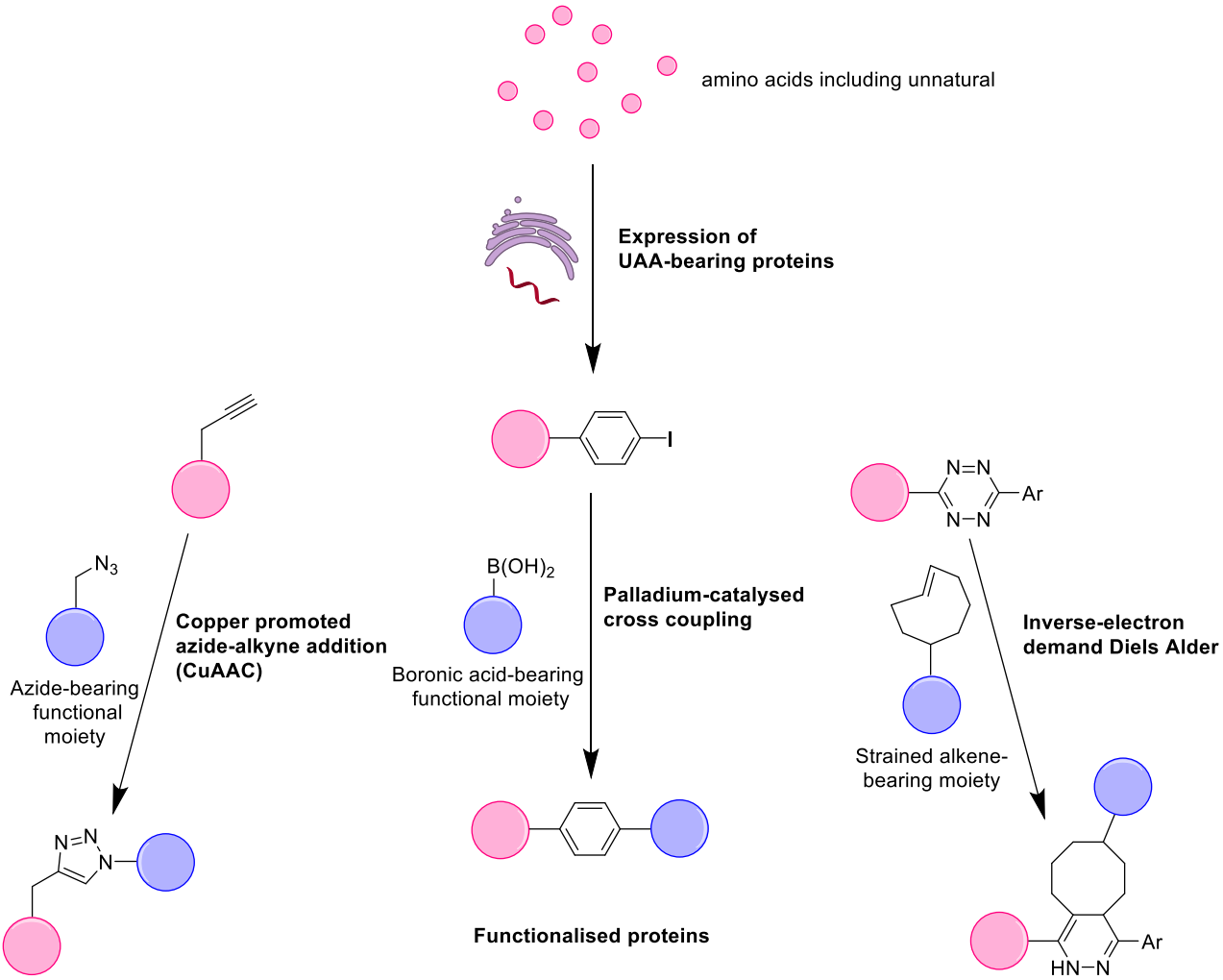

Scheme 1 The construction of proteins containing bioorthogonal handles is made possible through the incorporation UAAs *via* site-directed mutagenesis. Handles such as alkynes, halides and tetrazene have been incorporated facilitating further bioorthogonal chemical modification.

1.1.2 Naturally occurring amino acids

Targeting of natural occurring amino acids (NAAs) involves taking advantage of the differential reactivity of a functional handle present on one of the 22 proteinogenic amino acids (Figure 2). While this method limits the scope of bioorthogonal reactions that can be performed directly on the protein, there is an abundance of strategies that can still enable site-selective modification.[27] As with UAAs, NAAs can be incorporated into proteins using site-directed mutagenesis to provide convenient handles for further chemical modification. However, incorporation of NAAs *via* site-directed mutagenesis is less challenging; *i.e.* the codons for NAAs already exist and so optimisation of cell culture conditions is less

complicated. The degree of selectivity offered by this method is thus reliant on the reactivity and natural abundance of the NAA that is being introduced, *i.e.* only the amino acid that is being introduced will be available for reaction as it is the only amino acid of that type being introduced or it is the only amino acid of that type that is available for bioconjugation (other residues of the same type may be buried in the protein structure and, therefore, not accessible). Moreover, the modification of NAAs offers a facile strategy for the modification of native proteins.

The two NAAs that are most frequently targeted for bioconjugation are lysine and cysteine, on account of their high nucleophilicity under physiological conditions. Tyrosine and tryptophan can also be targeted but are typically less accessible due to often being buried within the hydrophobic interiors of proteins.[28-30]

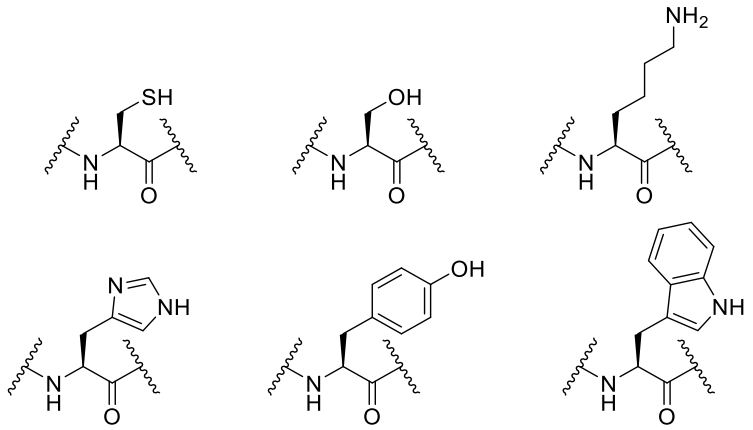

Figure 2 Some of the NAAs that serve as potential targets for protein modification; lysine and cysteine are the most common choices due their high nucleophilicity. Left to right: cysteine, serine, lysine; histidine, tyrosine and tryptophan.

1.1.2.1 Lysine modification

Lysine is a common choice for protein modification; the primary alkyl amine side chain is a functional group with high nucleophilicity.[31] The relatively high natural abundance of lysine residues on proteins often also nullifies the need for incorporation of extra lysine residues.[32, 33] The majority of Food and Drug Administration (FDA) approved bioconjugates have been synthesised using lysine modification strategies, most commonly through the use of amine-reactive succinimidyl esters.[31] Lysine's high natural abundance and high nucleophilicity make it well suited for instances when site-selectivity is not required.[32,33]

Under physiological conditions lysine has been shown to form irreversible amide linkages with *N*-hydroxysuccinimide (NHS) esters with no exogenous reagents. Moreover, lysine has been shown to react in good yields with isothiocyanates or isocyanates at higher pH (9.0-9.5). There is a plethora of strategies available for modification of lysines on the surface of proteins using a variety of reagents under a broad range of conditions (Scheme 2).[34-37]

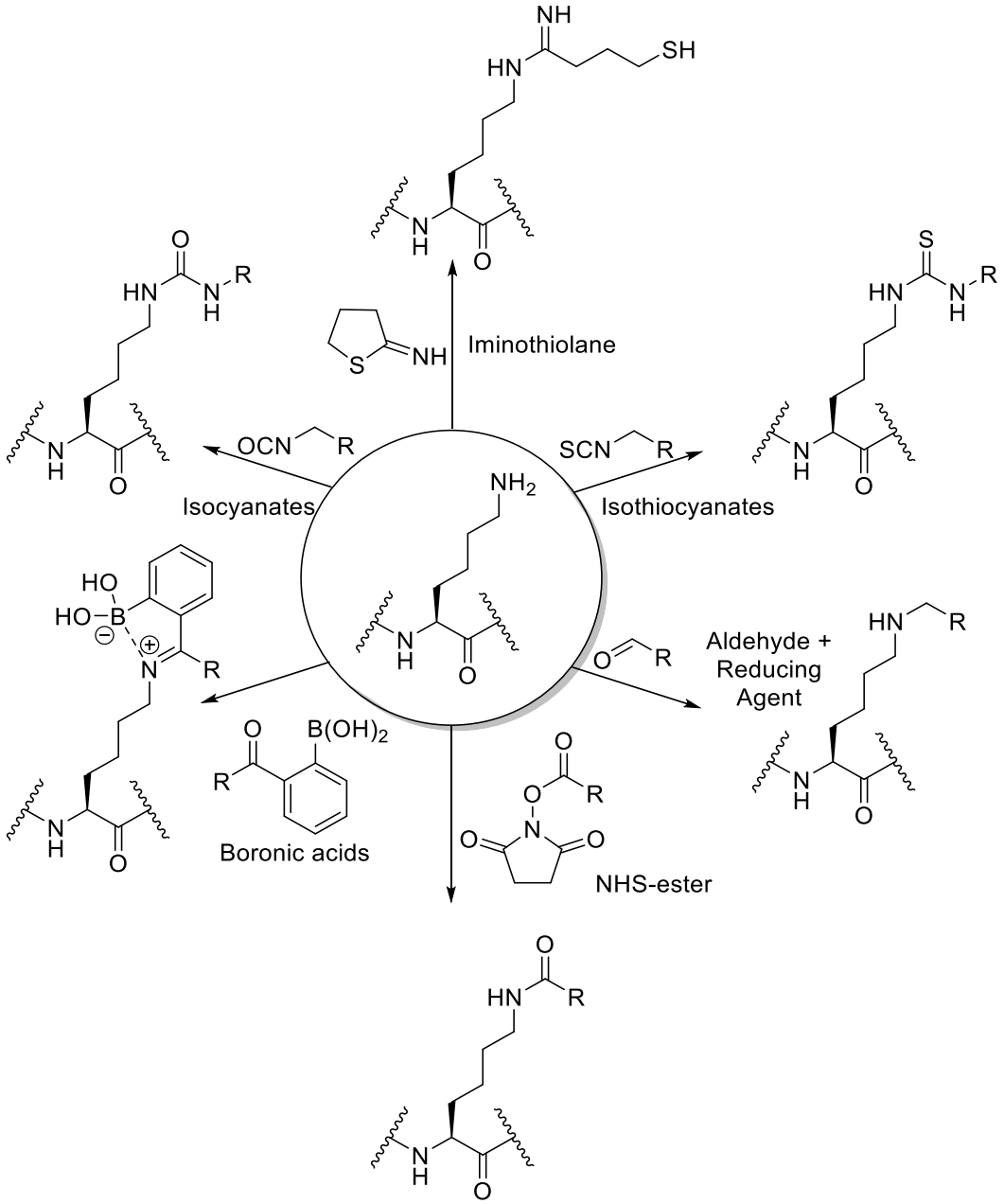

Scheme 2 Main reactions for the primary alkyl amine side chain of lysine.

An early example of lysine modification was demonstrated by Tuls *et al.* through conjugation of a fluorescein isothiocyanate (FITC) to an oxidative cytochrome

P-450 enzyme.[34] The isothiocyanate motif reacted readily with the primary amine side chain under basic pH to create a stable thiourea linkage. Interestingly, the authors found the modification took place at a specific lysine in the active site of the protein, reflected by a sharp loss in binding with adrenodoxin.[34] More recently, reductive amination, a common strategy for installation of secondary amines, has seen use in the context of lysine modification. Gildersleeve *et al*. demonstrate the use of reductive amination to install a series of oligosaccharides onto bovine serum albumin (BSA).[36] The technique serves as an especially convenient method for conjugation of sugars to lysine owing to the natural occurrence of the saccharide aldehyde groups, therefore mitigating any chemical preparation of either protein of conjugating reagent. Another example of lysine modification, that is currently applied in modern medicine, can be found in the synthesis of FDA approved drug Kadcyla™ (trastuzumab emtansine); an anti-HER2 monoclonal antibody, Herceptin™ (trastuzumab), linked to the microtubule assembly inhibiting drug maitansine (DM1) *via* lysine residues (Scheme 3).[38] Surface lysines on the antibody react preferentially with an NHS ester on a succinimidyl-4-(*N*-maleimidomethyl)cyclohexane-1-carboxylate linker leaving an exposed maleimide, through which the thiol-bearing DM1 drug is attached. The result of this modification method is a heterogeneous mixture of products with up to 10^6 distinct species when targeting averaged drug-to-antibody ratio (DAR) of 3.0-3.6.[38] This is a direct consequence of there being 88 lysines on trastuzumab, 40 of which are solvent accessible for modification.[39]

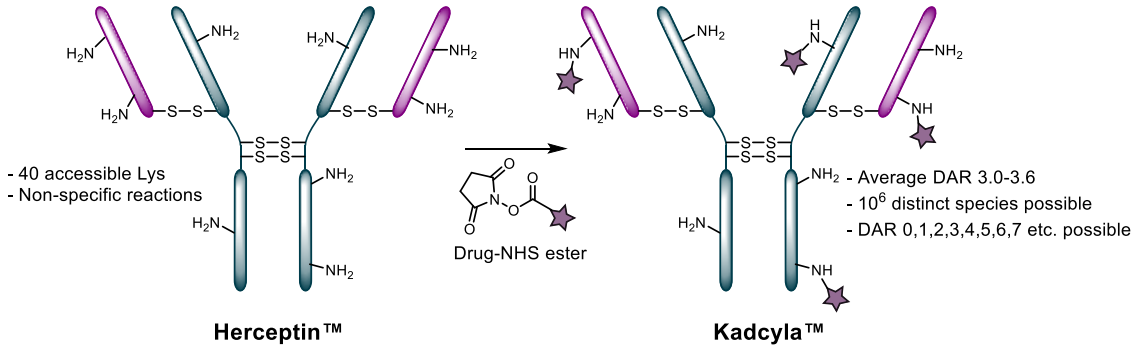

Scheme 3 The synthesis of FDA-approved ADC Kadcyla™ is achieved through reaction of surface lysine residues on native Herceptin™ *via* an NHS-ester bearing linker with the highly potent tubulin inhibitor emtansine.

It is a combination of lysine's high natural abundance and frequent appearance on the solvent-accessible surface of proteins that gives rise to heterogeneous product generation, making the technique suboptimal for some applications.[33, 40] Furthermore, solvent-exposed lysines are present on the surface of almost all proteins in addition to exposed *N*-termini. Varied batch-to-batch product distribution can be particularly problematic in the production of bioconjugate therapeutics and imaging agents as it can lead to broad pharmokinetic profiles; resulting in a narrow therapeutic window.[41, 42] Moreover, excessive lysine modification can result in a loss in solubility and rapid blood clearance rates when used to make therapeutics.[43, 44] This is primarily due to exchange of the solubilising protonated ammonium of the lysine side chain for neutral moieties, resulting in a loss of polar surface area. Furthermore, the presence of lysines in key areas of proteins, for example in the complementarity determining region of antibodies, is not uncommon and, if modified can lead to significant decreases in binding affinity and, therefore, a potential loss in efficacy.[45] Moreover, reactions at lysine residues often require very stringent control of pH or other conditions to slow the rate of reaction to ensure modification of only the most reactive lysine takes place.[46, 47] It is in light of these factors that cysteine makes the most promising candidate for NAA modification.

1.1.2.2 Cysteine modification

Cysteine makes an attractive target for modification of NAAs; the highly reactive thiolate side chain under basic pH reaction conditions (*i.e.* generally far more reactive than lysine or other nucleophilic side-chains under analogous conditions) allows for rapid reaction in a chemoselective manner with various conjugating agents.[48] This chemoselectivity is further increased due to the thiolate side chain being a 'soft' nucleophile; this means it has lower charge density than other nucleophiles, leading it to preferentially form more thermodynamically stable products. Moreover, free cysteine residues occur at only 0.2% abundance. Whilst total cysteine abundance is at 1.7% in the human proteome, the majority of cysteine residues exist in their oxidised form; disulfide bridges, which provide covalent support to a protein's tertiary structure and assists in preserving them in a given conformation.[49, 50] Cysteine modification has seen significant

development over the years having been shown to enable the synthesis of novel bioconjugates,[51-54] label proteins,[55] probe biochemical pathways and obtain structural information.[56-60] Furthermore, there are now a wide range of commercially available reagents for cysteine modification from large suppliers, in addition to new reagents being developed by academic groups. There are several main methods that are applied for cysteine modification including; alkylation, disulfide formation and oxidation (Scheme 4).

Site-selective reaction with cysteine is often achieved by incorporation of a single reactive cysteine into the protein structure at a solvent accessible site *via* site-directed mutagenesis followed by chemoselective bioconjugation. Due to the extreme rarity of free cysteine occurring in native proteins and its differential reactivity, through inclusion into a protein's sequence, a single cysteine can offer excellent selectivity.

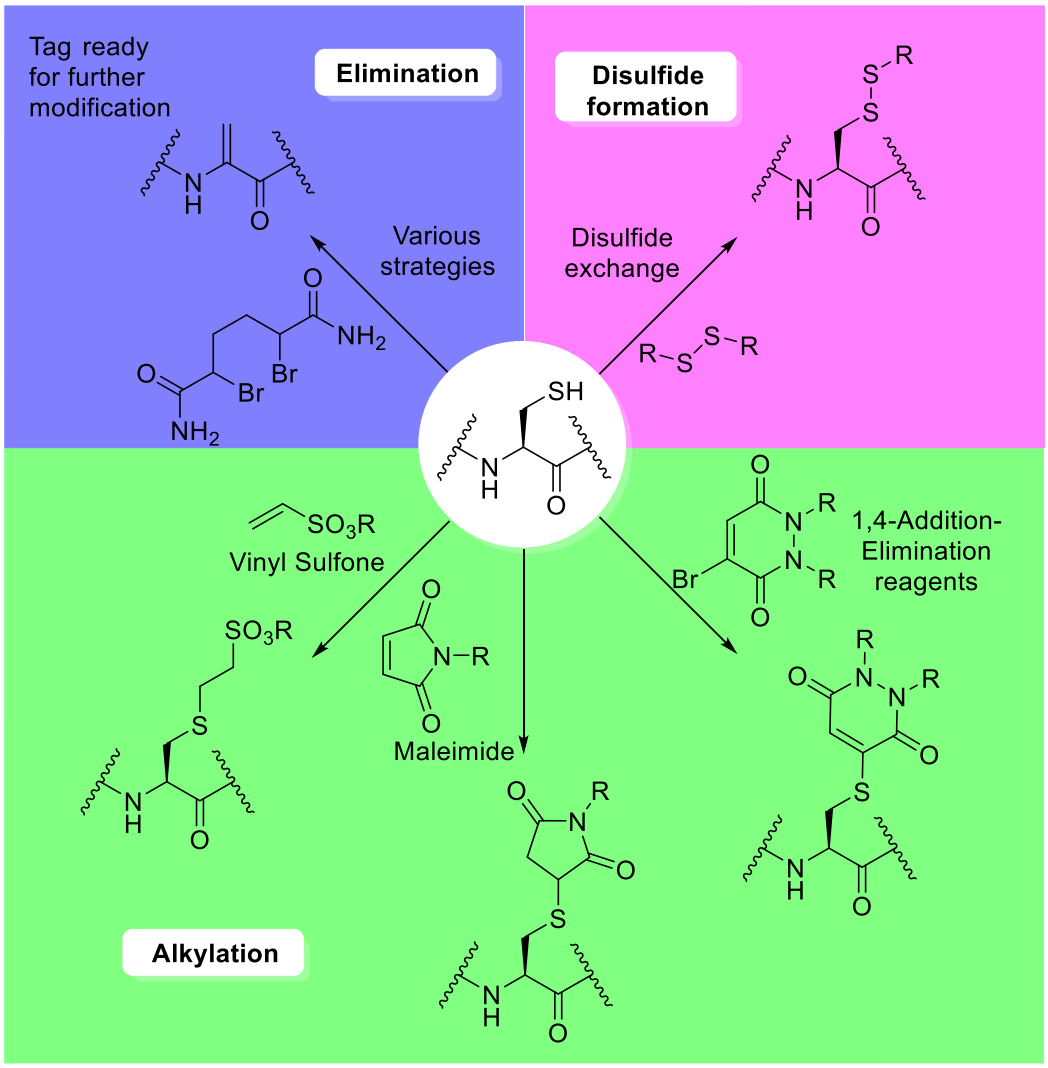

Scheme 4 There is an abundance of possible reactions and transformations that can be performed on cysteine residues that either occur in a protein's native sequence or are inserted *via* mutagenesis.[13, 49, 61-63]

Davis *et al.* describe several strategies for the *in situ* conversion of single free cysteines into the alkene-bearing amino acid, dehydroalanine, which can then be functionalised further by nucleophilic addition. This has been performed on a range of single cysteine containing proteins, both engineered and native.[13, 49, 61] This is an example of the general strategy that was coined as the 'tag and modify' approach; where an amino acid 'tag', either natural or unnatural, is converted *in situ* into a reactive handle followed by a highly selective functionalisation.

One of the most common classes of reagents used for alkylation of cysteines are maleimides. As good Michael acceptors, maleimides can react selectively and rapidly with cysteine thiols to form succinimide adducts, because of this feature

there are now many commercially available chemical probes with maleimide handles from leading suppliers (*e.g.* Sigma Aldrich). Further to this, bromomaleimides have been developed that react at comparable speeds, where the resulting thioether bond is reversible under certain conditions (*vide infra*, section 1.2.2).[62] More recently, a novel class of pyridazinediones (PDs) have been developed by Chudasama *et al.* that can feature two thiol-reactive centres and two *N*-linked handles.[63] Furthermore, they have shown exquisite selectivity for cysteine modification over lysine (*vide infra*, section 1.2.3).[63]

The majority of cysteine residues found in the sequences of native proteins exist in their oxidised format (Scheme 5); a pair of cysteines forming a disulfide bridge. Considering the high thiol reactivity and their higher abundance,[64] once reduced, they offer promising targets for site-selective modification of native proteins.

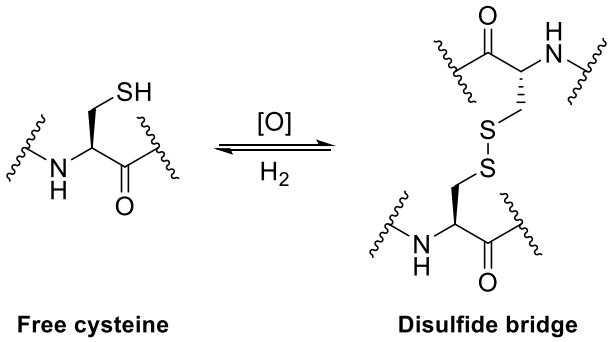

Scheme 5 Cysteine has relatively low natural abundance; 1.7% total abundance; 0.2% as free cysteine and 1.5% as the oxidised disulfide bond.

1.2 Disulfide modification

Disulfide bonds can be critical in providing structural integrity and conformational stability for a protein's tertiary structure and, as a result, its biological activity. Many proteins contain disulfide bridges either buried within the protein's hydrophobic interior (*i.e.* inaccessible for modification without denaturement) or on their solvent-accessible surface. As most proteins, including many therapeutically relevant ones, possess at least one solvent-accessible disulfide bridge they represent promising targets for site-selective modification.[65-68]

One of the more prominent examples of disulfide modification can be found in the synthesis of the FDA-approved antibody-drug conjugate (ADC), Adcetris™ (brentuximab vedotin) (Scheme 6). Reduction of disulfide bridges and subsequent conjugation of the liberated cysteines enabled conjugation of an anti-CD-30 monoclonal antibody (brentuximab) to the highly cytotoxic drug monomethylauristatin E (MMAE).[69] This method of inter-chain disulfide reduction and conjugation can give rise to a homogenous product if all the liberated thiols are reacted analogously, *i.e.* giving eight attachments per the antibody as brentuximab comprises four inter-chain disulfide bridges.[70] However, when targeting typical DARs of 4 (as in the case of Adcetris™), a heterogeneous, statistical mixture of products is obtained. Whilst reduction of disulfide bonds did not lead to a significant change in the protein's structure and conformation in this case, the antibody was less stable *in vivo* and no longer had antibody dependent cellular cytotoxicity (ADCC) associated with it, demonstrating the significance of the structural integrity and conformational support offered by disulfide bridges.[71]

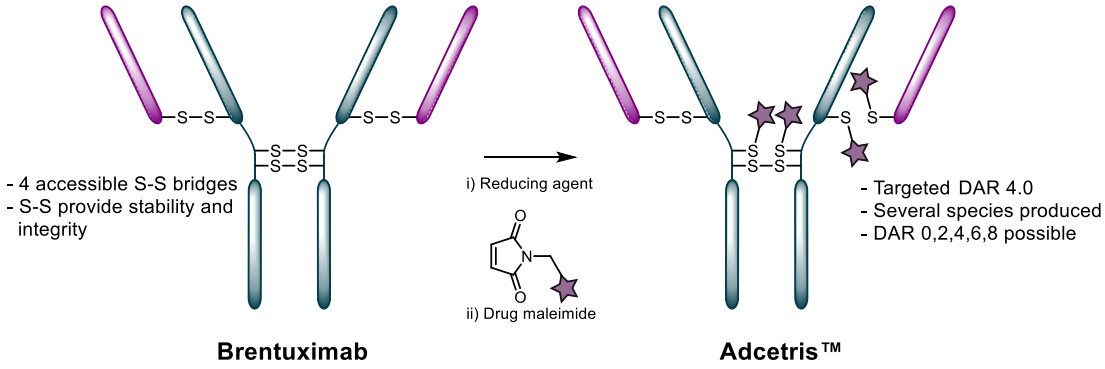

Scheme 6 Synthesis of FDA-approved ADC Adcetris™ is achieved through reduction of inter-chain disulfide bonds followed by conjugation to a maleimide linked drug (MMAE) giving an average DAR of 4.0 followed by careful re-oxidation of remaining non-conjugated thiols.

1.2.1 Functional disulfide re-bridging

The issues associated with disulfide reduction, *i.e.* change in conformation/loss of activity can be somewhat mitigated through a technique known as functional disulfide re-bridging. The technique involves the reduction of accessible disulfide

bridges, followed by introduction of a linker, bearing either a chemical probe or functional handle (to enable further modification) that will restore the connection. This simultaneously results in the functionalisation of the protein whilst restoring the structural and conformational stability offered by the original covalent bridge.[72] Over the past 10 years, since its inception by Brocchini *et al.*,[68, 73] the strategy has seen significant development and has been successfully applied to many different disulfide bearing targets, often with significant therapeutic relevance.[66, 67, 72, 74-76]

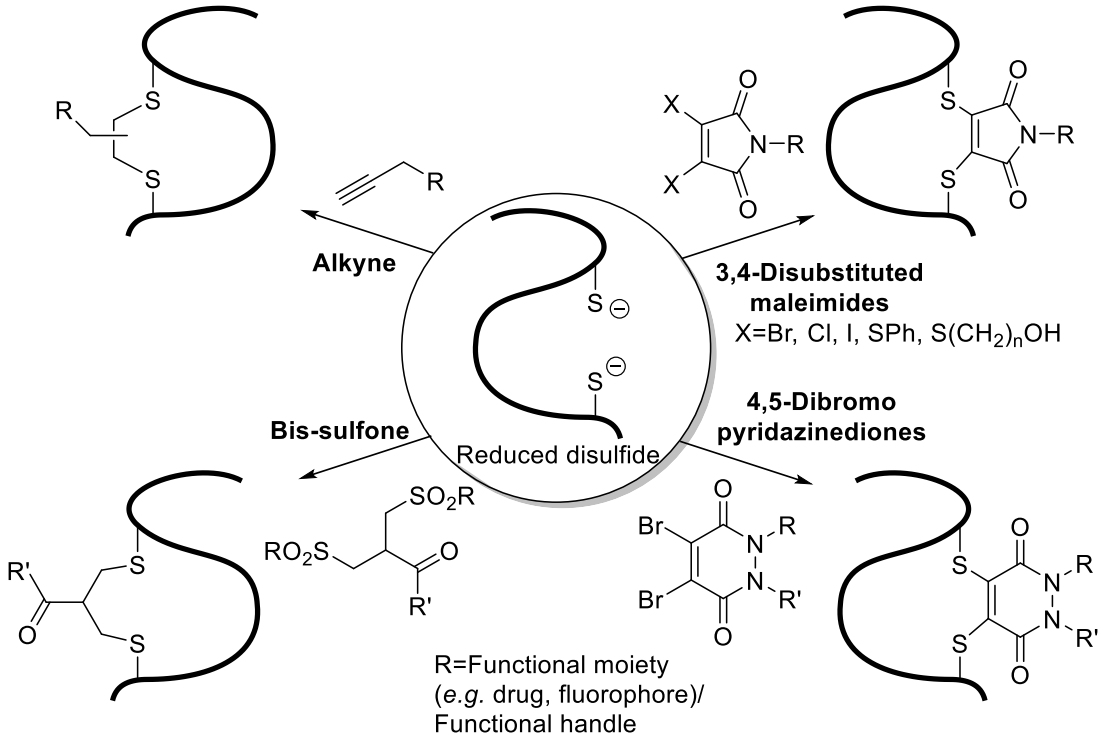

Scheme 7 Functional disulfide re-bridging enables functionalisation of proteins whilst retaining the structural stability offered by the native bridges; as such many strategies have been developed.

The seminal work in the field of functional disulfide re-bridging was carried out by Brocchini *et al.* in 2006, in which an interferon α-2b was conjugated to a polyethylene glycol (PEG) chain.[68] An enone-sulfonyl compound was synthesised that underwent *in situ* elimination to form a reactive species that reacts with a free thiol *via* a conjugate addition and elimination reaction. When applied to a reduced disulfide bond a second conjugate addition reaction with the other free thiol can take place, thereby re-connecting the cysteines with a three-carbon bridge (Scheme 8). This demonstrated the utility of functional disulfide re-bridging; the

native protein had been successfully site-selectively modified and in such a way that tertiary structure and biological activity were retained.[68]

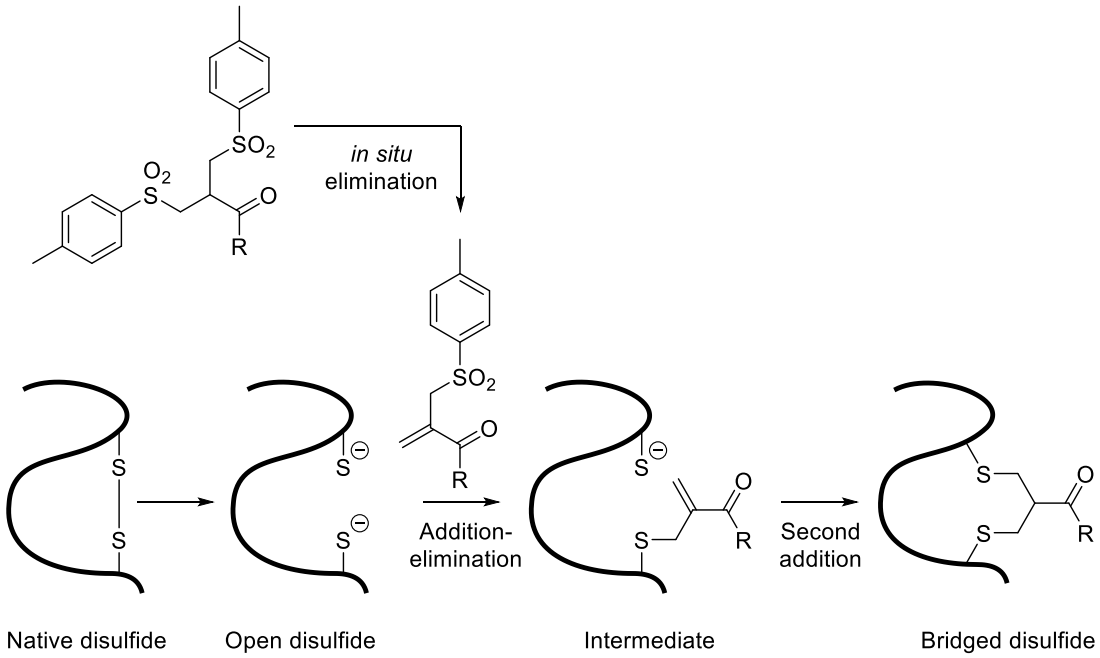

Scheme 8 Introduction of reduced disulfides to enone-sulfonyl reagent by Brocchini *et al.* resulted in first example of functional disulfide re-bridging.[68] The reactive enone species is generated *in situ* followed by two conjugate additions.

More recently, a photochemically driven thiol-yne reaction has been reported by Griebenow *et al.*, which, similar to Brocchini's strategy, leaves a saturated carbon bridge; in this case two carbons.[77] Following reduction, a disulfide-bearing peptide was incubated with a commercially available alkyl alkyne with radical initiator lithium phenyl-2,4-6-trimethylphosphinate and irradiated with UV light (365 nm). This strategy results in a stable re-bridged peptide construct, however, the yield for this reaction was 3% and substitution for more strained alkynes saw improvement to only 22% in the best case.[77]

1.2.2 Di-substituted maleimides

Previous work in the Baker, Chudasama and Caddick groups has demonstrated functional disulfide re-bridging on a wide variety of disulfide containing peptides and large proteins using *N*-functionalised dibromomaleimides.[65, 67] Unlike classical maleimides, once it has reacted with a thiol in its 3- or 4-position, a

dibromomaleimide retains the double bond due to the addition-elimination mechanism afforded by the presence of leaving groups (Scheme 9). This is as opposed to the 1,4-conjugate addition observed with a non-substituted maleimide. Through having two thiol-reactive centres and a versatile handle on the nitrogen, dibromomaleimides enable the formation of bis-thioether linked bioconjugates. Schumacher *et al.* initially demonstrated this class of molecule's utility by increasing the *in vivo* stability of the peptide hormone somatostatin through PEGylation (attachment of a polyethylene glycol chain);[78] the non-toxic, non-immunogenic and highly soluble polymer often sees use in drug delivery, owing to the fact it can improve resistance to enzymatic metabolism and decrease protein immunogenicity.[46] A stepwise protocol was employed where the first step involved using tris(2-carboxyethyl)phosphine (TCEP) to reduce the disulfide bridge between the Cys^{3} and Cys^{14} residues; TCEP is a mild alkyl-phosphine reducing agent. The excess TCEP is then removed by ultrafiltration and the newly liberated thiols from the disulfide bond then undergo two addition-elimination reactions to freshly added *N*-PEG dibromomaleimide, which re-bridge across the two cysteines. This method allowed efficient and selective conjugation of a PEG chain to somatostatin; increasing its *in vivo* stability, without affecting its biological activity or conformation.[15]

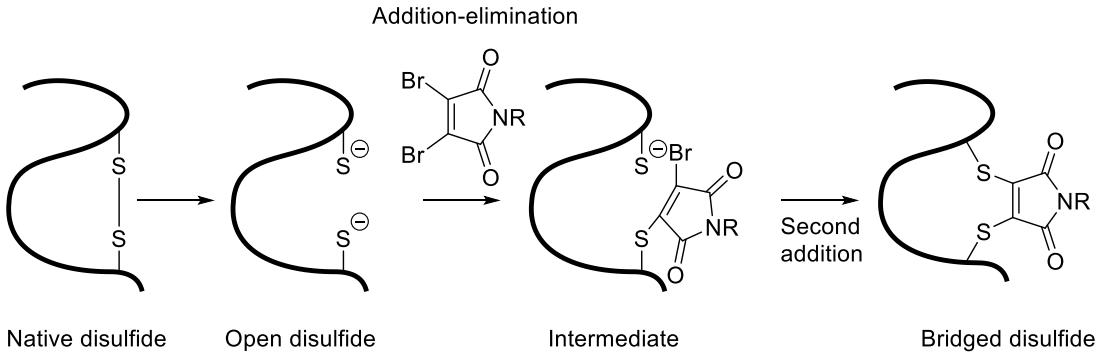

Scheme 9 3,4-Disubstituted maleimides enable functional disulfide re-bridging through two sequential addition-elimination reactions leaving an unsaturated rigid two-carbon bridge.

Since their inception, the scope of dibromomaleimides has been expanded through variation of the leaving groups in the 3- and 4- positions, *i.e.* at the thiol-reactive centres. Baker *et al.* attempted to overcome unwanted side-reactions, *e.g.* dibromomaleimide with TCEP, through the displacement of the bromo- groups

with thiophenol(Scheme 10, centre). This aided somewhat in reducing the large excess of maleimide required to affect re-bridging.[78] Mono-bromomaleimides were also reintroduced for disulfide re-bridging; Richards *et al.* demonstrate a strategy in which a reduced disulfide is introduced to an excess of bromomaleimide followed by a photochemically driven [2+2] cycloaddition between the C3-C4 unsaturated bonds on two adjacent maleimides (Scheme 10, left). This strategy showed potential not just for functionalisation of proteins but also as a potential photo-switchable tool to manipulate a protein's structure and effect conformational change.[79] Further to this, the functional scope of di-substituted maleimides was shown through the demonstration of a multimodal imaging strategy. A radiolabelled iodine was incorporated in to the triazole product resulting from a copper-catalysed azide-alkyne cycloaddition (CuAAC) between an alkyne-bearing dithioarylmaleimide and a fluorophore azide tag. The single-disulfide bearing peptide octreotide was then functionally re-bridged using the resultant multimodal imaging maleimide (Scheme 10, right).[80]

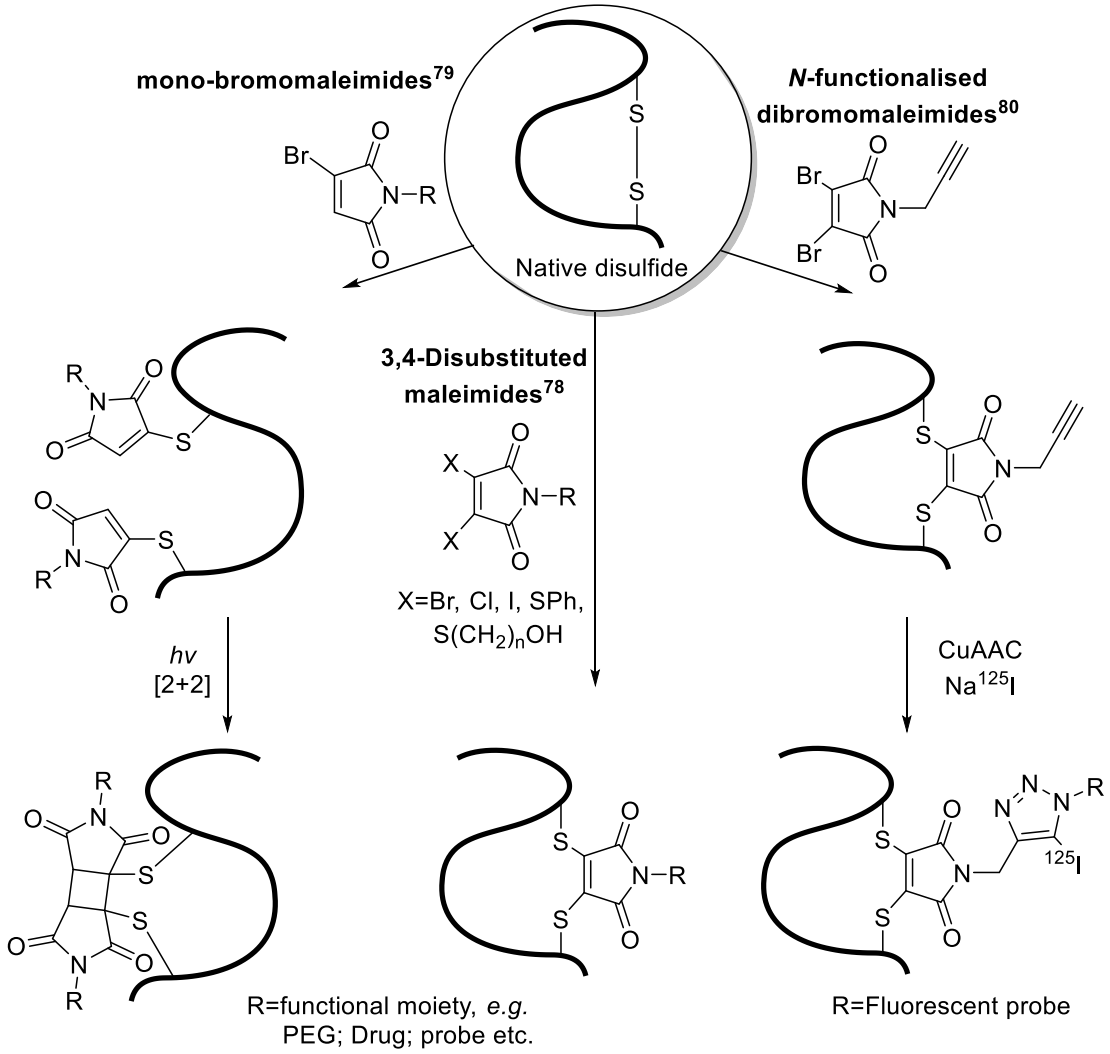

Scheme 10 Mono- and di-substituted maleimides have shown broad scope when applied to functional disulfide re-bridging.[78-80]

Under certain conditions maleimides linkers have been shown to bind reversibly to cysteines, allowing them to be cleaved from proteins when exposed to high concentrations of other thiols, *e.g.* glutathione. [81]

Whilst di-substituted maleimides are a powerful tool in protein modification they have shortcomings in some areas: i) the five-membered ring is prone to hydrolysis under basic conditions (Scheme 11) (although this has been used beneficially to afford thiol stability in some cases), the rate of hydrolysis can be between minutes and days, depending on substituents;[67] and ii) a maleimide re-bridged disulfide only has one point from which a functional handle can be easily constructed.

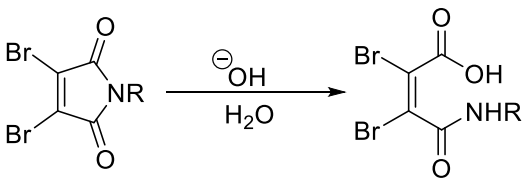

Scheme 11 Maleimide hydrolysis can occur under basic conditions.

The high reactivity of dibromomaleimides can also make them incompatible with certain reagents used in chemical biology, often necessitating the use of a large excess of either reducing agent or re-bridging agent. Chudasama *et al.* have, in recent years, reported on a new class of PD-based reagents, which have several desirable attributes that make them a more optimised platform for functional disulfide re-bridging.[63]

1.2.3 Pyridazinediones

In addition to having two thiol-reactive centres, PDs can comprise two orthogonal functional handles, which can be used to carry out two chemoselective transformations to yield multi-functionalised adducts (Figure 3).

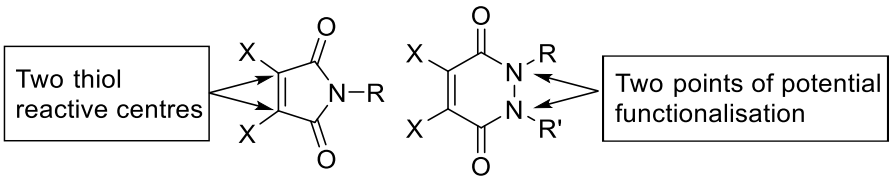

Figure 3 Di-substituted maleimides (left) and PDs (right) both have two thiol reactive centres, however, PDs have two points of attachment for functional moieties or handles, furthermore, PDs are tolerant to a broader range of reagents and conditions.

Furthermore, the 6-membered ring has been shown to be resistant to hydrolysis at a broad range of pH.[63] Recent work in the Chudasama and Caddick groups has highlighted the impressive scope of this scaffold (Figure 4).[82-84] The site-selective dual modification of proteins has been made possible using the 'dual click' strategy presented by Maruani *et al* (Figure 5).[83]

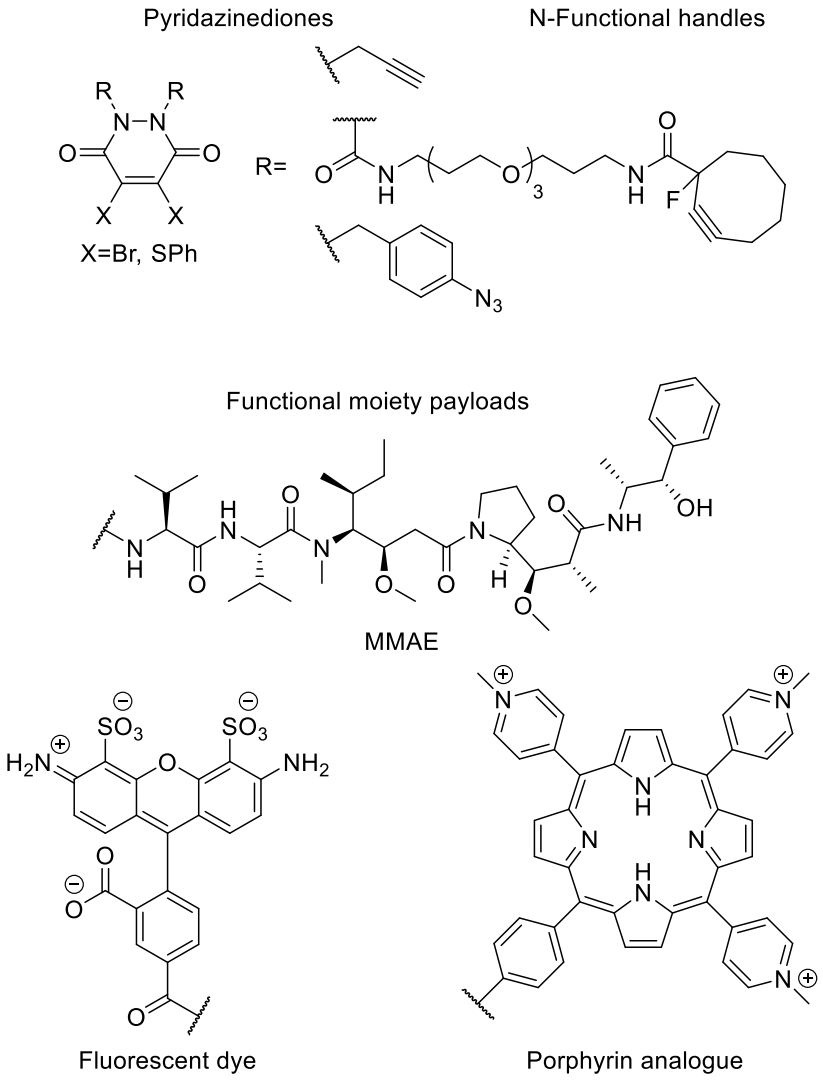

Figure 4 PDs have been shown to bear a range of orthogonal handles, of which a PD scaffold can bear two at once. A range of functional payloads have also been attached to antibodies and proteins demonstrating the scope of PDs in the field.

'Click' chemistry is a general term that is used to describe reactions that proceed in high yields with minimal by-product formation and typically can proceed in benign solvent conditions.[85, 86] Moreover, 'click' reactions usually feature a strong thermodynamic driving force that lead to the rapid and selective formation of a single product; they have seen widespread use in the field of protein modification due to their tendency to proceed *via* bioorthogonal reaction pathways.[21, 48] Through inclusion of a terminal alkyne handle on one nitrogen and of a cyclooctyne strained alkyne on the other, two distinct targets can be conjugated

via sequential copper-free strain promoted azide-alkyne cycloaddition (SPAAC) 'click' on the strained alkyne and a CuAAC 'click' on the non-strained alkyne.[83]

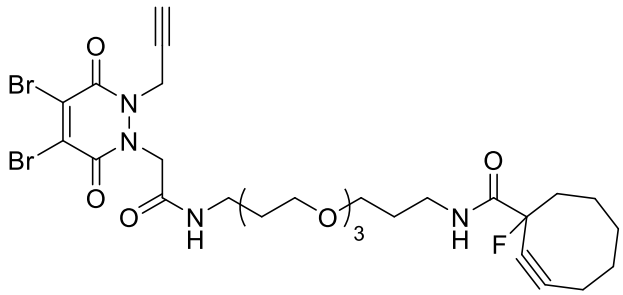

Figure 5 The 'dual click' strategy presented by Maruani *et al.* involves the use of orthogonal azide-alkyne cycloaddition reactions; a strained alkyne that can react under copper free conditions and an alkyl alkyne that reacts *via* a copper catalysed route.

The Chudasama group have also presented work demonstrating the advantages of PDs over succinimide linkers formed from maleimide-cysteine additions.[82] It has recently emerged that succinimide thiol linkages are unstable in blood serum due to thiol exchange with blood thiols (*e.g.* albumin).[87] It was shown that if one of the nitrogen atoms on a PD is unsubstituted then the molecule does not react with thiols at physiological pH or higher. It was speculated that this was a consequence of such a structure existing as its enol tautomer, which is likely to be significantly deprotonated under physiological conditions, thus significantly reducing the electrophilicity of the PD core and, therefore, it's susceptibility to thiol attack. Thus a novel strategy to unmask such an entity post-bioconjugation was developed (Scheme 12). This was done by reaction with a PD bearing a *p*-azidobenzyl group on the nitrogen, which when reacted with TCEP offered the desired thiol irreversible scaffold.[82]

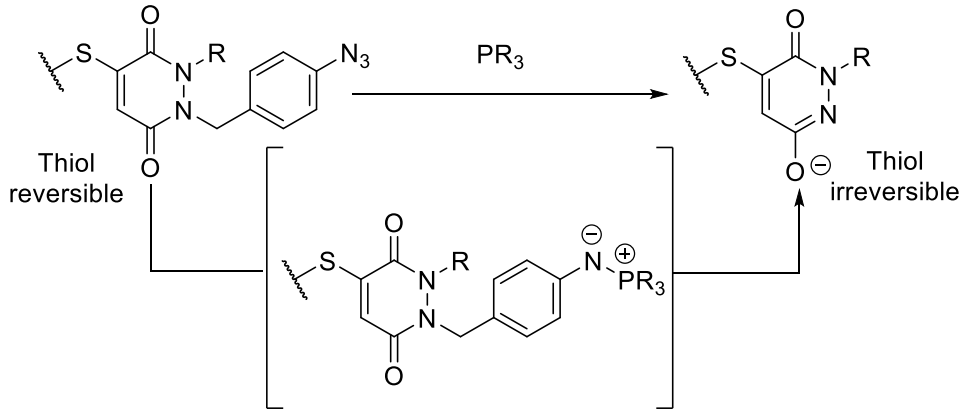

Scheme 12 Chudasama and co-workers developed thiol irreversible linkers by removing a para-azidobenzyl group on a conjugated PD *in situ* to convert reversible linkers into irreversible ones.

The broader functional applications of PDs were further demonstrated in the context of photo-dynamic therapy. Chudasama and Boyle *et al.* showed site-selective functionalisation of Herceptin™ to bear 4 porphyrin moieties to act as photosensitisers, which upon being directed to the tumour could be activated through the topical application of low energy light. The resultant conjugates were appraised *in vitro* and were shown to exude excellent selectivity and efficacy.[84]

1.3 Antibody-Drug Conjugates

Functional-disulfide re-bridging is broadly applicable to protein modification in general. However, much of the presented work has been performed in the context of the site-selective modification of antibodies and their fragments for use as therapeutic tools, often referred to as ADCs. As such a brief introduction to the current state of ADC synthesis and use will be given.

1.3.1 Antibodies

Antibodies (often referred to as immunoglobulin [Ig]) are large (*ca.* 150 kDa) protein complexes that are produced as part of the body's active immune response to invading pathogens. The Y-shaped complexes bind with excellent selectivity to their complementary antigens. This, combined with their inherent ADCC is why they have seen use as therapies on their own. However, their use as delivery

vehicles for cytotoxic drugs and imaging moieties has attracted much attention in previous years.

The most common class of antibody used to construct ADCs is IgG (the sub-classification G, its isotype, denotes the structure of the constant domain of the heavy chain), as they make up the greatest proportion of antibodies found in humans and are predominantly located in blood. More specifically the sub-type most commonly use is an IgG1; the general structural motif of which can be described as consisting of two distinct chains, the heavy chain and light chain (denoted by $_H$ and $_L$, respectively) (Figure 6). The chains themselves can be divided into constant and variable regions, where changes in the variable region dictate the antibody's complementarity to its given antigen. This structure means that IgG1s are bivalent, *i.e.* each antibody can bind two antigens.[88]

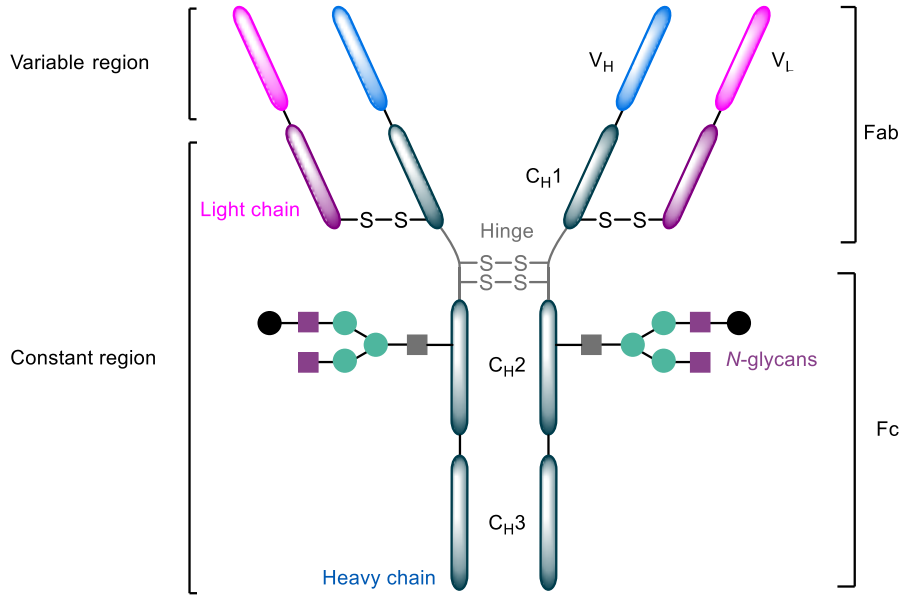

Figure 6 Generic structure of an IgG1 antibody displaying its general regions; 4 accessible disulfides and; 2 glycans; each of which represents a potential point of site-selective modification on native antibodies.

1.3.2 Current methods of antibody modification

The initial concept of delivering a toxic payload selectively to a tumour was conceived by Paul Ehrlich in 1913;[89] where he described a "haptophoric" or "fixing group", which could deliver a "toxophoric" or "injuring group" selectively to a

tumour. However, it was 45 years before an ADC was first created by Bernard *et al.*[90] and not until the 1970's that ADCs were first tested on animal models.[91, 92] The first ADCs using humanised monoclonal antibodies (mAbs) were reported in the 1990's.[43] Following this, the payloads used were developed to be more potent and selectivity of mAbs was improved.[93] By 2000 the first FDA approved ADC, Mylotarg™ (gemtuzumab ozogamicin) was released;[94] vindicating Ehrlich's initial hypothesis of an entity that could deliver the cytotoxic potency of a chemotherapy drug with the reduced off-target toxicity of an antibody.

Mylotarg™ has since been voluntarily withdrawn due to subsequent clinical trials showing no clinical benefit over conventional chemotherapy. However, two further ADCs have since seen approval; aforementioned Adcetris™ and Kadcyla™, which gained FDA approval in 2011 and 2013, respectively.[69, 95-97] There are currently *ca.* 50 ADCs in clinical trials, showing the impressive rate of growth in this sector.[98]

Kadcyla™ and Mylotarg™ were both constructed using lysine modification (*vide supra,* section 1.1.2.1), whereas Adcetris™ uses capping of reduced inter-chain disulfides (*vide supra,* section 1.2). All three exist as statistical heterogeneous mixtures of products, and while these remain the only entities to have gained FDA approval, the non-specific conjugation techniques used to create them are now seen as sub-optimal.

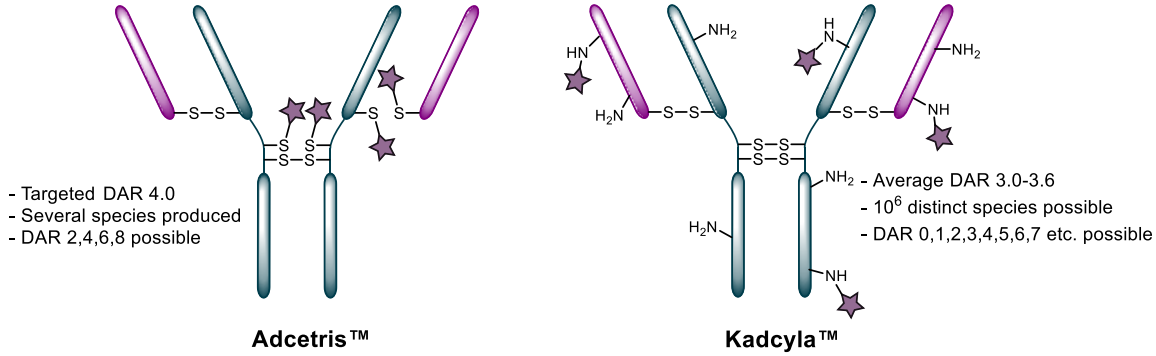

Figure 7 Kadcyla™ and Adcetris™ remain the only two currently FDA-approved ADCs; both use non-specific methods of modification in their synthesis.

1.3.3 Engineered antibodies

Many strategies have evolved in recent years that enable the site-selective modification of antibodies, due to recent advances in the field of protein engineering. These methods can be categorised into 3 main groups; (i) incorporation of cysteine into an antibody's sequence by mutagenesis; (ii) enzymatic conjugation; and (iii) incorporation of UAAs.

Engineered cysteines

The most widely applied example of engineered cysteine use was first demonstrated by Junutula *et al.* (Genentech) where additional cysteine residues were incorporated into a mAb *via* site-directed mutagenesis.[99] This enabled further site-selective attachment of functional moieties owing to the absence of other accessible free cysteines. This method is non-trivial, however, owing to the fact that the newly introduced cysteines can form disulfides with other available cysteines (*e.g.* forming mixed disulfides and protein dimers) that could disrupt the mAb's activity.[15, 100] This strategy of insertion of two additional cysteines into a mAb was coined THIOMAB™ by Genentech and has seen application in different mAbs including Herceptin™ (scheme 13).[101] While cysteine residues can be successfully introduced, they cannot be readily accessed due them mostly existing in the form of mixed disulfides with glutathione. Due to the lack of a method to selectively reduce the engineered cysteines, an alternative strategy was devised for modification at these points. All accessible disulfide bridges must be reduced, followed by re-oxidation under mild conditions to restore the inter-chain disulfide bonds, affording a mAb with its native disulfide bridges intact but featuring two engineered cysteines free for further chemical modification. THIOMABs™ have been used to create antibody conjugates with several different functional moieties (including drugs), with the ratio of payload to antibody typically being 1.9 (±0.1) with varying degrees of homogeneity.[50, 102]

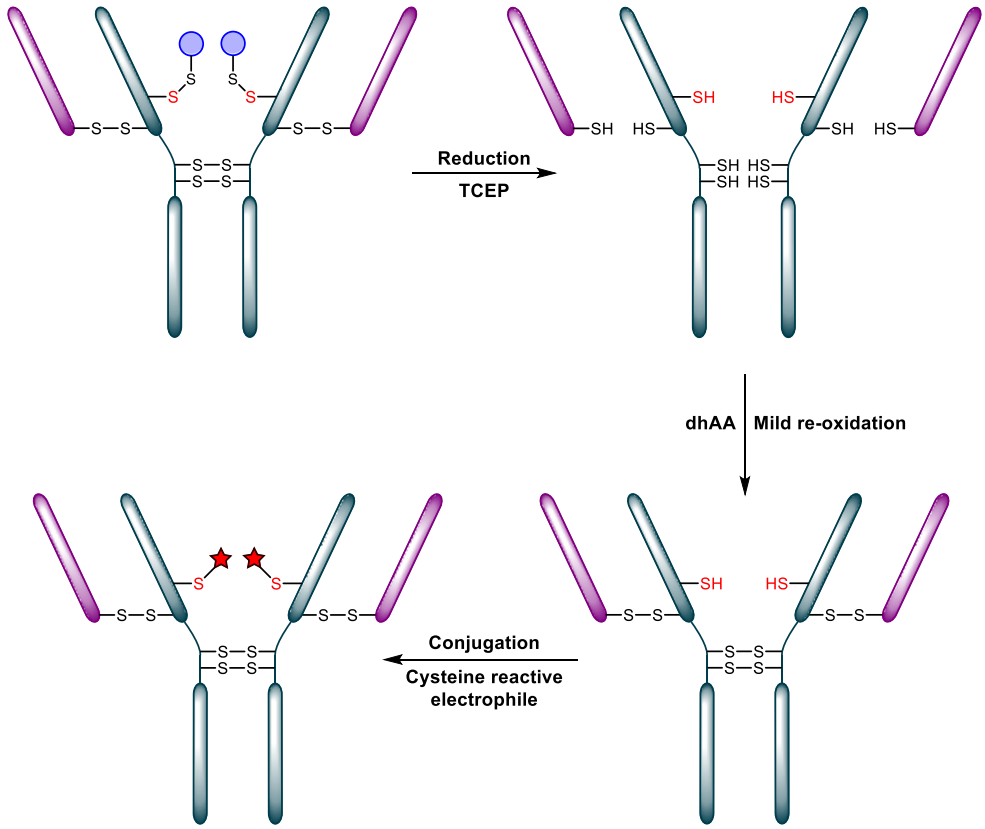

Scheme 13 THIOMAB™ technology enables site-selective incorporation of two cysteines into accessible points on a mAb's surface. As these are typically capped with a disulfide protecting group they require deprotection *via* reduction, then the inter-chain disulfides must be re-oxidised.

Enzymatic modification

Another strategy for the site-selective modification of engineered antibodies is through the incorporation of an amino acid sequence that acts as a tag to direct enzymatic modification. This approach has been used to site-selectively attach drugs to antibodies. An example of such a strategy has been through the use of certain transglutaminases (TGs). TGs are useful tools in biosynthesis owing to their ability to form amide linkages between a lysine primary amine side chain and the amide group on a glutamine.[103] Strop *et al.* demonstrated the use of a bacterial TG, isolated from *Streptoverticillium mobaraense*, which will only catalyse reactions of glutamines found in a 'glutamine (Q)-tag' (as in LLQG).[104] The authors identified two optimal positions in an anti-M1S1 mAb sequence for inclusion of Q-tags. This enabled the use of the bacterial TG to catalyse conjugation of two monomethyl dolastatin (MMAD, a potent tubulin inhibitor) to the mAb's

surface, resulting in the generation of ADCs with good biophysical properties and average DARs of 1.9.[104] These ADCs showed better *in vivo* tolerance in comparison with analogous ADCs with higher drug loadings synthesised through the use of cysteine modification following reduction of inter-chain disulfides.

Incorporation of UAAs

Incorporation of UAAs also remains a viable strategy and has been used for the successful construction of ADCs. Axup *et al*. presented the synthesis of an MMAD-Herceptin™ ADC with a DAR 2.0, through incorporation of the UAA *p*-acetylphenylalanine into the constant region of the mAb and a subsequent oxime-ligation reaction.[15] This method enabled production of several ADCs with good homogeneity. Incorporation of UAAs sees continued use in the field but is still hampered with the aforementioned issues (*vide supra,* section 1.1.1). Furthermore the potential immunogenicity of UAAs is not yet fully understood and more studies are required to fully appraise the implications of their use in bio-therapeutics.

1.3.4 Site-selective modification of native antibodies

Whilst the synthesis of near homogeneous ADCs is made possible through the use of engineered antibodies, it remains advantageous to carry out site-selective homogenous transformations on native mAbs. This is due to the increased overall costs associated with the optimisation of cell-culture conditions and site-directed mutagenesis that engineered mAb scaffolds necessitate. There are two main types of target available for the site-selective modification of antibodies; (i) glycans; and (ii) disulfide bridges.

N-Glycan modification

All antibodies possess *N*-glycosylated residues at a conserved position in their constant region, thus they serve as potential targets for site-selective modification. This is generally achieved through oxidation of the carbohydrate residues to produce aldehydes, which can then undergo further chemical

modification (scheme 14).[105, 106] However, this strategy employs harsh oxidative conditions that can result in oxidation of other residues on the antibody; this over-oxidation has been known to negatively affect the activity and half-life of resulting ADCs.[107] Whilst these issues have been somewhat mitigated through the use of milder enzymatic oxidation strategies, the fact remains that glycan populations are heterogeneous due to the existence of different glycoforms amongst antibodies of the same type. Thus, ADCs synthesised through glycan modification can suffer from poor homogeneity.[108]

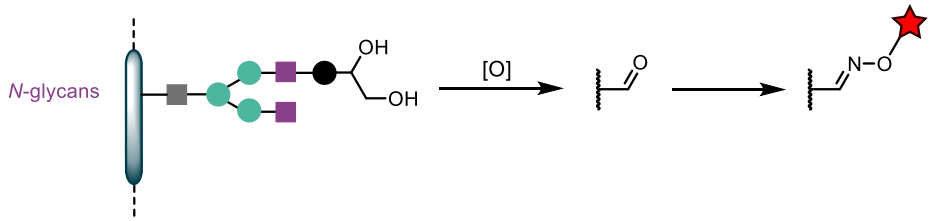

Scheme 14 Native glycan targeting to yield aldehyde-modified mAb by oxidation followed by reductive amination or O-substituted oxime functionalization.

Disulfide modification of antibodies

Reduction of inter-chain disulfide bonds and subsequent reaction with the free thiols has also been put to use in the site-selective modification of antibodies. This is due in part to the inter-chain disulfides being the only solvent-accessible ones on the antibody; *i.e.* on an IgG1 there four accessible inter-chain disulfide bridges, offering eight thiols once reduced.

Reaction at reduced disulfides can yield ADC species with a DAR of up to 8.0 as was the case in the early development of Adcetris™. Ultimately, however, it was discovered that a lower drug loading (averaging 4.0) provided the best balance between efficacy and pharmacokinetic properties. As such, carefully controlled stoichiometry of conjugating reagents was employed to ensure an average loading of 4.0, with homogeneity of up to 75%. Overall, due to a lack of control over selective disulfide reduction a heterogeneous mixture of products still arises.

In order to target more homogeneous ADCs with a DAR of 4.0, Badescu *et al.* (PolyTherics) considered the use of functional disulfide re-bridging.[66] It was proposed that the use of a bis-sulfone reagent would allow, through a bis-elimination-addition mechanism (*vide supra,* section 1.2.1), incorporation of a single cytotoxic drug into each accessible disulfide bridge. MMAE, another potent tubulin inhibitor, was chosen as the toxic payload and the resulting conjugates were shown to have improved efficacy and selectivity over the free drug alone *in vitro* and *in vivo*.[66]

The field of functional disulfide re-bridging in the context of ADCs has also seen considerable advancements from the Chudasama, Baker and Caddick groups through the use of di-substituted maleimides and PDs (*vide supra,* section 1.2.1). Nunes *et al.* describe methods that target a DAR 4 ADC using Herceptin™ that has undergone functional disulfide re-bridging with disubstituted maleimides. A bisthioaryl maleimide bearing MMAE was incorporated into the interchain disulfide bonds of the mAb using a sequential reduction/re-bridging protocol (figure 8). The resultant species had an average DAR of 3.89, as characterised by HIC.[67] Further to this, the utility of post-bioconjugation hydrolysis of the maleimide linkers was shown through dramatic increases in serum stability over conventional (non-hydrolysed) maleimides. The potency of the ADCs was assessed through *in vitro* assays against a HER2 positive cell line showing significantly reduced cell viability and increased cytotoxicity when compared to native Herceptin™.[67] The homogeneity of conjugates produced using this strategy has since been improved by Morais *et al.,* through the accelerated hydrolysis of maleimide linkers post-conjugation.[109] The presented conjugates undergo hydrolysis in 1 h; a stark improvement over the 72 h achieved previously by Nunes *et al.* This improved rate of hydrolysis prevented unwanted side reactions and increased homogeneity.

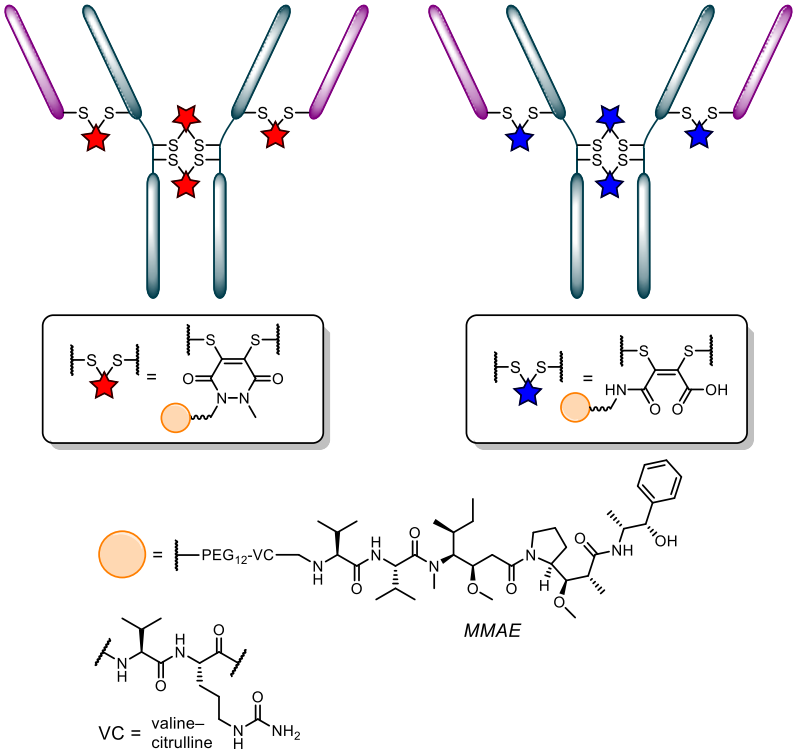

Figure 8 Conjugates prepared by Robinson *et al*. (left) and Nunes *et al.* (right). Both feature the use of functional disulfide re-bridging to create DAR 4 ADCs. Stable thioether linkages are essential to ensure selective delivery to cancer cells.

More recently, Robinson *et al.* described the use of PDs to synthesise Herceptin™-MMAE ADCs, targeting a DAR of 4.0 (figure 8).[110] Two different MMAE PDs were used to produce conjugates; one with a valine-citrulline linker, one without. In both cases an average DAR of 4.0 was achieved with 90% homogeneity, characterised by both HIC and LCMS. Furthermore, the PD conjugates showed comparable serum stability to the maleimide conjugates prepared by Nunes *et al.*, thereby mitigating the need for an extra hydrolysis step post-bioconjugation. The activity of the prepared ADCs was assessed through *in vitro* and *in vivo* studies.[110] The PD ADCs performed especially well in breast cancer xenograft mouse models; showing complete tumour regression in 18 days; a significant improvement over native Herceptin™ in the same study.

1.4 Aims

In recognition of the aforementioned challenges associated with the modification of antibodies, the need for improved biochemical techniques that would increase the homogeneity and control of such modifications was identified. Furthermore, in order to make the field of bioconjugation, and specifically the synthesis of ADCs, more accessible to groups and companies that do not have access to more expensive mutagenesis techniques, simple chemical strategies are required.

The work in this thesis centres on the development of two distinct technologies, both of which address hitherto unmet needs in the field. The first of which was designed to overcome two issues central to functional disulfide re-bridging in mAbs; to simplify the protocols used in functional disulfide re-bridging and to overcome incidence of non-native disulfide re-bridging in multi-disulfide systems, which can lead to a loss in activity. It was theorised that the creation of a single chemical entity that could both reduce and re-bridge a disulfide bond would circumvent both these issues (detailed further; *vide infra*, Chapter 2.0).

The second technology was envisaged to meet the growing demand in the field for the capability to construct ADCs with a functional loading of two moieties per mAb, without the use of antibody engineering techniques. The loading of two moieties per mAb is especially desirable in the case of large hydrophobic payloads where a compromise between efficacy and pharmacokinetic profile is required and has until now not been achieved with control over homogeneity of products using chemical methods alone (detailed further; *vide infra*, Chapter 3.0).

Both the presented technologies aim to use PD-based scaffolds to affect novel disulfide re-bridging on a variety of disulfide-containing systems. Specifically, however, they are both aimed at improving the control and homogeneity with which ADCs can be constructed from native mAbs.

Chapter 2: Reduction and re-bridging delivered by one reagent

Whilst pyridazinediones represent an important step towards providing reagents for efficient and versatile modification of proteins, there are still areas in which significant barriers remain. A commonly used protocol for functional disulfide re-bridging with pyridazinediones (as well as other bridging agents) is a stepwise procedure, whereby the disulfide bond on a protein is first reduced with TCEP; excess TCEP (and oxidised by-product) is then removed and the liberated cysteines are exposed to a pyridazinedione based conjugating reagent with two appropriate leaving groups at the thiol-reactive 4- and 5-positions.[75, 83] This sequential protocol works very efficiently with templated single disulfide systems (*e.g.* the fragment antigen-binding [Fab] of Herceptin™, Somatostatin), but certain protein complexes that are not templated and/or held together by a single disulfide bond would fall apart if this sequential reduction/re-bridging protocol were employed. Moreover, when this stepwise protocol is applied to multi-disulfide systems re-bridging of cysteines in a non-native configuration has been observed; this is especially likely when there are multiple disulfide bonds within close proximity to one another, *e.g.* in the hinge region of an IgG1 (Figure 9).[67, 111] Re-bridging in a non-native configuration can lead to significant changes in a protein's configuration that can impact its stability and activity.[112] Furthermore within a given bioconjugation reaction it can lead to a heterogeneous mixture of products. Whilst steps can be taken to avoid non-native disulfide re-bridging (*e.g.* running conjugation reactions at low temperature and modifying with a low concentration of TCEP and a high concentration of re-bridging reagent *in situ* to rapidly trap reduced disulfide bonds) these procedures are inefficient, reagent-specific and cumbersome.[83] Moreover, for many bridging reagents cross-reactivity between the bridging reagent and reducing reagent is a major issue. Hence, it would be highly desirable to be able to perform functional disulfide re-bridging rapidly and efficiently with a single reagent, and ideally if it facilitated functional re-bridging with native disulfide connectivity retained. Furthermore, such a reagent would eliminate the need to purify a protein post-reduction and/or

switch buffer, reducing the number of steps and associated costs of the conjugation.

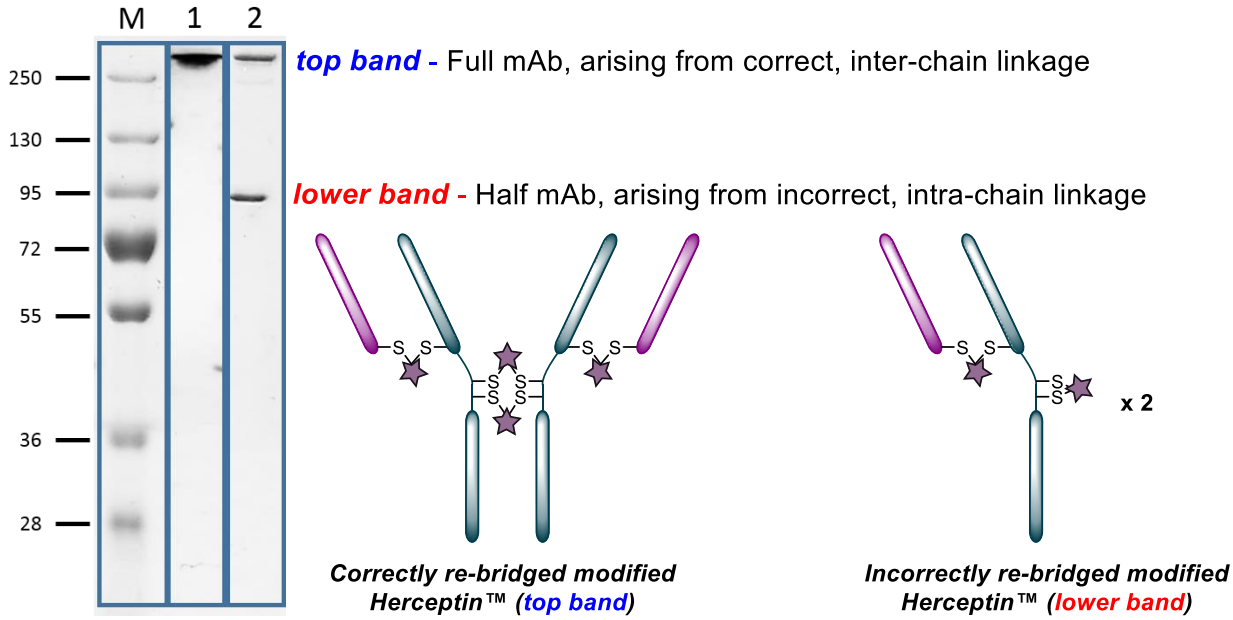

Figure 9 Left: SDS-PAGE analysis showing native Herceptin™ (lane 1) and Herceptin that has been re-bridged to give a mixture of native and non-natively re-bridged products (lane 2). Re-bridging in the native configuration gives rise to the full antibody band (top band) and non-native re-bridging gives rise to the half antibody band (lower band observed in lane 2).

2.1 A one-reagent procedure to create homogenous functional disulfide bridged proteins

Recently, Chudasama, Caddick *et al.* have shown dibromopyridazinediones to be viable candidates for functional disulfide re-bridging and that the resulting bisthioether is stable in blood plasma-mimicking conditions.[83] Whilst this approach, as well as others, offer advances in this growing field of disulfide labelling, a common limitation is the requirement for reduction and re-bridging in distinct steps. As highlighted above, this is mainly due to the incompatibility of the bridging and reducing agents. This introduces inefficiencies in terms of cost, time and practicality. Whilst one-pot *in situ* methods have been employed, this is only at the expense of using a vast excess of reducing and bridging agents to compensate for the reaction between the two reagents.[83]

The aim of this project is to develop a system that can, with a single reagent, convert a range of single and multi-disulfide systems into functional bioconjugates whilst retaining their native disulfide configuration. The proposal is to synthesise a molecule that can single-handedly reduce and conjugate across a disulfide bond in a rapid manner. In order to achieve this, a suitable molecule needed to be designed, which had to feature both a reduction and re-bridging moiety, this would turn the previously step-wise protocol into a one-reagent/one-addition procedure. Furthermore, it was theorised that immediately following reduction, by having the re-bridging moiety so close in space to the reduction moiety, the newly liberated thiol groups would be immediately exposed to a high local concentration of the conjugating molecule core (*i.e.* minimising reduced disulfide residency time and, thereby, the associated risk of non-native disulfide re-bridging) and rapidly undergoing functional re-bridging. During the course of previous studies within in the Chudasama and Caddick groups, dithiophenolpyridazinediones have been observed to be unreactive towards commonly used disulfide reducing agent TCEP.[63, 75, 83] In light of this, TCEP moieties were a logical choice for incorporation into a dithiophenolpyridazinedione. More specifically, the TCEP functional moieties were to be tethered onto the thiophenol groups of the dithiophenolpyridazinedione since these groups would be extruded during an addition-elimination reaction with a thiol following disulfide reduction (Figure 10).

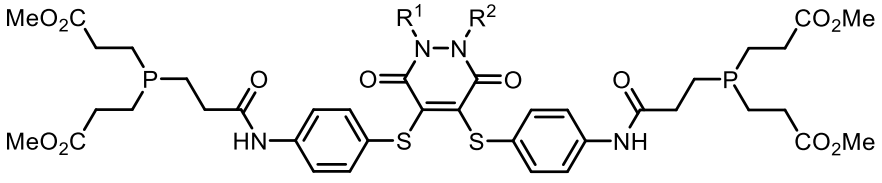

Figure 10 Proposed structure for dithioaryl(TCEP)pyridazinedione **7**; a molecule that can both reduce and subsequently conjugate across a disulfide bridge

2.2 Results and discussion

2.2.1 Synthesis of dithioaryl(TCEP)pyridazinedione

The synthesis of target pyridazinedione **7** started through bis-alkylation of di-*tert*-butyl hydrazine-1,2-dicarboxylate **1** using caesium carbonate with bromoethane in *N,N*-dimethylformamide (DMF) at 21 °C for 48 h to give di-*tert*-butyl 1,2-diethylhydrazine-1,2-dicarboxylate (**2**)(Scheme 15). The first alkylation, to give the mono-*N*-alkylated product proceeded rapidly (within 3-5 h), whereas the second, to give the desired bis-alkylated product, required significantly longer (*ca.* 40 h); the reaction progress was tracked by TLC. The bis-alkylation to give diethylhydrazine **2** proceeded with an 88% yield.

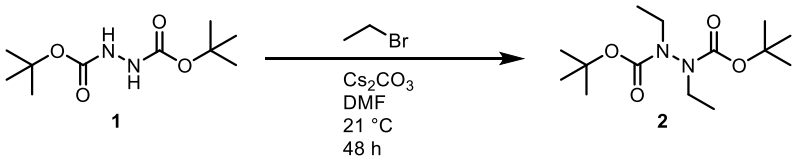

Scheme 15 Bis-alkylation of di-Boc protected hydrazine **1** to give diethyl analogue **2**.

Following this, TFA cleavage of the Boc groups of diethylhydrazine **2**, followed by reaction with dibromomaleic anhydride under reflux in AcOH afforded diethyl dibromopyridazinedione **3** in an overall yield of 73% (Route A, Scheme 16)**.** An alternative route for the formation of dibromopyridazinedione **3** where the deprotection and pyridazinedione formation steps are combined in a single-pot and the use of TFA avoided was also developed (Route B, Scheme 16).

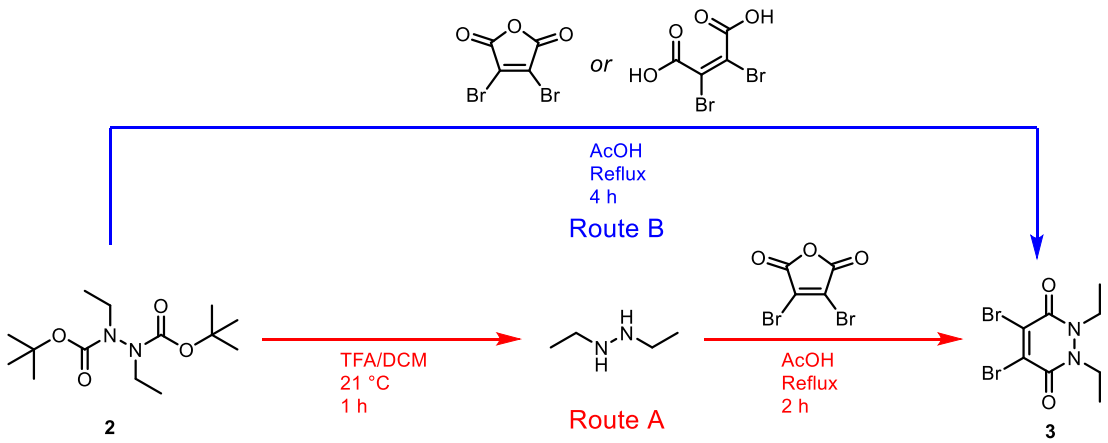

Scheme 16 Formation of pyridazinedione **3** was achieved through TFA deprotection of hydrazine **2** and subsequent treatment of the crude hydrazine with dibromomaleic anhydride in AcOH, refluxed for 2 h (Route A). Subsequent optimisation of the synthesis revealed deprotection of the hydrazine and pyridazinedione formation could both take place under reflux in AcOH (Route B).

Dibromopyridazinedione **3** was then reacted with 4-aminothiophenol in DCM with triethylamine at 21 °C for 2 h to form dithioarylpyridazinedione **4** in 66% yield (Scheme 17).

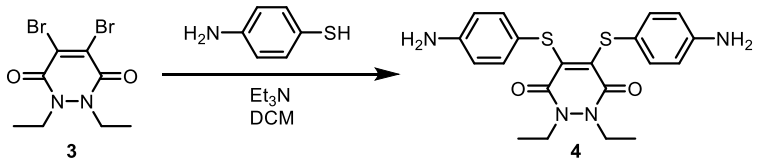

Scheme 17 Dibromopyridazinedione **3** was treated with 4-aminothiophenol and triethylamine in DCM

Following this a TCEP derivative (**6**), for attachment to the pyridazinedione core, was prepared through methyl esterification of two out of the three carboxylic acid groups give di-methylated species **6** (Scheme 18).

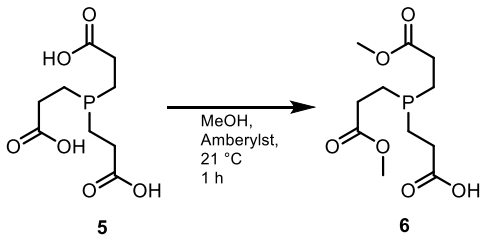

Scheme 18 TCEP·HCl was prepared for incorporation into final pyridazinedione scaffold **7** through methyl esterification of two out of the three carboxylic acid groups to give di-methylated TCEP analogue **6**.

To do this, TCEP·HCl **5** was treated with acidic resin Amberlyst® 15 in MeOH for 1 h at 21 °C to give a mixture of the mono-, di- and tri-methylated products. Gratifyingly, the three products were easily separated on silica using FCC,

affording dimethyl-TCEP analogue **6** as a colourless oil in a 17% yield. Finally the TCEP derivative **6**, now bearing only one carboxylic acid group, was coupled *via* an amide bond formation to the 4-amino groups on dithioarylpyridazinedione **4**. 1-[Bis(dimethylamino)methylene]-1*H*-1,2,3-triazolo[4,5-b]pyridinium 3-oxid hexafluorophosphate (HATU) was used to activate the carboxylic acid on TCEP analogue **6**, with DIPEA as base, prior to addition of the bis-aniline bearing dithioarylpyridazinedione **4**; the reaction was performed in DMF at 21 °C for 12 h and afforded target dithioaryl(TCEP)pyridazinedione **7** in a yield of 18% (Scheme 19).

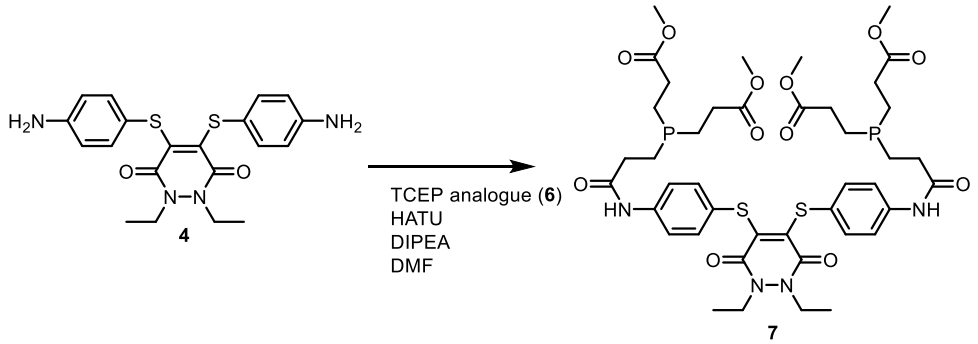

Scheme 19 Synthesis of dithioaryl(TCEP)pyridazinedione **7**. The thioaryl moiety was chosen for several reasons; it is reactive towards alkyl thiols; it is resistant to cross reactivity with TCEP; the 4-amino group served as a convenient point through the synthesis could be continued.

2.2.2 Proof of concept with single-disulfide containing systems

With dithioaryl(TCEP)pyridazinedione **7** in-hand, it's suitability as a bioconjugation reagent for both disulfide reduction and functional re-bridging was appraised. To do this, dithioaryl(TCEP)pyridazinedione **7** was incubated with a selection of biologically relevant disulfide containing proteins, *i.e.* the Fab (fragment antigen-binding) arm of Herceptin™, somatostatin, and octreotide.

2.2.2.1 Reaction of dithioaryl(TCEP)pyridazinedione 7 with Herceptin™ Fab fragment

To appraise the utility of dithioaryl(TCEP)pyridazinedione **7** it's suitability for the functional re-bridging of the Fab of Herceptin™ was examined. To do this, the single–disulfide containing Fab fragment was incubated in borate buffer solution (BBS) at pH8 with EDTA (0.5 mM) at 37 °C for 1 h with 1.25, 2, 5, and 10 equivalents of dithioaryl(TCEP)pyridazinedione **7** (scheme 20). A range of

equivalents were used to test the lower limit possible for dithioaryl(TCEP)pyridazinedione **7** to effect full re-bridging; 1.25 eq represents the lowest possible number that ensured a minimum ratio of 1:1 within the experimental degree of error. In each case significant conversion to the desired product was observed; the *N,N*'-diethylpyridazinedione core had been inserted into the one disulfide bond on the Fab fragment as assessed by LS-MS (Figure 11). In the acquired MS data, only one species is observed both before and after reaction showing a clear gain in mass corresponding to the mass of one diethyl-PD ring. The use of only 1.25 eq of dithioaryl(TCEP)pyridazinedione **7** was an especially significant result as conventional means of functional disulfide re-bridging typically require large excesses of either re-bridging or reduction components effect full conversion.

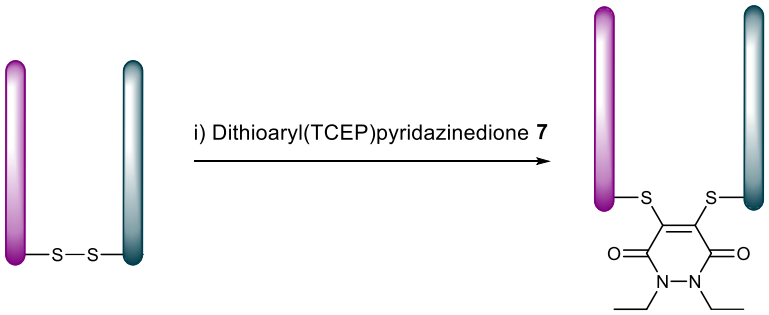

Scheme 20 Insertion of pyridazinedione core into the single disulfide bond present on a Herceptin™ Fab fragment through incubation with dithioaryl(TCEP)pyridazinedione **7**.

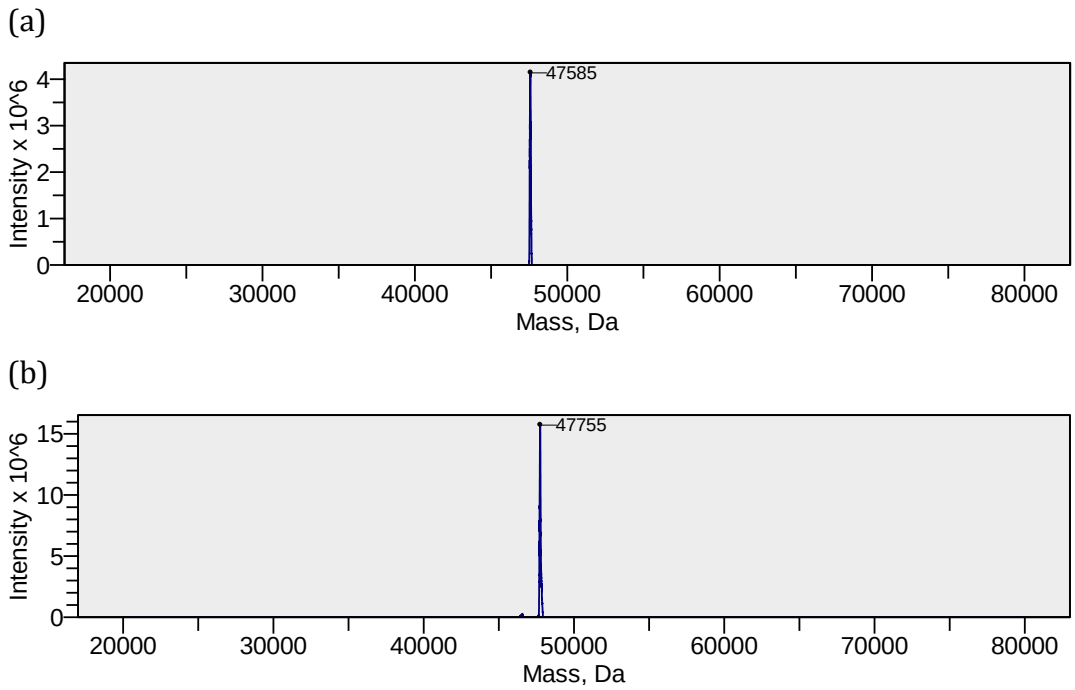

Figure 11 (a) deconvoluted MS data for native Fab fragment of Herceptin™ (b) deconvoluted MS data for Fab fragment of Herceptin™ reacted with dithioaryl(TCEP)pyridazinedione **7** (1.25 eq.).

2.2.2.2 Reaction of dithioaryl(TCEP)pyridazinedione 7 with octreotide

Octreotide is a peptide used in the treatment various conditions including growth hormone producing tumours.[113] It is a mimetic of somatostatin and has higher activity; it was chosen on the basis that it had only one disulfide bridge and that previous work on the peptide in the Caddick and Baker groups had provided insight to the peptide's characteristics with regards to its reactivity and solubility. In view of the optimisation on Fab and previous studies, the unmodified peptide was incubated with 1.25 equivalents of dithioaryl(TCEP)pyridazinedione **7**, as this was the previously discovered lowest number of equivalents used to effect re-bridging in a single disulfide system, in a 57.5:40:2.5 mixture of phosphate buffer (PB) (pH 6.2)/MeCN/DMF (peptide buffer) at 37 °C for 1 h (scheme 21). The octreotide underwent conversion to the desired product; the *N,N*'-diethylpyridazinedione core had been inserted into the one disulfide in the peptide as confirmed by LC-MS (Figure 11), which again showed a clear increase in the observed mass of the peptide corresponding to one PD ring.

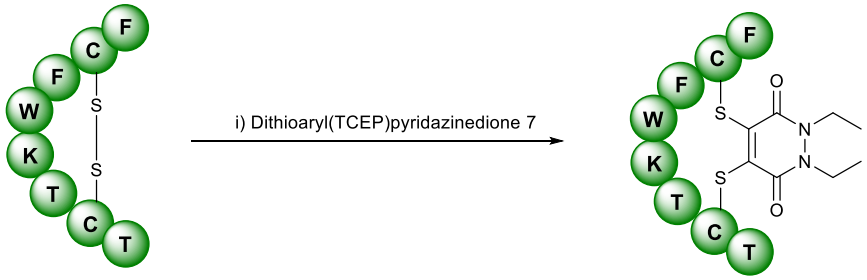

Scheme 21 Insertion of pyridazinedione core into the single disulfide bond present in octreotide through incubation with dithioaryl(TCEP)pyridazinedione **7**.

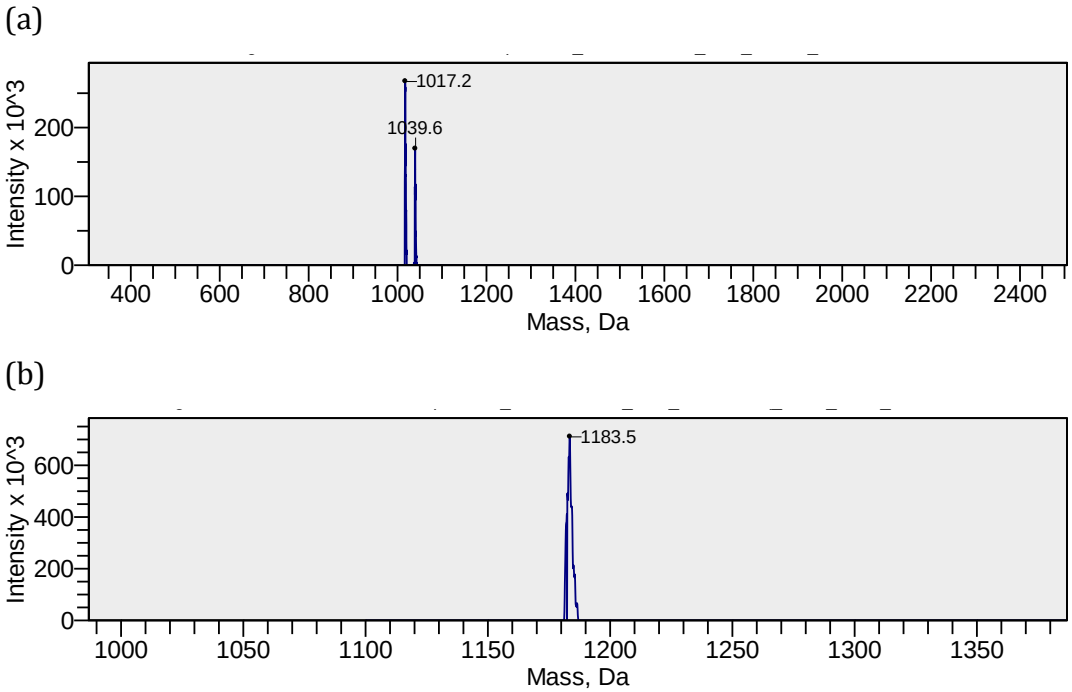

Figure 11 (a) deconvoluted MS data for unmodified octreotide, peak at m/z 1039.6 corresponds to $[M+Na]^+$ (b) deconvoluted MS data for octreotide reacted with dithioaryl(TCEP)pyridazinedione **7** (1.25 eq.).

2.2.2.3 Reaction of dithioaryl(TCEP)pyridazinedione 7 with somatostatin

The peptide somatostatin, an endocrine system regulatory hormone, was also chosen on the basis that it contained only one disulfide bond and on the familiarity that the Chudasama and Caddick groups have with reacting the peptide. In view of previous optimisation, the native peptide was incubated with 1.25 equivalents of dithioaryl(TCEP)pyridazinedione **7** in peptide buffer at 37 °C for 1 h (scheme 22). Gratifyingly, somatostatin underwent complete conversion to the desired

product; the *N,N'*-diethylpyridazinedione core had been inserted into the one disulfide in the peptide as confirmed by MALDI-TOF-MS (Figure 12).

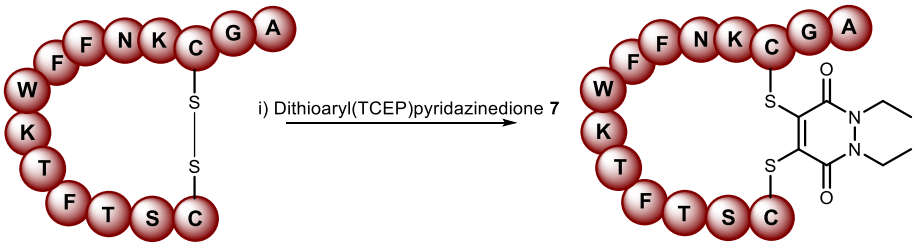

Scheme 22 Insertion of pyridazinedione core into the single disulfide bond present in a somatostatin through incubation with dithioaryl(TCEP)pyridazinedione **7**.

(a)

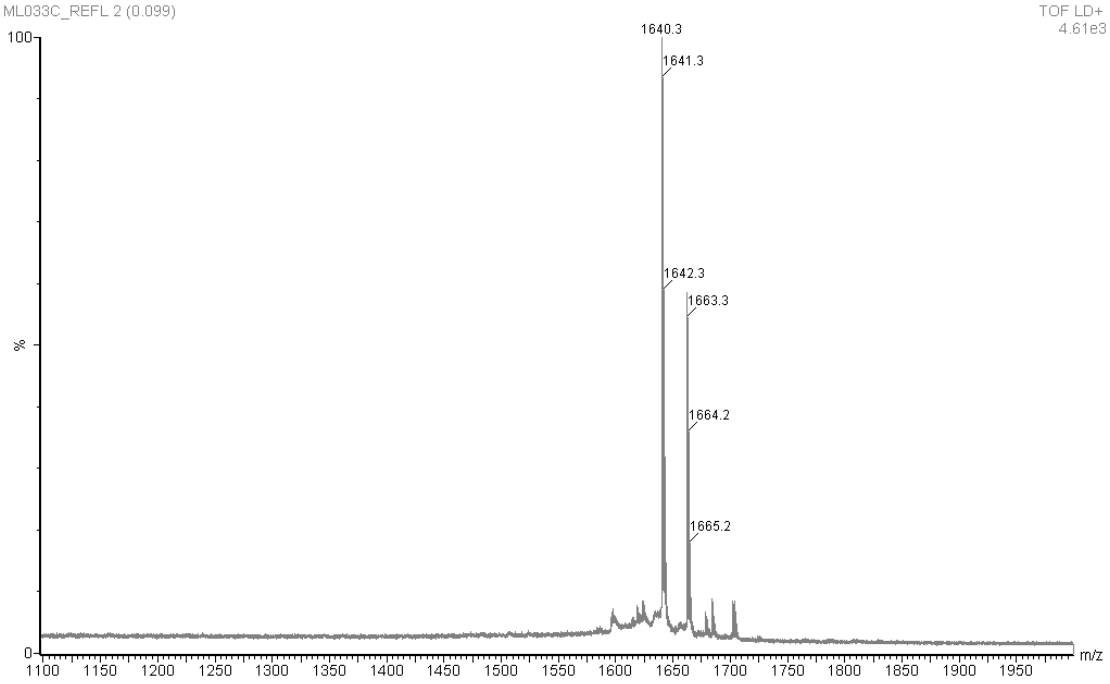

(b)

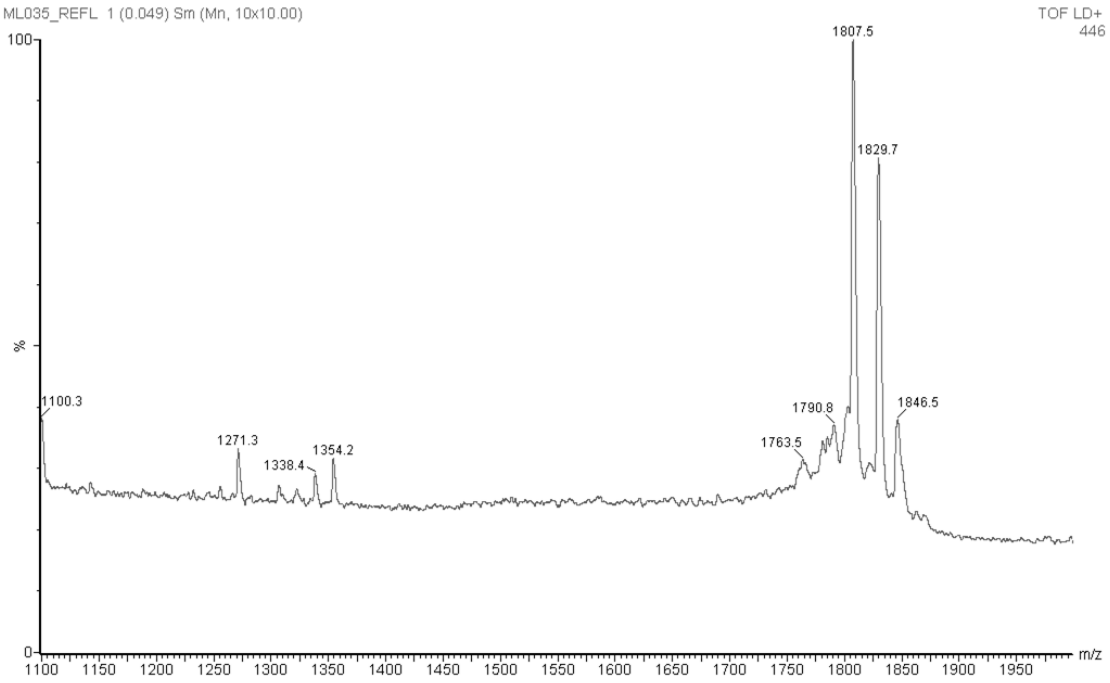

Figure 12 (a) MS data for unmodified somatostatin, peak at m/z 1663 corresponds to $[M+Na]^+$ (b) deconvoluted MS data for somatostatin reacted with dithioaryl(TCEP)pyridazinedione **7** (1.25 eq.), peak at m/z 1830 corresponds to $[M+Na]^+$.

2.2.2.4 Summary of results with single disulfide systems

Gratifyingly, in each case, dithioaryl(TCEP)pyridazinedione **7** was shown to reduce and functionally re-bridge the singly accessible disulfide of somatostatin, octreotide and Herceptin™ Fab. Moreover, only a small excess of dithioaryl(TCEP)pyridazinedione **7**, 1.25 equivalents, was required to effect complete conversion. Over the course of these studies it was also noted that dithioaryl(TCEP)pyridazinedione **7** could be stored with near complete stability over six months at -18 °C under argon. This was assessed by ^{31}P NMR, showing less than 10% oxidation after six months.

2.2.3 Competition studies

It was previously rationalised that a molecule with both reducing and re-bridging functions would minimise the residency time of the cysteines liberated from disulfide reduction due to the aforementioned high local concentration effect. This is especially in view of no reduced protein being observed upon incubation of the above peptides and proteins with dithioaryl(TCEP)pyridazinedione **7**. To appraise

this further, an analogous pyridazinedione with comparable thiol reactivity (to that of dithioaryl(TCEP)pyridazinedione **7**), which if incorporated into a peptide would give a product of distinct mass to that observed with reagent **7**, was designed and synthesized; pyridazinedione **10**.

2.2.3.1 Synthesis of pyridazinedione 10

Synthesis of the pyridazinedione **10** started with bis-alkylation of di-*tert*-butyl hydrazine-1,2-dicarboxylate **1** using caesium carbonate with 1-bromopropane in DMF at 21 °C for 48 h to give di-*tert*-butyl 1,2-dipropylhydrazine-1,2-dicarboxylate **8** in a 78% yield (Scheme 23).

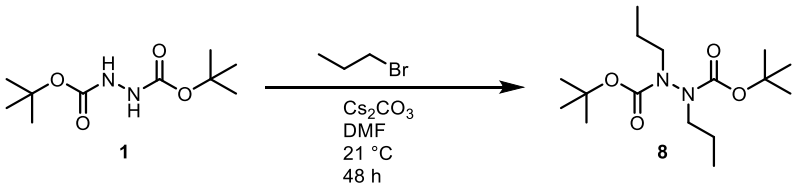

Scheme 23 Alkylation of di-Boc hydrazine **1** was achieved through treatment with 1-bromopropane and caesium carbonate to give bis-alkylated product **8.**

Following this, TFA cleavage of the Boc groups of dipropylhydrazine **8**, followed by reaction with dibromomaleic anhydride under reflux in AcOH afforded dipropyl dibromopyridazinedione **9** in an overall yield of 78%**.**

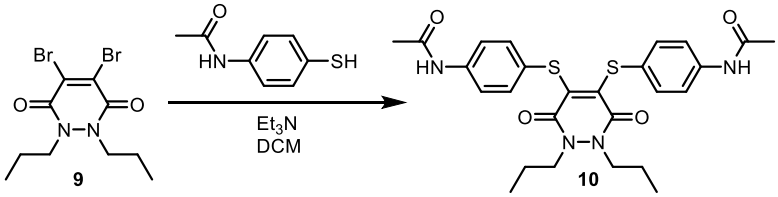

Scheme 24 Bromo groups were displaced with 4-acetimidothiphenol to create pyridazinedione **10**, which would feature comparable thiol-reactivity to that of pyridazinedione **7.**

Dibromopyridazinedione **9** was then reacted with 4-acetimidothiophenol in DCM with triethylamine at 21 °C for 2 h to form dithioarylpyridazinedione **10** in 40% yield (Scheme 24).

2.2.3.2 Application to Herceptin™ Fab fragment

In comparison to pyridazinedione **7**, dipropyl pyridazinedione **10** lacks the reducing function and it bears two *N*-propyl groups in place of the ethyl groups.

The mass difference of having two propyl groups in place of two ethyl groups is detectable by mass spectrometry.

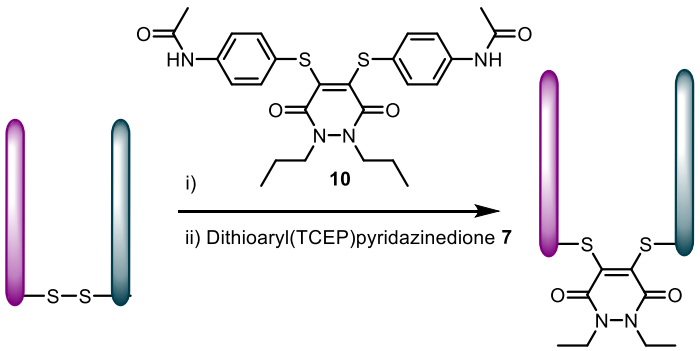

Scheme 25 Reaction of a Herceptin™ Fab fragment with dithioaryl(TCEP)pyridazinedione **7**; the Fab fragment was first incubated with dipropyl pyridazinedione **10** and subsequently incubated with **7**.

By having an excess of pyridazinedione **10** present in solution, incorporation of the diethyl pyridazinedione core from pyridazinedione **7**, would validate the high local concentration hypothesis *i.e.* the effective concentration of pyridazinedione **7** would be higher than that of competing pyridazinedione **10**. In the competition experiment, the Fab of Herceptin™ was incubated with 1, 2 and 5 equivalents of dipropyl pyridazinedione **10** in BBS with EDTA at pH 8 prior to incubation with 2 equivalents of diethyl pyridazinedione **7** (Scheme 25). Validating our hypothesis, re-bridging was only observed with the dithioaryl(TCEP)pyridazinedione **7**, *i.e.* only the *N,N'*-diethylpyridazinedione core from the parent scaffold of **7** was incorporated. The control reaction of reducing the Fab prior to adding a mixture of pyridazinediones **7** and **10** afforded a mixture of bioconjugates, confirming the validity of the competition studies; *i.e.* dipropyl pyridazinedione **10** did indeed have comparable thiol reactivity; this was validated by LC-MS (figure 13).

(a)

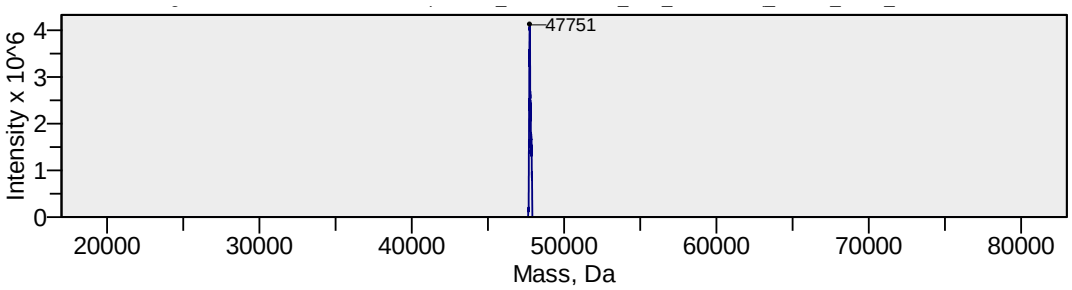

(b)

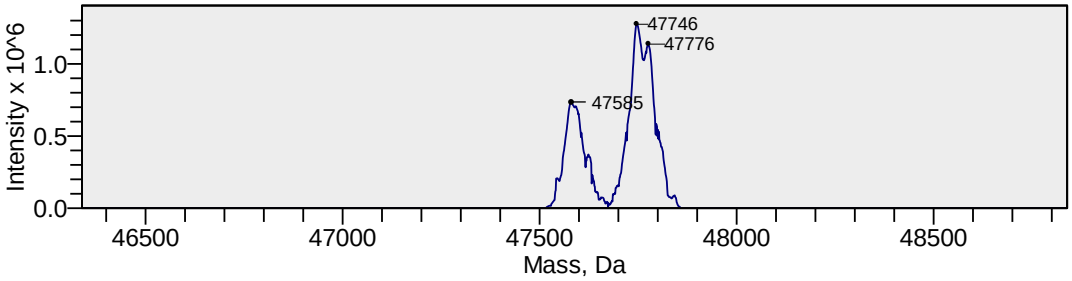

Figure 13 (a) deconvoluted MS data for Fab fragment of Herceptin reacted with dithioaryl(TCEP)pyridazinedione **7** in the presence of dipropyl pyridazinedione **10** (ratio of **7**:**10** = 2:5). (b) Deconvoluted MS data for reduction of Fab fragment of Herceptin and subsequent reaction with dithioaryl(TCEP)pyridazinedione **7** and dipropyl pyridazinedione **10** (1:1 ratio 0.5 eq.:0.5 eq); the three species observed are unmodified Fab, Fab modified with the diethyl species and Fab modified with the dipropyl species at m/z 47565, 47746 and 47776, respectively.

2.2.4 Multi-disulfide system

With the knowledge of the use of dithioaryl(TCEP)pyridazinedione **7** resulting in a high local concentration of the specific pyridazinedione incorporated into the parent scaffold of pyridazinedione **7**, the use of this reagent was appraised in the context of a multi-disulfide system, *i.e.* to apprise if it minimised non-native disulfide re-bridging.

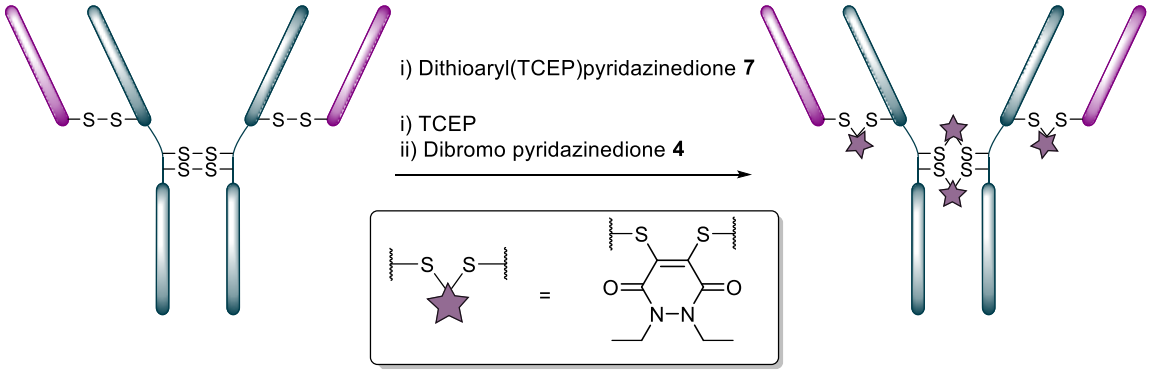

Scheme 26 Reaction of a Herceptin™ full antibody with dithioaryl(TCEP)pyridazinedione **7** was chosen as a way to appraise the utility of the technology, as the modification of full antibodies to produce homogeneous bioconjugates is seen as a significant challenge. Control reactions with conventional pyridazinedione **4** (not containing integrated reducing agent) were also carried out.

To do this, the multi-disulfide system of Herceptin™ was chosen as the model system. Herceptin™ is an antibody comprising four disulfide bonds – whose

disulfide bonds can be re-bridged in a non-native configuration on attempted functional disulfide re-bridging using traditional methods.[111] Although the incidence of non-native disulfide re-bridging can be minimised, the leading strategy is reagent specific.[83] It was rationalised that the use of dithioaryl(TCEP)pyridazinedione **7** would ensure minimisation of non-native disulfide re-bridging in a general sense (Scheme 26). To this end, pyridazinediones **4** (with no internal reducing agent function) and **7** (with reducing agent function) were reacted with Herceptin™ under the appropriate reaction conditions, *i.e.* reaction with dithioarylpyridazinedione **4** required pre-reduction of Herceptin™ with TCEP. Gratifyingly, no non-native disulfide re-bridging was observed by SDS-PAGE for reagent **7**, with complete re-bridging of all disulfides confirmed by UV-Vis (Figure 14, lane 4). Analogous reagent **4**, with no inherent reducing capability, afforded an appreciable amount of non-natively re-bridged product (Figure 14, lane 2). Even when dithioarylpyridazinedione **4** was used in excess and TCEP was added in small portions multiple times (6 × 0.33 eq. per disulfide every 30 mins), *i.e.* to minimise the number of open disulfides at any given time, non-native re-bridging was still observed (Figure 14, lane 3). Although the degree of non-native re-bridging was far less pronounced, the reaction protocol is highly cumbersome and inefficient. Reaction of dithiopyridazinedione **4** at 37 °C also afforded a mixture of products (Figure 14, lane 5). Furthermore, reaction of dibromopyridazinedione **3** at 4 °C and 37 °C also afforded a mixture of correctly and incorrectly re-bridged modified Herceptin™ conjugates. All re-bridged samples analysed by SDS-PAGE were subjected to pre-incubation with TCEP, thereby ensuring that any non-re-bridged interchain disulfides would be shown through fragmentation. An example of a fully reduced mAb is shown in Figure S61.

*SDS-Page gel of Herceptin™ and use of pyridazinediones **4** & **7**:*

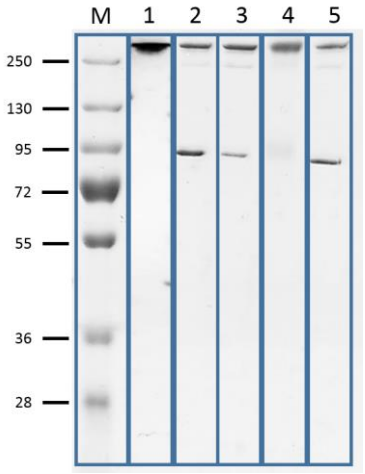

M) Molecular weight marker. 1) Untreated Herceptin. 2) *In situ* reduction of Herceptin mAb and reaction with pyridazinedione **4** at 4 °C (25 eq.). 3) Portion-wise *in situ* reduction of Herceptin mAb and reaction with pyridazinedione **4** at 4 °C (25 eq.). 4) Reaction of Herceptin mAb with pyridazinedione **7** at 4 °C (8 eq.). 5) *In situ* reduction of Herceptin mAb and reaction with pyridazinedione **4** at 37 °C (25 eq.)

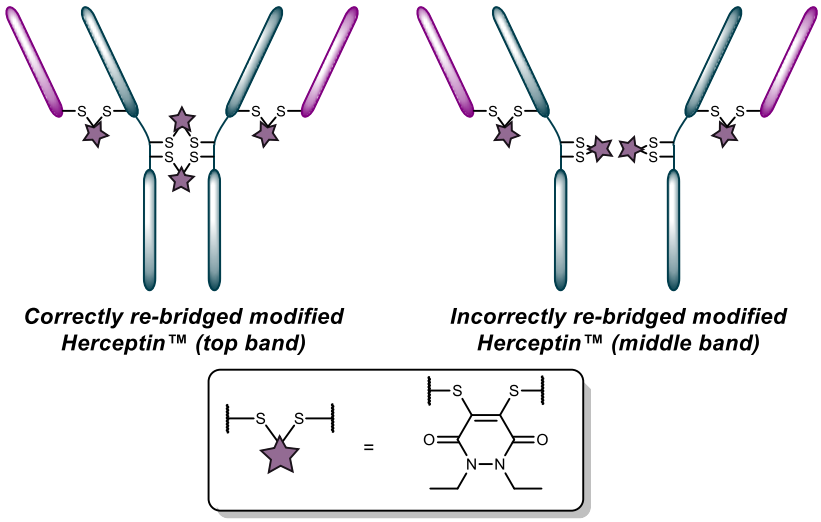

Correctly re-bridged modified Herceptin™ (top band)

Incorrectly re-bridged modified Herceptin™ (middle band)

Figure 14 Appraisal of the use of pyridazinediones **4** *(in situ 4°C (pre-reduced, portion-wise reduction), 37 °C)* and **7** for functional re-bridging of Herceptin™ (lane 4).

Providing a reagent that can functionally re-bridge the disulfide bonds of Herceptin™ without non-native disulfide re-bridging is a major contribution in view of the desire to create homogenous conjugates in the field of antibody–drug conjugates.[11] Use of Herceptin™, in view of its clinical validation alone and as the antibody component of FDA-approved ADC Kadcyla™,[114, 115] provides direct applicability of the chemistry to this exciting area of targeted therapy.

2.2.5 Extension of technology to incorporate a "click" handle

To make this approach modular and expand its scope, an analogue of pyridazinedione **7** was synthesised, which contained an alkyne handle for further

chemical functionalisation, *i.e.* alkyne-pyridazinedione **15.** The alkyne group enables further chemical modification through the use of CuAAC 'click' chemistry.

2.2.5.1 Synthesis of alkyne-bearing dithioaryl(TCEP)pyridazinedione analogue 15

For the synthesis of an alkyne-bearing analogue of dithioaryl(TCEP)pyridazinedione, an analogous route to that described for dithioaryl(TCEP)pyridazinedione **7** was followed, with the exception of the use of asymmetric *N*-substituents on the pyridazinedione core. Initially, mono-alkylation was carried out by treating a large excess of di-*tert*-butyl hydrazine-1,2-dicarboxylate **1** with caesium carbonate and bromoethane in DMF at 21 °C for 18 h to give di-*tert*-butyl 1-ethylhydrazine-1,2-dicarboxylate **11** in a 41% yield. The other major product from this reaction is the di-alkylated hydrazine, which is a common feedstock molecule within the Chudasama group and, therefore, is not undesired. Alkylation of the mono-ethyl hydrazine product **11** was achieved through treatment with caesium carbonate and propargyl bromide in DMF at 21 °C for 72 h to give di-*tert*-butyl 1-ethyl-2-(prop-2-yn-1-yl)hydrazine-1,2-dicarboxylate **12** in a 35% yield (Scheme 27). This yield was lower than desired; the reaction had only reached 35% conversion even after 3 days, this is likely due to the poor nucleophilicity of the remaining non-alkylated nitrogen.

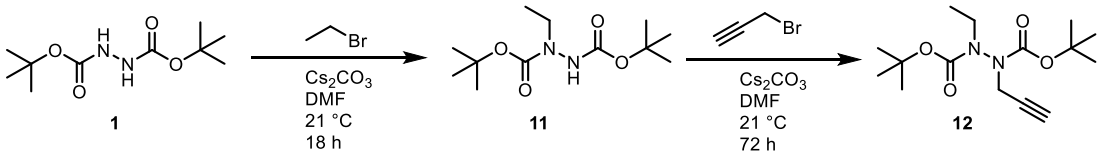

Scheme 27 Two separate alkylations were performed on di-Boc hydrazine to create alkyne-bearing Boc protected hydrazine **12**.

The pyridazinedione formation (Scheme 28), involving TFA cleavage of the Boc groups of dipropylhydrazine **12**, followed by reaction with dibromomaleic anhydride under reflux in AcOH afforded dipropyl dibromopyridazinedione **13** in an overall yield of 43%.

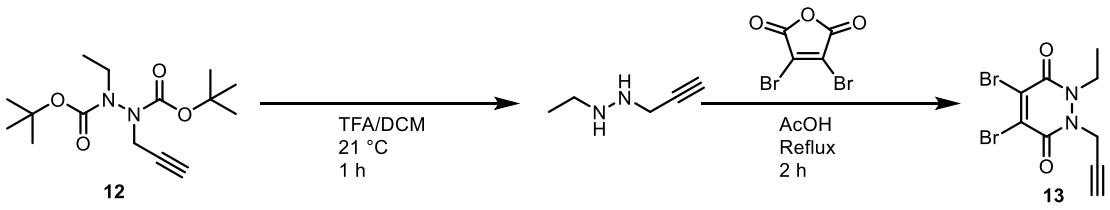

Scheme 28 Hydrazine **12** was treated first with TFA for deprotection followed by reflux with dibromomaleic anhydride to give alkyne-bearing dibromopyridazinedione **13**.

The alkyne-bearing dibromopyridazinedione product **13** was subsequently treated with 4-aminothiophenol with triethylamine in DCM at 21 °C to give alkyne-bearing thioarylpyridazinedione **14** in a 95% yield (scheme 29).

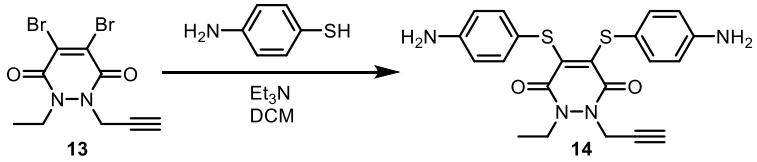

Scheme 29 Dibromopyridazinedione **13** was treated with 4-aminothiophenol and triethylamine in DCM to give alkyne-bearing dithioarylpyridazinedione **14**.

Finally, amide coupling to dimethyl-esterified TCEP analogue **6** was carried out through treatment with HATU and triethylamine in DMF at 21 °C for 12 h to give the alkyne-bearing dithioaryl(TCEP)pyridazinedione **15** in a 32% yield (scheme 30).

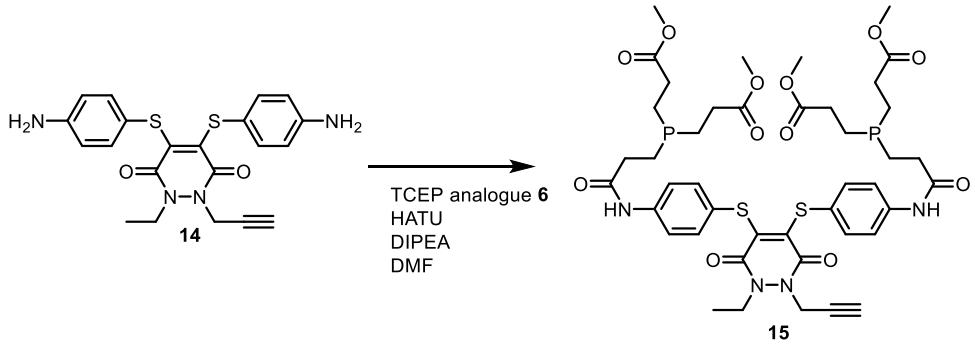

Scheme 30 Final alkyne-bearing analogue 15 was created through amide coupling of TCEP analogue **6** to pyridazinedione **14**.

2.2.5.2 Application to Herceptin™

The appraisal of this molecule was carried on the Fab fragment of Herceptin™ as this would allow extensive analysis by UV-Vis, MS, SDS-PAGE and ELISA (for binding). The optimised conditions for the insertion of

dithioaryl(TCEP)pyridazinedione **7**, were applied to the alkyne bearing analogue **15** for the functional re-bridging of the Fab of Herceptin™ to form conjugate **16**. The efficiency of reduction and re-bridging was translated cleanly from reagent **7** to alkyne analogue **15**.

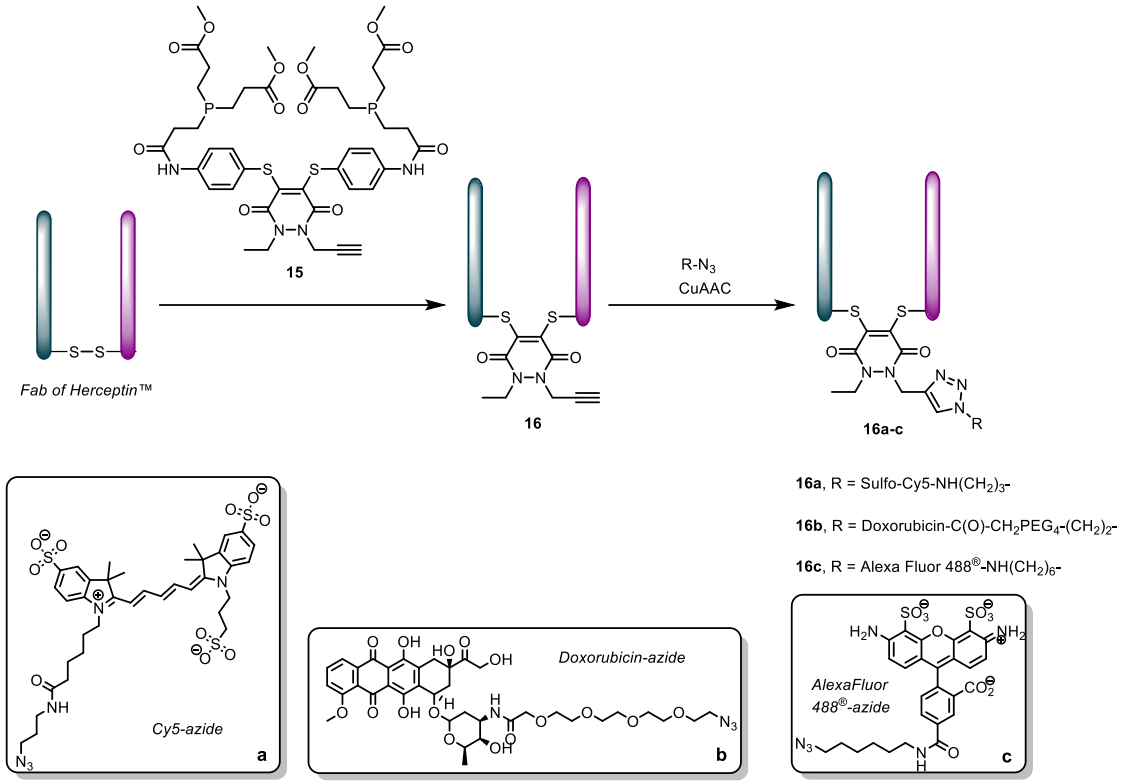

Scheme 31 Application of alkyne bearing pyridazinedione **15** for disulfide reduction and re-bridging as well as "click" functionalisation of the product with various azides to form bioconjugates **16a-c**.

Finally, conjugate **16** was functionalised by "click" modification using doxorubicin, AlexaFluor488™ and sulfo-cyanine5 azides (see Scheme 31); three biologically relevant functional moieties. In all cases, complete conversion was observed to afford functionalised conjugates **16a-c**, thus demonstrating how the platform may be used for efficient introduction of functional modalities as well as reduction and re-bridging. The "click" reactions were carried out in BBS with copper (II) sulfate, tris(3-hydroxypropyltriazolylmethyl)amine (THPTA) and sodium ascorbate for

1.5 h at 21 °C. Samples were analysed by LC-MS, showing only one species in each case (figure 15).

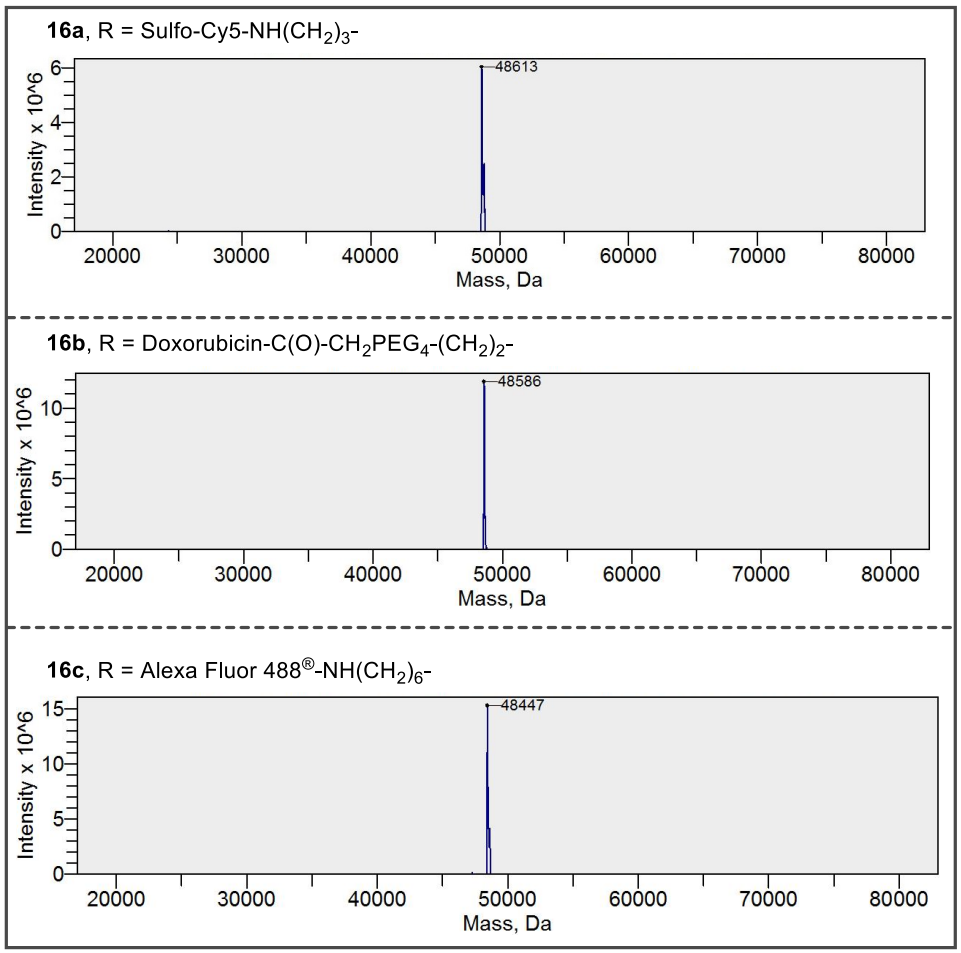

Figure 15 Deconvoluted MS data for "click" functionalised conjugates **16a-c**.

Finally, pyridazinedione **15** was also used to re-bridge Herceptin™ mAb under the same conditions as those used for pyridazinedione **7**. The compound was shown to successfully re-bridge the full antibody system and was amenable to further "click" functionalisation with doxorubicin azide to create a homogeneous ADC (Scheme 32). The creation of homogeneous ADCs from native antibody scaffolds was a significant achievement and a hitherto unmet need in the field. Such technology opens the ability to readily functionalise multi-disulfide containing

systems to groups and researchers, for whom custom protein expression or antibody engineering is too expensive or impractical.

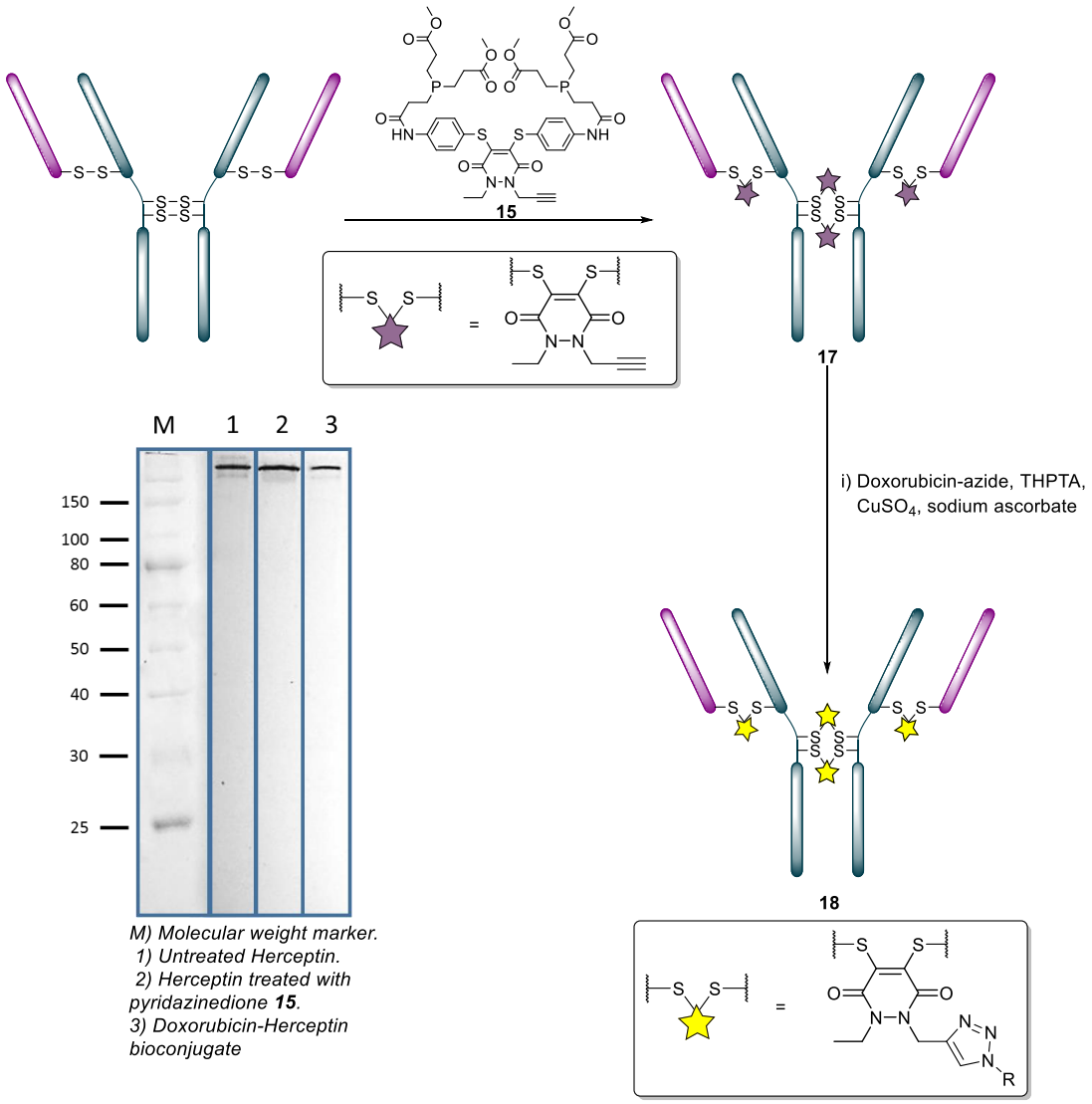

Scheme 32 Incubation with pyridazinedione **15** to give alkyne-bearing bioconjugate, **17**, followed by further chemical modification *via* a CuAAC reaction to give doxorubicin-bearing ADC **18.**

2.2.6 Activity of bioconjugates

It was important that the bioconjugates obtained through reaction with pyridazinedione **15** retained the binding activity offered by their native counterparts, as it is indicative of how the bioconjugates could perform as therapeutics. The Herceptin™ fab fragment (**16a-c**) (Figure 16) and full antibody (**18**) (Figure 17) bioconjugates were all submitted to analysis by enzyme linked immunosorbent assay (ELISA). ELISA is a biochemical assay used to measure the

strength with which a protein, typically an antibody, binds to a complementary fragment (or antigen) (a fully detailed protocol is given in Chapter 5: Experimental). For all modified Fab fragments (bioconjugates 16a-c) and the modified mAb (bioconjugate 18), no loss in activity was observed, *i.*e. the curves generated for the tested conjugates closely fit those of the native analogues, therefore indicating that, relative to the native proteins, no binding activity has been lost.

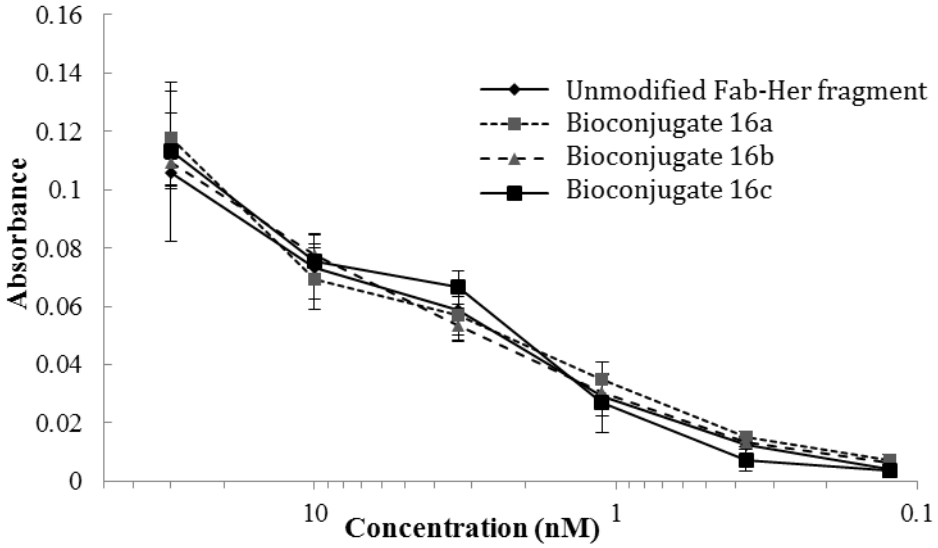

Figure 16 Binding activity of Fab-Her bioconjugates **16a**, **16b** and **16c** against untreated Fab fragment of Herceptin™.

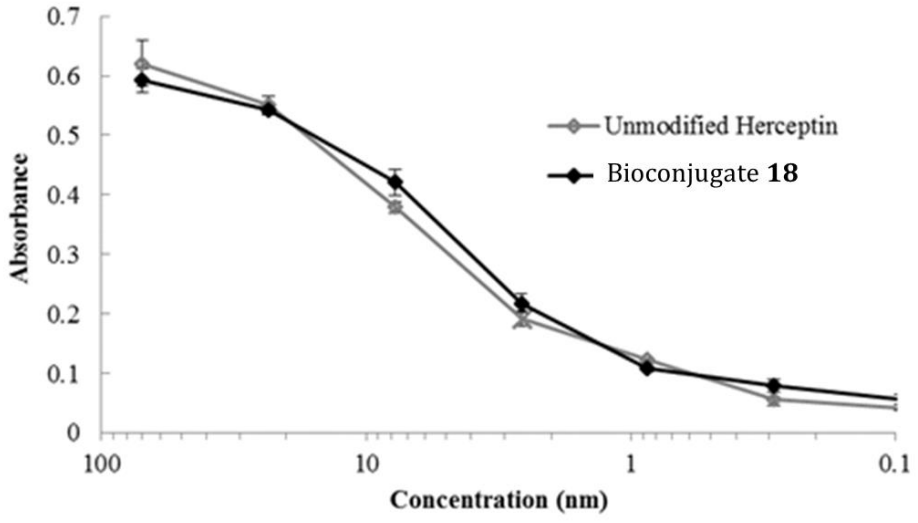

Figure 17 Binding activity of bioconjugate **18** against native unmodified Herceptin™.

2.3 Conclusion

In conclusion, an important step towards delivering on next-generation functional disulfide re-bridging has been demonstrated. This technology allows for reduction and functional re-bridging by the use of a single reagent. The technology was demonstrated on a series of single disuflide bearing systems. Furthermore, this strategy has been shown to result in a high local concentration of bridging agent, which has been exploited for the functional re-bridging of a multi-disulfide system (*i.e.* Herceptin™) whilst retaining native disulfide configuration. Finally, facile "click" functionalisation and retention of binding affinity, using our strategy, has been demonstrated on a full antibody Herceptin™ and its Fab fragment. This has resulted in the construction of a DAR 4 ADC from a native antibody scaffold, a hitherto unmet need.

Chapter 3: Controlled loadings on native mAb scaffolds

Whilst a large number of reagents and strategies have been developed to create new ADCs, novel approaches for site-specific conjugation continue to attract considerable interest.[48, 72] This is especially important as it is coming to light that specific requirements are essential for each particular ADC to operate at its optimum. Specifically, much attention has been given to the generation of ADCs with controlled drug loadings due to the varied physical properties of payloads requiring different degrees of drug loading. Whilst engineered antibodies have worked well in meeting the demand for these tailor-made antibody conjugates, *e.g.* by using engineered cysteine residues, UAAs, selenocysteine or enzymatic conjugation, there is a requirement for methods that are based on native antibody modification (*vide supra,* section 1.3).[48] This is to ensure that technologies to make these "designer" ADCs are more accessible and cost-effective; engineered approaches often require significant optimisation on each antibody scaffold they are applied to, as well as not being accessible to a broad range of scientists.

It has recently come to light that in various tailor-made ADCs, one of the most desirable ratios of drugs to antibody is two. The reason for this is that for certain hydrophobic drugs, a loading of two is preferable as it provides a good balance between efficacy and pharmacokinetic profile (higher payload loading tends to result in a too rapid clearance and lower loadings reduce efficacy). This is an issue that has been especially prominent in the construction of pyrrolobenzodiazepine–protein conjugates. Pyrrolobenzodiazepines (PBDs) are a class of compound containing a substituted aromatic A-ring, a diazepine B-ring and a pyrrolidine C-ring, with a chiral centre at the carbon connecting the B and C rings (Figure 18). Overall this grants PBDs the ideal 3-dimesional shape to fit within the DNA minor groove, making them well suited for use as anti-tumour agents. Moreover, the PBD motif typically features an electrophilic imine (N10-C11) which reacts preferentially with the C2-NH_2 group on the nucleotide base guanine. This feature was exploited to create DNA cross-linking agents by constructing PBD dimers that would feature two of the alkylating imine moieties capable of producing both inter-strand and intra-strand cross-links in addition to mono-alkylated products

(figure 19). Due to the greater variety of possible adducts and better adduct stability, PBD dimers typically offer greater cytotoxicity than their monomer counterparts.[116, 117]

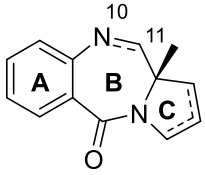

Figure 18 The core template of PBD drugs, the alkylating capability is offered by the electrophilic imine between N10-C11.

Due to the significant cytotoxicity of PBD dimers, they have seen use as payloads in ADCs. Seattle Genetics have two PBD dimer-based ADCs in early and late stage clinical development; SGN-CD33A and SGN-CD70A (in Phase I and Phase III clinical trials, respectively). Both of which have a targeted DAR of 2 (average 1.9), which has been shown to be optimal for providing the best balance between efficacy and pharmacokinetic profile.[118, 119] Higher loadings of the drug, while synthetically feasible, produce conjugates with undesirable physicochemical properties due to the high hydrophobicity and large size of the PBD dimers, in spite of attempts to offset this through the use of solubilising groups as linkers *e.g.* PEG chains. For both SGN-CD33A and SGN-CD70A a DAR 2 is achieved through the use of two serine-to-cysteine point mutations on the heavy chains (one on each chain) to give two free solvent-accessible thiols that can attack PBD dimer maleimide-based linkers.

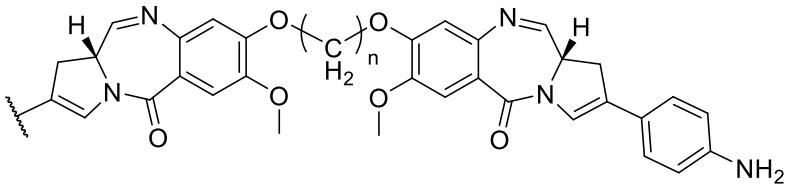

Figure 19 Example of PBD dimer, featuring two electrophilic imines; increased ability to cross link DNA strands comes at the cost of larger hydrophobic surface area.

Whilst the challenge of producing lower loadings of hydrophobic drug conjugates has been addressed to some extent through the use of the above methods and similar antibody engineering strategies in the field *e.g.* THIOMABS™, they are not

readily accessible and there are issues associated with the methodology (*e.g.* potential for non-native disulfide re-bridging and the inefficiency of having to reduce, carefully re-oxidise and then conjugate).[48, 98, 120, 121] Thus, there is a need for a reliable method of constructing antibody conjugates with a loading of two entities starting from a native antibody construct. This is especially in the context of: (i) the rapid progression in the development of further hydrophobic drugs being used and developed in the field;[117, 118, 122-125] and (ii) the major attempts on native antibodies (*i.e.* based on the selective reduction of the Fab or hinge disulfides of an IgG1)[111, 126, 127] proving to lack broad applicability, as evidenced by the lack of uptake in the field, or having to employ harsh oxidation conditions or enzymes under highly specific conditions.

3.1 A reagent that enables a controlled loading of two entities per mAb

While much progress has been made in the synthesis of DAR 4 ADCs, *i.e.* through the use of the integrated reduction-enabled PDs (*vide supra,* section 2.0), dibromomaleimides and other methods (*vide supra,* section 1.2), the construction of DAR 2 conjugates from native antibody scaffolds remains a hitherto unmet need. Given their recent successes in functional disulfide re-bridging of mAbs,[48, 75, 82, 83] DiBrPDs were chosen as a platform on which to base a technology that could enable the controlled assembly of a DAR 2 ADC. It was envisaged that conjugation of two bis-DiBrPDs (each containing a single functional modality) with an appropriate linker length could "tie up" two pairs of the four disulfides on

an IgG1 to allow the formation of a conjugate with an overall loading of two functional modules (Figure 20).

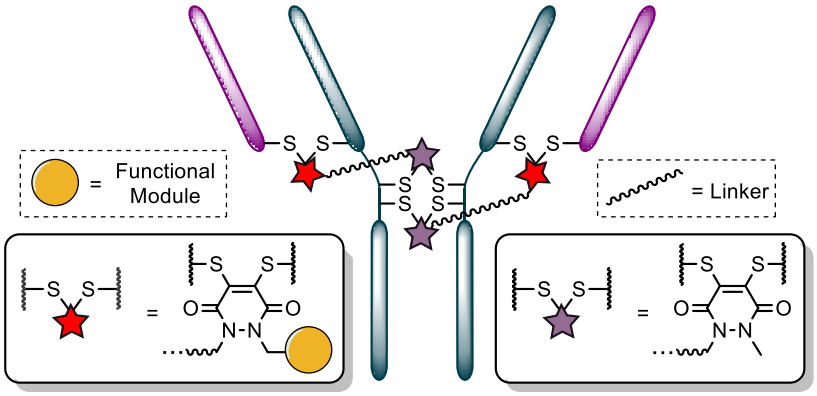

Figure 20 The envisaged molecule would feature four cysteine-reactive centres and one functional handle; thereby, upon introduction to a reduced mAb, each molecule would 'tie-up' two disulfide bonds. A flexible tether was essential to ensure mAb would not be conformationally constricted.

3.2 Results and discussion

The study commenced with the design and synthesis of an appropriately spaced bis-dibromopyridazinedione, bis-diBrPD **19**. Given the aim to react a pair of disulfides using bis-diBrPD **19** it was rationalised from the outset that the linker length would be key. If too short, the bis-PD could not react with a pair of disulfides as it could not span the appropriate length; too long and it would increase the likelihood of undesirable intermolecular reaction(s) by losing the high local concentration effect – thus resulting in inefficient bridging of bis-diBrPD **19** across a pair of disulfides. In an effort to avoid these issues a linker was designed based

on the spacing of the disulfides on an IgG1 for which a crystal structure has been obtained (~16.1 Å = maximum linear distance) (Figure 21).[128]

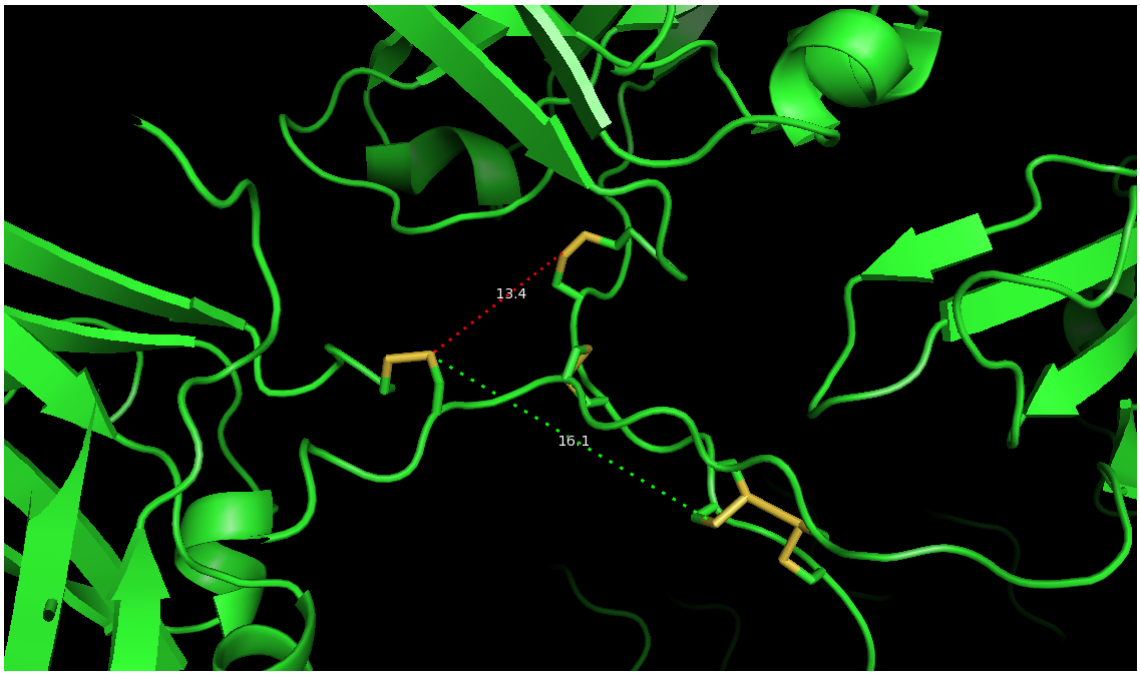

Figure 21 Image of crystal structure for an IgG1 hinge region with inter-Fab (Red - 13.4 Å) disulfide and hinge-Fab (Green - 16.1 Å) disulfide distances highlighted. The bis-DiBrPD was designed to be long and flexible enough to cause minimum hindrance of mAb.

To ensure flexibility, and improve water solubility of the bis-DiBrPD, a PEG spacer was used to link together the PD bioconjugation sites. A single alkyne was installed on the bis-PD scaffold to eventually allow a loading of two modules, through the use of click chemistry, post-conjugation of bis-DiBrPD **19** on a full antibody. The click handle was also positioned by design to be close to a PD-disulfide bridging site to minimise exposure of the clicked entity.[83] The length of the PEG linker was chosen to give the final bis-DiBrPD a maximum linear distance of ~25 Å as this was anticipated to be a suitable separation between the bridging sites when taking

into account the resolution of the measurement,[128] given the flexibility of this region of the antibody, and the PEG chain not being structurally linear (figure 22).

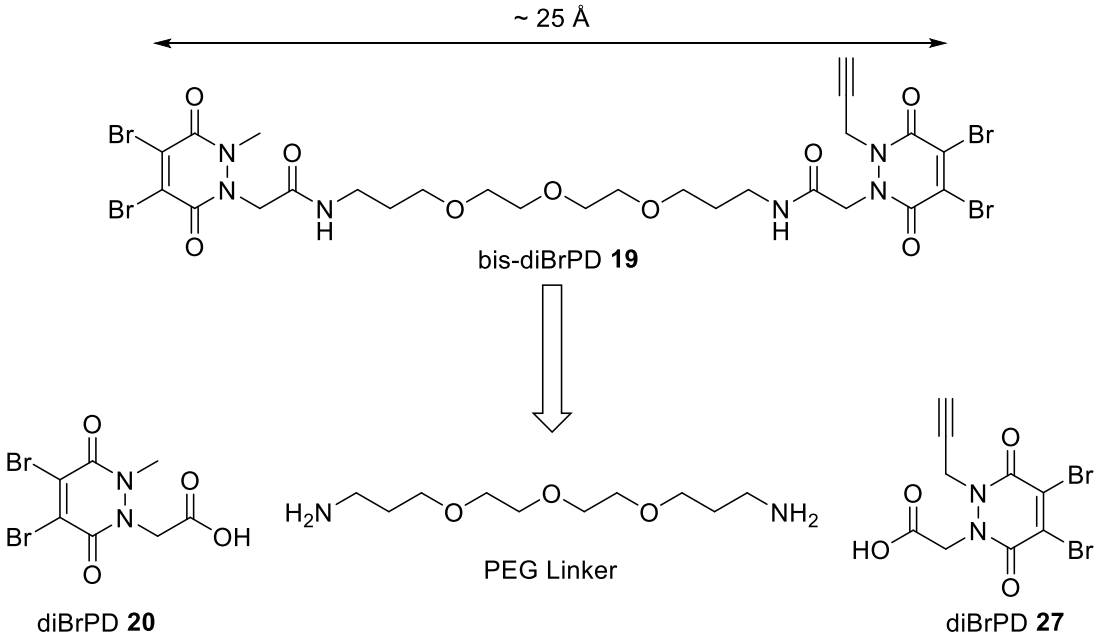

Figure 22 The proposed structure of bis-DiBrPD **19**, which features four cysteine reactive centres on the PD end groups, a flexible PEG linker and a single functional handle (terminal alkyne) – and its substituent components.

3.2.1 Synthesis of bis-DiBrPD

Synthesis of bis-DiBrPD **19** began with assembly of asymmetric DiBrPD **20** using a protocol analogous to those used to synthesise previously mentioned PDs (*vide supra* section 2.1). Methyl hydrazine **21** was reacted with di-*tert*-butyl dicarbonate, triethylamine and 4-(dimethylamino)pyridine in DCM at 20 °C for 72 h to afford tri-*tert*-butyl 2-methylhydrazine-1,1,2-tricarboxylate **22** as a yellow oil in quantitative yield. Selective mono-deprotection of the non-methyl substituted nitrogen was carried out through reaction of tri-*tert*-butyl 2-methylhydrazine-1,1,2-tricarboxylate **22** with magnesium perchlorate in MeCN at

20 °C for 1 h, which yielded di-*tert*-butyl 1-methylhydrazine-1,2-dicarboxylate **23** as a white solid in an 89% yield (scheme 33).[84]

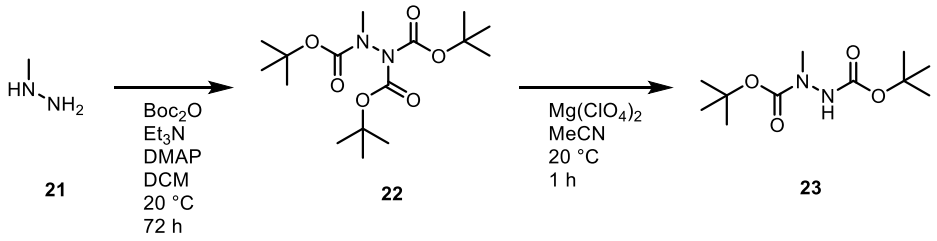

Scheme 33 Methyl hydrazine was prepared for selective alkylation through triple Boc-protection followed by selective removal of one of the Boc groups from the *N*-diBoc nitrogen using magnesium perchlorate.

Di-*tert*-butyl 1-methylhydrazine-1,2-dicarboxylate **23** then underwent an alkylation with *tert*-butyl bromoacetate with caesium carbonate in DMF at 20 °C for 16 h to give di-*tert*-butyl 1-(2-(*tert*-butoxy)-2-oxoethyl)-2-methylhydrazine-1,2-dicarboxylate **24** as a colourless oil in a 98% yield (scheme 34).

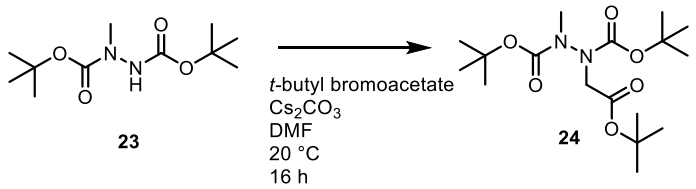

Scheme 34 Alkylation of hydrazine with *tert*-butyl bromoacetate

The PD precursor **24** then underwent Boc-deprotection with TFA in DCM at 20 °C for 2 h. The crude product was then refluxed with dibromomaleic anhydride in acetic acid for 16 h to give 2-(4,5-dibromo-2-methyl-3,6-dioxo-3,6-

dihydropyridazin-1(2*H*)-yl)acetic acid **25** (scheme 35). With DiBrPD **25** in hand synthesis of the second DiBrPD **27** was undertaken.

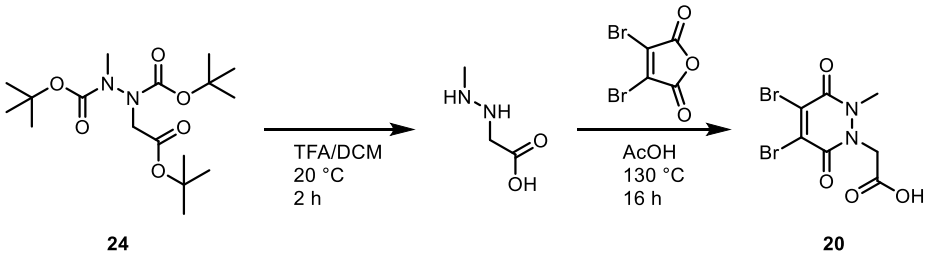

Scheme 35 *N*-Boc and *t*-butyl ester removal with TFA followed by DiBrPD formation with dibromomaleic anhydride

Di-*tert*-butyl hydrazine-1,2-dicarboxylate **1** was alkylated with propargyl bromide and TBAB in a mixture of toluene and aqueous sodium hydroxide at 20 °C for 16 h to afford di-*tert*-butyl-1-(prop-2-yn-1-yl)hydrazine-1,2-dicarboxylate **25** as a white solid in a yield of 83% (scheme 36).[83] This yield was a significant improvement over the yield obtained from the previous mono-alkylation strategy used in the synthesis of the asymmetric dithioaryl(TCEP)pyridazinedione **15** (*vide supra,* Section 2.2.5). The biphasic reaction, adapted from a literature protocol, uses TBAB as a phase transfer catalyst that prevents over alkylation, resulting in a relatively high yield of the desired mono-alkylated hydrazine.[129]

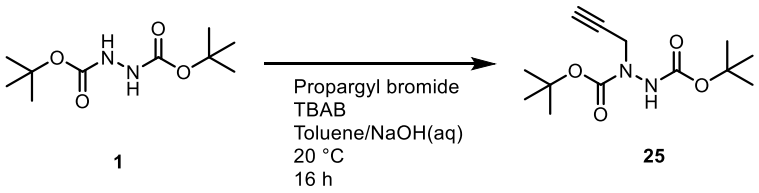

Scheme 36 Selective mono-alkylation of di-Boc hydrazine with propargyl bromide.

The alkyne-bearing hydrazine **25** was then alkylated further with *tert*-butyl bromoacetate and caesium carbonate in DMF at 20 °C for 16 h, which gave di-*tert*-

butyl 1-(2-(*tert*-butoxy)-2-oxoethyl)-2-(prop-2-yn-1-yl)hydrazine-1,2-dicarboxylate **26** as a colourless oil in a 97% yield (Scheme 37).[83]

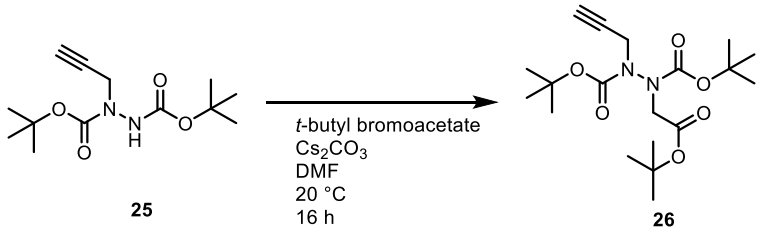

Scheme 37 Alkylation alkyne hydrazine with *tert*-butyl bromoacetate.

The bis-substituted di-Boc hydrazine **26** underwent Boc-deprotection with TFA in DCM followed by reaction with dibromomaleic anhydride under reflux in acetic acid, which afforded the second DiBrPD, 2-(4,5-dibromo-3,6-dioxo-2-(prop-2-yn-1-yl)-2,3-dihydropyridazin-1(6*H*)-yl) acetic acid **27** as a white solid in a 65% yield (Scheme 28).

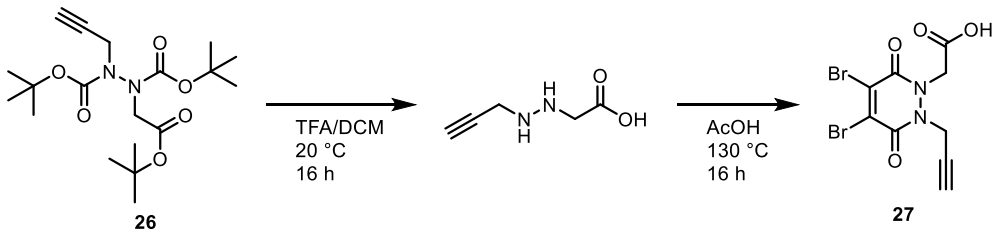

Scheme 28 *N*-Boc and *tert*-butyl ester removal with TFA followed by DiBrPD formation with dibromomaleic anhydride.

The PEG linker that would tether the two DiBrPDs, **20** and **27**, was prepared through dropwise addition of Boc-anhydride in 1,4-dioxane over 2 h to a stirring solution of the bis-amine PEG, 3,3'-((oxybis(ethane-2,1-diyl))bis(oxy))bis(propan-1-amine) in 1,4-dioxane. After a further 30 min at 20°C, the mono-Boc protected product, tert-butyl (3-(2-(2-(3-

aminopropoxy)ethoxy)ethoxy)propyl)carbamate **28**, was given as a colourless oil in a 75% yield (Scheme 39).

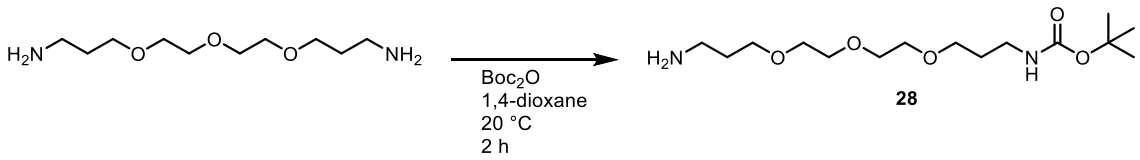

Scheme 39 Mono *N*-Boc protection of bis-amine PEG in dioxane.

To couple the first bis-DiBrPD **20** to PEG linker **28**, the two species were reacted with 1,1'-carbonyldiimidazole (CDI) in DMF at 20 °C for 12 h to afford Boc-protected PEG-DiBrPD **29** as a yellow gum in an 8% yield (scheme 40). Whilst this yield was disappointingly low, the synthesis was continued in interest of expediting the testing of the final product. In future work, a reagent screen of conditions and other carboxylic acid-activating reagents would be desirable.

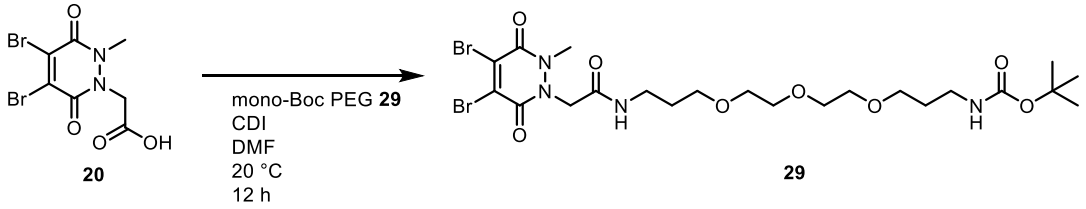

Scheme 40 Amide coupling between DiBrPD **20**, and mono-Boc PEG using CDI to make Boc-PEG-DiBrPD **29**.

The Boc-protected PEG-DiBrPD **29** then underwent deprotection through reaction with TFA in DCM at 21 °C for 30 mins. After removal of all volatiles, the crude deprotected product was taken through to form the second amide bond *via*

reaction with DiBrPD **27** with HATU and DIPEA in DMF at 21°C for 16 h to afford final product, bis-DiBrPD **19** as a yellow gum in a 30% yield (scheme 41).

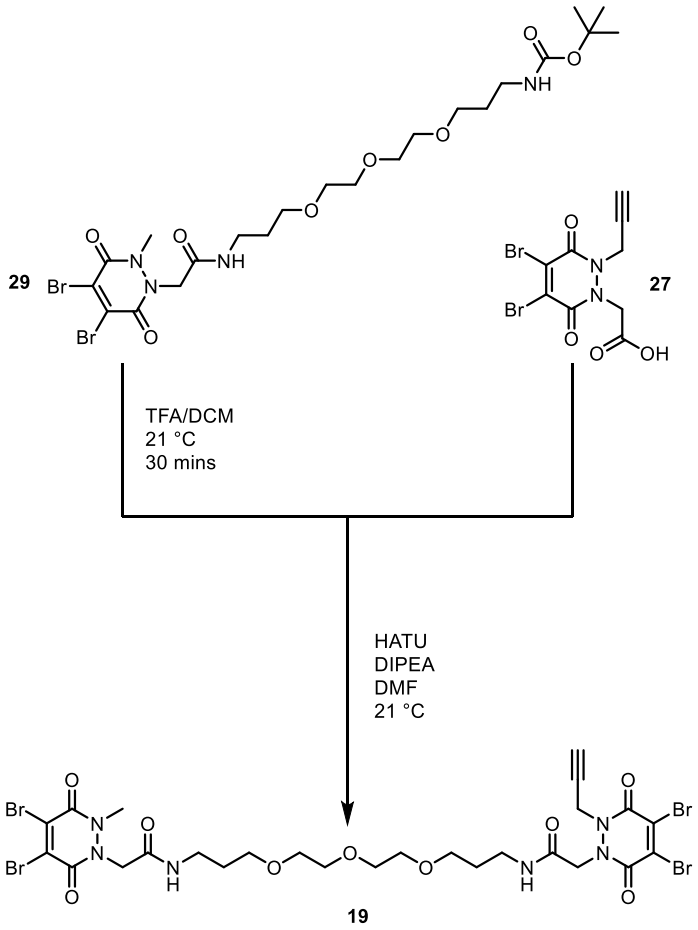

Scheme 41 Deprotection of Boc-PEG-DiBrPD **29**, followed by coupling of crude amine to second DiBrPD **27** with HATU to give final product bis-DiBrPD **19**.

3.2.2 Conjugation of Herceptin™ with bis-DiBrPD 19 and click functionalisation

Following the successful synthesis of DiBrPD **19**, its ability to conjugate a mAb had to be appraised. The clinically relevant IgG1 antibody Herceptin™ was chosen as a platform upon which to assess the technology. Herceptin™ was reduced with TCEP following pre-incubation with bis-DiBrPD **19** in BBS with EDTA at pH 8 for 1 h at 37 °C to give bioconjugate **30** (scheme 42). Gratifyingly, following purification, the sample was analysed *via* UV-vis, SDS-PAGE gel and LC-MS to show a pyridazinedione-to-antibody ratio (PDAR) of 4.0 with complete functional re-bridging confirmed by SDS-PAGE (Figure 23). Further to this conjugate **30** was incubated with excess TCEP, which showed no change in fragmentation profile as assessed by SDS-PAGE, further confirming that all disulfides were re-bridged. This result supported the original hypothesis, as it suggested each bis-diBrPD had re-bridged two disulfides; *i.e.* only such a result could have yielded the observed SDS-PAGE profile and PDAR. Despite the challenges of using mass spectrometry for characterisation of full antibody conjugates,[130] especially for disulfide modified conjugates,[131] mass spectrometry data for conjugate **30** was obtained which further verified two additions of bis-diBrPD **19** to Herceptin™. The observed mass, 146,328 Da (Expected mass: 146,320 Da.) showed addition of two bis-DiBrPD **19** molecules for one mAb (Figure 24). The MS data clearly shows one major species,

representing a single mAb with two bis-PDs conjugated to it; the raw data shows a small amount of half mAb arising from non-native disulfide re-bridging

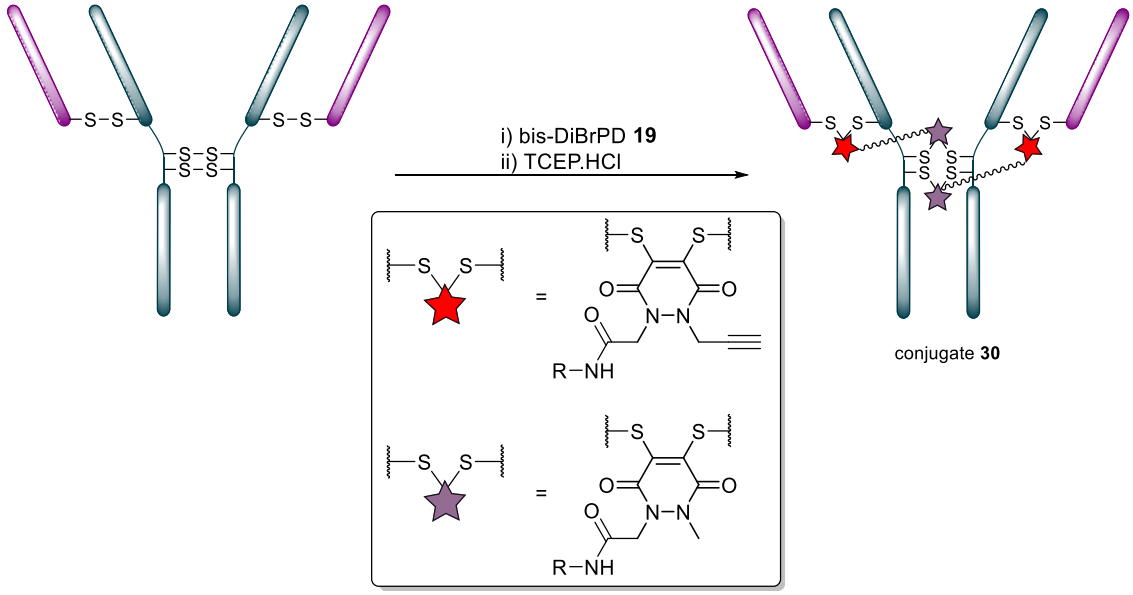

Each pair of red and purple stars per linker molecule are independently interchangeable, and other disulfide pairs (e.g. Fab-Fab, Hinge-Hinge) may be functionally re-bridged.

Scheme 42 Pre-incubation with bis-DiBrPD **19**, followed by reduction with TCEP yielded conjugate **30**, with all four disulfide bonds 'tied-up' with two molecules of bis-DiBrPD **19**, giving a PDAR of 4.0.

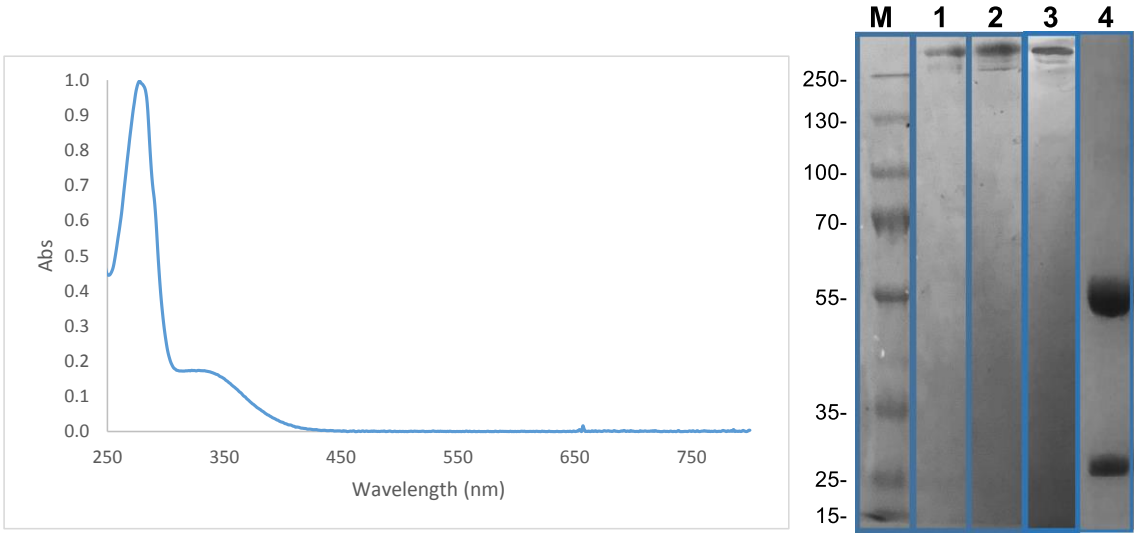

Figure 23 Left) UV-Vis data for conjugate **30**. (Right) SDS-PAGE gel; M.) Molecular weight marker; 1) Unmodified Herceptin™; 2) Conjugate **30**; 3) Conjugate **30** treated with TCEP·HCl; 4) Herceptin™ reduced with TCEP·HCl displaying heavy chain and light chain fragments.

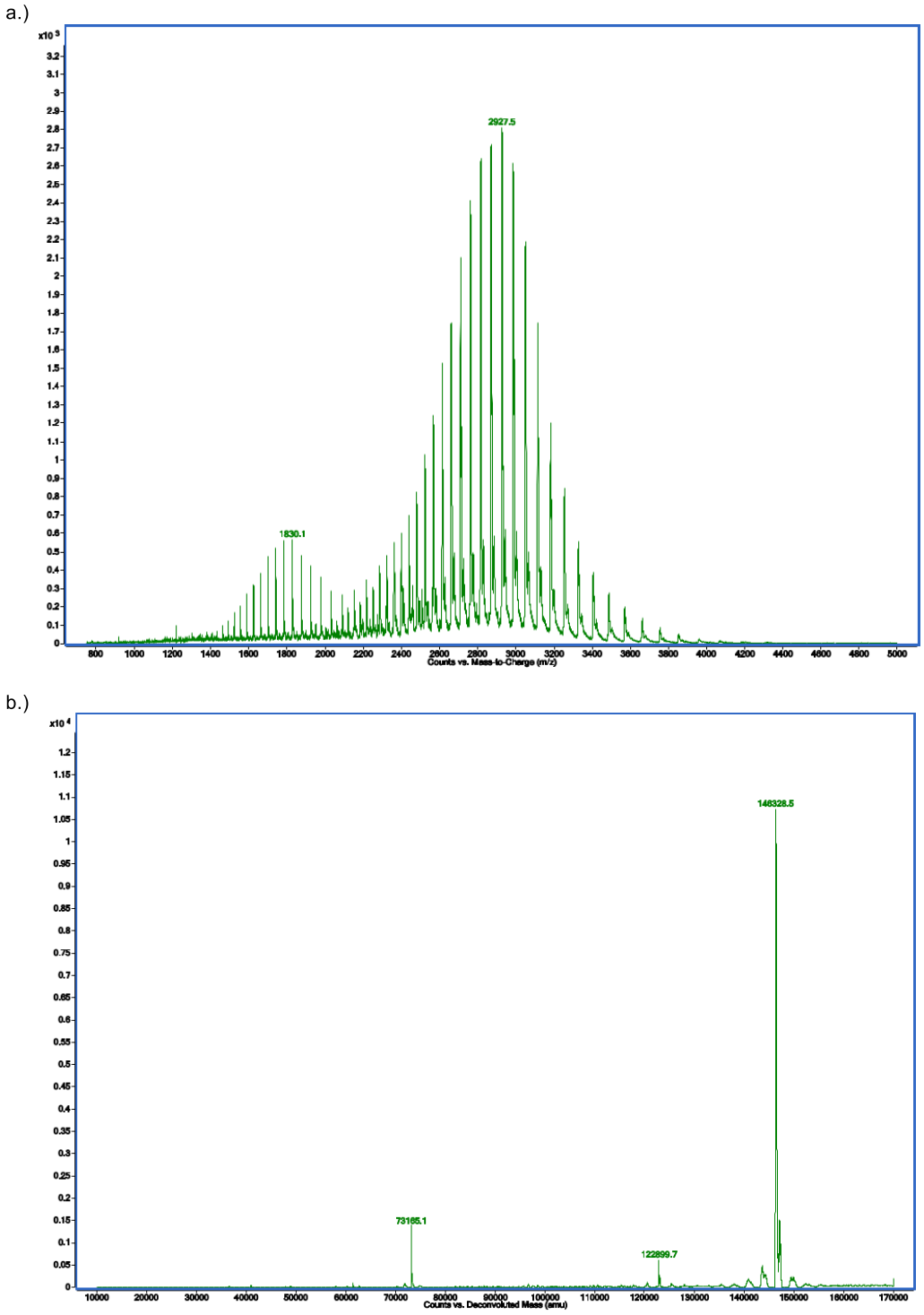

Figure 24 (a) non-deconvoluted and (b) deconvoluted MS data for conjugate **30** (deglycosylated).

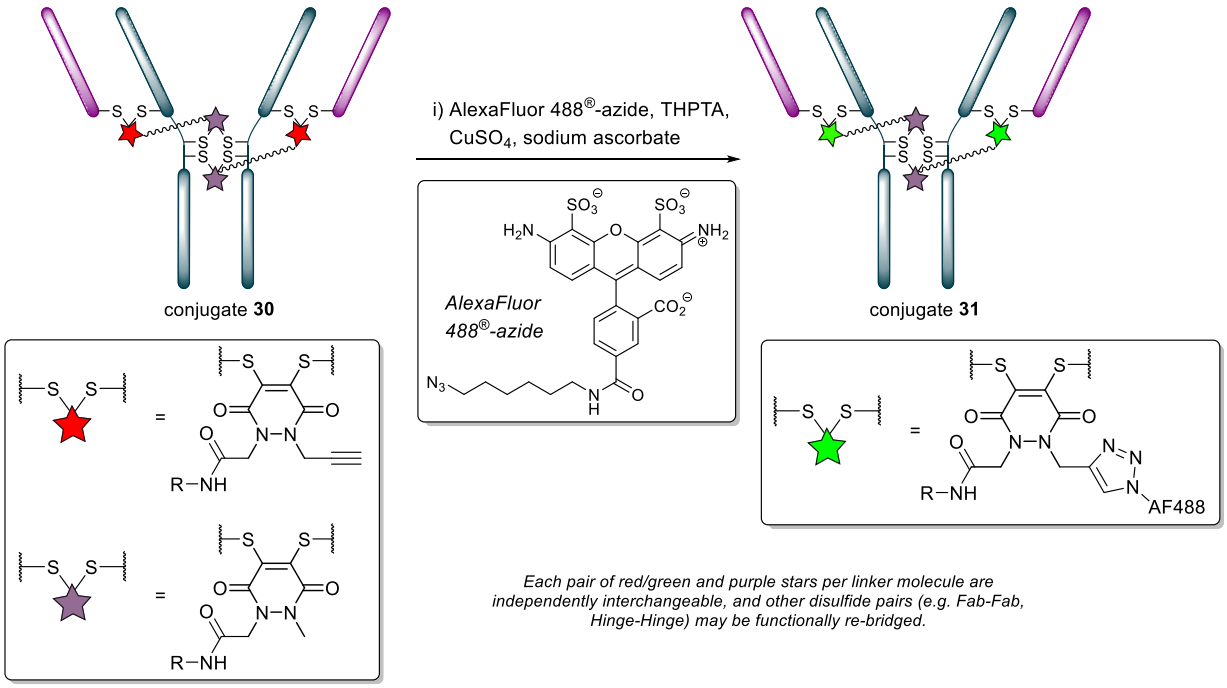

Scheme 43 "Click" functionalisation, *via* CuAAC, of conjugate **30** with AF488 azide to give FAR 2 species conjugate **31**.

As conjugate **30** was in possession of two alkyl alkyne handles it was theorised that a copper click reaction to a fluorophore azide would yield a conjugate with a FAR of 2.0 (Scheme 43). Thus, conjugate **30** was reacted with a large excess (20 eq) of AlexaFluor488™ azide with copper (II) sulfate, THPTA and sodium ascorbate in BBS pH 8 at 21 °C for 1.5 h to afford conjugate **31**, which was characterised by SDS-PAGE and UV-Vis spectroscopy. An excess of azide was used to ensure all pendant alkynes were reacted. Analysis showed the conjugate had a loading (FAR) of 2.0, furthermore the result was highly reproducible (n=7) reporting FAR in the range 1.9-2.1 by UV-Vis spectroscopy (Figure 25). Following

the copper click no degradation of the mAb was observed as monitored by SDS-PAGE.

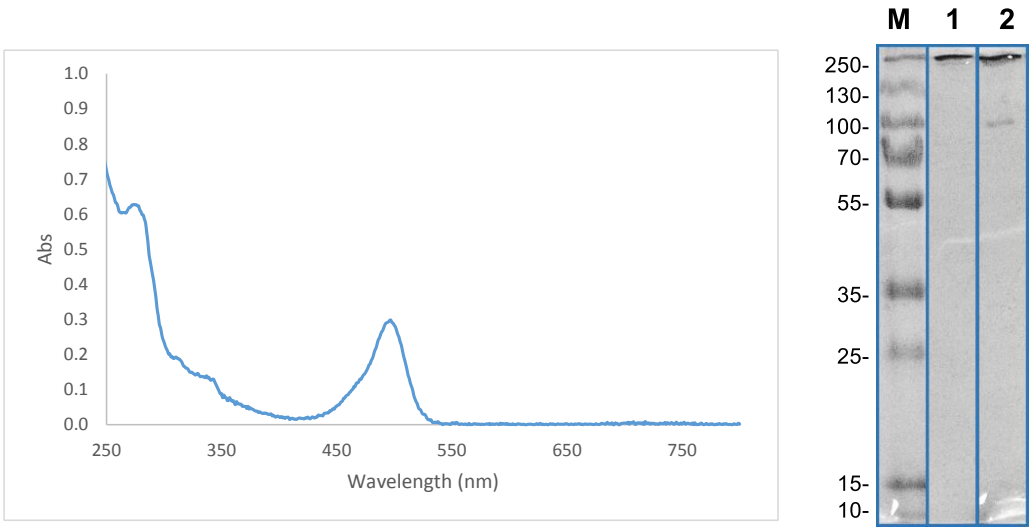

Figure 25 (Left) UV-Vis data for conjugate **31**. (Right) SDS-PAGE gel; M.) Molecular weight marker; 1) Unmodified Herceptin™; 2) Conjugate **31**.

To ensure the binding capability of the antibody remained unperturbed by the conjugation and subsequent click functionalisation, conjugate **31** was submitted to an ELISA study. The conjugate was found to have retained binding capability completely (with respect to the native mAb) (Figure 26a). Finally, as the effectiveness of the platform is dependent on the ability of the resultant conjugates to deliver the payloads selectively to the internal cellular environment of cancer cells, the ability of the conjugates to be internalised also had to be assessed. As such, their internalisation into a HER2 positive cell line was assessed *via* confocal microscopy (Figure 26b). Internalisation can be effectively assessed through incubation of appropriate cells with the conjugates at two different temperatures; 4 °C and 37 °C. At the lower temperature, the conjugates can be seen bound to the cell membrane, incubation at a higher temp allows the receptor-mediated internalisation to take place as it is an active process. If movement of the conjugates from the membrane to the cytoplasm can be observed following incubation at 37 °C, it can be concluded that the activity of the antibody has not been retarded following modification. Gratifyingly, the conjugate was shown to be

internalised rapidly, showing the mechanism of the native mAb had not been negatively affected by the conjugation or click procedures.

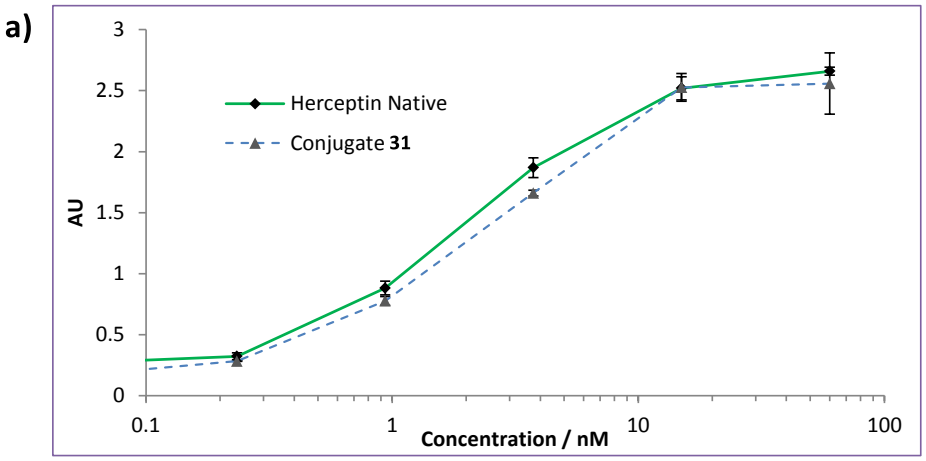

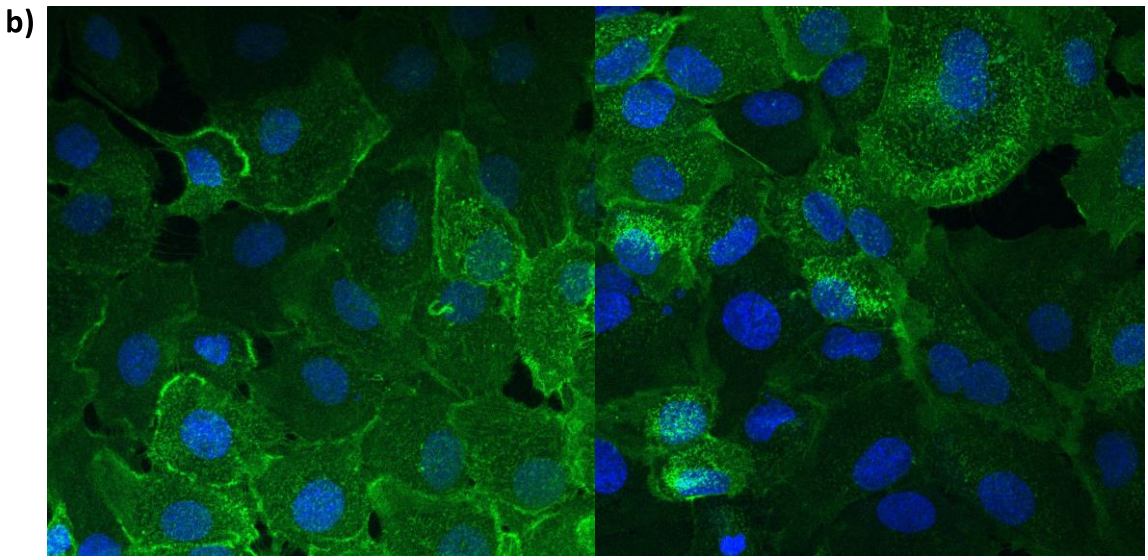

Figure 26 a) ELISA for conjugate **31** against native unmodified Herceptin™ mAb, showing binding affinity was unaffected by conjugation and "click"" functionalisation. b) Internalisation analysis by confocal microscopy – movement of conjugates from membrane to cytoplasm was observed at 37 °C.

Drug conjugation

Given that the intended end purpose of the bis-DiBrPD platform was to enable the synthesis of DAR 2 ADCs, it was prudent to demonstrate the utility of the platform

with a clinically relevant chemotherapy drug. Doxorubicin was chosen at it offered an acceptable balance between toxicity (and associated risk to scientists involved with the project) and relevance; more hydrophobic (and toxic) payloads such as MMAE/PBD dimers would have required use of specialised facilities certified for handling of such materials.

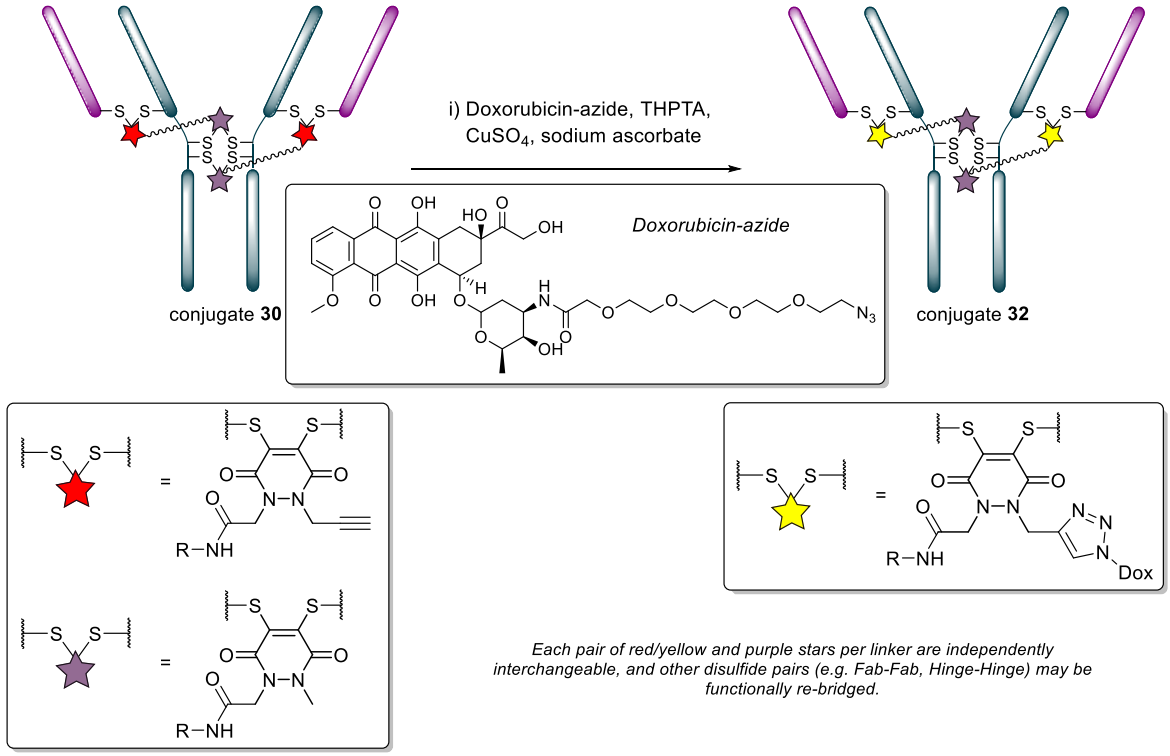

Scheme 44 "Click" functionalisation, *via* CuAAC, of conjugate **30** with doxorubicin azide to give a DAR 2 ADC, conjugate **32**.

The DAR 2 doxorubicin ADC was assembled per the protocol established for conjugate **31**. Following a copper click of doxorubicin azide to conjugate **30**, a Herceptin™ – doxorubicin ADC with a loading of 2.0, conjugate **32**, was achieved

(Scheme 44). The drug loading and re-bridging were assessed by SDS-PAGE gel and UV-Vis spectroscopy (Figure 27).

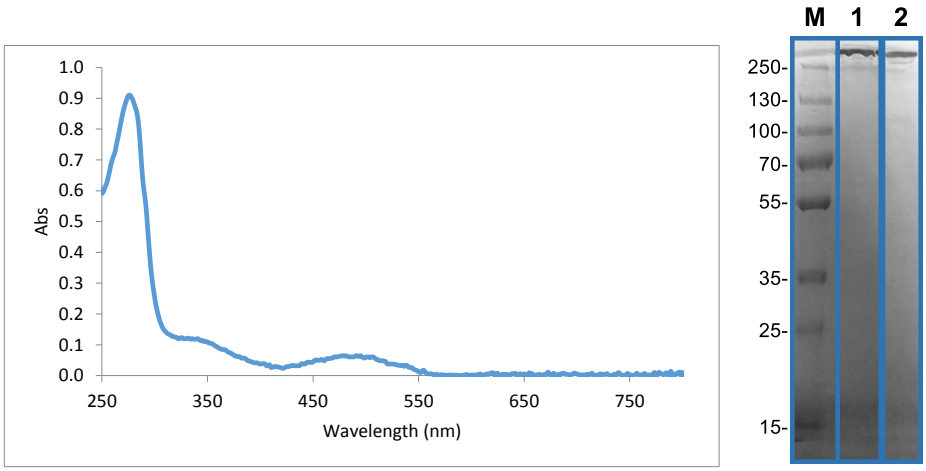

Figure 27 (Left) UV-Vis data for conjugate **32**. (Right) SDS-PAGE gel; M.) Molecular weight marker; 1) Unmodified Herceptin™; 2) conjugate **32**.

3.2.3 Extension of strategy to loadings of four

In order to demonstrate the utility of the bis-DiBrPD platform and expand its utility, it was decided that synthesis of an antibody conjugate with a loading of four would showcase the flexibility of the strategy, *i.e.* for cases when a loading of four moieties is appropriate. This would also serve as further proof of the disulfide pair functional re-bridging hypothesis as well as provide a novel conjugation strategy for making antibody conjugates with a loading of four. To this end, a second bis-DiBrPD was synthesised; while conceptually similar to bis-DiBrPD **19**, the new iteration would feature two functional handles instead of one, *i.e.* once

installed on a mAb scaffold bis-DiBrPD **33** would furnish an antibody with four points of attachment (Figure 28).

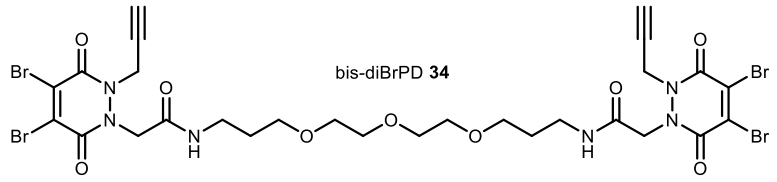

Figure 28 Proposed structure of bis-DiBrPD **34**, designed to conjugate in the same modes as bis-DiBrPD **19** but to feature two functional handles instead of one, enabling synthesis of DAR 4 ADCs.

In light of the success of bis-DiBrPD **19**, both in its ability to successfully re-bridge a Herceptin™ mAb and in that the binding and internalisation ability of the resulting conjugates was undisturbed, bis-DiBrPD **33** was designed to match its properties as closely as possible (Figure 28).

3.2.3.1 Synthesis of bis-DiBrPD 33

Due to the symmetrical nature of bis-DiBrPD **33** the synthesis was technically simpler. DiBrPD **27** was coupled to both ends of bis-amine PEG 3,3'-((oxybis(ethane-2,1-diyl))bis(oxy))bis(propan-1-amine) with DCC in DMF at 21 °C for 12 h giving bis-DiBrPD **33** as a yellow gum in an 18% yield (scheme 45).

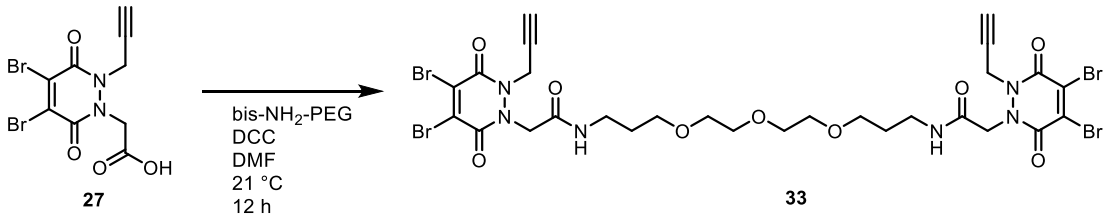

Scheme 45 Preparation of bis-DiBrPD **33** *via* amide coupling of DiBrPD **27** to both ends of bis-amine PEG with DCC.

3.2.3.2 Conjugation to Herceptin and subsequent click functionalisation

Conjugation to Herceptin was performed under analogous conditions for conjugate **30**. Herceptin™ was reduced with TCEP following pre-incubation with bis-DiBrPD **33** in BBS with EDTA at pH 8 for 1 h at 37 °C to give conjugate **34**

(Scheme 46). Following purification, the sample was analysed *via* UV-Vis and SDS-PAGE gel to show a PDAR of 3.9 with complete functional re-bridging (Figure 29).

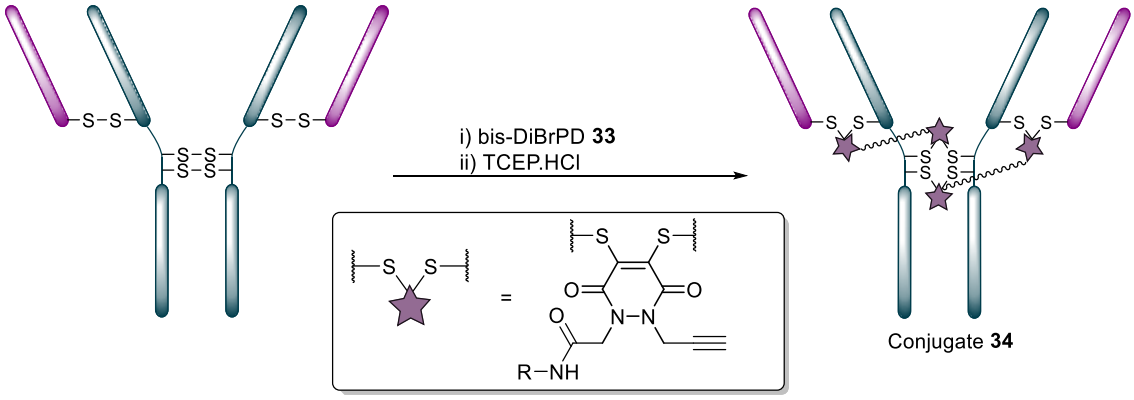

Scheme 46 Pre-incubation with bis-DiBrPD **33**, followed by reduction with TCEP yielded conjugate **34**, with all four disulfide bonds 'tied-up' with two molecules of bis-DiBrPD **33**, giving a PDAR of 4.0.

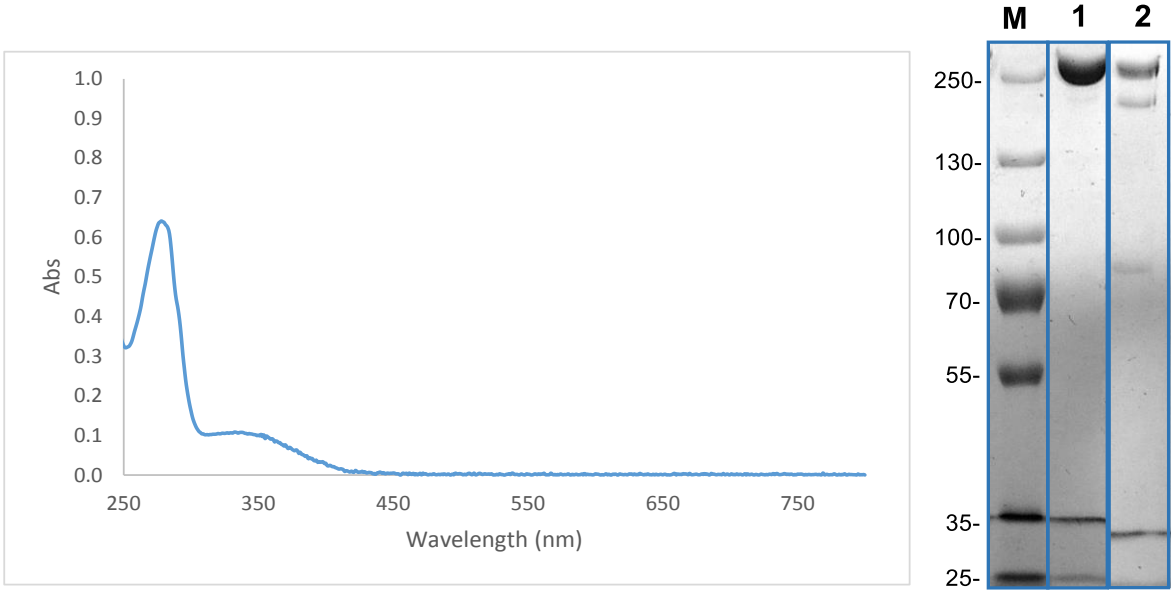

Figure 29 (Left) UV-Vis data for conjugate **34**. (Right) SDS-PAGE gel; M) Molecular weight marker; 1) Untreated Herceptin™; 2) conjugate **34**. Artefact in SDS-PAGE gel observed in both samples (*ca.* 35 kDa).

As conjugate **34** was in possession of four alkyl alkyne handles, it was theorised that a copper click reaction to a fluorophore azide would yield a conjugate with an FAR of 4.0. Thus, conjugate **34** was reacted with a large excess (40 eq) of AlexaFluor488™ azide with copper (II) sulfate, THPTA and sodium ascorbate in BBS pH 8 at 21 °C for 1.5 h to afford conjugate **35** (Scheme 47), which was

characterised by SDS-PAGE and UV-Vis spectroscopy (Figure 30). An excess of azide was used again to ensure all pendant alkynes were reacted. Analysis showed the conjugate had a loading (FAR) of 4.0. Following the copper click no degradation of the mAb was observed as monitored by SDS-PAGE.

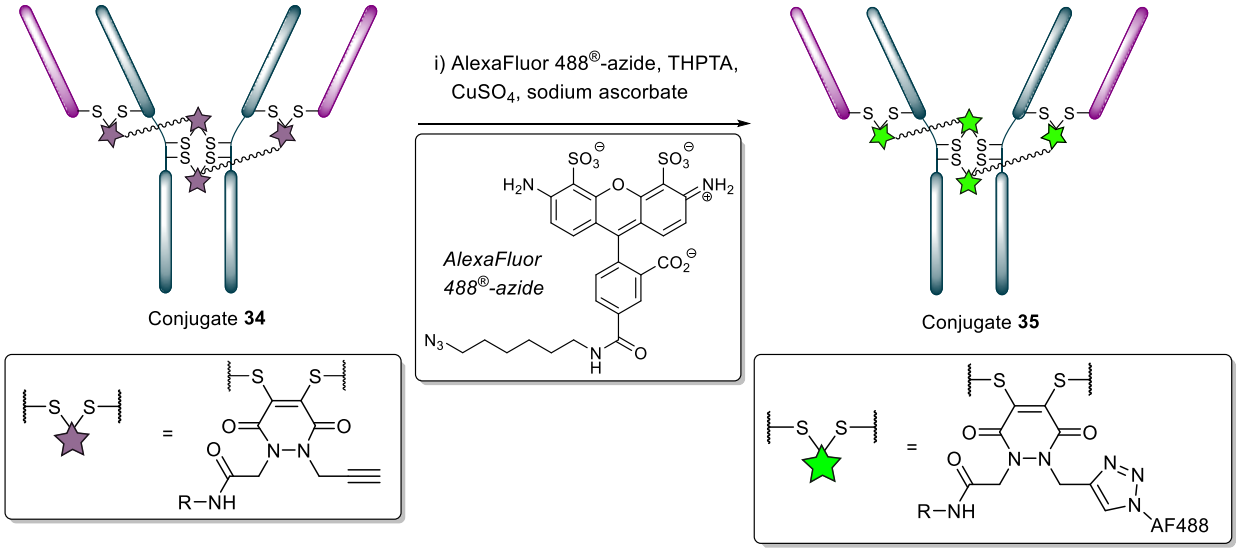

Scheme **47** "Click" functionalisation, *via* CuAAC, of conjugate **34** with AlexaFluor488™ azide to give a FAR 4 species, conjugate **35**.

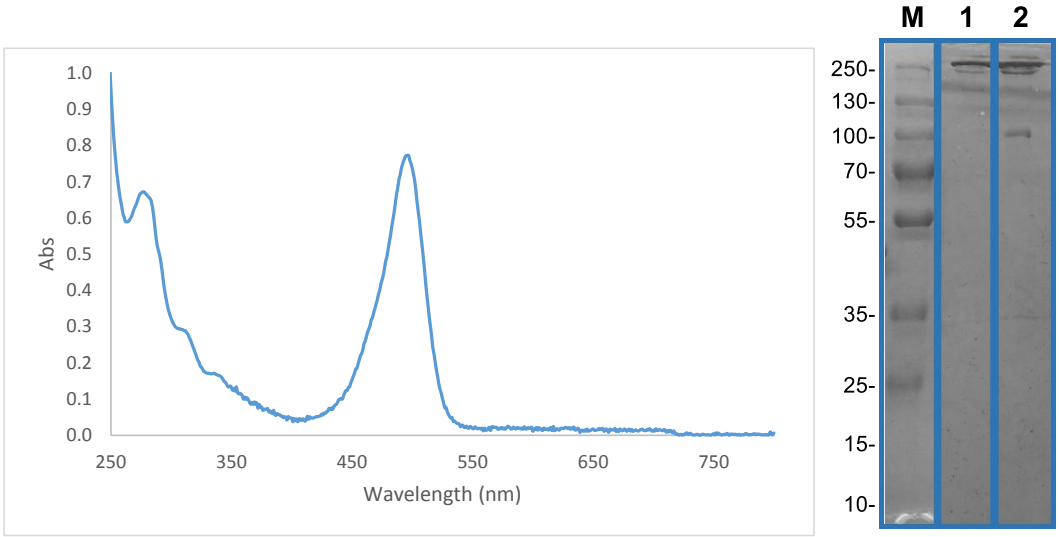

Figure 30 (Left) UV-Vis data for conjugate **35** modified with AF488-azide. (Right) SDS-PAGE gel; M) Molecular weight marker; 1) Unmodified Herceptin™; 2) Conjugate **35**.

Finally, to assess that the higher loading of fluorophores had not disturbed the activity of the mAb scaffold, conjugate **35** was submitted to ELISA study and its internalisation assessed as per conjugate **31** (Figure 31). Gratifyingly, both the

conjugates binding capability and internalisation were unaffected by the functionalisation procedure.

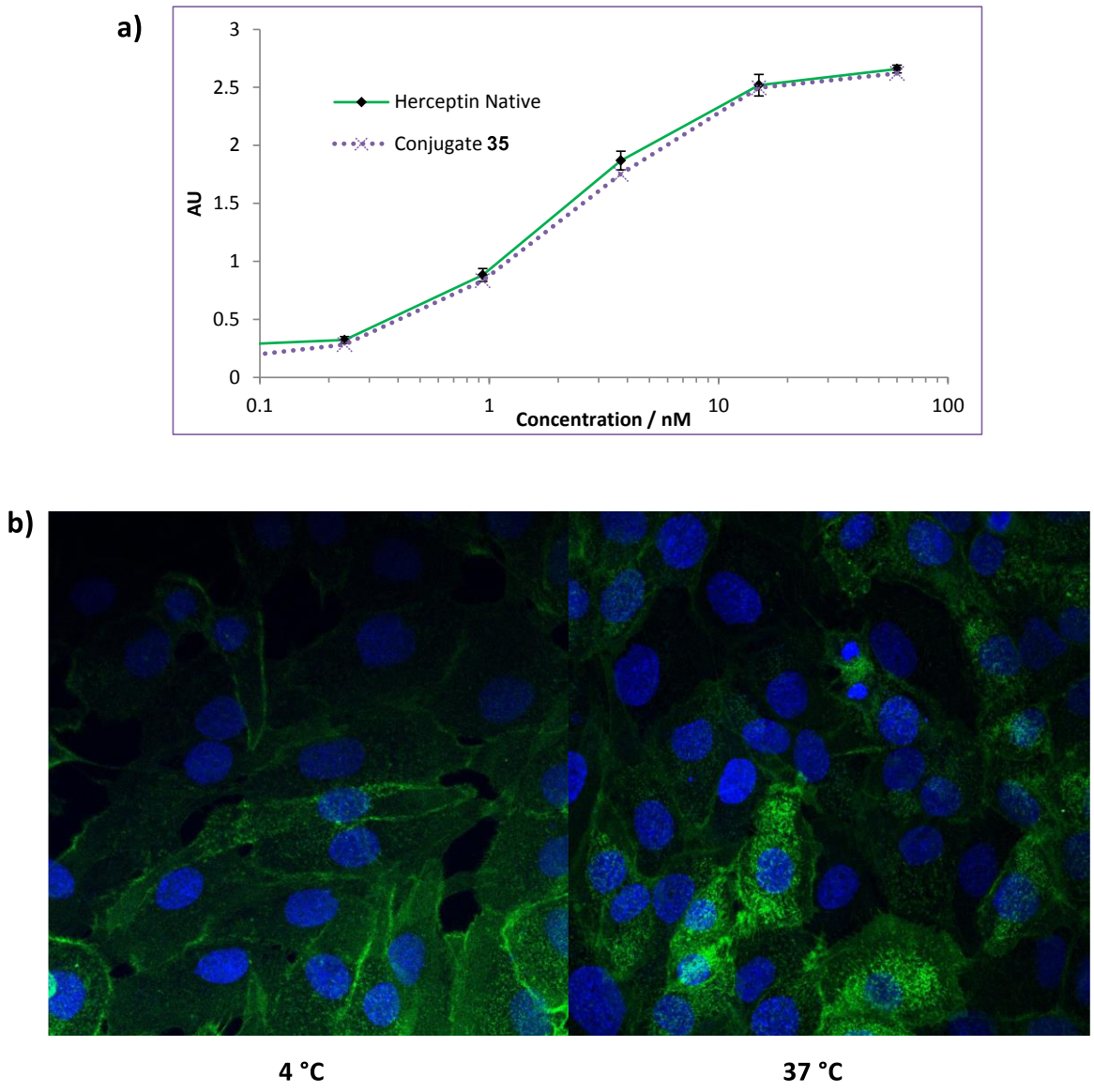

Figure 31 a) ELISA for conjugate **35** against native unmodified Herceptin™ mAb, showing binding affinity was unaffected by conjugation and "click"" functionalisation. b) Internalisation analysis by confocal microscopy – movement of conjugates from membrane to cytoplasm was observed at 37 °C.

3.3 Conclusion

In conclusion, a strategy for enabling the controlled, reproducible loading of two modules onto a native antibody scaffold has been produced. This was enabled by the successful synthesis and application of an entity, containing one "click" handle and four cysteine reactive centres, which functionally re-bridges two pairs of disulfide bonds on an IgG1. Subsequent reaction of the formed conjugate with an azide-fluorophore and azide-drug showed that the controlled loading of two modules was feasible and reproducible. The strategy, starting from the same branch point, was also readily adapted for the formation of a conjugate with a loading of four modules. Furthermore, all final conjugates were shown to retain binding by ELISA and internalisation by study with confocal microscopy. Given the practical simplicity and effectiveness of the bis-DiBrPD conjugation strategy to facilitate the loading of two modules starting from a native antibody scaffold, it will likely find application in multiple fields where the controlled loading of lower than four entities is desirable (*e.g.* antibody conjugates bearing highly hydrophobic modules) and especially in laboratories where antibody engineering techniques are not accessible, too expensive or not practical.

Chapter 4: Conclusions

In conclusion, two technologies have been developed that enable the construction of ADCs with previously unmet degrees of homogeneity. The first, dithioaryl(TCEP)pyridazinedione, features a molecule that has two cysteine-reactive centres, through which phosphine reducing agents are linked. This enables a strategy to both reduce and re-bridge disulfide containing proteins, allowing for the creation of protein conjugates (that are ready for further chemical modification) with a single reagent. Moreover, due to a high local concentration effect, in multi-disulfide containing systems only re-bridging in the native configuration is observed. This allowed for the construction of homogeneous ADCs using only biochemical techniques on native mAb scaffolds, a hitherto unmet need in the field. The activity of the resultant ADC, which featured doxorubicin as a payload, the activity of which was shown to be unperturbed by the modification as shown by ELISA.

The second technology, bis-DiBrPDs, feature two DiBrPDs connected *via* a flexible PEG linker, which can re-bridge mAbs in such a way that all four accessible disulfides are 'tied up' whilst only installing two chemical handles. By varying the terminal PD groups on these molecules a loading of two or four functional moieties per mAb can be achieved. The length of the bis-DiBrPDs was designed to span the maximum distance between any two accessible disulfide bonds on a mAb, thus the conformational freedom of the mAbs would not be hampered. This technology was used to synthesise a series of antibody conjugates that with a functional loading of two, exemplified with a fluorophore (AlexaFluor488™) and a drug (doxorubicin). The resulting conjugates were shown to have precise loadings, as assessed by UV-Vis, SDS-PAGE, and LC-MS. Furthermore, the activity of the conjugates was shown by ELISA (binding) and confocal microscopy (cell internalisation).

Both reported technologies represent significant breakthroughs within the field of ADCs. They are both biochemical techniques that provide companies and research groups around the globe the means to create ADCs with previously

unmet levels of control. Thus, mitigating the need for more expensive protein engineering techniques such as mutagenesis and protein expression.

4.1 Outlook

Given the success of the technologies presented in this work, it is prudent to appraise their future in the field, both in their commercial and academic applications.

4.1.1 Dithioaryl(TCEP)pyridazinedione

The key success of the dithioaryl(TCEP)pyridazinedione, and its analogues, lie in the streamlining of the functional disulfide re-bridging protocol and in its ability to re-bridge multi-disulfide systems whilst maintaining the native disulfide configuration. While this has been applied, with great success, to the IgG1 mAb Herceptin™, there are many proteins that see use in therapeutic settings that remain challenging targets for disulfide functionalisation.

Insulin

Insulin is a vital endocrine peptide hormone, which comprises two small peptide chains of 21 and 30 amino acids. It plays a major role in glucose regulation as well as other critical biological mechanisms and, defects in insulin secretion result in diabetes type I and II, thus efficient preparation and use of insulin is key to its ever-growing role in replacement therapy. Over the last decade, recombinant production, conversion of porcine insulin and high-yielding total syntheses have made the preparation of this peptide relatively inexpensive.[132] Unfortunately, to date, even state-of-the-art regimes of replacement therapy are insufficient to simulate hormone levels that match the physiological profile and, since all insulin analogues must be administered subcutaneously, patient compliance is poor. Thus, there is great demand for stable, longer lasting analogues that would allow

for less frequent dosing structures, which in turn, will lead to better patient compliance and welfare.

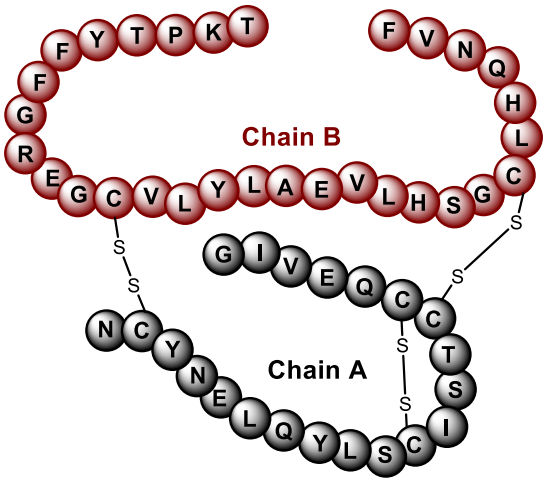

Figure 32 The structure of the endocrine hormone insulin, featuring three disulfide bridges; one intra-chain and two inter-chain.

The challenges associated with insulin use as a therapeutic lie in that it has a poor pharmacokinetic profile with low physicochemical stability, inherent immunogenicity and short plasma half-life.[133, 134] Additionally, the hormone becomes inactive and highly immunogenic upon partial unfolding.[135] The chemical modification of insulin to create stable and long acting analogues has generated a significant amount of research.

In most approaches lysines were non-specifically targeted to increase the hydrodynamic radius. This resulted in low-yielding and heterogenous mixtures of products.[46, 134, 136] Moreover, activity of the protein was abrogated as the interaction of the hormone with its receptor is governed by ionic interactions, which are inhibited through reaction with charged amino acids.

Attempts to functionalise the two interchain and one intrachain disulfide have met varying success. Upon reduction of the disulfides, they rapidly scramble, the hormone unfolds and loses biological activity.[137] Furthermore, the thiol groups of insulin are highly reactive and disulfide exchange is often observed. Modifying insulin *via* its disulfide bonds represents a significant challenge yet would allow

for functionalisation of the hormone whilst retaining and potentially stabilising the conformation associated with its native, most active disulfide configuration. A direct parallel can be made between the intricate 3-disulfide system of insulin and IgG1 antibodies 4-disulfide architecture. Indeed, when attempting to natively modify IgG1's essential disulfides, scrambling is almost always observed.[48]

Dithioaryl(TCEP)pyridazinedione was successfully applied to the full IgG1 mAb Herceptin™, resulting in successful re-bridging to produce homogenous ADCs. A similar strategy could be used to great effect to functionalise insulin with a broad range of modules. Moreover, the unique "built-in" reduction function would allow for re-bridging of the protein in its native configuration, thus retaining its conformational stability and associated activity. After optimisation of the conditions, re-bridged insulin conjugates could be covalently modified further with a diverse portfolio of biologically-relevant adducts with the intention of prolonging half-life and serum stability. To this end, PEG chains of varying sizes, including high molecular weight (20–60 kDa) dendritic PEG chains to prevent glomerular filtration of the insulin conjugates, could be attached. Other sought-after targets for insulin conjugation would be biotin, albumin, and albumin-binder proteins, which have also been shown to improve serum stability. Work could then be conducted to assess the activity of the insulin conjugates and their viability for use as therapeutics.

4.1.2 bis-DiBrPDs

In this work the scope of the presented bis-DiBrPDs are limited to controlled loadings of two and four of the same functional moiety. Whilst the use of asymmetric bis-DiBrPDs was exploited to allow loadings of two by tying using a methyl dummy handle (PD **20**) on one end, the same position could be used by a functional handle that could react in an orthogonal mode to the PD on the other end. This would allow the construction of ADCs bearing two distinct functional moieties, with two of each moiety; a highly significant achievement as a controlled dual-functionalisation of such a large protein scaffold has hitherto not been achieved. An example of the reactive handles that would be applicable could be borrowed from Maruani *et al.*'s aforementioned "dual click" strategy, featuring

one strained alkyne, for a SPAAC 'click' reaction and a terminal alkyne, for a CuAAC.[83]

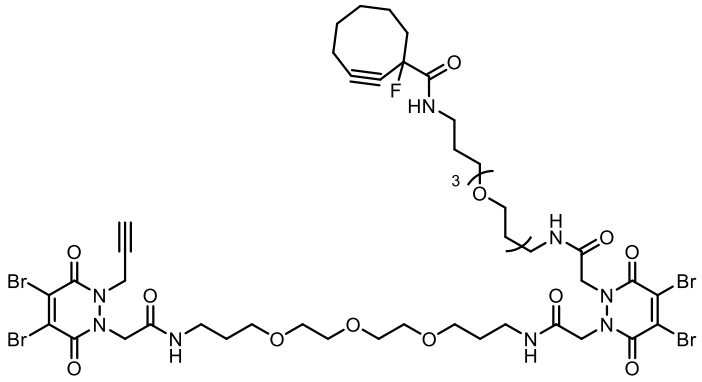

Figure 33 A proposed structure for a bis-DiBrPD bearing orthogonally reactive functional handles.

4.1.3 Combination of technologies: bis-dithioaryl(TCEP)PDs

Dithioaryl(TCEP)pyridazinedione, while capable of producing homogeneous ADCs is limited to loadings of four, or eight if two handle per pyridazinedione are used. Whereas, the bis-DiBrPDs are not capable of the same consistent homogeneous native re-bridging seen with dithioaryl(TCEP)pyridazinediones. Individually, the reported technologies have significant utility, however if the two technologies were combined, *i.e.* a bis-thioaryl(TCEP)PDs linked by a flexible PEG, the synthesis of homogenous ADCs could be achieved with modular loadings of two or four. While the synthesis of such a molecule would be difficult, due to its size and complexity, its capability and versatility (with respect to drug loading) would be of great value in the creation of new ADCs.

Chapter 5: Experimental

5.1 Experimental for Chapter 2

General Experimental

All reagents were purchased from Aldrich, AlfaAesar or Lumiprobe and were used as received. Where described below Pet. refers to petroleum ether (40–60 °C). All reactions were monitored by thin-layer chromatography (TLC) on pre-coated SIL G/UV254 silica gel plates (254 μm) purchased from VWR. Flash column chromatography was carried out with Kiesegel 60M 0.04/0.063 mm (200–400 mesh) silica gel. ^{1}H and ^{13}C NMR spectra were recorded at ambient temperature on a Bruker Avance 300 instrument operating at a frequency of 300 MHz for ^{1}H and 75 MHz for ^{13}C, a Bruker Avance 500 instrument operating at a frequency of 500 MHz for ^{1}H and 125 MHz for ^{13}C, and a Bruker Avance 600 instrument operating at a frequency of 600 MHz for ^{1}H and 150 MHz for ^{13}C in $CDCl_3$ or CD_3OD (as indicated below). The chemical shifts (δ) for ^{1}H and ^{13}C are quoted relative to residual signals of the solvent on the ppm scale. ^{1}H NMR peaks are reported as singlet (s), doublet (d), triplet (t), quartet (q), m (multiplet), br (broad) and doublet of quartets (dq). Coupling constants (*J* values) are reported in Hertz (Hz) and are H-H coupling constants unless otherwise stated. Signal multiplicities in ^{13}C NMR were determined using the distortionless enhancement by phase transfer (DEPT) spectral editing technique. Infrared spectra were obtained on a Perkin Elmer Spectrum 100 FTIR Spectrometer operating in ATR mode with frequencies given in reciprocal centimetres (cm^{-1}). Melting points were measured with a Gallenkamp apparatus and are uncorrected. All reagents containing phosphine were stored at −18 °C under argon. All bioconjugation reactions were carried out in duplicate.

Protein LC-MS for Figures S14-S24, S32-S36

LC-MS was performed on protein samples using a Thermo Scientific uPLC connected to MSQ Plus Single Quad Detector (SQD). Column: Hypersil Gold C4, 1.9 μm, 2.1 × 50 mm. Wavelength: 254 nm. Mobile Phase: 99:1 Water (0.1% formic acid): MeCN (0.1% formic acid) to 1:9 Water (0.1% formic acid): MeCN (0.1% formic acid) gradient over 4.5 min. Flow Rate: 0.3 mL/min. MS Mode: ES+. Scan Range: m/z = 500–2000. Scan time: 1.5 s. Data obtained in continuum mode. The electrospray source of the MS was operated with a capillary voltage of 3.5 kV and a cone voltage of 50 V. Nitrogen was used as the nebulizer and desolvation gas at a total flow of 600 L/h. Ion series were generated by integration of the total ion chromatogram (TIC) over the 3.0–5.0 min range. Total mass spectra for

protein samples were reconstructed from the ion series using the pre-installed ProMass software using default settings for large proteins in m/z range 500–1500.

Peptide MALDI-TOF MS for Figure S25

Samples were prepared by diluting with matrix (α-cyano-4-hydroxy-cinnamic acid in water-acetonitrile (2:8, v/v)), 0.5% formic acid. 3 μL of sample was spotted onto the MALDI target plate and allowed to dry. Samples were analysed using a Waters MALDI micro MX (Waters, UK) with a nitrogen laser in positive reflectron mode using source TLF delay (500 ns), an accelerating voltage of 120 V, pulse 2500 and detector 2000. Acquisition was between 500–30000 Da with 100 shots/spectrum.

UV-Vis spectroscopy

UV-vis spectroscopy was used to determine protein concentrations and pyridazinedione to antibody ratios (PAR) using a nanodrop ND-1000 spectrophotometer (Figure **S26**–**29**) and a Varian Cary 100 Bio UV-Visible spectrophotometer (Figure **S30**, **S31**, **S41** and **S42**), operating at room temperature. Sample buffer was used as blank for baseline correction.

SDS-PAGE gels

Non-reducing glycine-SDS-PAGE at 12% acrylamide gels were performed following standard lab procedures. A 6% stacking gel was used and a broad-range MW marker (10–250 kDa, Prestained PagerulerPlus Protein Standards, Bio-Rad) was co-run to estimate protein weights. Samples (15 μL at ~12 μM construct) were mixed with loading buffer (3 μL, composition for 6 × SDS: 1 g SDS, 3 mL glycerol, 6 mL 0.5 M Tris buffer pH 6.8, 2 mg bromophenol blue in 10 mL) and heated at 75 °C for 3 min. The gels were run at 30 mA for 50 min in 1 × SDS running buffer. The gels were stained with Coomassie dye.

5.1.1 Synthesis of compounds

Di-*tert*-butyl 1,2-diethylhydrazine-1,2-dicarboxylate (2)

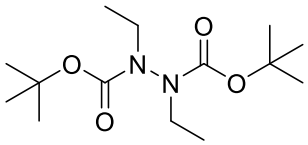

To a solution of di-*tert*-butyl hydrazine-1,2-dicarboxylate **1** (1.0 g, 4.3 mmol) and caesium carbonate (5.6 g, 17.2 mmol) in DMF (20 mL) was added bromoethane (1.1 g, 10.1 mmol) and the reaction mixture stirred at 21 °C for 24 h. After this time, the reaction mixture was diluted with EtOAc (50 mL) and washed with deionised water (4 × 20 mL) and brine (2 × 20 mL). The organic phase was then concentrated *in vacuo* and the crude residue purified by flash column chromatography (50% EtOAc:Pet.). The appropriate fractions were combined and concentrated *in vacuo* to afford di-*tert*-butyl 1,2-diethylhydrazine-1,2-dicarboxylate **2** (1.1 g, 3.8 mmol, 88%) as a colourless oil as a mixture of rotamers. ^{1}H NMR (300 MHz, $CDCl_3$) δ 3.57–3.33 (m, 4H), 1.50–1.39 (m, 18H), 1.16 (t, *J* = 7.2 Hz, 6H); ^{13}C NMR (75 MHz, $CDCl_3$) δ 155.1 (C), 80.6 (C), 46.37 (CH_2), 44.37 (CH_2), 28.35 (CH_3), 28.27 (CH_3), 13.56 (CH_3), 12.95 (CH_3); IR (thin film) 2980, 2927, 2881, 1698 cm^{-1}; LRMS (ES+) 288 (100, $[M+H]^+$); HRMS (ES+) calcd for $C_{16}H_{32}N_2O$ $[M+H]^+$ 288.2049, observed 288.2054.

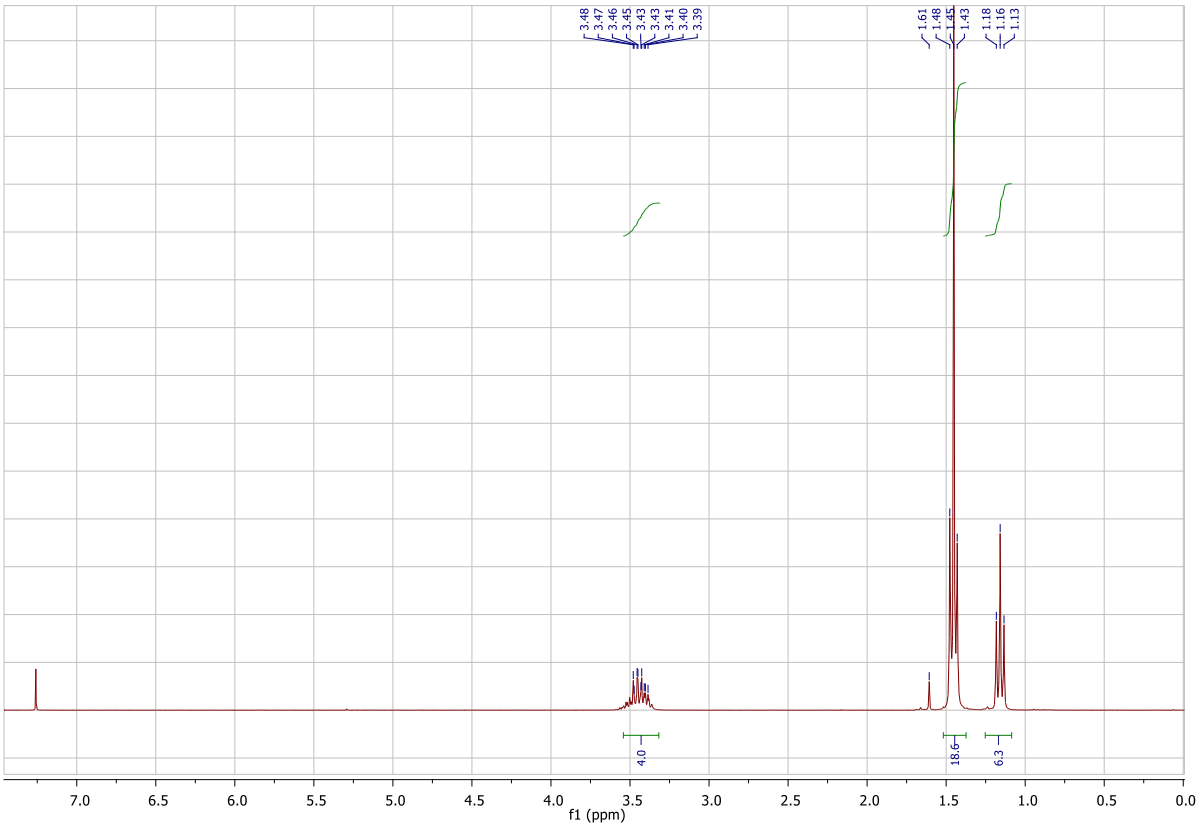

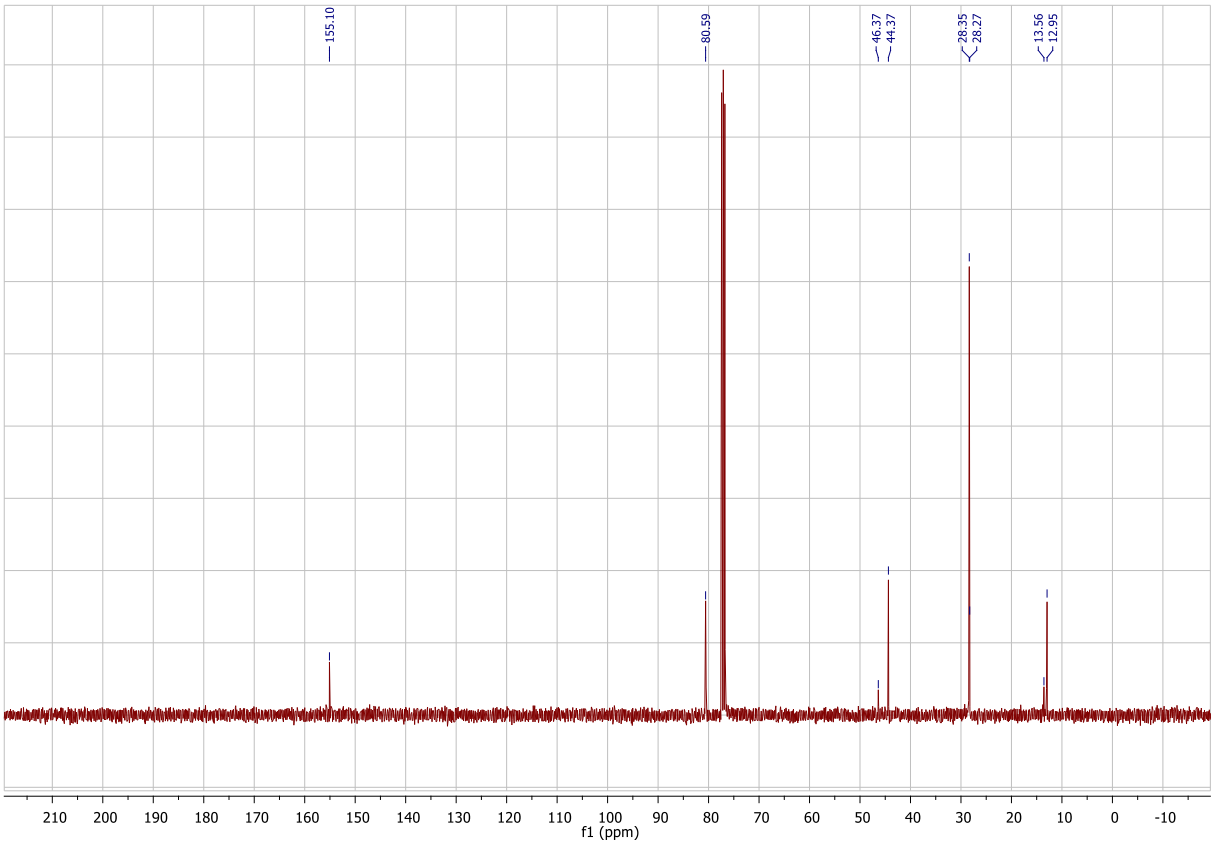

Figure **S1**. ^{1}H and ^{13}C NMR data for di-*tert*-butyl 1,2-diethylhydrazine-1,2-dicarboxylate (**2**).

4,5-Dibromo-1,2-diethyl-1,2-dihydropyridazine-3,6-dione (Pyridazinedione 3)[1]

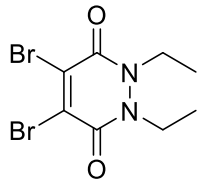

To a 1:1 solution of CH_2Cl_2:TFA (5 mL:5 mL) was added di-*tert*-butyl 1,2-diethylhydrazine-1,2-dicarboxylate **2** (348 mg, 1.21 mmol) and the reaction mixture stirred at 21 °C for 1 h. The reaction mixture was then concentrated *in vacuo*, taking care to ensure all the TFA was removed by use of toluene to form an azeotrope. The crude residue was then dissolved in AcOH (10 mL), to which was added 3,4-dibromomaleic anhydride (310 mg, 1.21 mmol) and the reaction mixture heated under reflux for 2 h. The reaction mixture was then concentrated *in vacuo* and the crude residue was purified by flash column chromatography (30–50 % EtOAc:Pet.). The appropriate fractions were then combined and concentrated *in vacuo* to afford 4,5-dibromo-1,2-diethyl-1,2-dihydropyridazine-3,6-dione (288 mg, 0.88 mmol, 73%) as a pale yellow solid. ^{1}H NMR (600 MHz, $CDCl_3$) δ 4.17 (q, *J* = 7.0 Hz, 4H), 1.28 (t, *J* = 7.0 Hz, 6H); ^{13}C NMR (150 MHz, $CDCl_3$) δ 153.3 (C), 136.1 (C), 42.4 (CH_2), 13.2 (CH_3); IR (solid) 2979, 2937, 1630, 1574 cm^{-1}; LRMS (EI) 328 (50, $[M^{81}Br^{81}Br]^+$), 326 (100, $[M^{81}Br^{79}Br]^+$), 324 (50, $[M^{79}Br^{79}Br]^+$); HRMS (EI) calcd for $C_8H_{10}Br_2N_2O_2$ $[M^{79}Br^{79}Br]^+$ 323.9104, observed 323.9097.

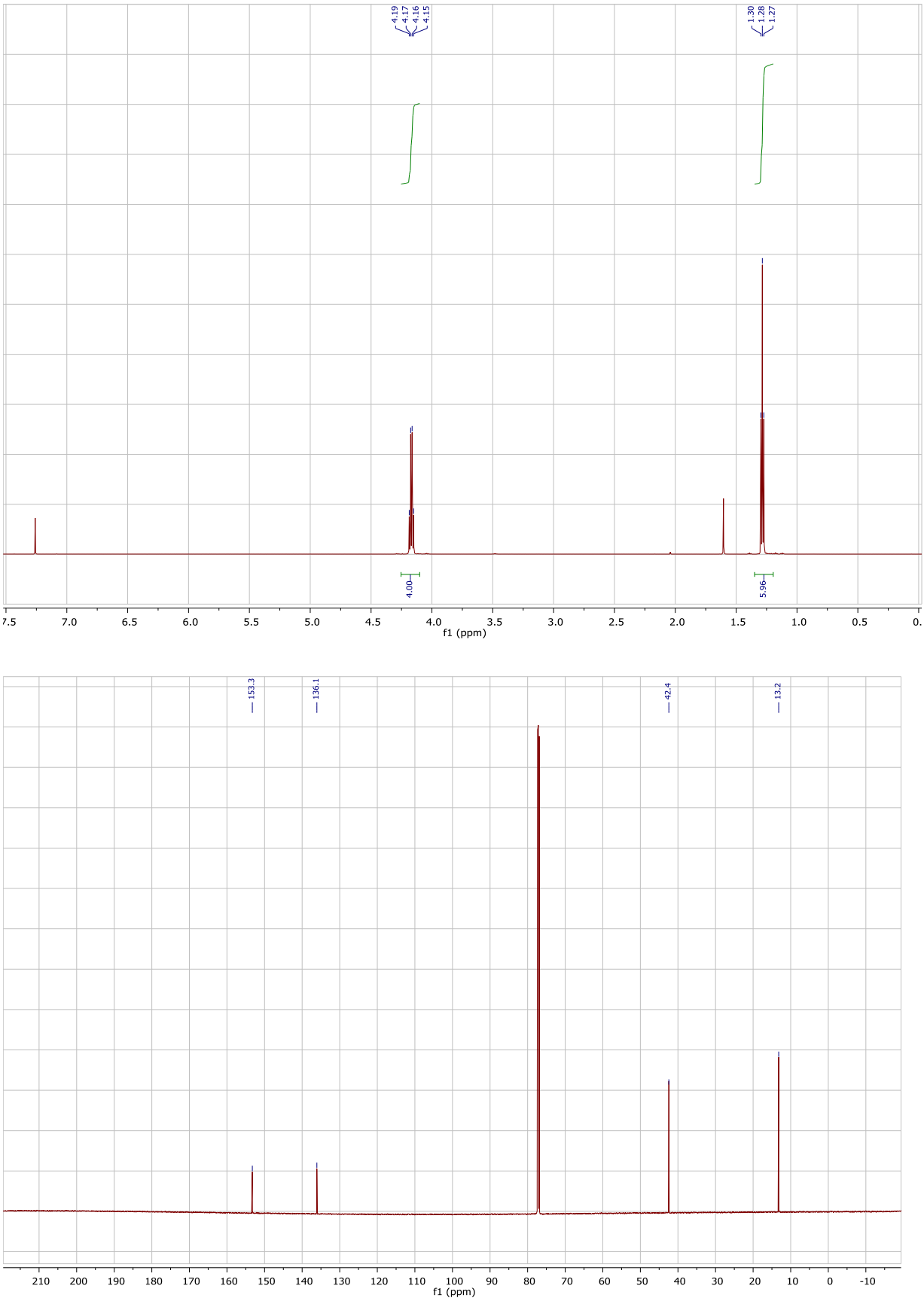

Figure **S2**. ^{1}H and ^{13}C NMR data for 4,5-dibromo-1,2-diethyl-1,2-dihydropyridazine-3,6-dione (Pyridazinedione **3**).

4,5-Bis((4-aminophenyl)thio)-1,2-diethyl-1,2-dihydropyridazine-3,6-dione (Pyridazinedione 4)

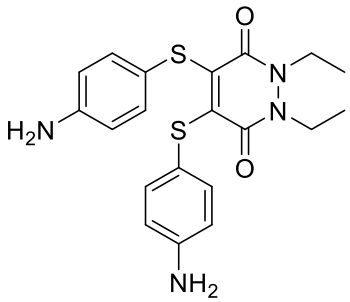

To a solution of 4,5-dibromo-1,2-diethyl-1,2-dihydropyridazine-3,6-dione **3** (193 mg, 0.60 mmol) and 4-aminothiophenol (89 mg, 0.71 mmol) in CH_2Cl_2 (20 ml) was added NEt_3 (166 µL, 1.20 mmol) and the reaction mixture stirred at 21 °C for 2 h. The reaction mixture was then washed with deionised water (3 × 15 mL), the organic phase was concentrated *in vacuo* and the crude residue purified by flash column chromatography (40–60% EtOAc:Pet.). The appropriate fractions were combined and concentrated *in vacuo* to give 4,5-bis((4-aminophenyl)thio)-1,2-diethyl-1,2-dihydropyridazine-3,6-dione **4** (163 mg, 0.39 mmol, 66%) as an orange-red crystalline solid. m.p. 158–162 °C; ^{1}H NMR (300 MHz, $CDCl_3$) δ 7.18–7.08 (m, 4H), 6.62–6.52 (m, 4H), 3.98 (q, *J* = 7.0 Hz, 4H), 3.75 (br. s, 4H), 1.17 (t, *J* = 7.0 Hz, 4H); ^{13}C NMR (75 MHz, $CDCl_3$) δ 156.4 (C), 146.8 (C), 142.3 (C), 134.1 (C), 120.4 (CH), 115.6 (CH), 41.0 (CH_2), 12.7 (CH_3); IR (solid) 3420, 3247, 2975, 1708, 1653, 1596, 1495, 1397 cm^{-1}; LRMS (ES+) 415 (100, $[M+H]^+$); HRMS (ES+) calcd for $C_{20}H_{22}N_4O_2S_2$ $[M+H]^+$ 415.1262, observed 415.1272.

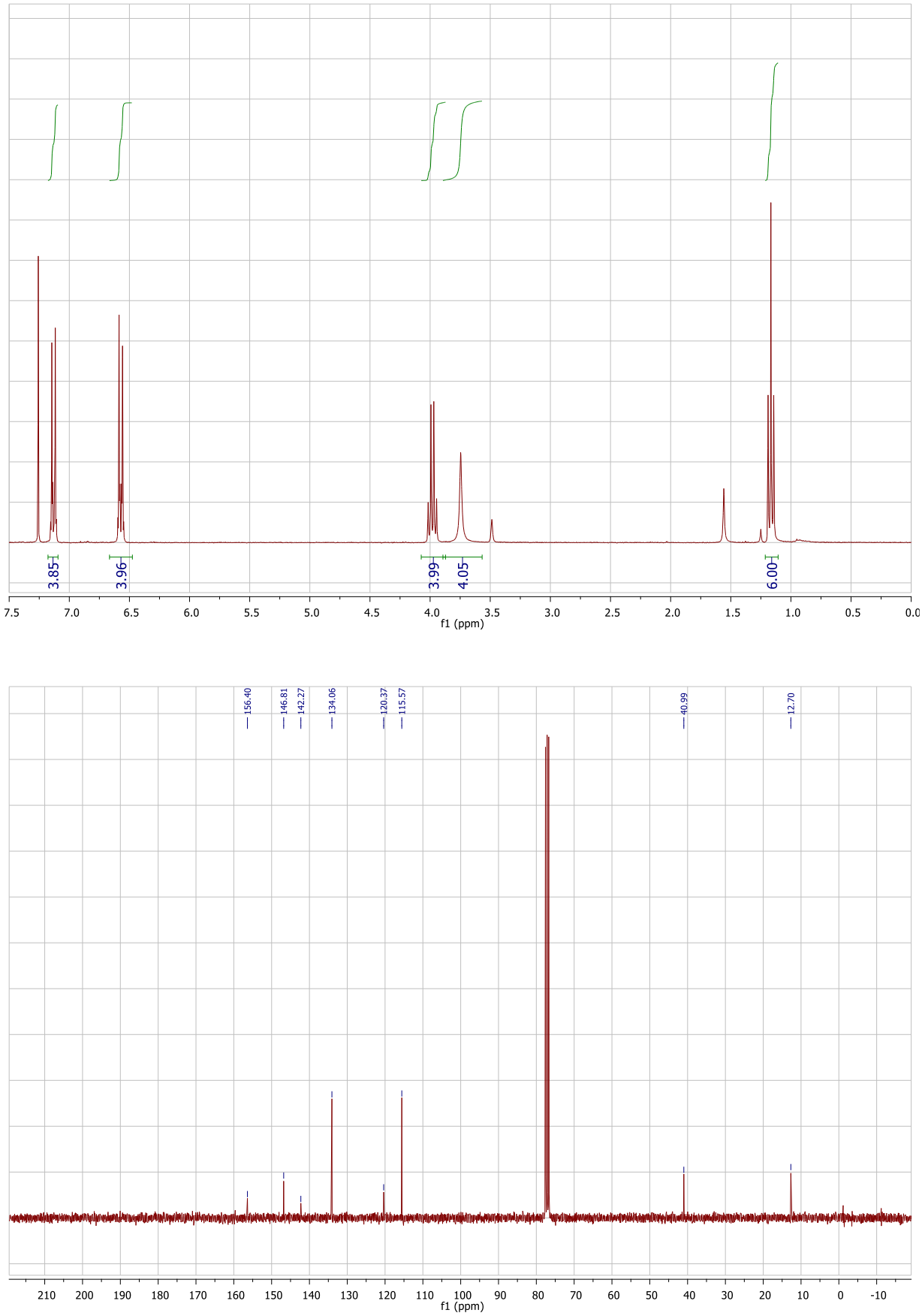

Figure **S3**. ^{1}H and ^{13}C NMR data for 4,5-bis((4-aminophenyl)thio)-1,2-diethyl-1,2-dihydropyridazine-3,6-dione (Pyridazinedione **4**).

3-(Bis(3-methoxy-3-oxopropyl)phosphanyl)propanoic acid (6)[138]

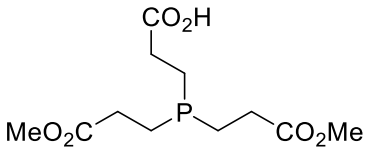

To a solution of tris(2-carboxyethyl)phosphine hydrochloride **5** (1.0 g, 3.5 mmol) in MeOH (15 mL), was added Amberlyst® 15 beads (1.0 g), which had been freshly pre-washed with MeOH (10 mL) for 10 mins, filtered and then dried. The reaction mixture was stirred at 21 °C for 1 h. The reaction mixture was then filtered to remove the Amberlyst® beads, the filtrate was concentrated *in vacuo* and the crude residue purified by flash column chromatography (1–2% MeOH:CH_2Cl_2). The appropriate fractions were collected and concentrated *in vacuo* to give 3-(bis(3-methoxy-3-oxopropyl)phosphanyl)propanoic acid **6** (170 mg, 0.61 mmol, 17%) as a clear oil. ^{1}H NMR (600 MHz, $CDCl_3$) δ 3.70 (s, 6H), 2.62–2.36 (m, 6H), 1.76 (t, J = 7.9 Hz, 6H); ^{13}C NMR (150 MHz, $CDCl_3$) δ 173.8 (C), 173.7 (C), 52.0 (CH_3), 30.7 (CH_2), 30.5 (CH_2), 21.5 (CH_2) (d, $J_{C\text{-}P}$ = 13.1 Hz), 21.3 (CH_2) (d, $J_{C\text{-}P}$ = 13.2 Hz); LRMS (ES-) 277 (100, $[M\text{-}H]^-$); HRMS (ES-) calcd for $C_{11}H_{19}O_6P$ $[M\text{-}H]^-$ 277.0841, observed 277.0838.

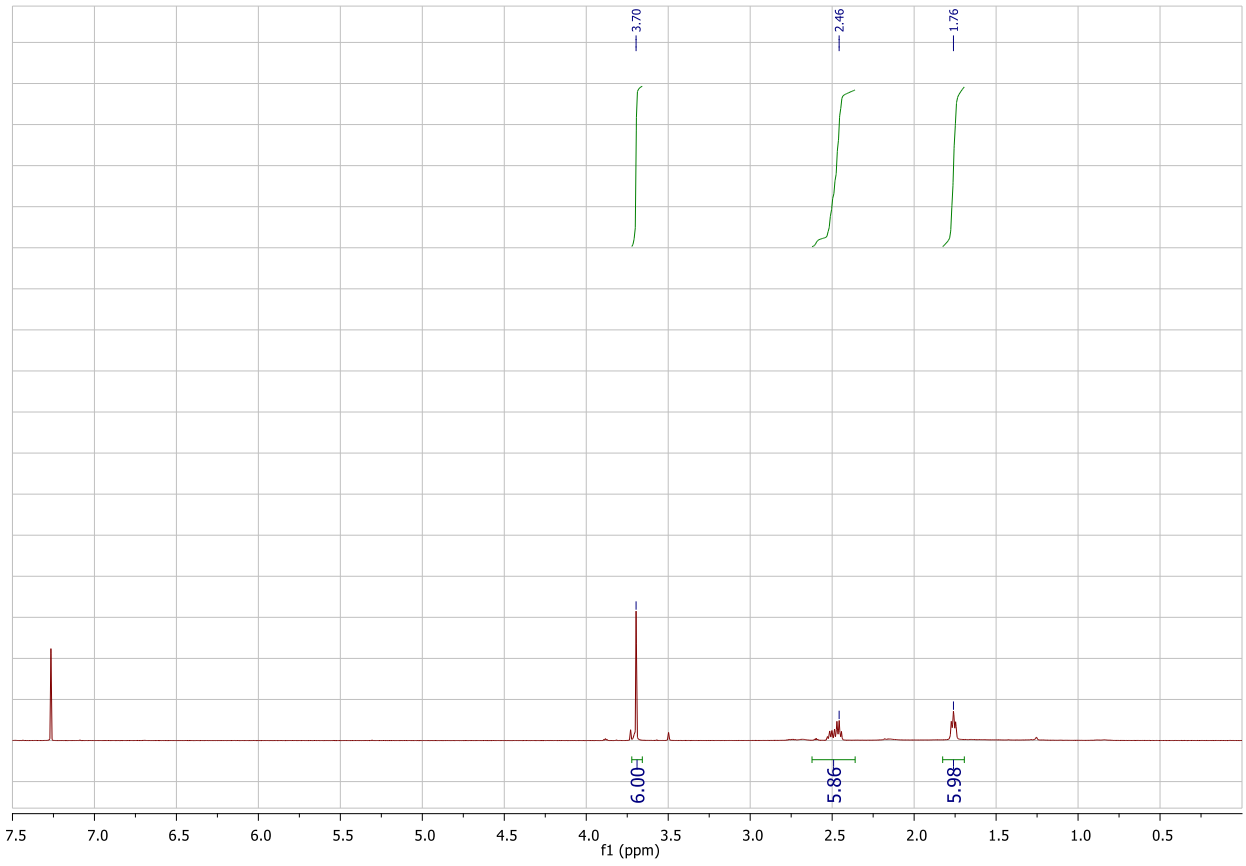

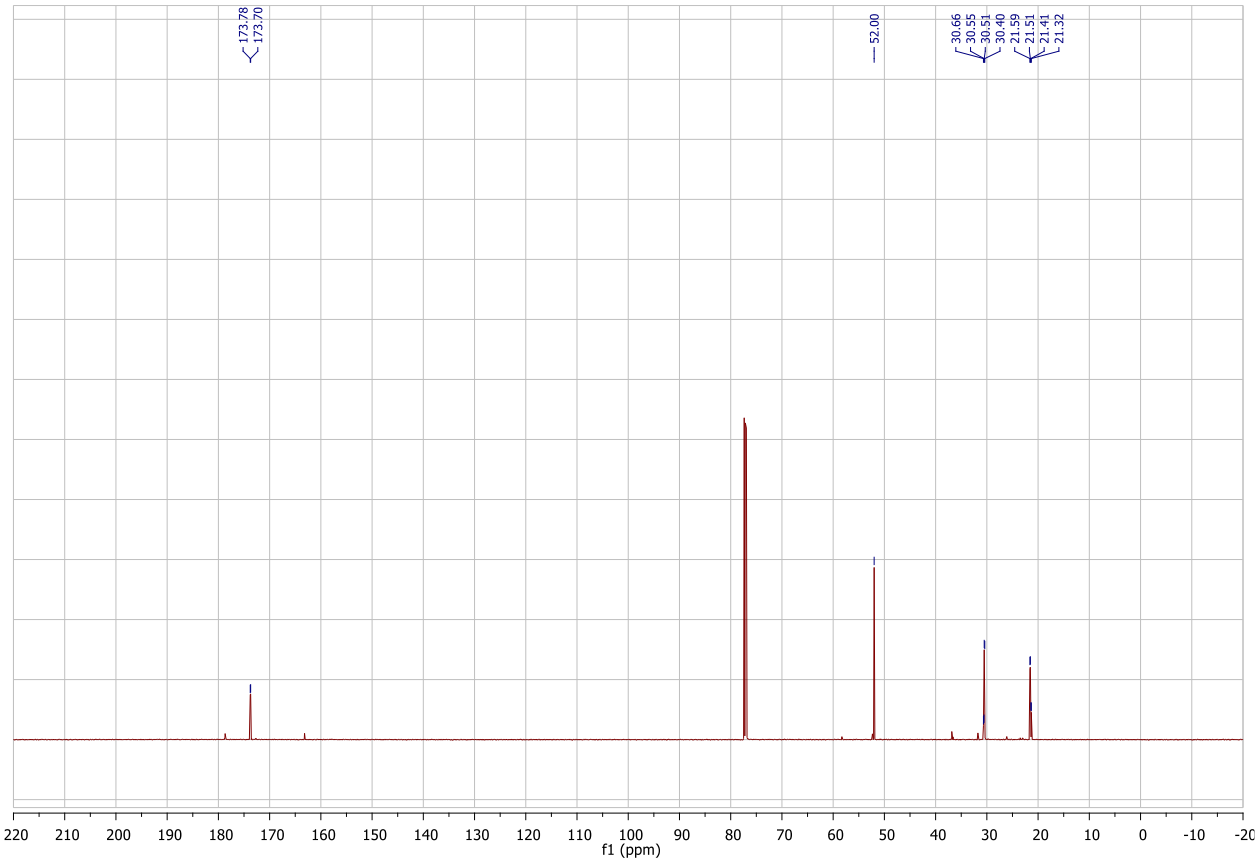

Figure **S4**. ^{1}H and ^{13}C NMR data for 3-(bis(3-methoxy-3-oxopropyl)phosphanyl)propanoic acid (**6**).

Tetramethyl 3,3',3'',3'''-((((((1,2-diethyl-3,6-dioxo-1,2,3,6-tetrahydropyridazine-4,5-diyl)bis(sulfanediyl))bis(4,1-phenylene))bis(azanediyl))bis(3-oxopropane-3,1-diyl))bis(phosphanetriyl))tetrapropionate (Pyridazinedione 7)

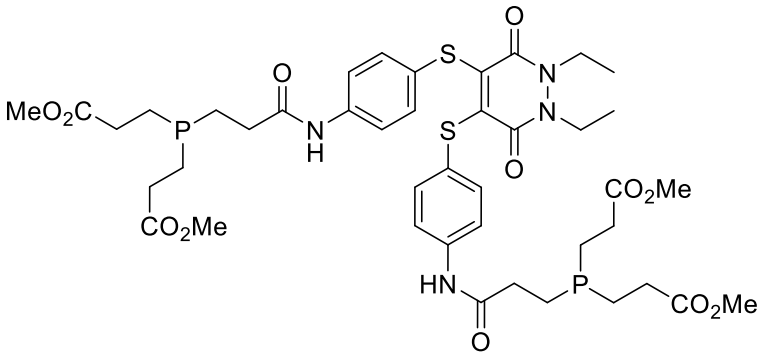

To a solution of **6** (31 mg, 0.11 mmol) in DMF (3 ml) was added HATU (42 mg, 0.11 mmol) and the reaction stirred at 21 °C for 15 mins. Following this, 4,5-bis((4-aminophenyl)thio)-1,2-diethyl-1,2-dihydropyridazine-3,6-dione **3** (12 mg, 0.03 mmol) was added and the reaction mixture stirred for a further 5 mins. After this, *N,N*-diisopropylethylamine (DIPEA) (20 µL, 0.11 mmol) was added and the reaction mixture stirred at 21 °C for 12 h. Following this, the reaction mixture was diluted with EtOAc (20 mL), and washed with deionised water (3 × 10 mL) and brine (3 × 10 mL). The organic phase was then concentrated *in vacuo* and the crude residue purified by flash column chromatography (0–2% MeOH:CH_2Cl_2). The appropriate fractions were then combined and concentrated *in vacuo* to give pyridazinedione **7** (6 mg, 0.01 mmol, 18%) as a yellow gum. ^{1}H NMR (600 MHz, $CDCl_3$) δ 7.80 (s, 2H), 7.45 (d, *J* = 8.4 Hz, 4H), 7.16 (d, *J* = 8.3 Hz, 4H), 4.04 (q, *J* = 7.0 Hz, 4H), 3.69 (s, 12H), 2.50 (s, 12H), 1.91–1.67 (m, 12H), 1.22 (t, *J* = 7.0 Hz, 6H); ^{13}C NMR (150 MHz, $CDCl_3$) δ 174.0 (C), 173.9 (C), 170.9 (C), 156.0 (C), 138.1 (C), 132.2 (C), 127.1 (C), 120.1 (C), 52.1 (CH_3), 41.2 (CH_2) , 33.9 (CH_2), 30.6 (d, $J_{C\text{-}P}$ =16.5, CH_2), 22.3 (d, $J_{C\text{-}P}$=13.5, CH_2), 21.6 (d, $J_{C\text{-}P}$=13.5, CH_2), 12.9 (CH_3); IR (thin film) 3325, 2953, 1725, 1614, 1593, 1527, 1494, 1409, 1367; LRMS (ES+) 951 (100, $[M(O)+H]^+$); HRMS (ES+) calcd for $C_{42}H_{56}O_{13}P_2S_2$ $[M(O)+H]^+$ 951.2839, observed 951.2887.

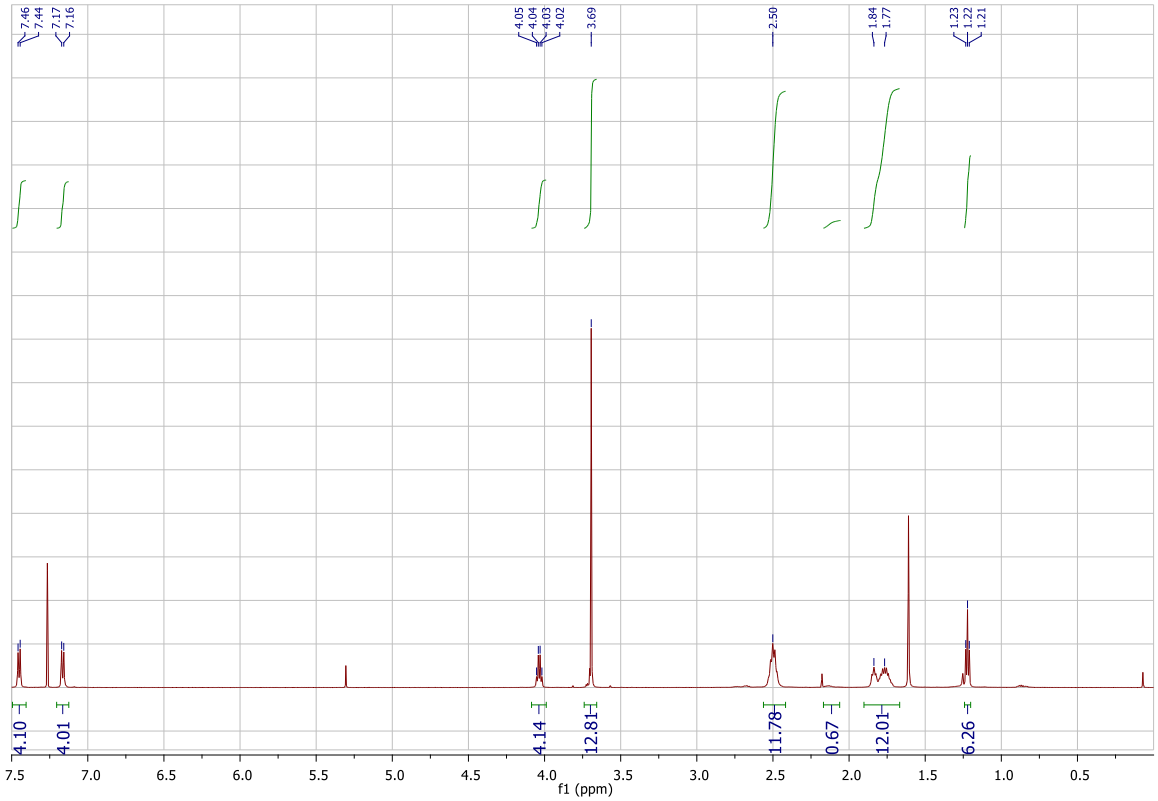

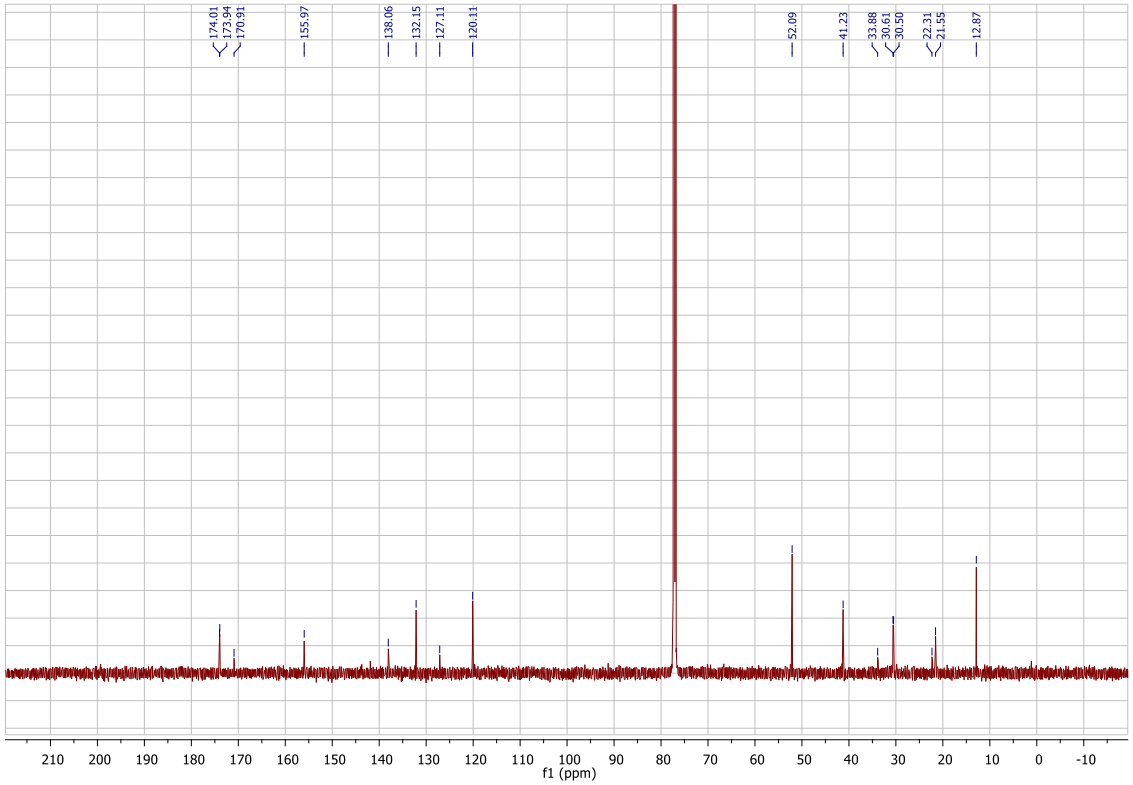

Figure **S5**. ^{1}H and ^{13}C NMR data for tetramethyl 3,3',3'',3'''-((((((1,2-diethyl-3,6-dioxo-1,2,3,6-tetrahydropyridazine-4,5-diyl)bis(sulfanediyl))bis(4,1-phenylene))bis(azanediyl))bis(3-oxopropane-3,1-diyl))bis(phosphanetriyl))tetrapropionate (Pyridazinedione **7**).

Di-*tert*-butyl 1,2-dipropylhydrazine-1,2-dicarboxylate (8)

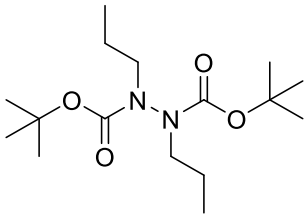

To a solution of di-*tert*-butyl hydrazine-1,2-dicarboxylate **1** (1.0 g, 4.3 mmol) and caesium carbonate (5.6 g, 17.2 mmol) in DMF (20 mL) was added bromopropane (1.1 g, 9.5 mmol) and the reaction mixture stirred at 21 °C for 24 h. After this time, the reaction mixture was diluted with EtOAc (50 mL) and washed with deionised water (4 × 20 mL) and brine (2 × 20 mL). The organic phase was then concentrated *in vacuo* and the crude residue purified by flash column chromatography (50% EtOAc:Pet.). The appropriate fractions were combined and concentrated *in vacuo* to afford di-*tert*-butyl 1,2-dipropylhydrazine-1,2-dicarboxylate (1.1 g, 3.36 mmol, 78%) as a colourless oil as a mixture of rotamers. ^{1}H NMR (600 MHz, $CDCl_3$) δ 3.50–3.17 (m, 4H), 1.61 (s, 4H), 1.51–1.38 (m, 18H), 0.90 (t, *J* = 7.4 Hz, 6H); ^{13}C NMR (150 MHz, $CDCl_3$) δ 156.0 (C), 155.3 (C), 154.9 (C), 80.9 (C), 80.7 (C), 80.7 (C), 80.6 (C), 53.5 (CH_2), 51.8 (CH_2), 51.7 (CH_2), 28.4 (CH_3), 28.3 (CH_3), 22.0 (CH_3), 21.3 (CH_3), 21.1 (CH_3), 11.7 (CH_3), 11.6 (CH_3), 11.5 (CH_3); IR (thin film) 2974, 2934, 2877, 1707 cm^{-1}; LRMS (ES+) 317 (100, $[M+H]^+$); HRMS (ES+) calcd for $C_{16}H_{32}N_2O$ $[M+H]^+$ 317.2440, observed 317.2425.

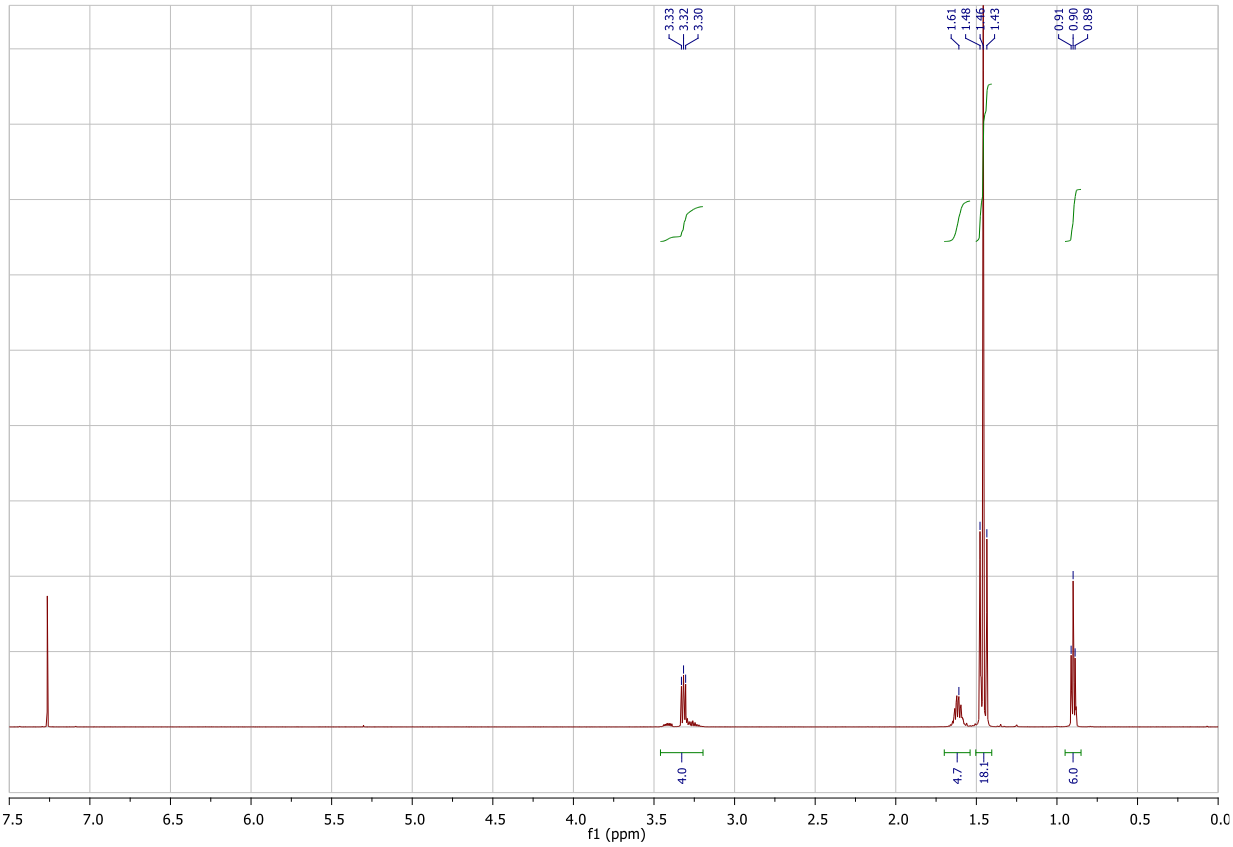

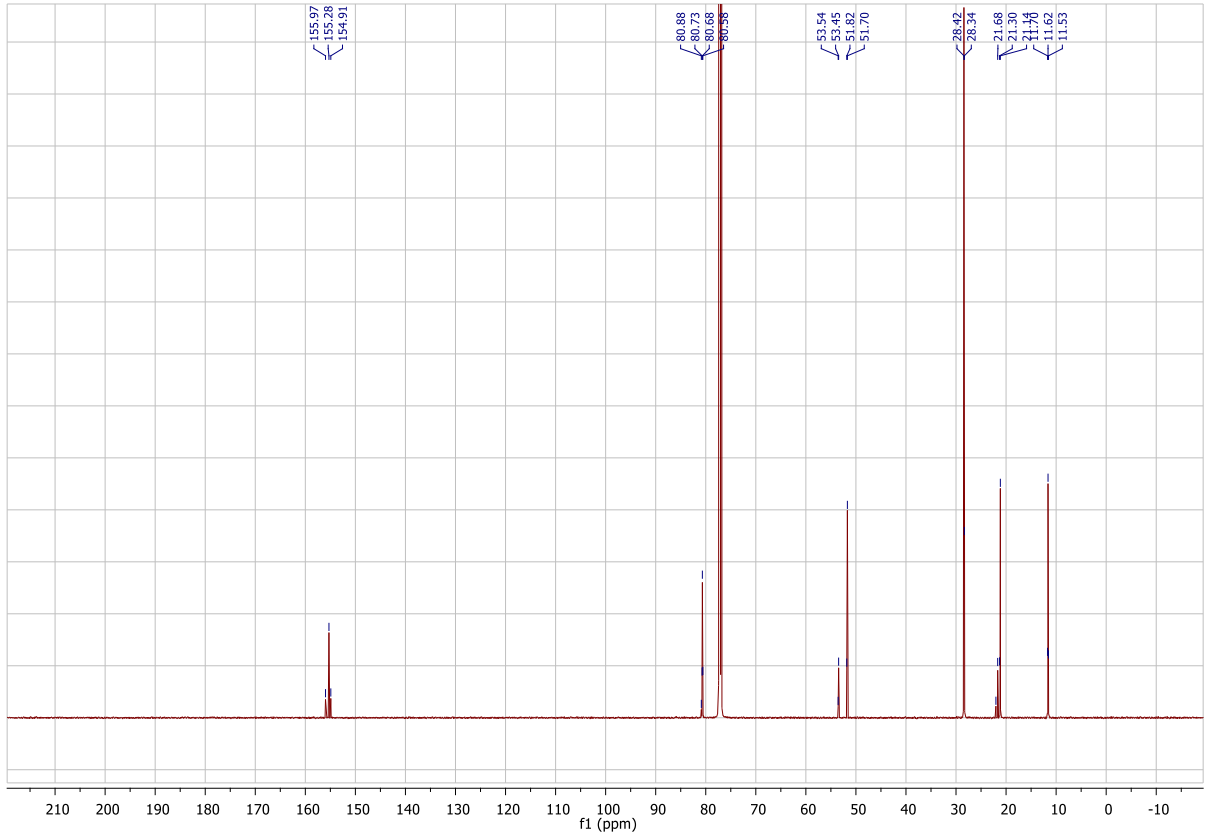

Figure **S6**. ^{1}H and ^{13}C NMR data for di-*tert*-butyl 1,2-dipropylhydrazine-1,2-dicarboxylate (**8**).

4,5-Dibromo-1,2-dipropyl-1,2-dihydropyridazine-3,6-dione (9)

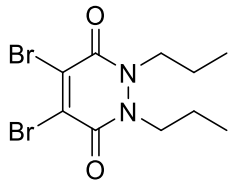

To a 1:1 solution of CH_2Cl_2:TFA (5 mL:5 mL) was added di-*tert*-butyl 1,2-dipropylhydrazine-1,2-dicarboxylate (**8**) (150 mg, 0.47 mmol) and the reaction mixture stirred at 21 °C for 1 h. The reaction mixture was then concentrated *in vacuo*, taking care to ensure all the TFA was removed by use of toluene as an azeotrope. The crude residue was then dissolved in AcOH (10 mL), to which was added 3,4-dibromomaleic anhydride (121 mg, 0.47 mmol) and the reaction mixture heated under reflux for 2 h. The reaction mixture was then concentrated *in vacuo* and the crude residue was purified by flash column chromatography (30–50 % EtOAc:Pet.). The appropriate fractions were then combined and concentrated *in vacuo* to afford 4,5-dibromo-1,2-dipropyl-1,2-dihydropyridazine-3,6-dione (130 mg, 0.37 mmol, 78%) as a pale yellow gum. ^{1}H NMR (300 MHz, $CDCl_3$) δ 4.04 (t, *J* = 7.2 Hz, 4H), 1.67 (dq, *J* = 7.5 Hz, 4H), 0.93 (t, *J* = 7.5 Hz, 6H); ^{13}C NMR (75 MHz, $CDCl_3$) δ 153.6 (C), 135.9 (C), 48.5 (CH_2), 21.5 (CH_2), 11.0 (CH_3); LRMS (EI) 356 (50, $[M^{81}Br^{81}Br+H]^+$), 354 (100, $[M^{81}Br^{79}Br+H]^+$), 352 (50, $[M^{79}Br^{79}Br+H]^+$); HRMS (EI) calcd for $C_{10}H_{14}Br_2N_2O_2$ $[M^{79}Br^{79}Br]^+$ 351.9422, observed 351.9420.

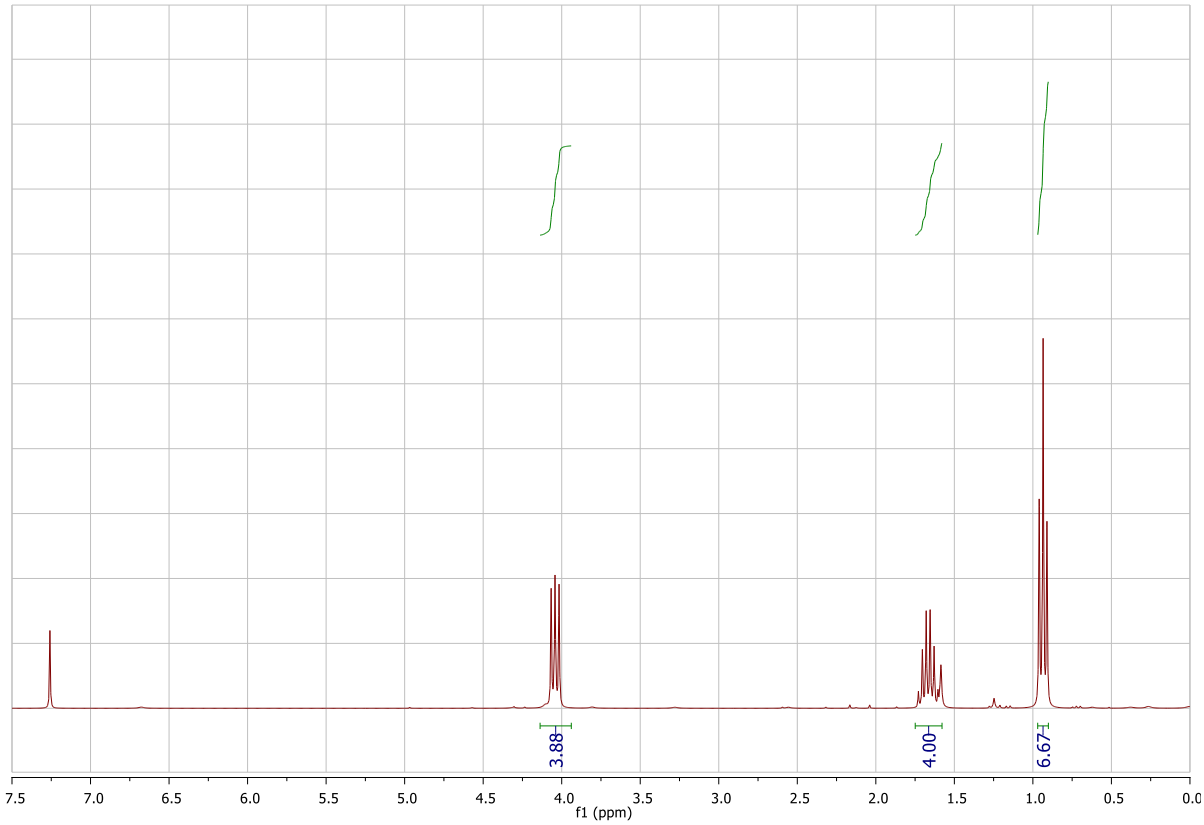

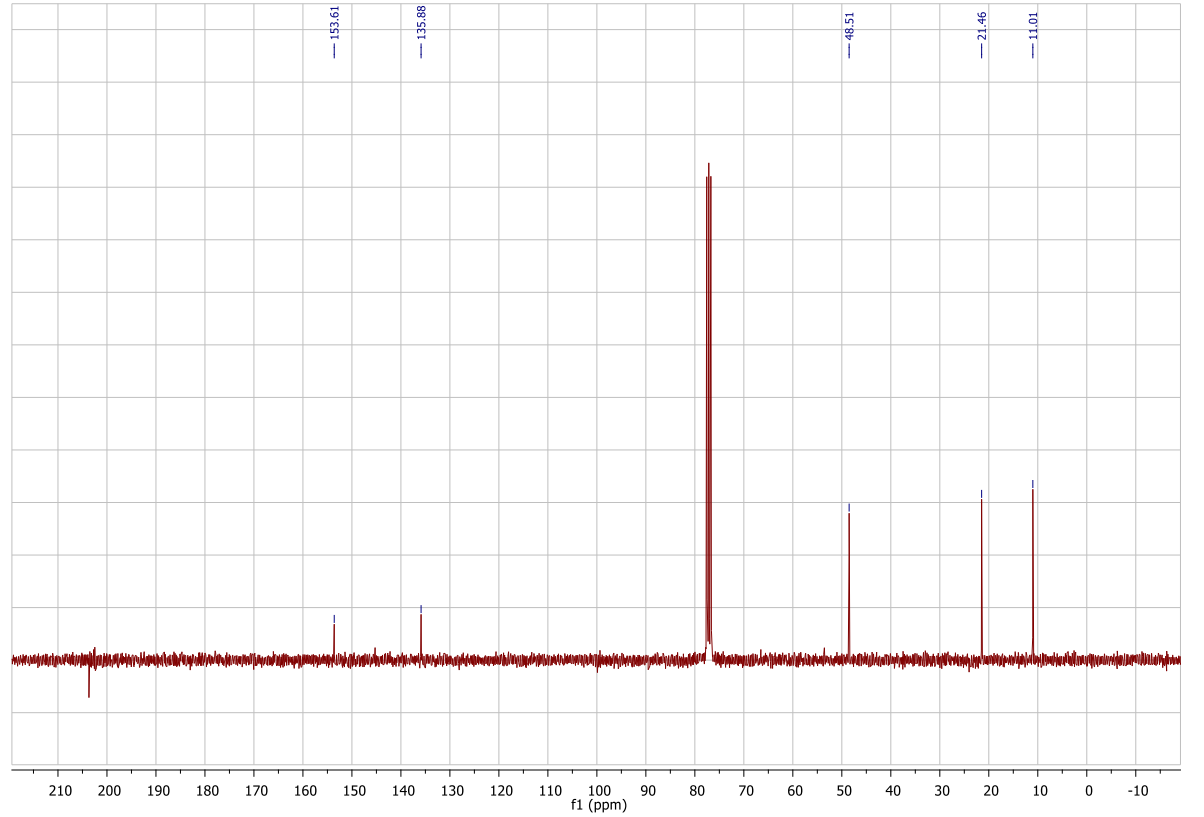

Figure **S7**. ^{1}H and ^{13}C NMR data for 4,5-dibromo-1,2-dipropyl-1,2-dihydropyridazine-3,6-dione (**9**).

***N,N′*-(((3,6-Dioxo-1,2-dipropyl-1,2,3,6-tetrahydropyridazine-4,5-diyl)bis(sulfanediyl))bis(4,1-phenylene))diacetamide (Pyridazinedione 10)**

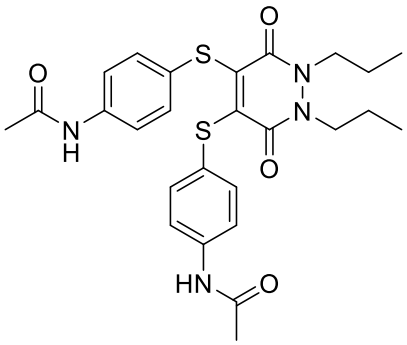

To a solution of 4-acetimidothiophenol (169 mg, 1.01 mmol) and 4,5-dibromo-1,2-dipropyl-1,2-dihydropyridazine-3,6-dione **9** (136 mg, 0.37 mmol) in CH_2Cl_2 (20 mL) was added NEt_3 (212 µL, 1.47 mmol) and the reaction mixture stirred at 21 °C over 72 h. The reaction mixture was then washed with deionised water (3 × 15 mL) and the organic phase concentrated *in vacuo*. The crude residue was then purified by flash column chromatography (2% MeOH:CH_2Cl_2), and the appropriate fractions combined and concentrated *in vacuo* to give *N,N′*-(((3,6-dioxo-1,2-dipropyl-1,2,3,6-tetrahydropyridazine-4,5-diyl)bis(sulfanediyl))bis(4,1-phenylene))diacetamide **10** (78 mg, 0.15 mmol, 40%) as a bright red crystalline solid. m.p. 147–150 °C; ^{1}H NMR (600 MHz, $CDCl_3$) δ 7.40 (d, *J* = 8.2 Hz, 4H), 7.15 (d, *J* = 8.5 Hz, 4H), 3.94 (t, *J* = 7.3 Hz, 4H), 2.18 (s, 4H), 1.62 (dq, *J* = 7.3 Hz, 6H), 0.89 (t, *J* = 7.4 Hz, 6H); ^{13}C NMR (150 MHz, $CDCl_3$) δ 168.5 (C), 156.5 (C), 137.9 (C), 132.1 (C), 127.3 (CH), 120.2 (CH), 120.1 (CH), 47.0 (CH_2), 24.8 (CH_2), 21.1 (CH_2), 11.0 (CH_3); IR (solid) 3314, 2966, 2929, 2876, 1694, 1632, 1592, 1527, 1493 cm^{-1}; LRMS (ES+) 527 (100, $[M+H]^+$); HRMS (ES+) calcd for $C_{26}H_{30}N_4O_4S_2$ $[M+H]^+$ 527.1787, observed 527.1798.

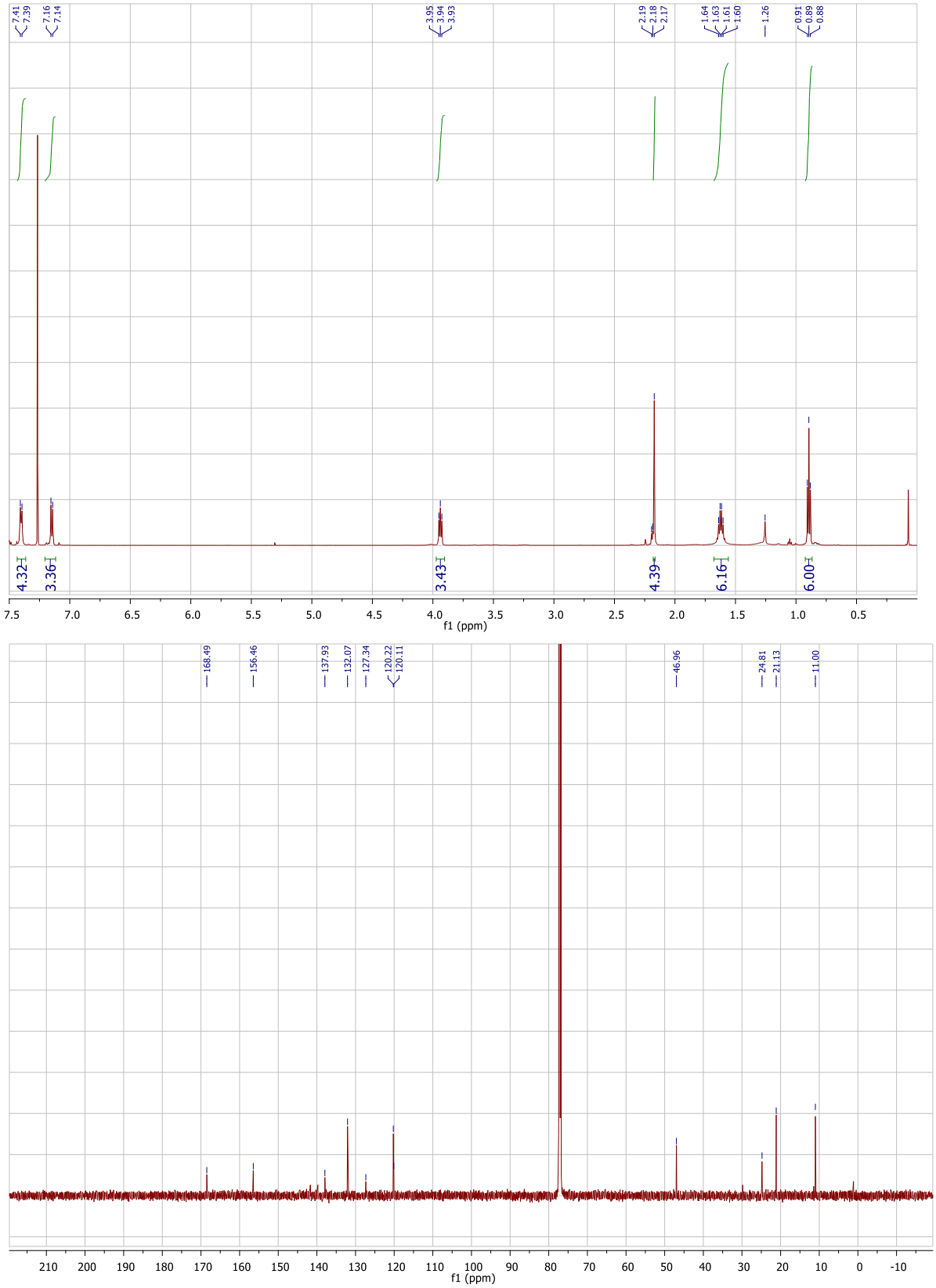

Figure **S8**. ^{1}H and ^{13}C NMR data for *N,N′*-(((3,6-dioxo-1,2-dipropyl-1,2,3,6-tetrahydropyridazine-4,5-diyl)bis(sulfanediyl))bis(4,1-phenylene))diacetamide (Pyridazinedione **10**).

Di-*tert*-butyl 1-ethylhydrazine-1,2-dicarboxylate (11)

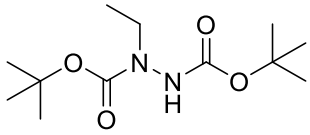

To a solution of di-*tert*-butyl hydrazine-1,2-dicarboxylate **1** (7.0 g, 30.13 mmol) and caesium carbonate (4.0 g, 12.06 mmol) in DMF (50 mL) was added bromoethane (644 µL, 6.03 mmol) and the reaction mixture left to stir at 21 °C for 18 h. After this time, the reaction mixture was diluted with EtOAc (75 mL) and washed with deionised water (3 × 40 mL) and brine (3 × 30 mL). The organic phase was then concentrated *in vacuo*, and cold hexane was added to the crude residue to precipitate out and recover the excess di-*tert*-butyl hydrazine-1,2-dicarboxylate as a white solid through recrystallisation and filtration. The filtrate was then concentrated further *in vacuo* and purified by flash column chromatography (5–15% EtOAc:Pet.). The appropriate fractions were combined and concentrated *in vacuo* to give di-*tert*-butyl 1-ethylhydrazine-1,2-dicarboxylate (642 mg, 2.46 mmol, 41%) as a white crystalline solid (rotamers present in solution NMR). m.p. 54–57 °C ^{1}H NMR (600 MHz, $CDCl_3$) δ 6.15 (br. d, 1H), 3.49 (br. s, 2H), 1.48-1.45 (m, 18H), 1.14 (t, *J* = 7.2 Hz, 3H); ^{13}C NMR (150 MHz, $CDCl_3$) δ 155.3 (C), 81.2 (C), 81.0 (C), 45.8 (CH_2), 44.1 (CH_2), 28.4 (CH_3), 28.3 (CH_3), 12.7 (CH_3); IR (solid) 3313, 2978, 2934, 1706 cm^{-1}; LRMS (ES+) 261 (100, $[M+H]^+$); HRMS (ES+) calcd for $C_{12}H_{24}N_2O_4$ $[M+H]^+$ 261.1814, observed 261.1813.

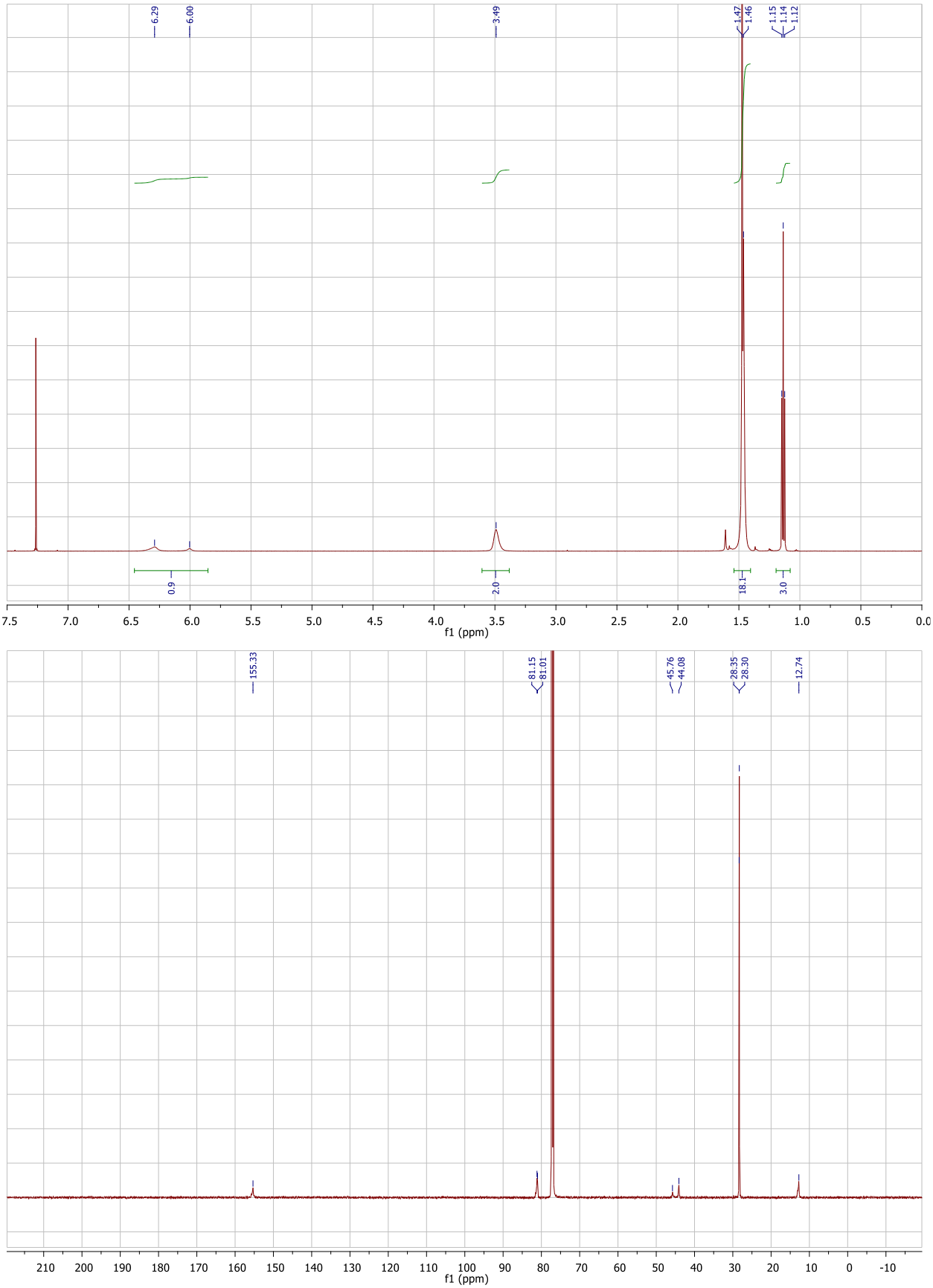

Figure **S9**. ^{1}H and ^{13}C NMR data for di-*tert*-butyl 1-ethylhydrazine-1,2-dicarboxylate (**11**).

Di-*tert*-butyl 1-ethyl-2-(prop-2-yn-1-yl)hydrazine-1,2-dicarboxylate (12)

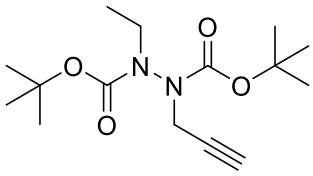

To a solution of di-*tert*-butyl 1-ethylhydrazine-1,2-dicarboxylate (**11**) (642 mg, 2.47 mmol) and caesium carbonate (2.0 g, 6.14 mmol) in DMF (20 mL) was added propargyl bromide (1 mL, 19.4 mmol) and the reaction mixture stirred at 21 °C for 72 h. The reaction mixture was then diluted with EtOAc (30 mL) and washed with deionised water (3 × 20 mL) and brine (3 × 20 mL). The organic phase was then concentrated *in vacuo* and purified by flash column chromatography (60% EtOAc:Pet.). The appropriate fractions were collected and concentrated *in vacuo* to give di-*tert*-butyl 1-ethyl-2-(prop-2-yn-1-yl)hydrazine-1,2-dicarboxylate (259 mg, 0.87 mmol, 35%) as a colourless oil as a mixture of rotamers. ^{1}H NMR (600 MHz, $CDCl_3$) δ 4.70–4.26 (m, 1H), 4.04–3.89 (m, 1H), 3.71–3.35 (m, 2H), 2.25 (s, 1H), 1.53–1.41 (m, 18H), 1.30–1.14 (m, 3H); ^{13}C NMR (150 MHz, $CDCl_3$) δ 155.6 (C), 154.9 (C), 154.5 (C), 82.0 (C), 81.7 (C), 81.6 (C), 81.2 (C), 81.1 (C), 81.0 (C), 79.5 (C), 79.0 (C), 78.7 (C), 72.7 (C), 72.4 (C), 72.2 (C), 46.6 (CH_2), 44.7 (CH_2), 41.6 (CH_3), 39.6 (CH_3), 39.4 (CH_3), 28.4 (CH_3), 28.3 (CH_3), 28.3 (C), 28.2 (C), 13.7 (CH_3), 13.1 (CH_3), 13.0 (CH_3); IR (solid) 3262, 2977, 2934, 2126, 1709 cm^{-1}; LRMS (ES+) 299 (100, $[M+H]^+$); HRMS (ES+) calcd for $C_{15}H_{26}N_2O_4$ $[M+H]^+$ 299.1971, observed 299.1963.

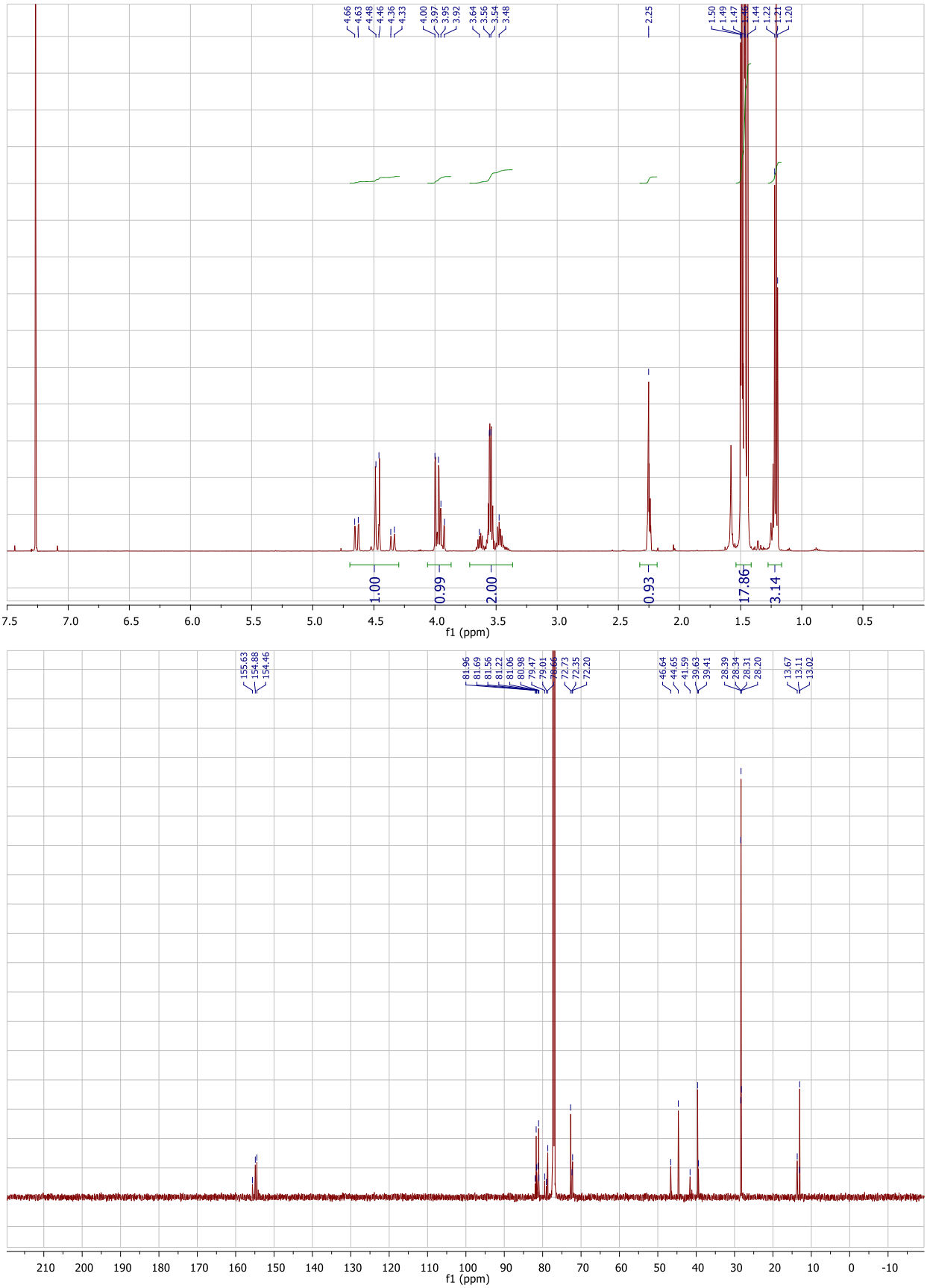

Figure **S10**. ^{1}H and ^{13}C NMR data for di-*tert*-butyl 1-ethyl-2-(prop-2-yn-1-yl)hydrazine-1,2-dicarboxylate (**12**).

4,5-Dibromo-1-ethyl-2-(prop-2-yn-1-yl)-1,2-dihydropyridazine-3,6-dione (13)

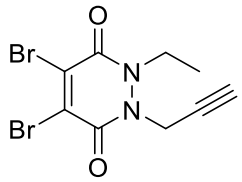

To a 1:1 solution of CH_2Cl_2:TFA (5 mL: 5 mL) was added di-*tert*-butyl 1-ethyl-2-(prop-2-yn-1-yl)hydrazine-1,2-dicarboxylate **12** (259 mg, 0.87 mmol) and the reaction mixture stirred at 21 °C for 1 h. The reaction mixture was then concentrated *in vacuo*, taking care to ensure all the TFA was removed by use of toluene as an azeotrope. The crude residue was then dissolved in AcOH (10 mL), to which was added 3,4-dibromomaleic anhydride (222 mg, 0.87 mmol) and the reaction mixture heated under reflux for 2 h. The reaction mixture was then concentrated *in vacuo* and the crude residue purified by flash column chromatography (60% EtOAc:Pet.). The appropriate fractions were then combined and concentrated *in vacuo* to give 4,5-dibromo-1-ethyl-2-(prop-2-yn-1-yl)-1,2-dihydropyridazine-3,6-dione (124 mg, 0.37 mmol, 43%) as a pale yellow gum. ^{1}H NMR (600 MHz, $CDCl_3$) δ 4.89 (s, 2H), 4.29 (q, *J* = 7.1 Hz, 2H), 2.42 (t, *J* = 2.5 Hz, 1H), 1.32 (t, *J* = 7.1 Hz, 3H); ^{13}C NMR (150 MHz, $CDCl_3$) δ 153.6 (C), 152.9 (C), 137.3 (C), 135.2 (C), 75.6 (C), 75.0 (C), 43.0 (CH_2), 37.1 (CH_2), 13.2 (CH_3); IR (thin film) 3243, 2985, 2123, 1639, 1576 cm^{-1}; LRMS (EI) 338 (50, $[M^{81}Br^{81}Br+H]^+$), 336 (100, $[M^{81}Br^{79}Br+H]^+$), 334 (50, $[M^{79}Br^{79}Br+H]^+$); HRMS (EI) calcd for $C_9H_8Br_2N_2O_2$ $[M^{79}Br^{79}Br]^+$ 333.8953, observed 333.8950.

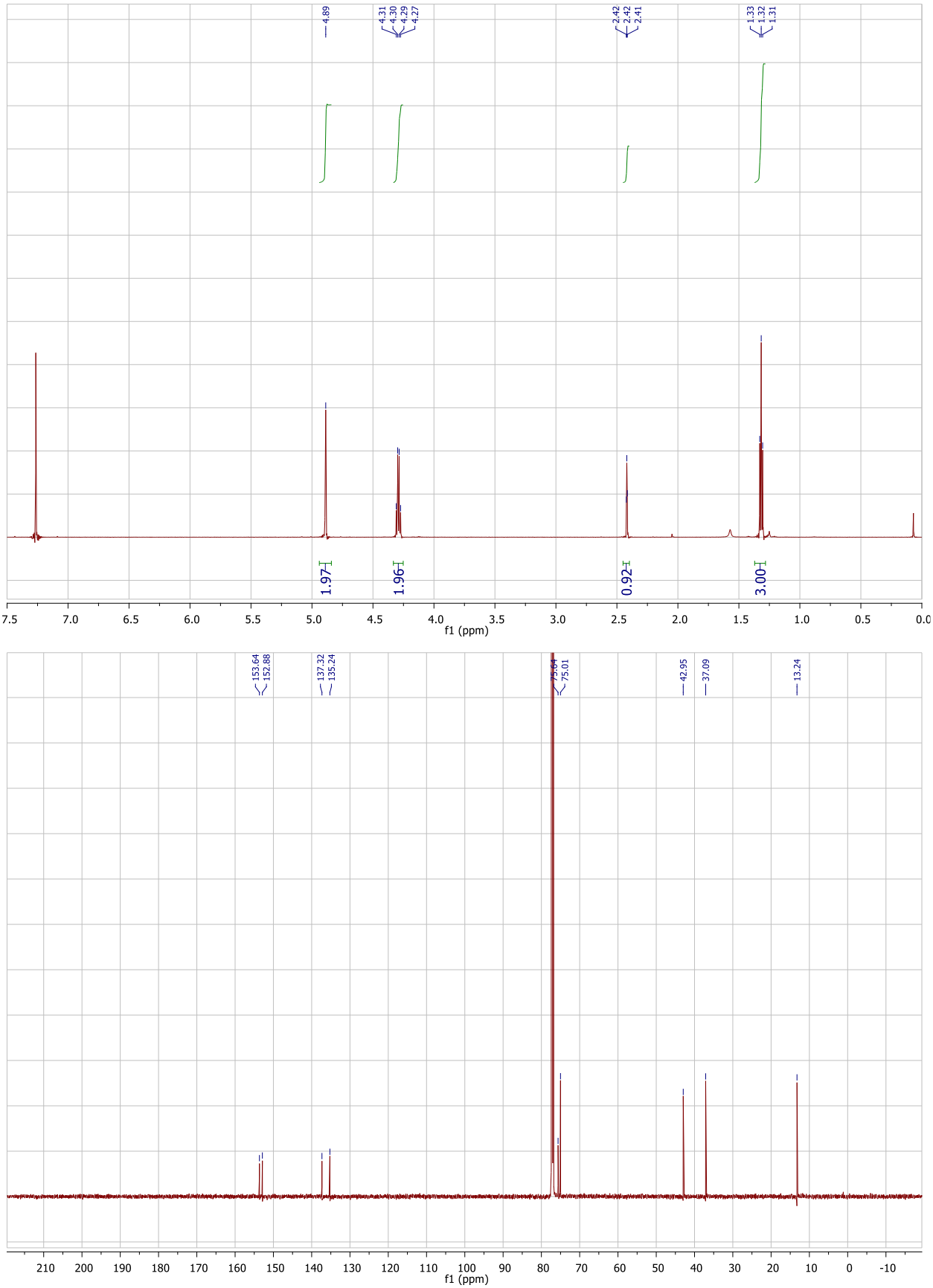

Figure **S11**. ^{1}H and ^{13}C NMR data for 4,5-dibromo-1-ethyl-2-(prop-2-yn-1-yl)-1,2-dihydropyridazine-3,6-dione (**13**).

4,5-Bis((4-aminophenyl)thio)-1-ethyl-2-(prop-2-yn-1-yl)-1,2-dihydropyridazine-3,6-dione (14)

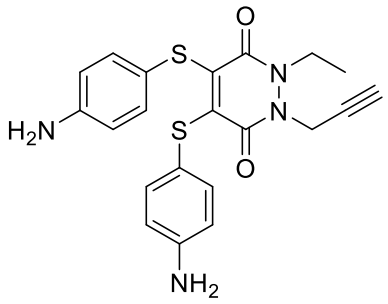

To a solution of 4,5-dibromo-1-ethyl-2-(prop-2-yn-1-yl)-1,2-dihydropyridazine-3,6-dione **13** (124 mg, 0.37 mmol) and 4-aminothiophenol (185 mg, 1.49 mmol) in CH_2Cl_2 (15 mL), was added triethylamine (215 µL, 1.49 mmol), and the reaction mixture was left to stir at 21 °C for 18 h. The reaction mixture was then washed with deionised water (3 × 10 mL), and the organic phase was concentrated *in vacuo* and the crude residue purified by flash column chromatography (2–5% MeOH:CH_2Cl_2). The appropriate fractions were then combined and concentrated *in vacuo* to give 4,5-bis((4-aminophenyl)thio)-1-ethyl-2-(prop-2-yn-1-yl)-1,2-dihydropyridazine-3,6-dione **14** (150 mg, 0.35 mmol, 95%) as an orange crystalline solid. m.p. 161–164 °C; ^{1}H NMR (600 MHz, $CDCl_3$) δ 7.17–7.12 (m, 4H), 6.62–6.56 (m, 4H), 4.71 (d, *J* = 2.5 Hz, 2H), 4.07 (q, *J* = 7.1 Hz, 1H), 3.77 (br. s, 4H), 2.31 (t, *J* = 2.5 Hz, 1H), 1.20 (t, *J* = 7.1 Hz, 3H); ^{13}C NMR (150 MHz, $CDCl_3$) δ 156.8 (C), 156.0 (C), 146.9 (C), 143.7 (C), 141.0 (C), 134.12 (C), 134.1 (C), 120.1 (C), 120.0 (C), 115.6 (C), 115.5 (C), 76.5 (C), 74.0 (CH), 41.5 (CH_2), 36.2 (CH_2), 12.7 (CH_3); IR (solid) 3450, 3359, 3275, 2128, 1619, 1595, 1517, 1495 cm^{-1}; LRMS (ES+) 425 (100, $[M+H]^+$); HRMS (ES+) calcd for $C_{21}H_{20}N_4O_2S_2$ $[M+H]^+$ 425.1106, observed 425.1107.

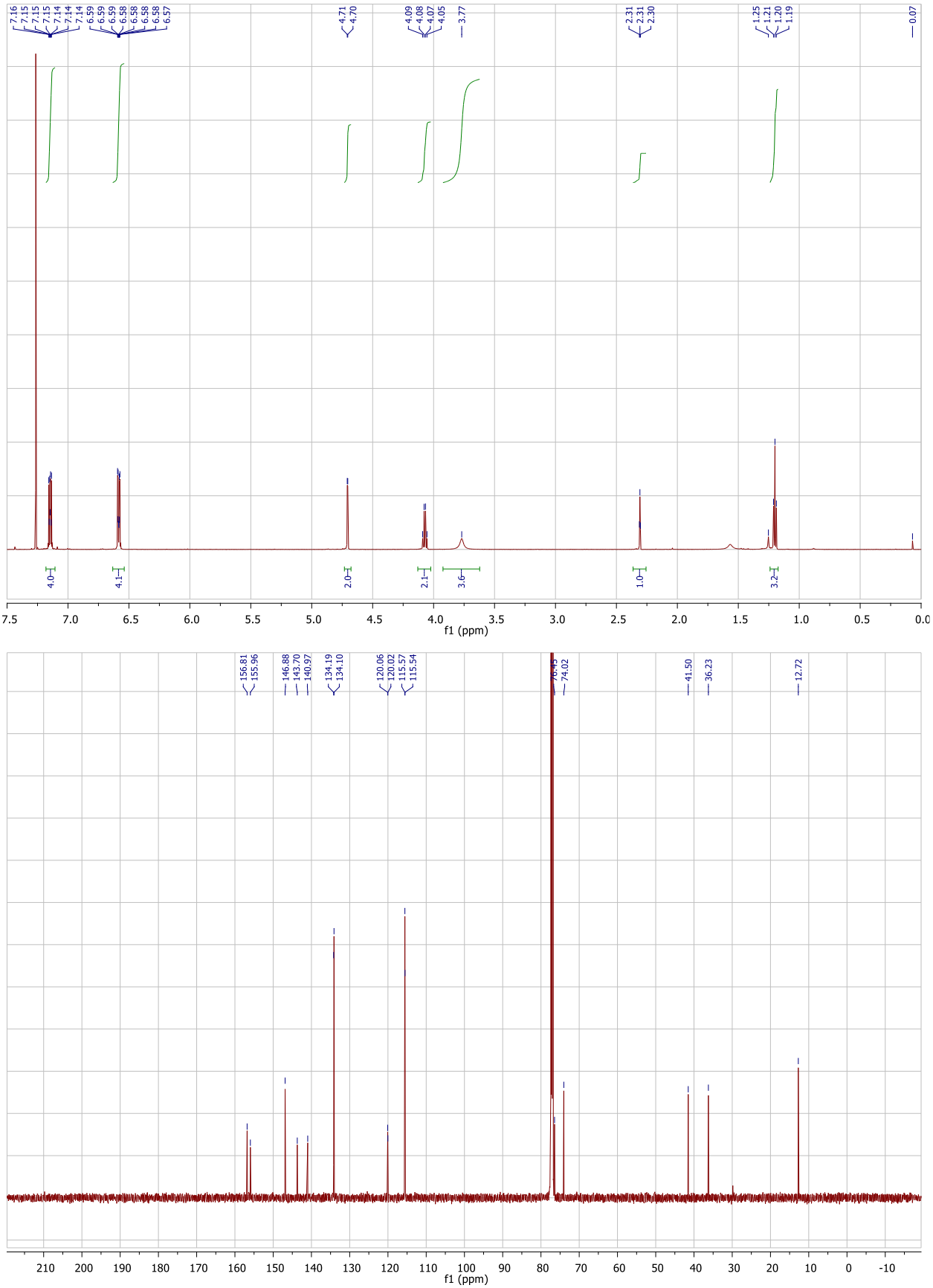

Figure **S12**. ^{1}H and ^{13}C NMR data for 4,5-bis((4-aminophenyl)thio)-1-ethyl-2-(prop-2-yn-1-yl)-1,2-dihydropyridazine-3,6-dione (**14**).

Tetramethyl 3,3',3'',3'''-((((((1-ethyl-3,6-dioxo-2-(prop-2-yn-1-yl)-1,2,3,6-tetrahydropyridazine-4,5-diyl)bis(sulfanediyl))bis(4,1-phenylene))bis(azanediyl))bis(3-oxopropane-3,1-diyl))bis(phosphanetriyl))tetrapropionate (Pyridazinedione 15)

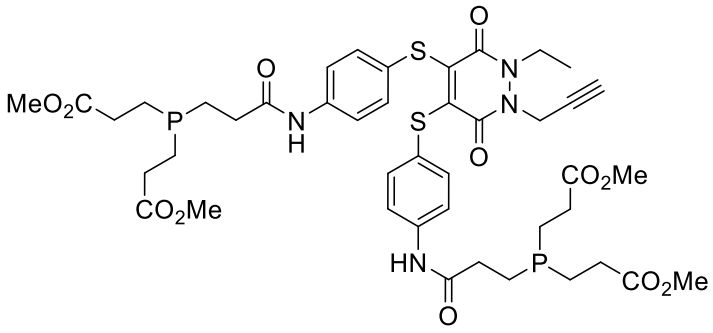

To a solution of 3-(bis(3-methoxy-3-oxopropyl)phosphanyl)propanoic acid **6** (170 mg, 0.61 mmol) in DMF (10 mL), was added HATU (232 mg, 0.61 mmol) and the reaction mixture stirred at 21 °C for 15 mins. After this time, to the reaction mixture was added 4,5-bis((4-aminophenyl)thio)-1-ethyl-2-(prop-2-yn-1-yl)-1,2-dihydropyridazine-3,6-dione (118 mg, 0.28 mmol) and the reaction mixture stirred for a further 5 mins. Following this, to the reaction mixture was added *N,N*-diisopropylethylamine (DIPEA) (195 µL, 1.12 mmol), and the mixture left to stirr at 21 °C for 12 h. After this time, the reaction mixture was diluted with EtOAc (20 mL) and washed with deionised water (3 × 10 mL) and brine (3 × 10 mL). The organic phase was then concentrated *in vacuo* and the crude residue purified by flash column chromatography (0–2% MeOH:CH_2Cl_2). The appropriate fractions were then combined and concentrated *in vacuo* to give pyridazinedione **15** (84 mg, 0.09 mmol, 32%) as a yellow oil. ^{1}H NMR (600 MHz, $CDCl_3$) δ 7.53–7.41 (m, 3H), 7.25–7.02 (m, 5H), 6.59 (d, *J* = 8.4 Hz, 2H), 4.82–4.65 (m, 3H), 4.21–3.94 (m, 4H), 3.80–3.59 (m, 12H), 2.99–1.74 (m, 24H), 1.33–1.16 (m, 6H); ^{13}C NMR (150 MHz, $CDCl_3$) δ 174.0 (C), 156.7 (C), 155.8 (C), 147.3 (C), 137.9 (C), 134.2 (C), 132.0 (CH), 120.0 (CH), 115.7 (CH), 76.3 (C), 74.2 (CH), 52.5 (CH_2), 52.1 (CH_2), 41.7 (CH_2), 36.3 (CH_2), 30.5 (CH_2), 29.8 (CH_2), 26.3 (CH_3), 23.8 (CH_2), 21.4 (CH_2), 12.8 (CH_3); IR (thin film) 3212, 2925, 2852, 2120, 1734, 1687, 1624, 1531, 1494 cm^{-1}; LRMS (ES+) 944 (100, $[M+H]^+$); HRMS (ES+) calcd for $C_{43}H_{54}N_4O_{12}P_2S_2$ $[M+H]^+$ 944.2655, observed 944.2651.

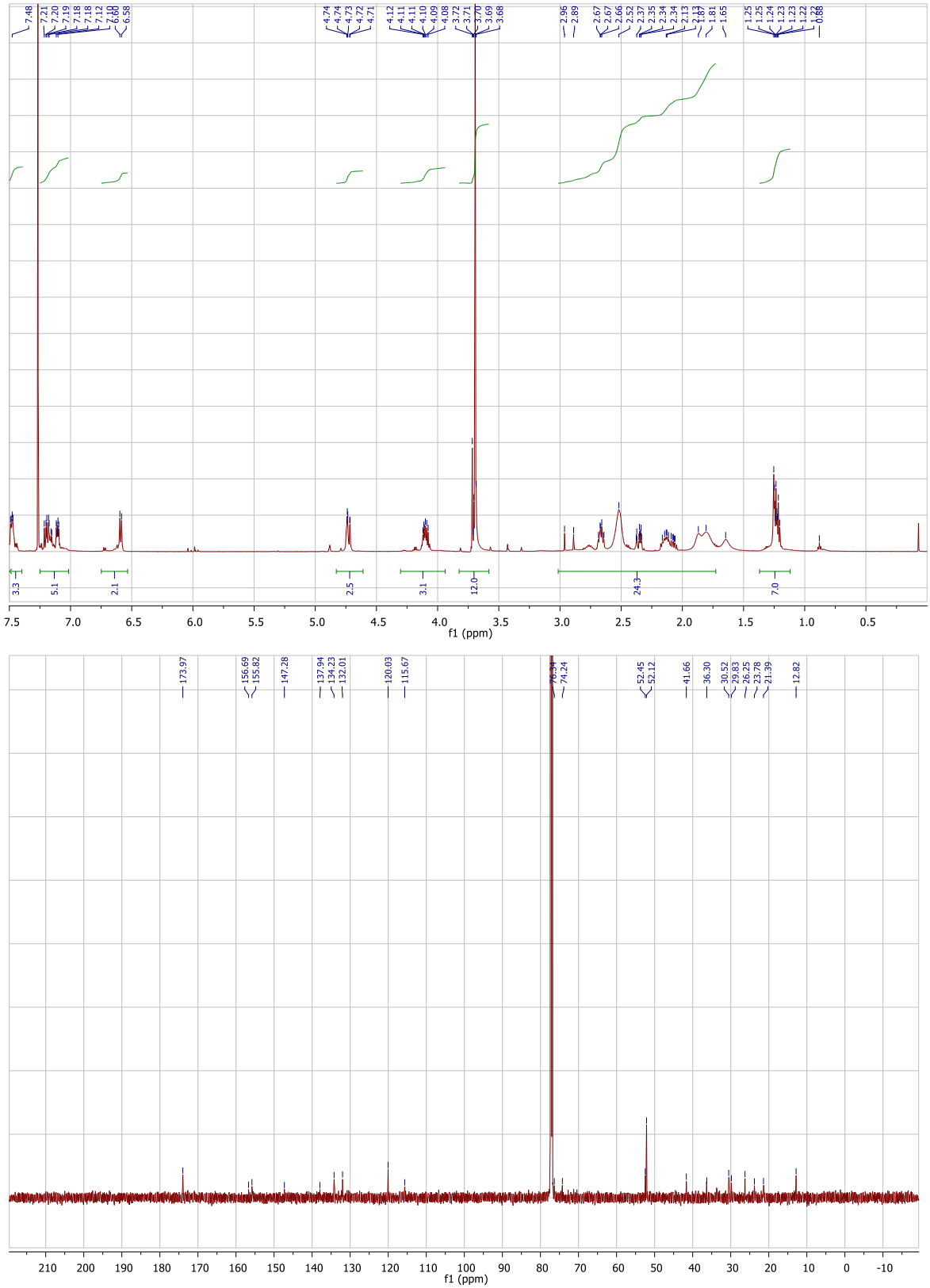

Figure **S13**. ^{1}H and ^{13}C NMR data for tetramethyl 3,3',3'',3'''-((((((1-ethyl-3,6-dioxo-2-(prop-2-yn-1-yl)-1,2,3,6-tetrahydropyridazine-4,5-diyl)bis(sulfanediyl))bis(4,1-phenylene))bis(azanediyl))bis(3-oxopropane-3,1-diyl))bis(phosphanetriyl))tetrapropionate (Pyridazinedione **15**).

5.1.2 Bioconjugation Reactions for Chapter 2

Trastuzumab Fab fragment (Fab fragment) preparation[83]

Preparation of Fab fragment using sequential digests with pepsin and papain

Immobilized pepsin (0.15 mL) was washed with digestion buffer (20 mM sodium acetate trihydrate, pH 3.1) four times and trastuzumab (0.5 mL, 6.41 mg·mL^{-1} in digestion buffer) was added. The mixture was incubated for 5 h at 37 °C whilst shaking (1100 rpm). The resin was separated from the digest using a filter column, and washed with digest buffer (50 mM phosphate, 1 mM EDTA, 150 mM NaCl, pH 6.8) three times. The digest was combined with the washes and the volume adjusted to 0.5 mL.

After this, immobilized papain (0.5 mL, 0.25 mg·mL^{-1}) was activated with 10 mM DTT (in digest buffer: 50 mM phosphate, 1 mM EDTA, 150 mM NaCl, pH 6.8) whilst shaking (1100 rpm) for 1 h at 37 °C. The resin was washed with digest buffer (without DTT) four times and the 0.5 mL of Herceptin-F(ab')$_2$ added. The mixture was incubated for 16 h at 37 °C whilst shaking (1100 rpm). Then the resin was separated from the digest using a filter column, and washed with BBS (25 mM sodium borate, 25 mM NaCl, 0.5 mM EDTA, pH 8.0) three times. The digest was combined with the washes and the buffer was exchanged completely for BBS using diafiltration columns (GE Healthcare, 10000 MWCO) and the volume adjusted to 0.5 mL. The digest was analysed by SDS-PAGE and LCMS to reveal formation of a single trastuzumab Fab fragment: observed mass 47585. The concentration of the Fab fragment was determined by UV/VIS using a molecular extinction coefficient of ε_{280} = 68590 M^{-1}·cm^{-1}. [Fab-Her fragment] 2.6 mg·mL^{-1} (0.5 mL), 62%.

Bioconjugation reactions involving Fab fragment of Herceptin

Control for untreated Fab fragment of Herceptin for experiments using pyridazinediones 7 and 10

(a)

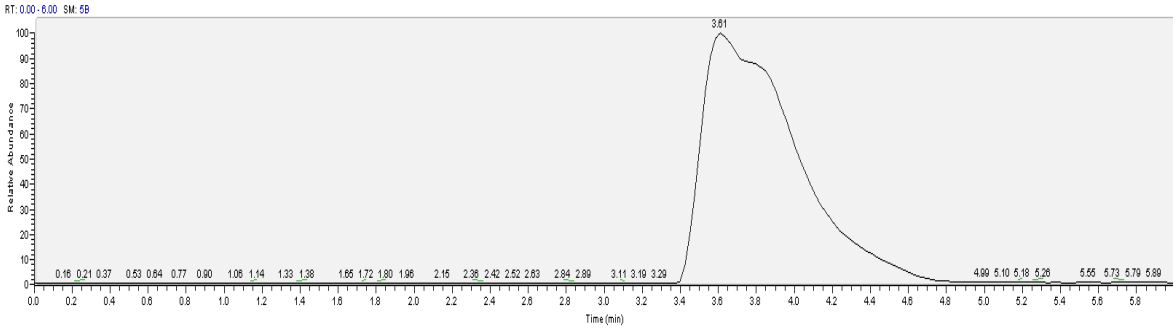

(b)

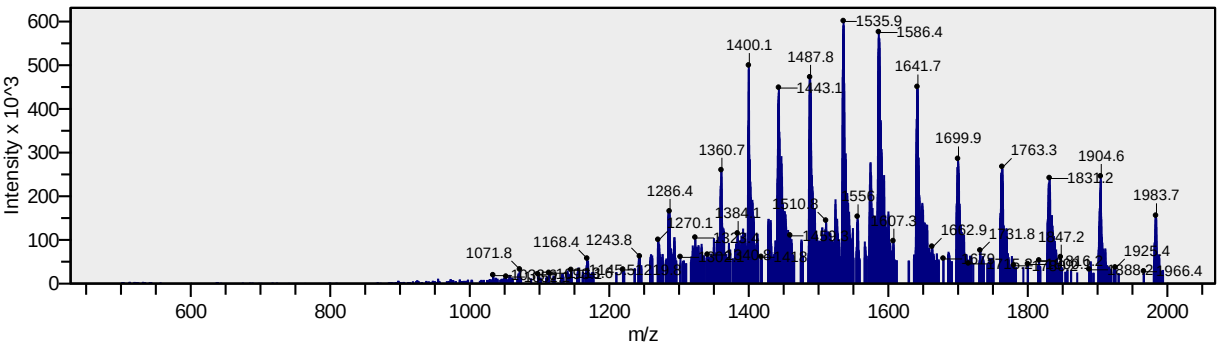

(c)

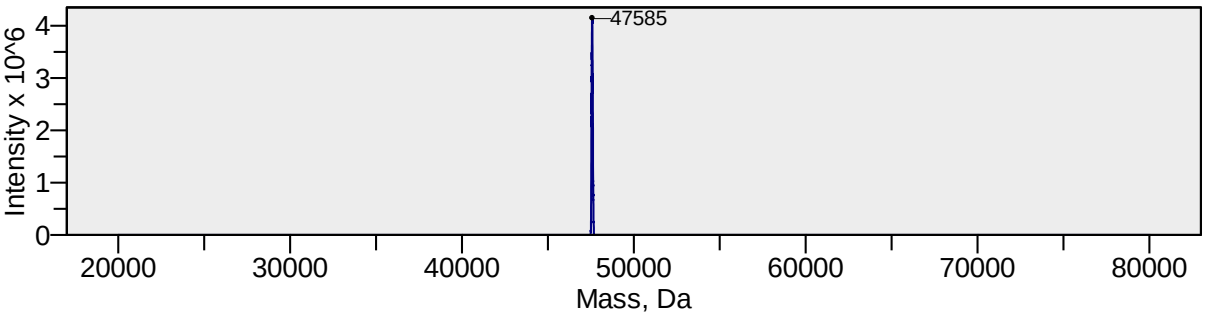

Figure **S14**. (a) TIC, (b) non-deconvoluted and (c) deconvoluted MS data for untreated Fab fragment of Herceptin for experiments using pyridazinediones **7** and **10**.

Reaction of Fab fragment of Herceptin with pyridazinedione 7 (1.25 eq.)

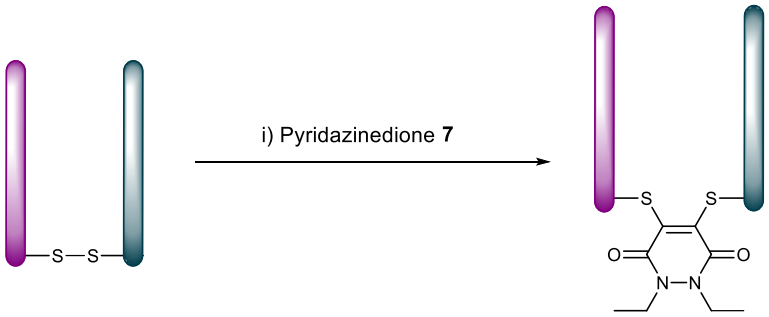

Pyridazinedione **7** (0.56 µL, 2.0 mM in DMF, 1.25 eq) was added to Fab fragment of Herceptin (30 µL, 1.4 mg/mL, 30 µM) in BBS (25 mM sodium borate, 25 mM NaCl, 0.5 mM EDTA, pH 8.0). The reaction mixture was incubated at 37 °C for 1 h. Excess reagents were removed by repeated diafiltration into deionised water using VivaSpin sample concentrators (GE Healthcare, 10,000 MWCO). The samples were analysed by LCMS. Expected mass: 47,751 Da. Observed mass: 47,755 Da.

(a)

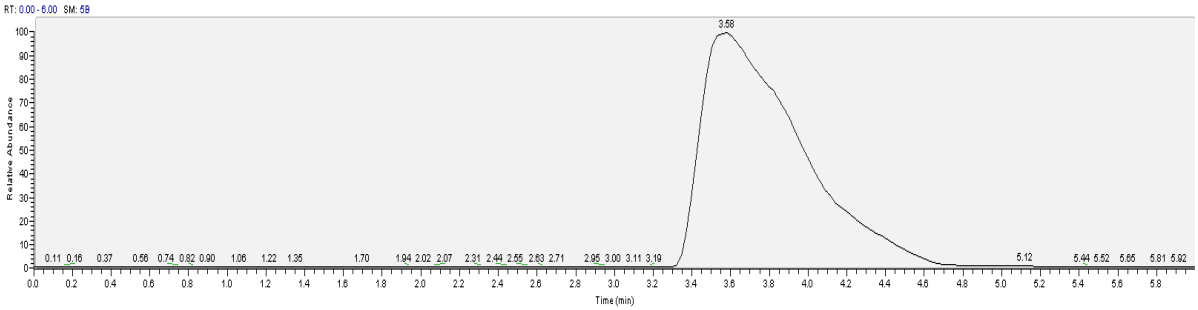

(b)

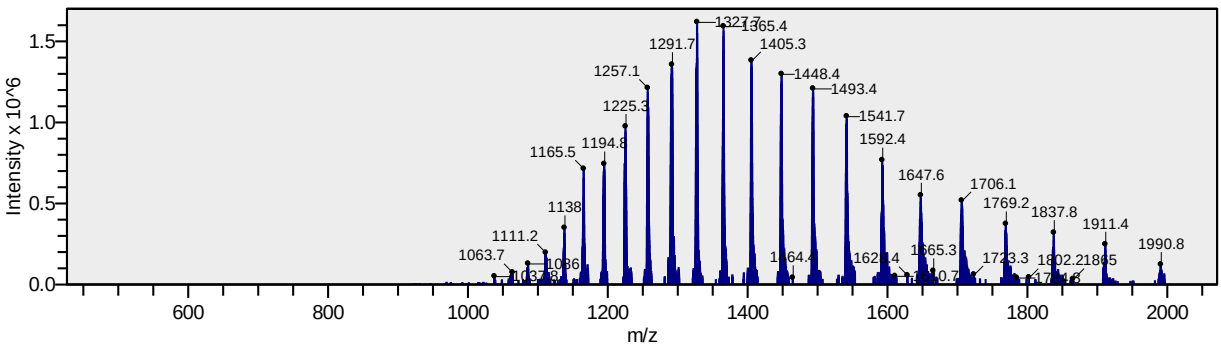

(c)

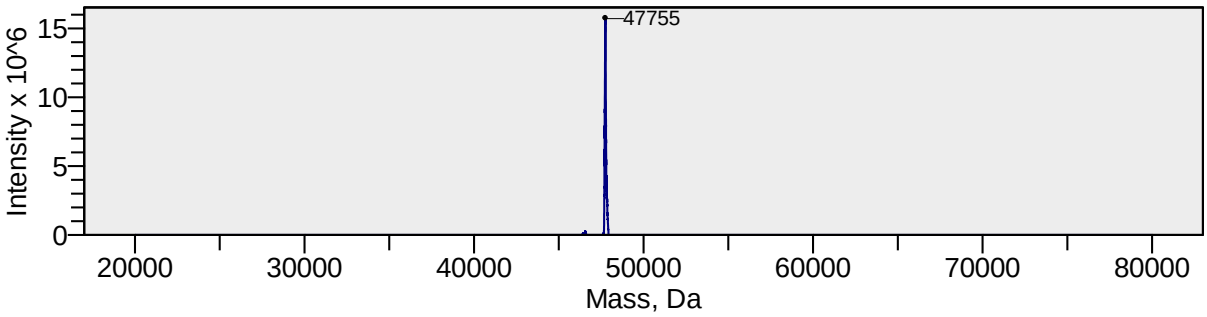

Figure **S15**. (a) TIC, (b) non-deconvoluted and (c) deconvoluted MS data for Fab fragment of Herceptin reacted with pyridazinedione **7** (1.25 eq.).

Reaction of Fab fragment of Herceptin with pyridazinedione 7 (2 eq.)

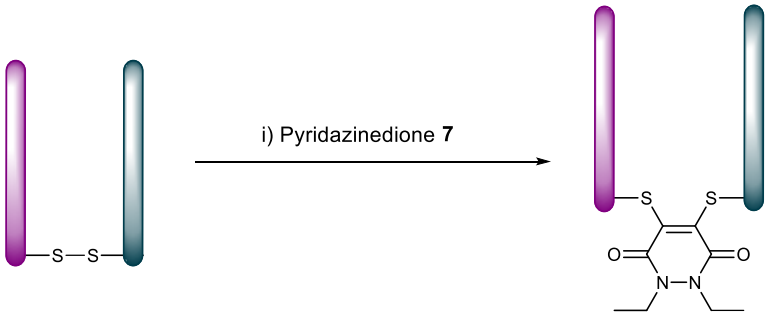

Pyridazinedione **7** (0.9 µL, 2.0 mM in DMF, 2 eq) was added to Fab fragment of Herceptin (30 µL, 1.4 mg/mL, 30 µM) in BBS (25 mM sodium borate, 25 mM NaCl, 0.5 mM EDTA, pH 8.0). The reaction mixture was incubated at 37 °C for 1 h. Excess reagents were removed by repeated diafiltration into deionised water using VivaSpin sample concentrators (GE Healthcare, 10,000 MWCO). The samples were analysed by LCMS. Expected mass: 47,751 Da. Observed mass: 47,743 Da.

(a)

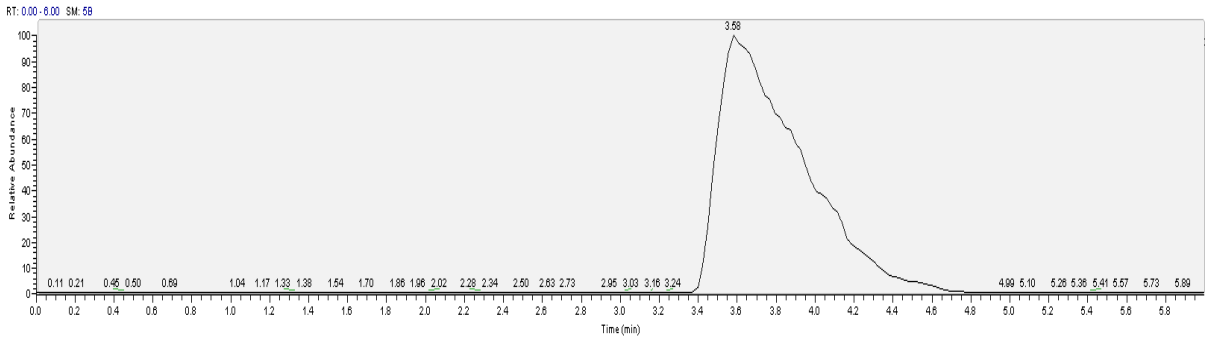

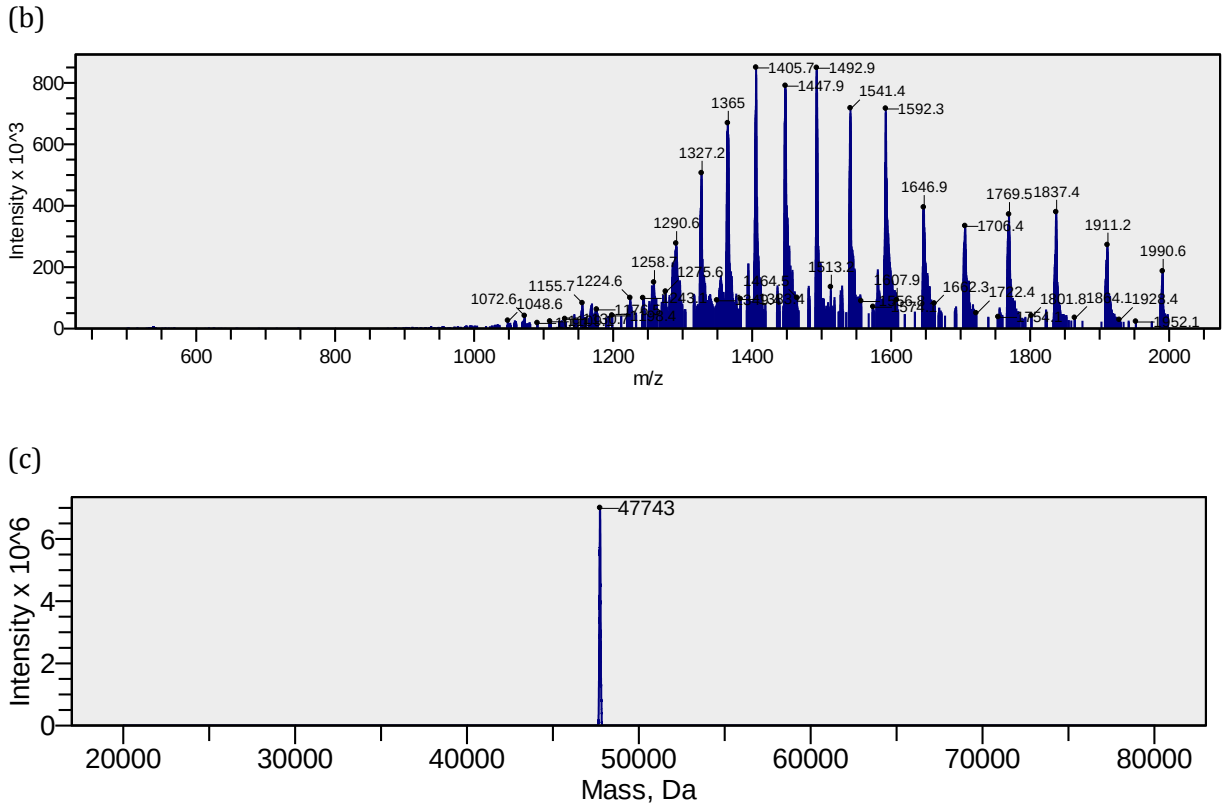

Figure **S16**. (a) TIC, (b) non-deconvoluted and (c) deconvoluted MS data for Fab fragment of Herceptin reacted with pyridazinedione **7** (2 eq.).

Reaction of Fab-Her fragment with pyridazinedione 7 (5 eq.)

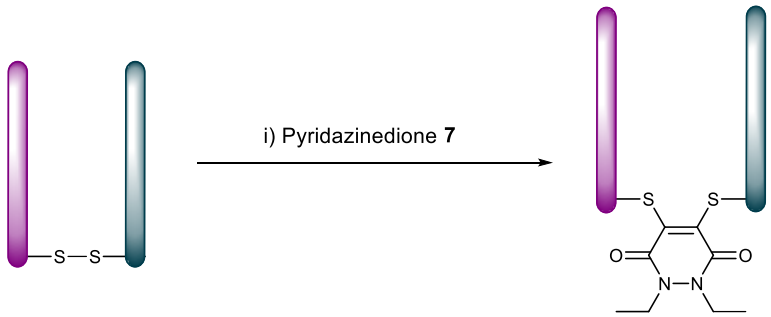

Pyridazinedione **7** (2.3 µL, 2.0 mM in DMF, 5 eq) was added to Fab fragment of Herceptin (30 µL, 1.4 mg/mL, 30 µM) in BBS (25 mM sodium borate, 25 mM NaCl, 0.5 mM EDTA, pH 8.0). The reaction mixture was incubated at 37 °C for 1 h. Excess reagents were removed by repeated diafiltration into deionised water using VivaSpin sample concentrators (GE Healthcare, 10,000 MWCO). The samples were analysed by LCMS. Expected mass: 47,751 Da. Observed mass: 47,753 Da.

(a)

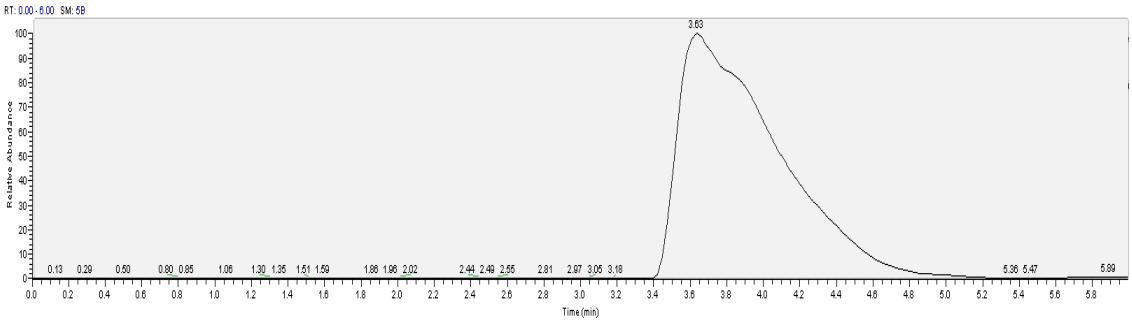

(b)

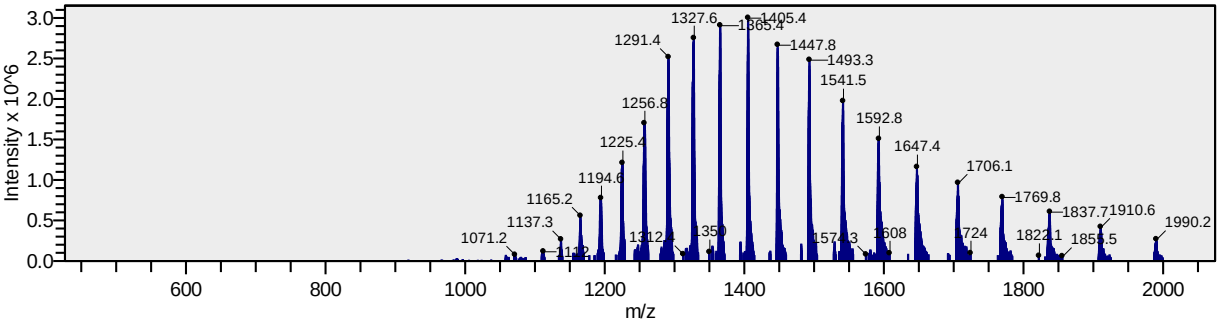

(c)

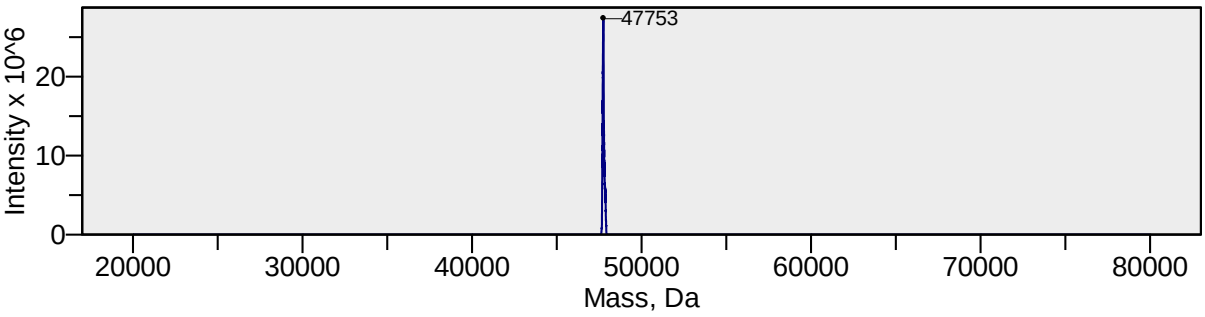

Figure **S17**. (a) TIC, (b) non-deconvoluted and (c) deconvoluted MS data for Fab fragment of Herceptin reacted with pyridazinedione **7** (5 eq.).

Reaction of Fab fragment of Herceptin with pyridazinedione 7 (10 eq.)

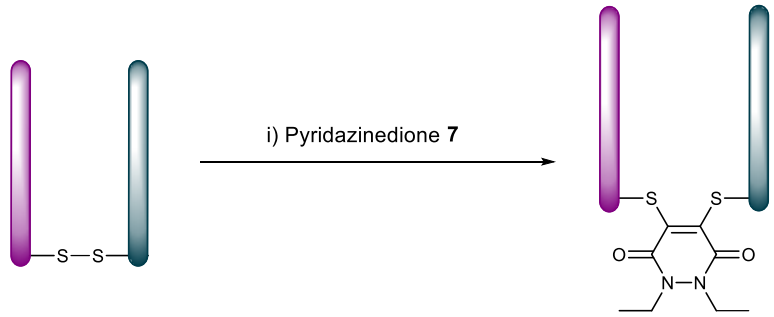

Pyridazinedione **7** (4.5 µL, 2.0 mM in DMF, 10 eq) was added to Fab fragment of Herceptin (30 µL, 1.4 mg/mL, 30 µM) in BBS (25 mM sodium borate, 25 mM NaCl, 0.5 mM EDTA, pH 8.0). The reaction mixture was incubated at 37 °C for 1 h. Excess reagents were removed by repeated diafiltration into deionised water using VivaSpin sample concentrators (GE Healthcare, 10,000 MWCO). The samples were analysed by LCMS. Expected mass: 47,751 Da. Observed mass: 47,750 Da.

(a)

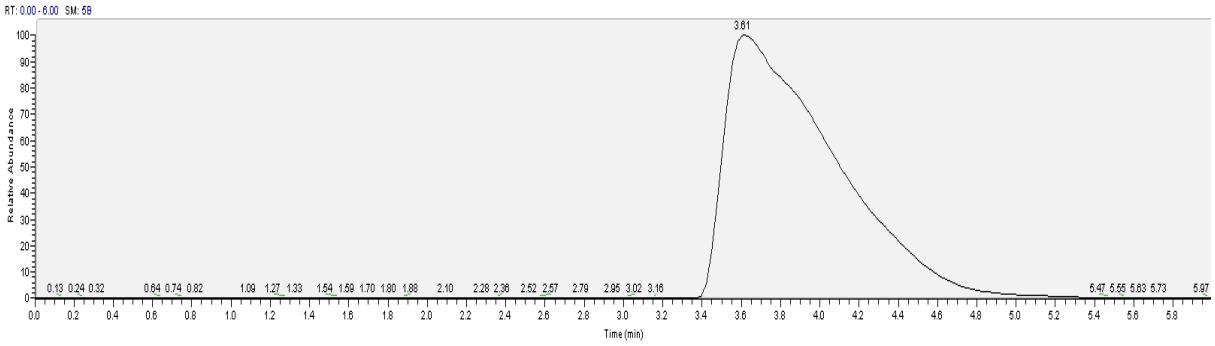

(b)

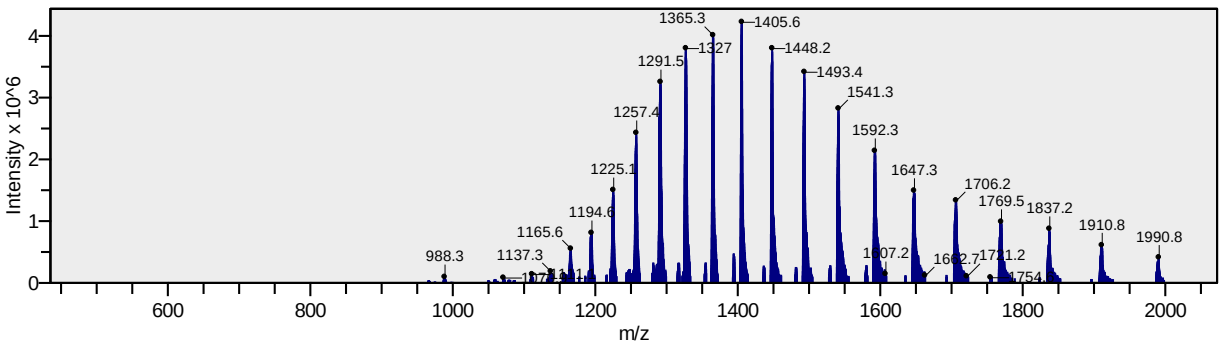

(c)

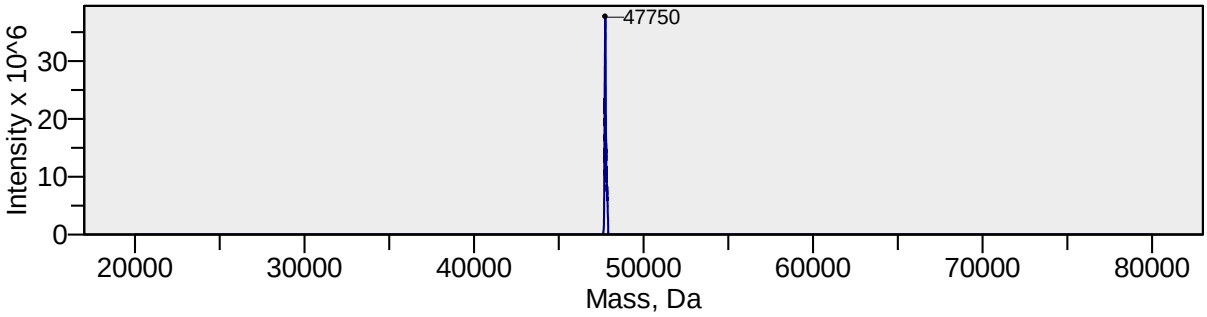

Figure **S18**. (a) TIC, (b) non-deconvoluted and (c) deconvoluted MS data for Fab fragment of Herceptin reacted with pyridazinedione **7** (10 eq.).

Reduction of Fab fragment of Herceptin and subsequent reaction with pyridazinedione 10

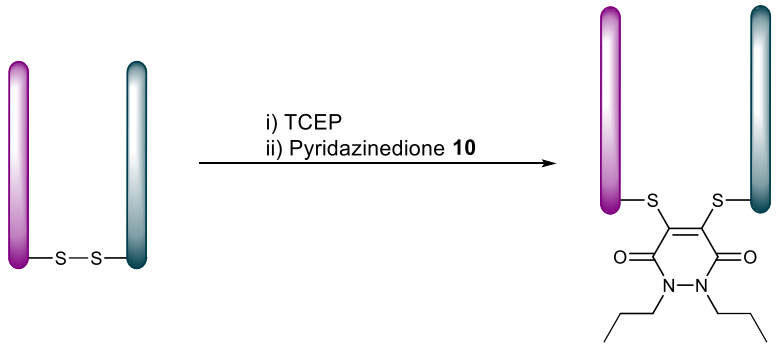

TCEP (4.5 µL, 2.0 mM, 10 eq) was added to the Fab fragment of Herceptin (30 µL, 1.4 mg/mL, 30 µM) in BBS (25 mM sodium borate, 25 mM NaCl, 0.5 mM EDTA, pH 8.0). The reaction was incubated at 37 °C for 1 h. Excess reagents were removed by repeated diafiltration into fresh BBS (25 mM sodium borate, 25 mM NaCl, 0.5 mM EDTA, pH 8.0) using VivaSpin sample concentrators (GE Healthcare, 10,000 MWCO). Pyridazinedione **10** (4.5 µL, 2.0 mM, 10 eq) was subsequently added to the reaction mixture and incubated at 37 °C for 1 h. Excess reagents were removed by repeated diafiltration into deionised water using VivaSpin sample concentrators (GE Healthcare, 10,000 MWCO). The samples were analysed by LCMS. Expected mass: 47,779 Da. Observed mass: 47,782 Da.

(a)

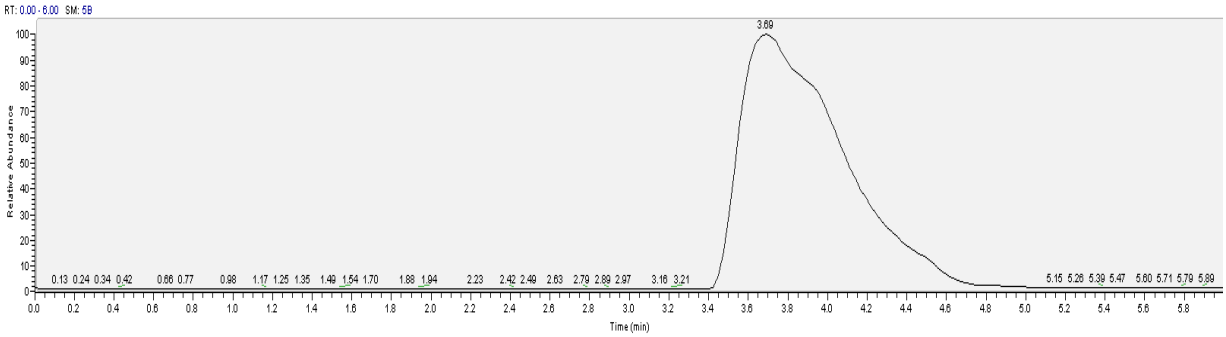

(b)

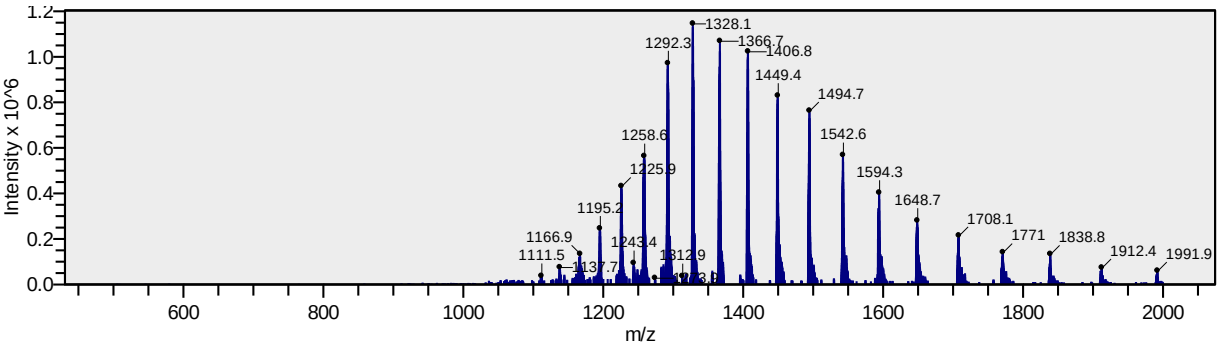

(c)

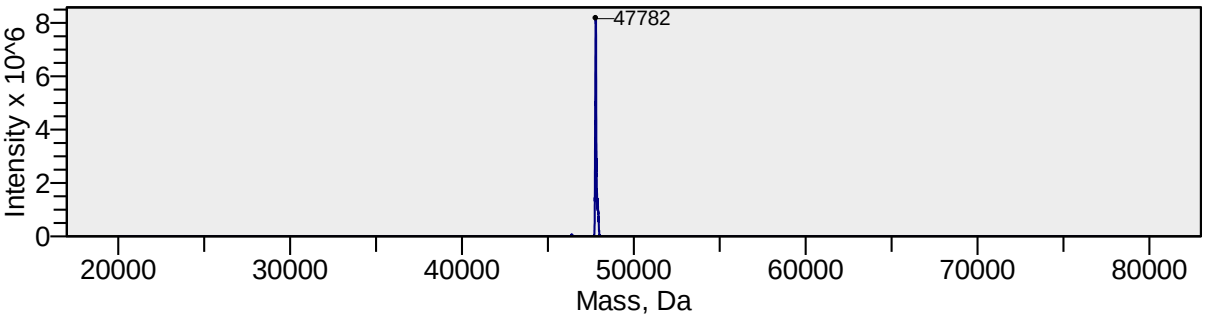

Figure **S19**. (a) TIC, (b) non-deconvoluted and (c) deconvoluted MS data for Fab fragment of Herceptin reacted with pyridazinedione **10**.

Reaction of Fab fragment of Herceptin with pyridazinedione 7 (2 eq.) in the presence of pre-incubated pyridazinedione 10 (1 eq.)

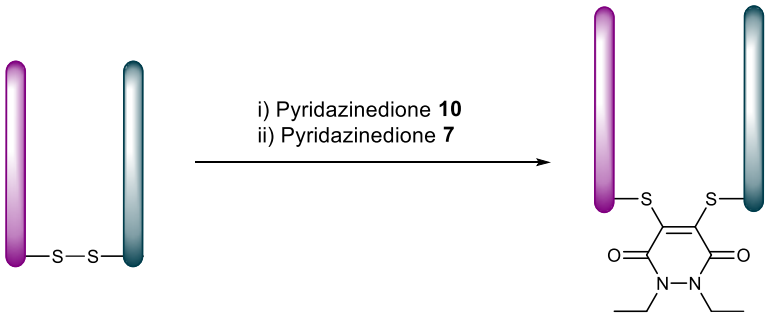

Pyridazinedione **7** (0.9 µL, 2.0 mM in DMF, 2 eq) was added to Fab fragment of Herceptin (30 µL, 1.4 mg/mL, 30 µM) in BBS (25 mM sodium borate, 25 mM NaCl, 0.5 mM EDTA, pH 8.0), which had been pre-incubated at 37 °C for 0.5 h with pyridazinedione **10** (0.45 µL, 2.0 mM in DMF, 1 eq). The reaction mixture was incubated further at 37 °C for 1 h. Excess reagents were removed by repeated diafiltration into deionised water using VivaSpin sample concentrators (GE Healthcare, 10,000 MWCO). The samples were analysed by LCMS. Expected mass: 47,751 Da. Observed mass: 47,745 Da.

(a)

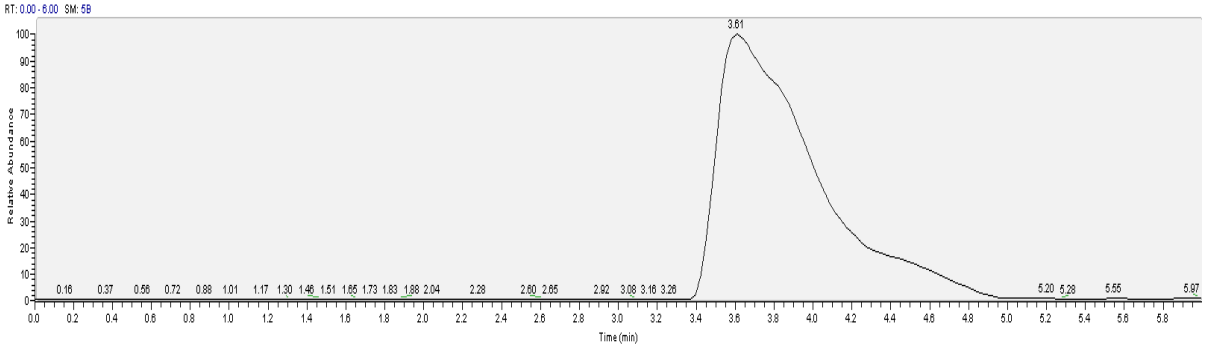

(b)

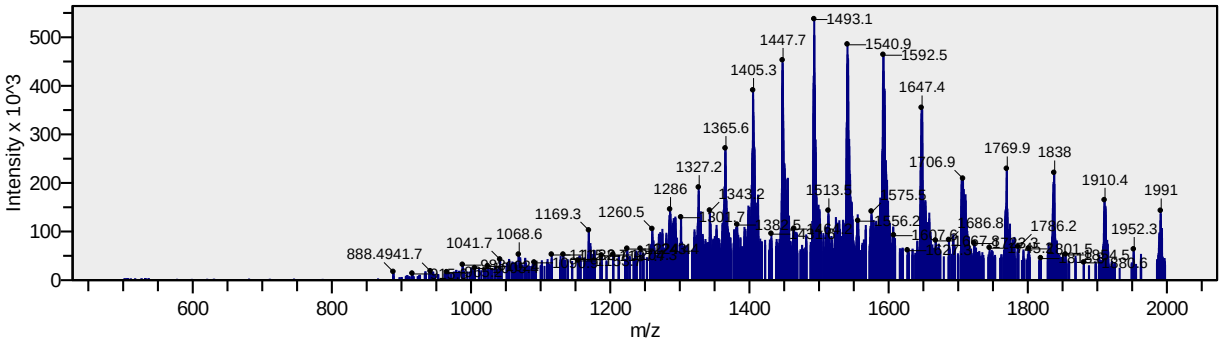

(c)

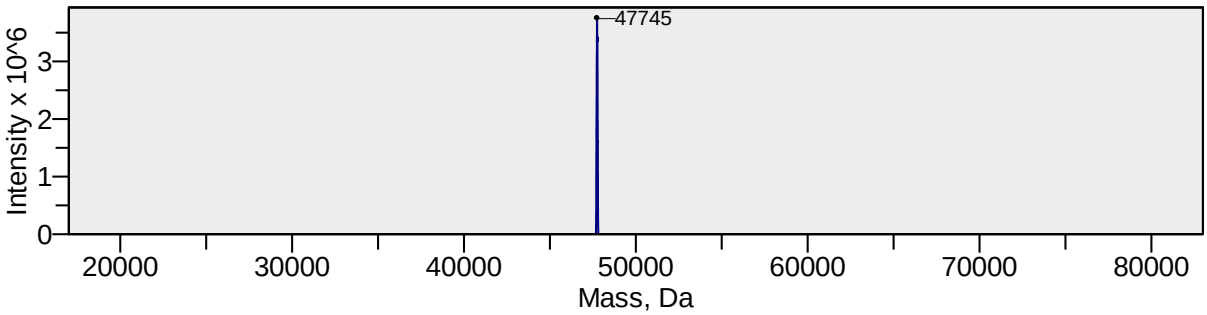

Figure **S20**. (a) TIC, (b) non-deconvoluted and (c) deconvoluted MS data for Fab fragment of Herceptin reacted with pyridazinedione **7** in the presence of pyridazinedione **10** (ratio of **7**:**10** = 2:1).

Reaction of Fab fragment of Herceptin with pyridazinedione 7 (2 eq.) in the presence of pre-incubated pyridazinedione 10 (2 eq.)

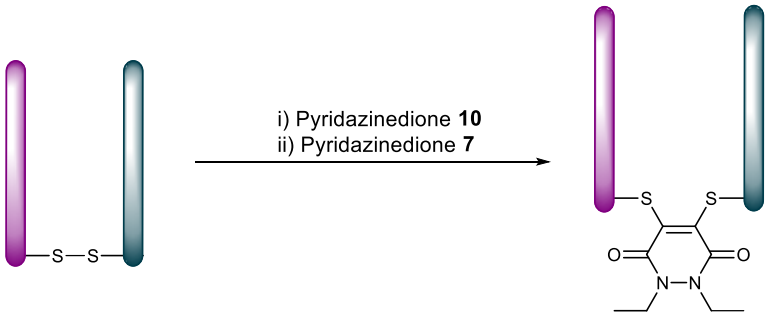

Pyridazinedione **7** (0.9 µL, 2.0 mM in DMF, 2 eq) was added to Fab fragment of Herceptin (30 µL, 1.4 mg/mL, 30 µM) in BBS (25 mM sodium borate, 25 mM NaCl, 0.5 mM EDTA, pH 8.0), which had been pre-incubated at 37 °C for 0.5 h with pyridazinedione **10** (0.9 µL, 2.0 mM in DMF, 2 eq). The reaction mixture was incubated further at 37 °C for 1 h. Excess reagents were removed by repeated diafiltration into deionised water using VivaSpin sample concentrators (GE Healthcare, 10,000 MWCO). The samples were analysed by LCMS. Expected mass: 47,751 Da. Observed mass: 47,749 Da.

(a)

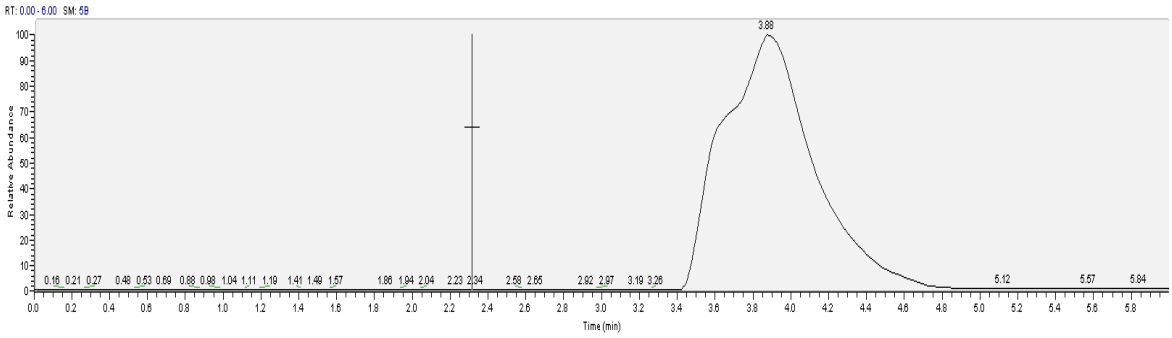

(b)

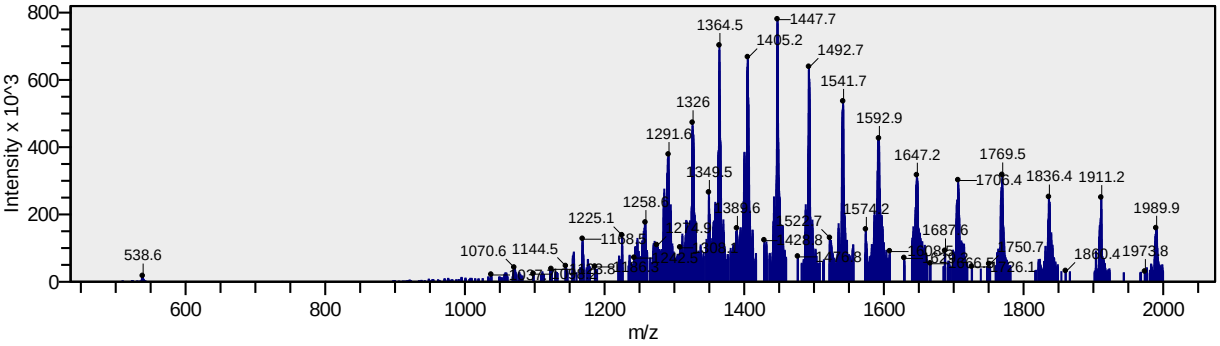

(c)

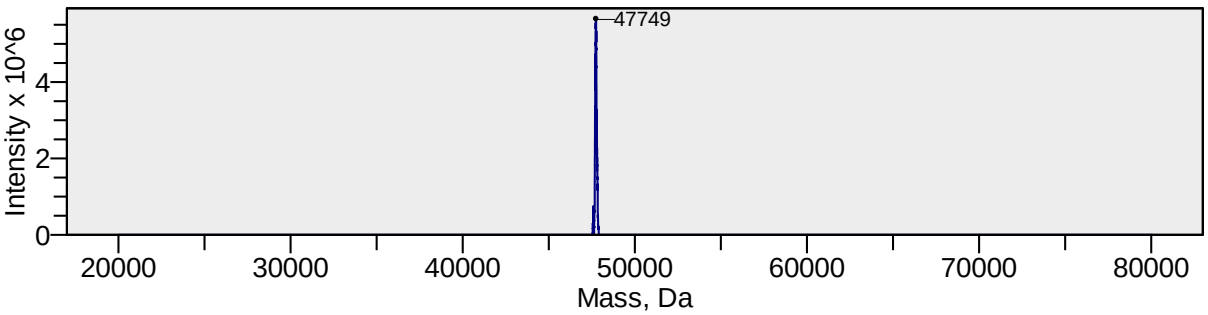

Figure **S21**. (a) TIC, (b) non-deconvoluted and (c) deconvoluted MS data for Fab fragment of Herceptin reacted with pyridazinedione **7** in the presence of pyridazinedione **10** (ratio of **7**:**10** = 2:2).

Reaction of Fab fragment of Herceptin with pyridazinedione 7 (2 eq.) in the presence of pre-incubated pyridazinedione 10 (5 eq.)

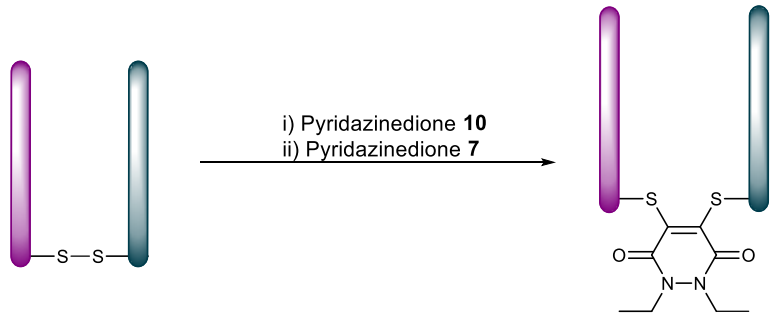

Pyridazinedione **7** (0.9 µL, 2.0 mM in DMF, 2 eq) was added to Fab fragment of Herceptin (30 µL, 1.4 mg/mL, 30 µM) in BBS (25 mM sodium borate, 25 mM NaCl, 0.5 mM EDTA, pH 8.0), which had been pre-incubated at 37 °C for 0.5 h with pyridazinedione **10** (2.3 µL, 2.0 mM in DMF, 5 eq). The reaction mixture was incubated further at 37 °C for 1 h. Excess reagents were removed by repeated diafiltration into deionised water using VivaSpin sample concentrators (GE Healthcare, 10,000 MWCO). The samples were analysed by LCMS. Expected mass: 47,751 Da. Observed mass: 47,751 Da.

(a)

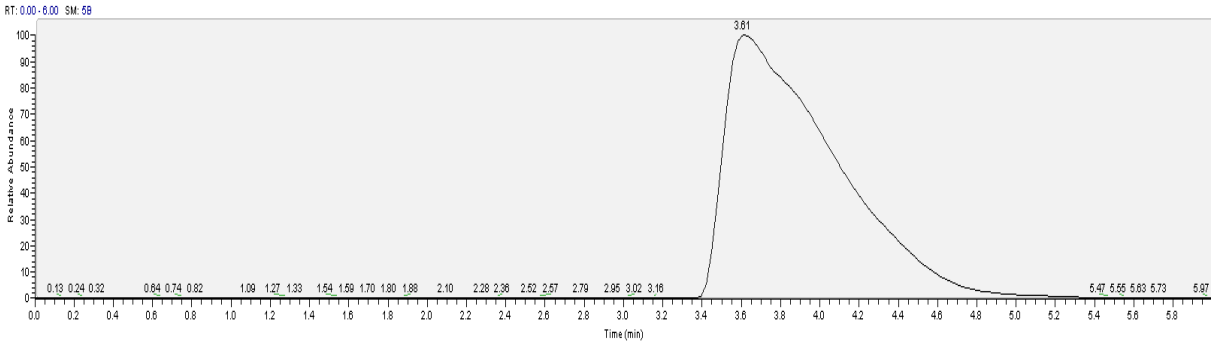

(b)

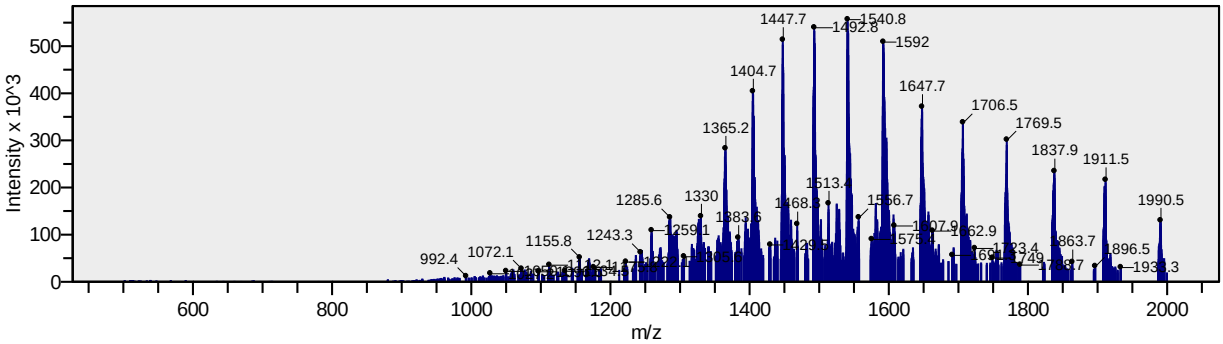

(c)

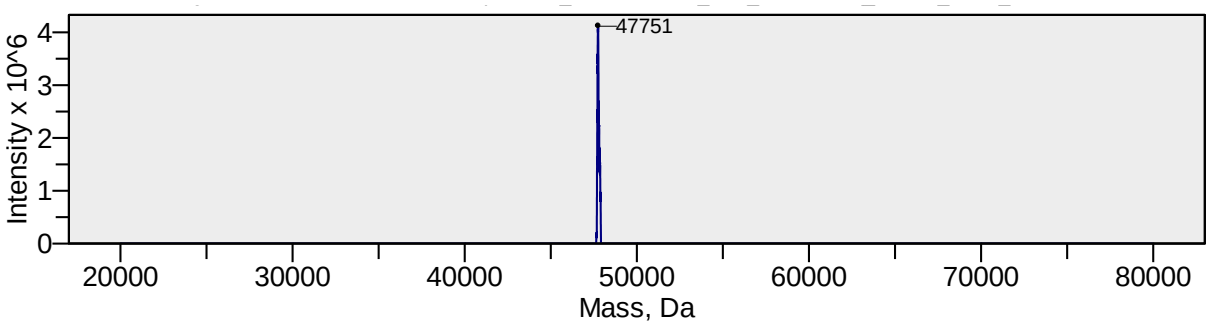

Figure **S22**. (a) TIC, (b) non-deconvoluted and (c) deconvoluted MS data for Fab fragment of Herceptin reacted with pyridazinedione **7** in the presence of pyridazinedione **10** (ratio of **7**:**10** = 2:5).

Reduction of Fab fragment of Herceptin and subsequent reaction with pyridazinedione 10 and pyridazinedione 7 (1:1 ratio 0.5 eq.:0.5 eq)

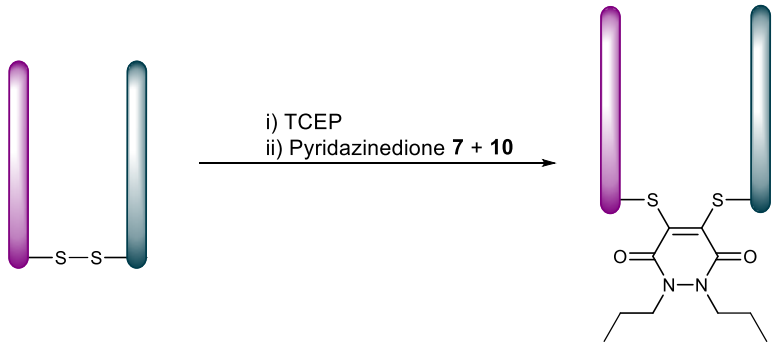

TCEP (4.5 µL, 2.0 mM, 10 eq) was added to the Fab fragment of Herceptin (30 µL, 1.4 mg/mL, 30 µM) in BBS (25 mM sodium borate, 25 mM NaCl, 0.5 mM EDTA, pH 8.0). The reaction was incubated at 37 °C for 1.0 h. Excess reagents were removed by repeated diafiltration into fresh BBS (25 mM sodium borate, 25 mM NaCl, 0.5 mM EDTA, pH 8.0) using VivaSpin sample concentrators (GE Healthcare, 10,000 MWCO). Pre-mixed pyridazinediones **7** and **10** ([1.1 µL, 0.2 mM in DMF, 0.5 eq] each) were subsequently added to the reaction mixture and incubated at 37 °C for 1.0 h. Excess reagents were removed by repeated diafiltration into deionised water using VivaSpin sample concentrators (GE Healthcare, 10,000 MWCO). The samples were analysed by LCMS. Expected mass: 47,751 Da [Fab fragment reacted with pyridazinedione **7**] and 47,779 Da [Fab fragment reacted with pyridazinedione **10**]. Observed mass:47,585 Da [unreacted Fab fragment], 47,746 Da [Fab fragment reacted with pyridazinedione **7**] and 47,776 Da [Fab fragment reacted with pyridazinedione **10**].

(a)

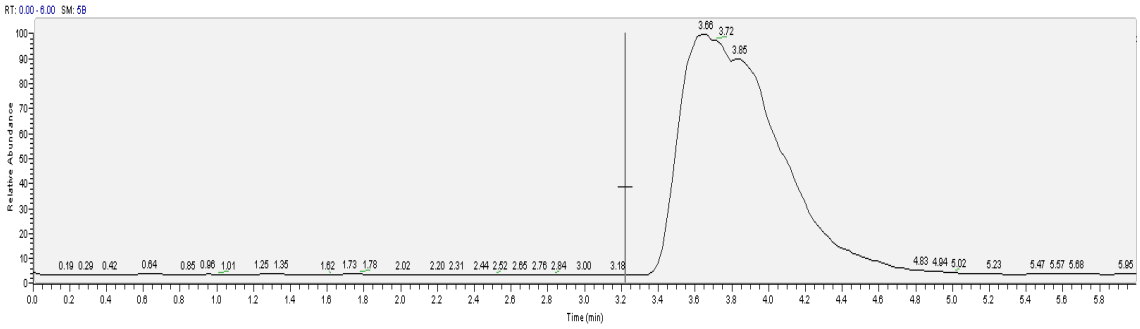

(b)

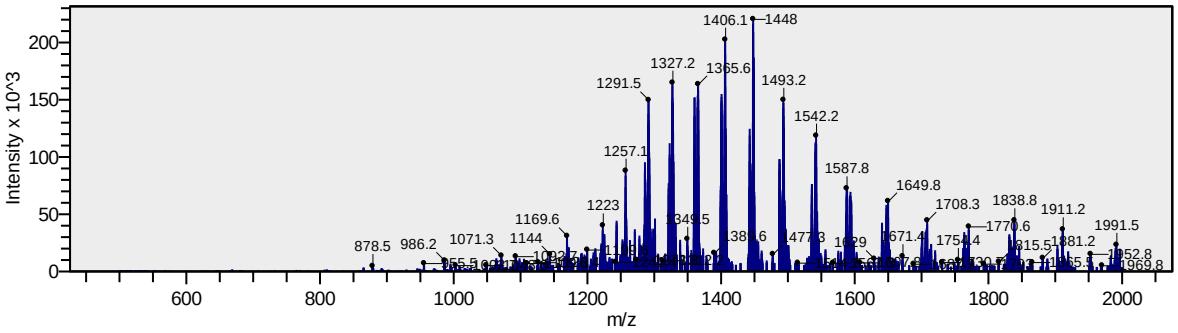

(c)

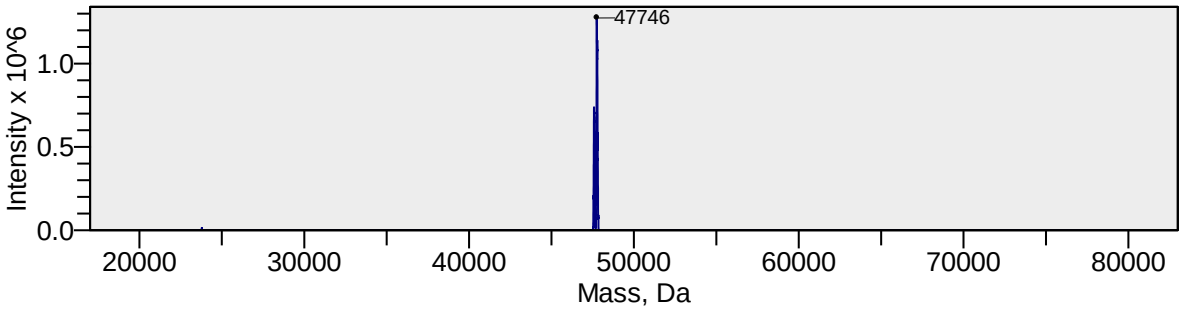

(d)

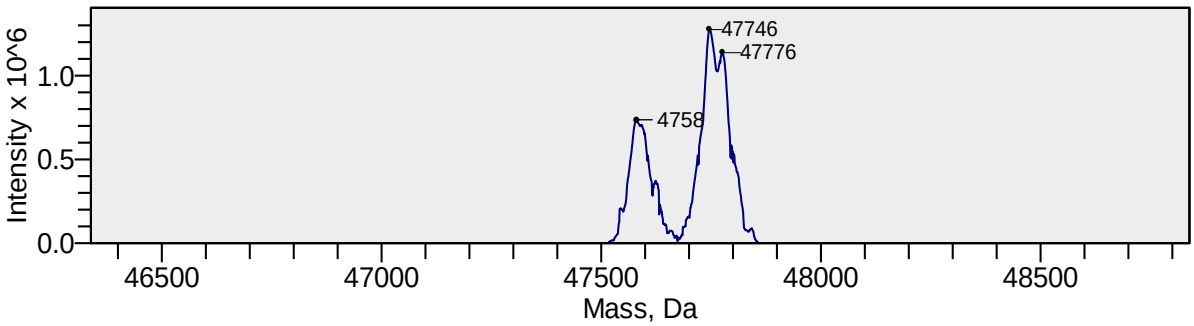

Figure **S23**. (a) TIC, (b) non-deconvoluted, (c) deconvoluted MS data over range 20,000–80,000 Da and (d) deconvoluted data over range 46,500–48,500 Da for reduction of Fab fragment of Herceptin and subsequent reaction with pyridazinedione **7** and pyridazinedione **10** (1:1 ratio 0.5 eq.:0.5 eq).

Reaction of Octreotide peptide with pyridazinedione 7 (1.25 eq.)

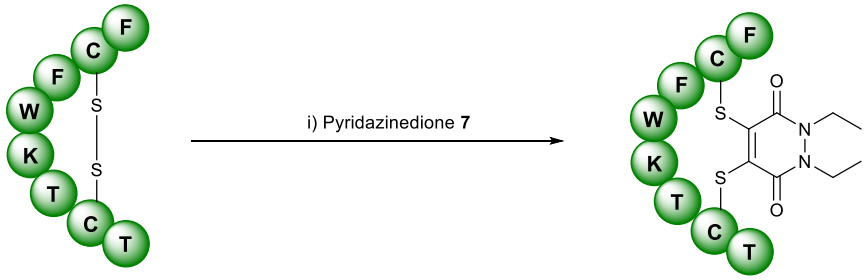

Pyridazinedione **7** (0.56 µL, 2.0 mM in DMF, 1.25 eq) was added to octreotide (30 µL, 30 µg/mL, 30 µM) in peptide buffer (40% MeCN, 2.5% DMF, 57.5% phosphate buffer [50 mM, pH 6.2]). The reaction mixture was incubated at 37 °C for 1 h. The samples were analysed by LCMS. Expected mass: 1185 Da. Observed mass: 1184 Da.

(a)

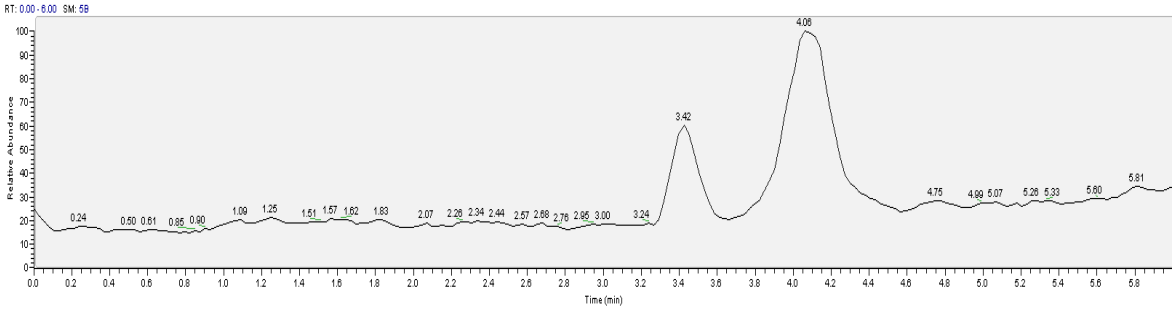

(b)

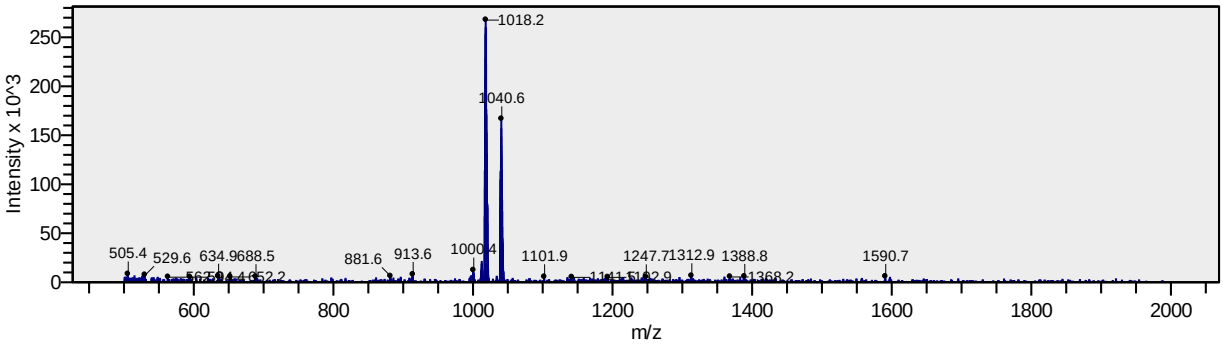

(c)

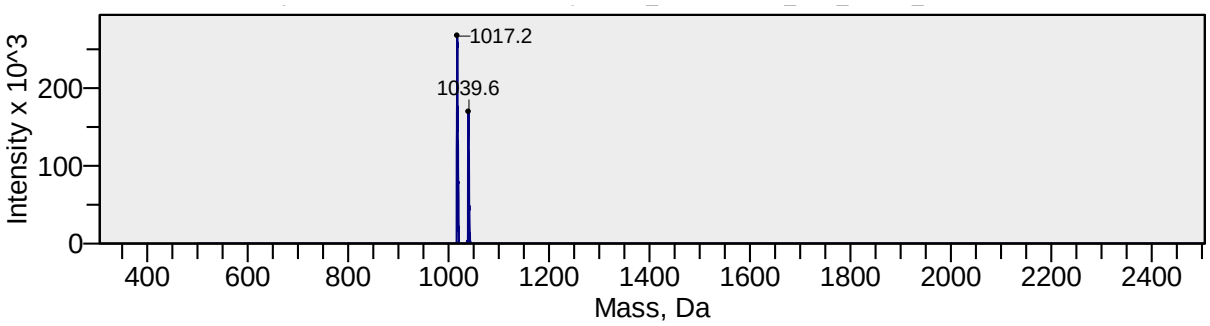

(d)

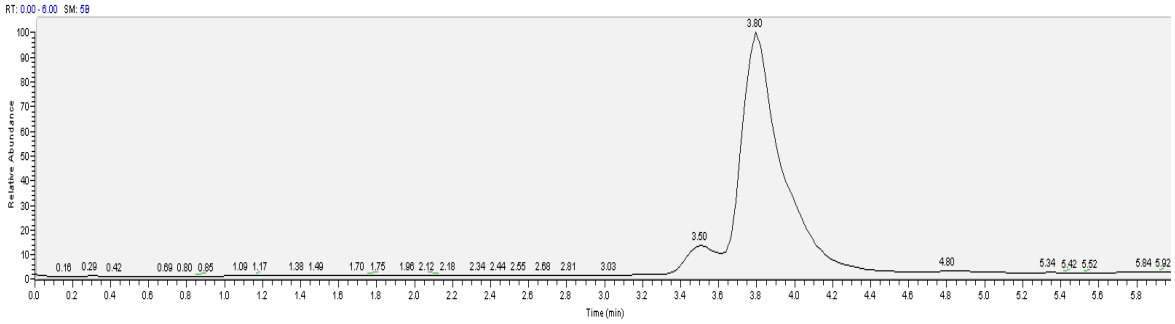

(e)

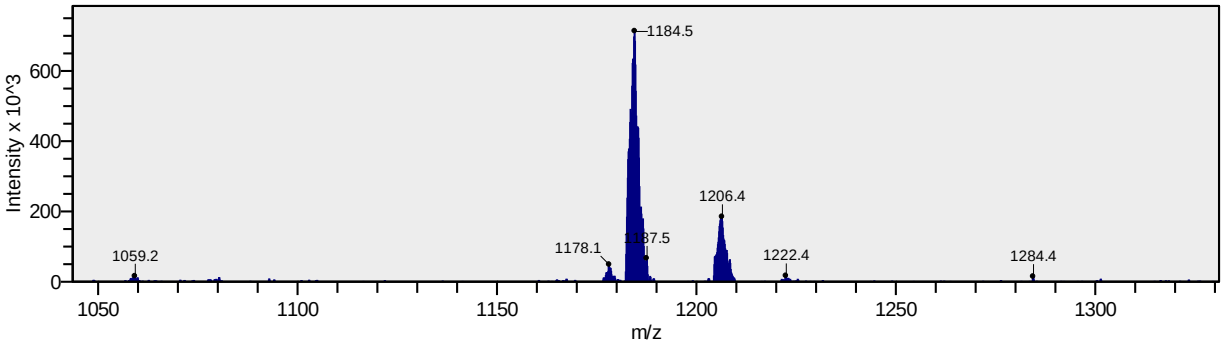

(f)

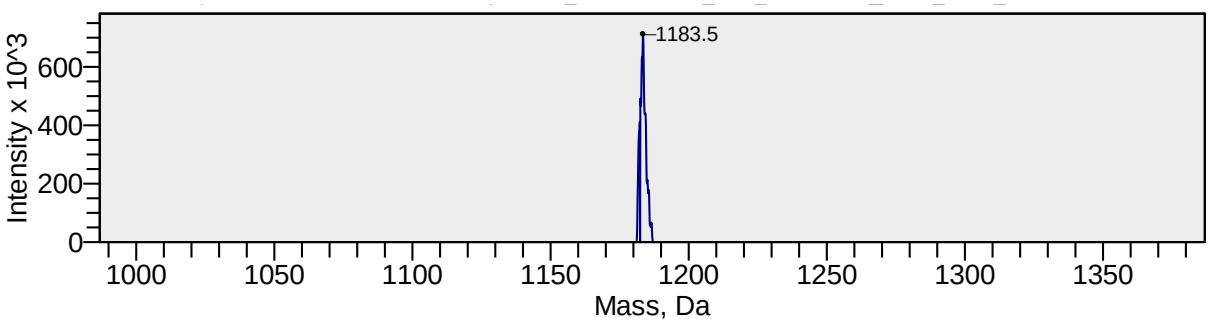

Figure **S24**. (a) TIC, (b) non-deconvoluted and (c) deconvoluted MS data for native octreotide; (d) TIC, (e) non-deconvoluted and (f) deconvoluted MS data for modified octreotide.

Reaction of Somatostatin peptide with pyridazinedione 7(1.25 eq.)

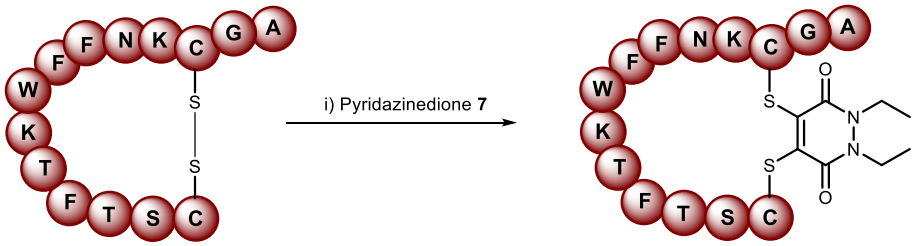

Pyridazinedione **7** (0.56 µL, 2.0 mM in DMF, 1.25 eq) was added to somatostatin (30 µL, 30 µg/mL, 30 µM) in peptide buffer (40% MeCN, 2.5% DMF, 57.5% phosphate buffer [50 mM, pH 6.2]) The reaction mixture was incubated at 37 °C for 1 h. The samples were analysed by MALDI-TOF. Expected mass: 1,804 Da. Observed mass: 1,808 Da $[M+H]^+$, 1,830 Da $[M+Na]^+$, 1,847 Da $[M+K]^+$.

(a)

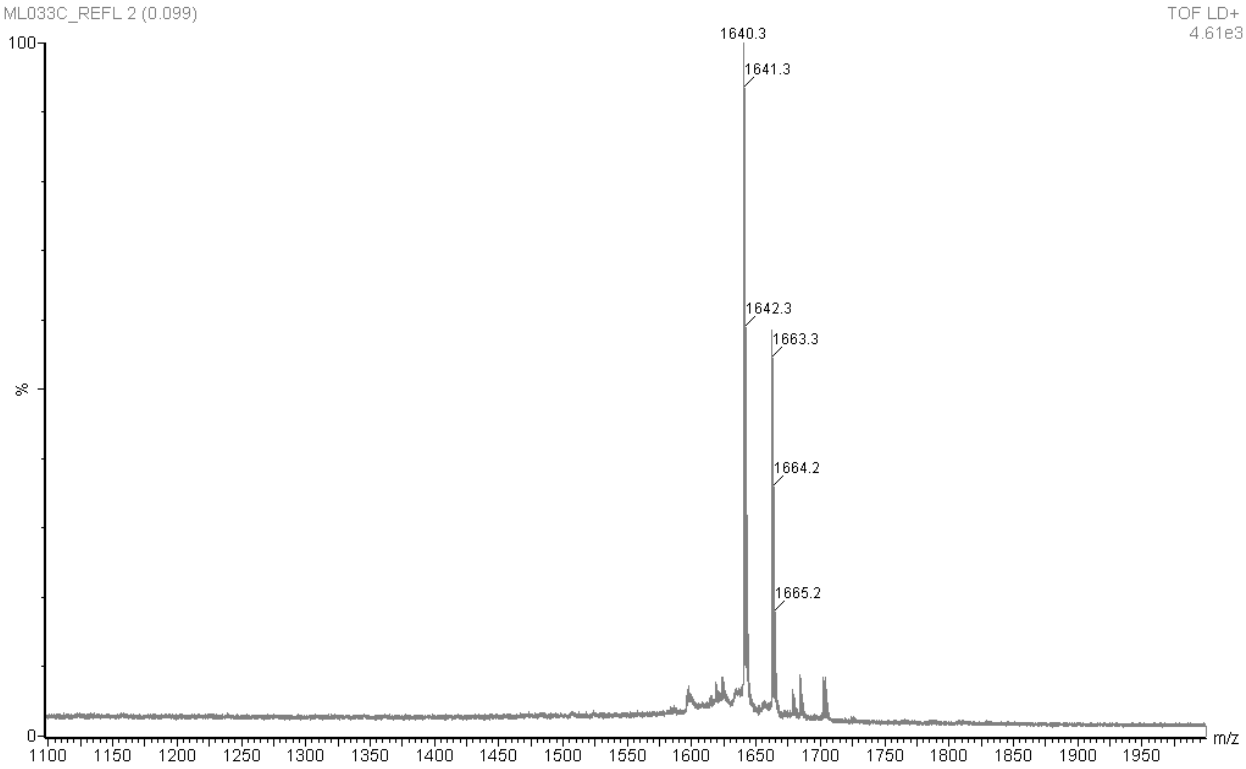

(b)

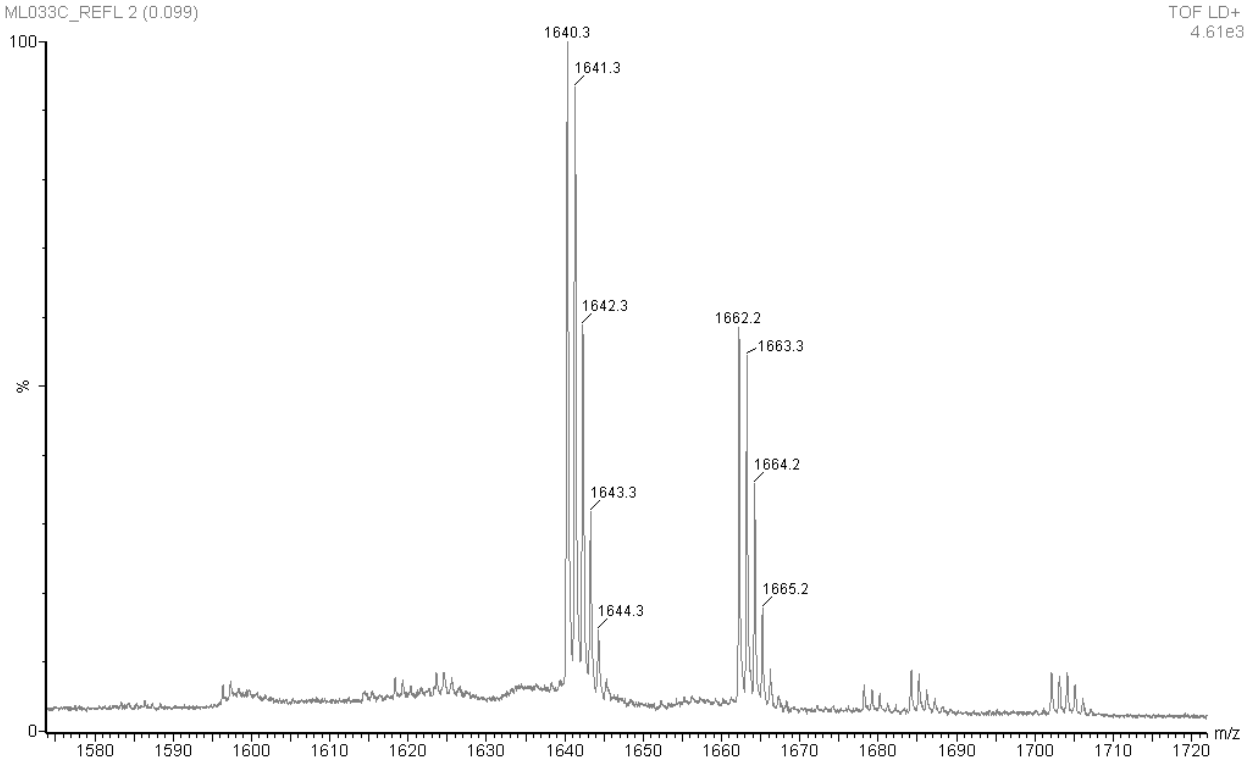
ML033C_REFL 2 (0.099)
TOF LD+
4.61e3
100
%
0
1640.3
1641.3
1642.3
1662.2
1663.3
1664.2
1643.3
1665.2
1644.3
1580
1590
1600
1610
1620
1630
1640
1650
1660
1670
1680
1690
1700
1710
1720
m/z

(c)

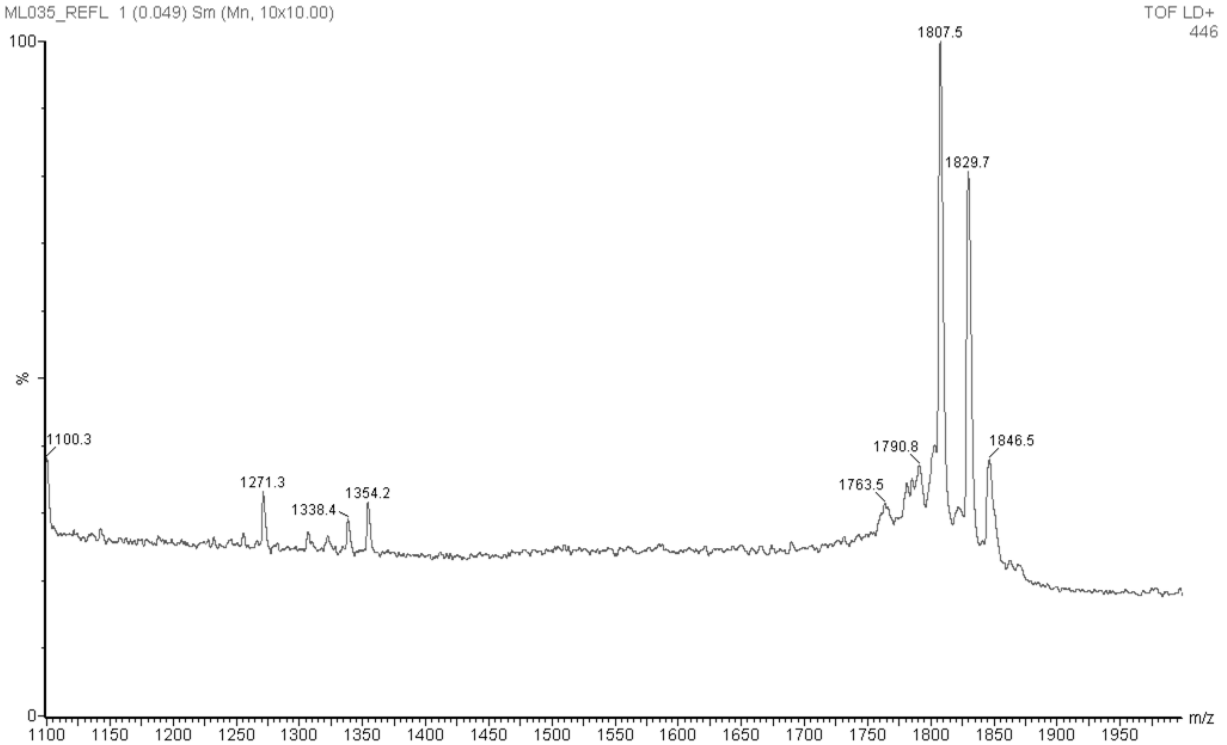
ML035_REFL 1 (0.049) Sm (Mn, 10x10.00)
TOF LD+
446
100
%
0
1807.5
1829.7
1100.3
1790.8
1846.5
1271.3
1763.5
1354.2
1338.4
1100
1150
1200
1250
1300
1350
1400
1450
1500
1550
1600
1650
1700
1750
1800
1850
1900
1950
m/z

(d)

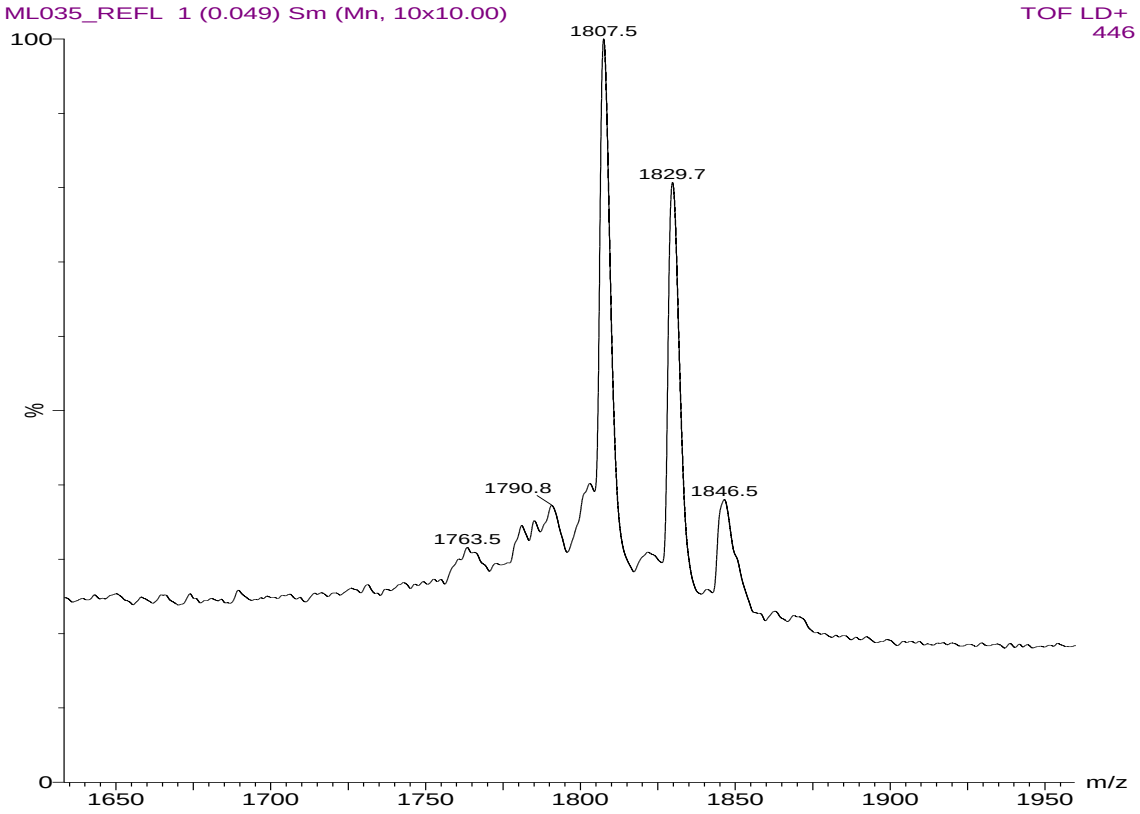

Figure **S25**. (a) MS data for native Somatostatin (1100–2000 m/z), (b) MS data for native Somatostatin (1580–2000 m/z), (c) MS data for modified Somatostatin (1100–2000 m/z) and (d) MS data for modified Somatostatin (1650–2000 m/z).

***In situ* reduction of Herceptin mAb and reaction with pyridazinedione 4 at 4 °C (25 eq.)**

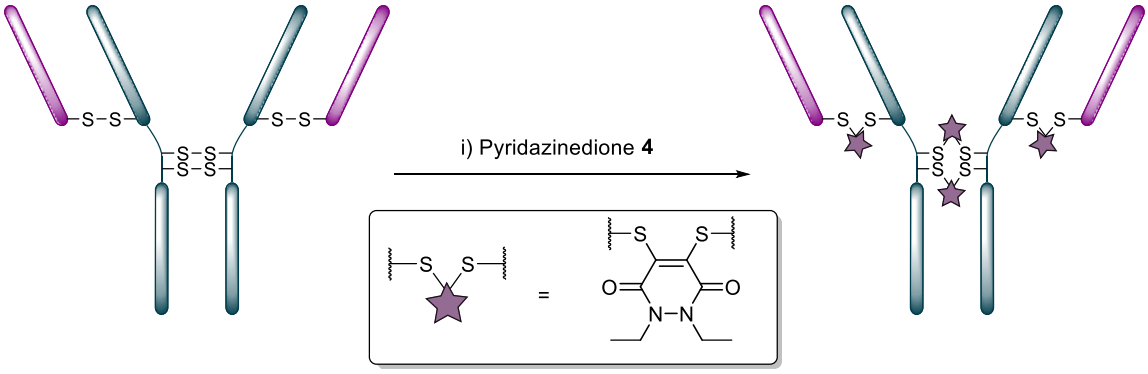

TCEP.HCl (2.3 µL, 20 mM in deionised water, 50 eq.) was added to Herceptin (30 µL, 4.4 mg/mL, 30 µM) in BBS (25 mM sodium borate, 25 mM NaCl, 0.5 mM EDTA, pH 8.0) which had been pretreated and stored at 4 °C for 1 h previously with pyridazinedione **4** (5.6 µL, 4 mM in DMF, 25 eq.). The reaction mixture was then stored at 4 °C for 15 h. Excess reagents were removed by repeated diafiltration into deionised water using VivaSpin sample concentrators (GE Healthcare, 10,000 MWCO). The samples were analysed by SDS-PAGE gel (see Figure **S37**. [lane 2]) and UV-vis spectroscopy was used to determine a PAR of 4.2. PAR was calculated according to that previously described.[3]

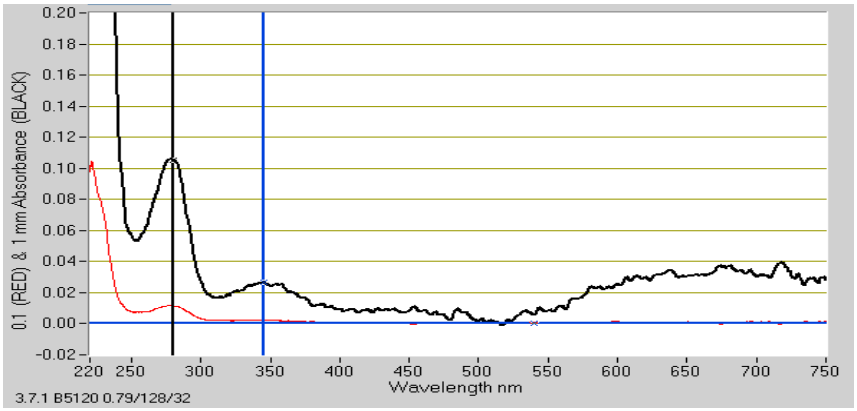

Figure **S26**. UV-vis data for Herceptin modified with pyridazinedione **4** at 4 °C *in situ*.

Portion-wise *in situ* reduction of Herceptin mAb and reaction with pyridazinedione 4 at 4 °C (25 eq.)

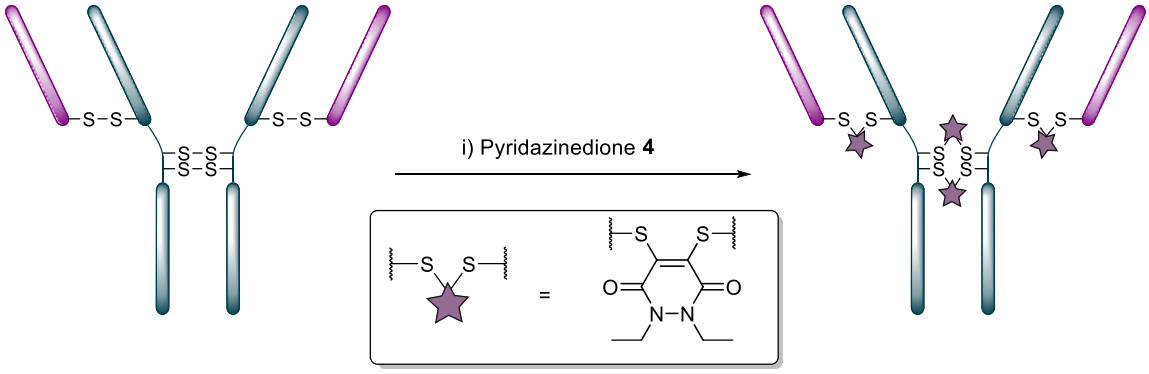

TCEP.HCl (1.2 µL, 0.2 mM in deionised water, 1.34 eq. [0.33 eq. per disulfide]) was added once every 0.5 h for 2.5 h (6 additions in total) to Herceptin (30 µL, 4.4 mg/mL, 30 µM) in BBS (25 mM sodium borate, 25 mM NaCl, 0.5 mM EDTA, pH 8.0) which had been pretreated and stored at 4 °C for 1 h previously with pyridazinedione **4** (5.6 µL, 4 mM in DMF, 25 eq.). The reaction mixture was then stored at 4 °C for 15 h. Excess reagents were removed by repeated diafiltration into deionised water using VivaSpin sample concentrators (GE Healthcare, 10,000 MWCO). The samples were analysed by SDS-PAGE gel (see Figure **S37**. [lane 3]) and UV-vis spectroscopy was used to determine a PAR of 4.0. PAR was calculated according to that previously described.[3]

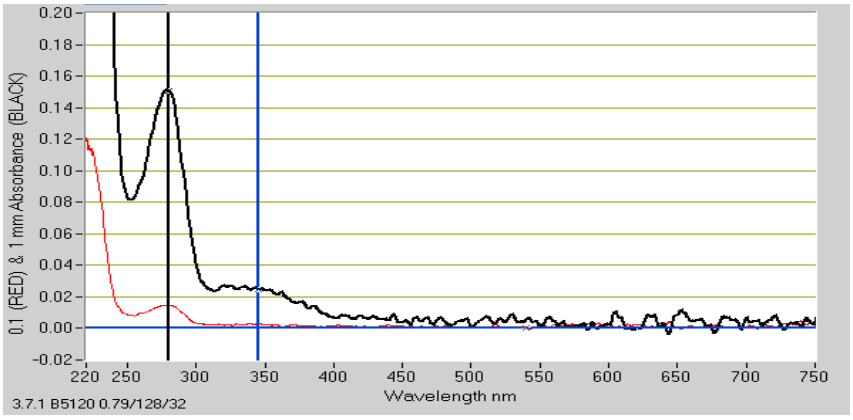

Figure **S27**. UV-vis data for Herceptin modified with pyridazinedione **4** *in situ* with portion-wise addition of TCEP.HCl.

Reaction of Herceptin mAb with pyridazinedione 7 at 4 °C (8 eq.)

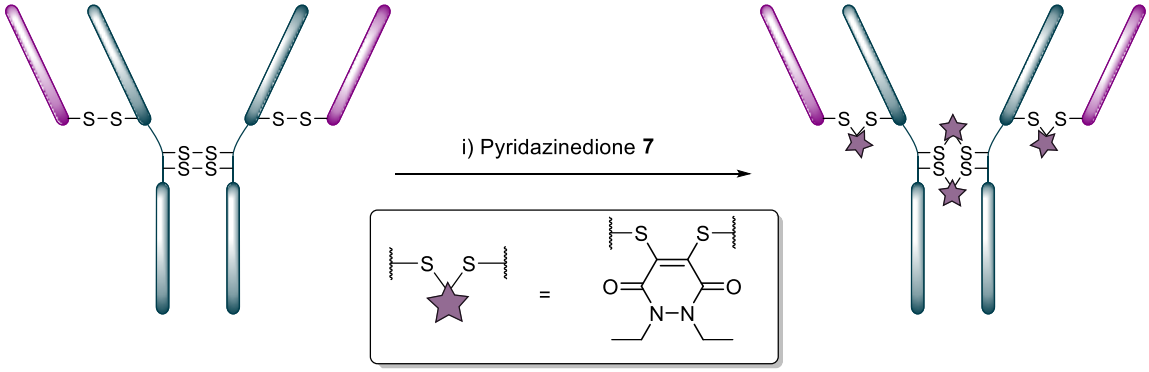

Pyridazinedione **7** (1.9 µL, 4.0 mM in DMF, 8 eq.) was added to Herceptin (30 µL, 4.4 mg/mL, 30 µM) in BBS (25 mM sodium borate, 25 mM NaCl, 0.5 mM EDTA, pH 8.0) which had been stored at 4 °C for 1 h previously. The reaction mixture was then stored at 4 °C for 15 h. Excess reagents were removed by repeated diafiltration into deionised water using VivaSpin sample concentrators (GE Healthcare, 10,000 MWCO). The samples were analysed by SDS-PAGE gel (see Figure **S37**. [lane 4]) and UV-vis spectroscopy was used to determine a PAR of 4.0. PAR was calculated according to that previously described.[3]

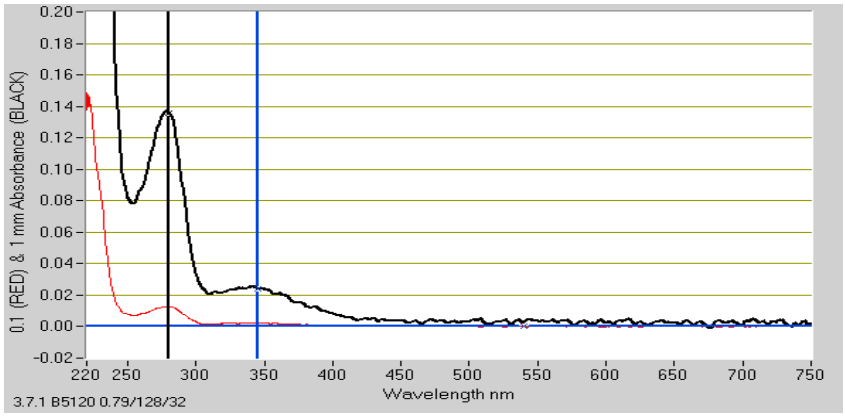

Figure **S28**. UV-vis data for Herceptin modified with pyridazinedione **7** at 4 °C.

***In situ* reduction of Herceptin mAb and reaction with pyridazinedione 4 at 37 °C (25 eq.)**

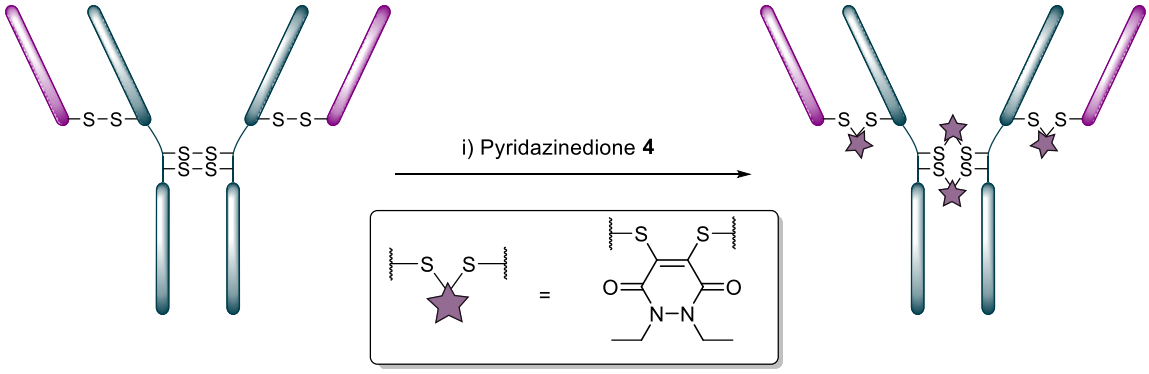

TCEP.HCl (2.3 µL, 20 mM in deionised water, 50 eq.) was added to Herceptin (30 µL, 4.4 mg/mL, 30 µM) in BBS (25 mM sodium borate, 25 mM NaCl, 0.5 mM EDTA, pH 8.0) which had been pretreated and stored at 37 °C for 1 h previously with pyridazinedione **4** (5.6 µL, 4.0 mM in DMF, 25 eq). The reaction mixture was then stored at 37 °C for 2 h. Excess reagents were removed by repeated diafiltration into deionised water using VivaSpin sample concentrators (GE Healthcare, 10,000 MWCO). The samples were analysed by SDS-PAGE gel (see Figure **S37**. [lane 5]) and UV-vis spectroscopy was used to determine a PAR of 4.2. PAR was calculated according to that previously described.[3]

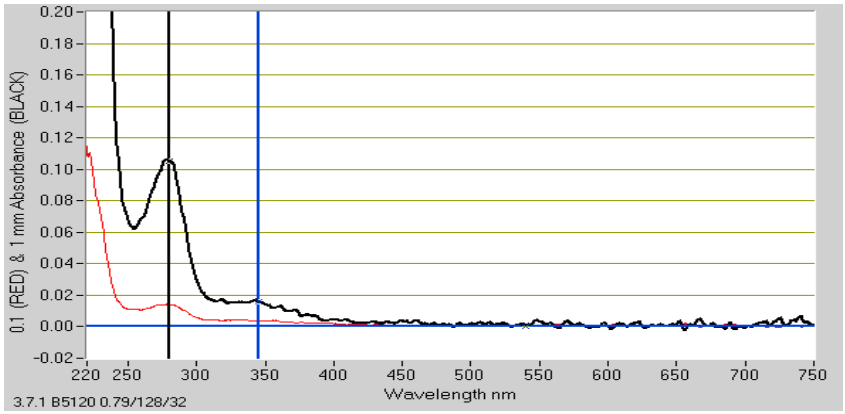

Figure **S29**. UV-vis data for Herceptin modified with pyridazinedione **4** at 37 °C *in situ*.

***In situ* reduction of Herceptin mAb and reaction with pyridazinedione 3 at 37 °C (25 eq.)**

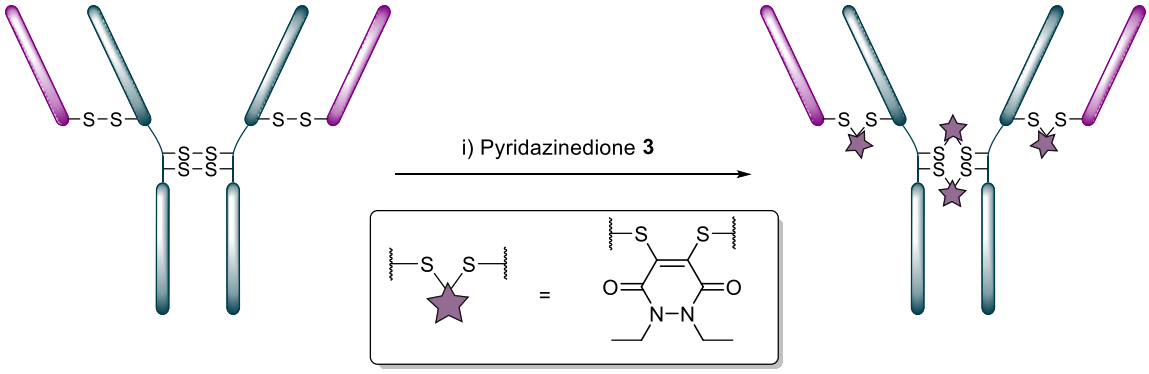

TCEP.HCl (2.3 µL, 20 mM in deionised water, 50 eq.) was added to Herceptin (30 µL, 4.4 mg/mL, 30 µM) in BBS (25 mM sodium borate, 25 mM NaCl, 0.5 mM EDTA, pH 8.0) which had been pretreated and stored at 37 °C for 1 h previously with pyridazinedione **3** (5.6 µL, 4.0 mM in DMF, 25 eq). The reaction mixture was then stored at 37 °C for 2 h. Excess reagents were removed by repeated diafiltration into deionised water using VivaSpin sample concentrators (GE Healthcare, 10,000 MWCO). The samples were analysed by SDS-PAGE gel (see Figure **S38**. [lane 3]) and UV-vis spectroscopy was used to determine a PAR of 4.1. PAR was calculated according to that previously described.[3]

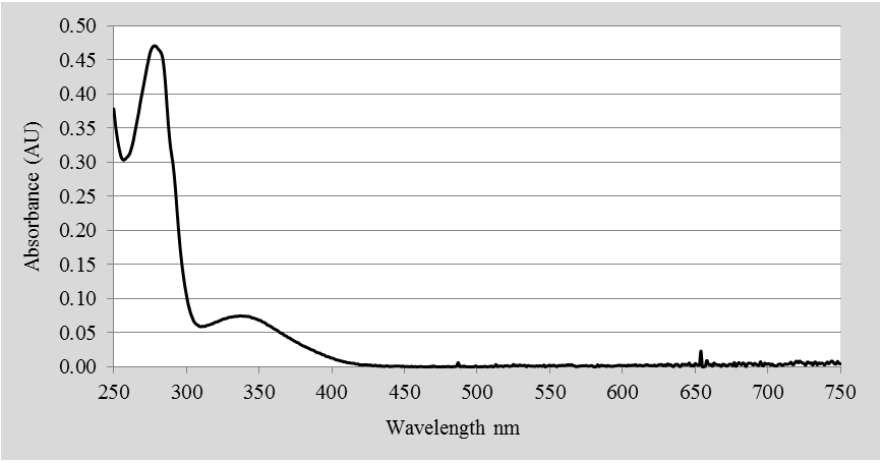

Figure **S30**. UV-vis data for Herceptin modified with pyridazinedione **3** at 37 °C *in situ*.

***In situ* reduction of Herceptin mAb and reaction with pyridazinedione 3 at 4 °C (25 eq.)**

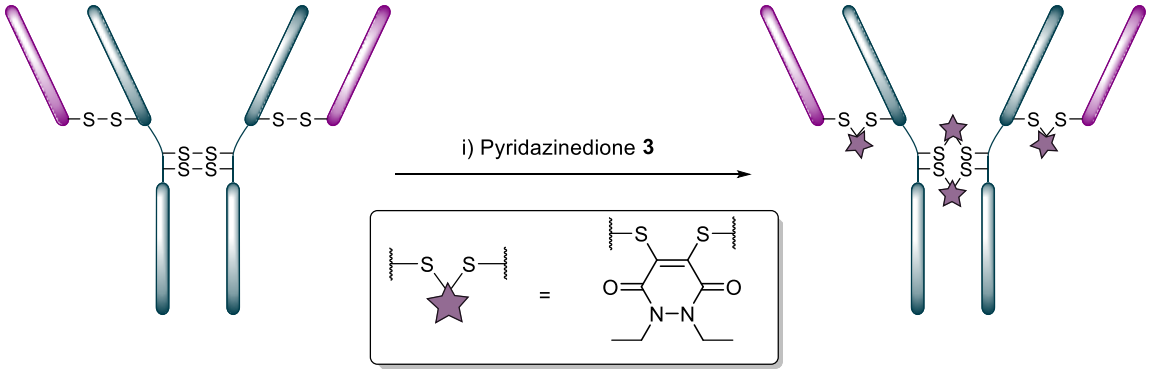

TCEP.HCl (2.3 µL, 20 mM in deionised water, 50 eq.) was added to Herceptin (30 µL, 4.4 mg/mL, 30 µM) in BBS (25 mM sodium borate, 25 mM NaCl, 0.5 mM EDTA, pH 8.0) which had been pretreated and stored at 4 °C for 1 h previously with pyridazinedione **3** (5.6 µL, 4 mM in DMF, 25 eq.). The reaction mixture was then stored at 4 °C for 15 h. Excess reagents were removed by repeated diafiltration into deionised water using VivaSpin sample concentrators (GE Healthcare, 10,000 MWCO). The samples were analysed by SDS-PAGE gel (see Figure **S38**. [lane 2]) and UV-vis spectroscopy was used to determine a PAR of 3.9.

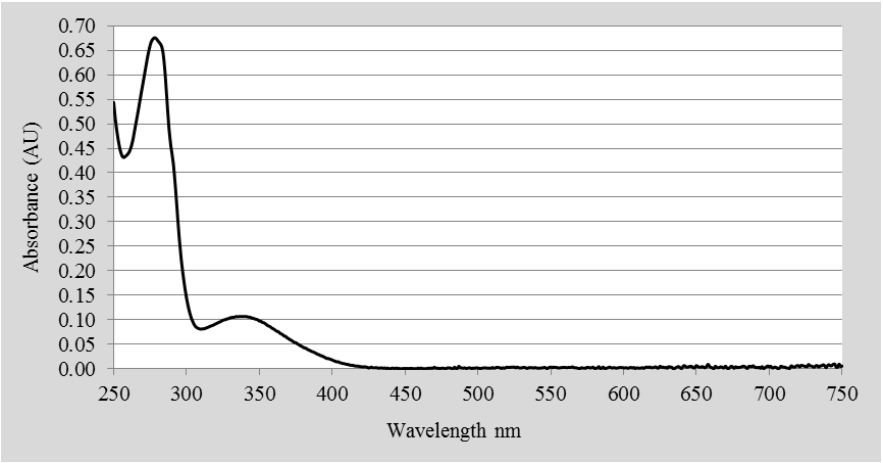

Figure **S31**. UV-vis data for Herceptin modified with pyridazinedione **3** at 4 °C *in situ*.

Control for untreated Fab fragment of Herceptin for experiments using pyridazinedione 15

During the course of this study the LC-MS device used (Thermo Scientific uPLC connected to MSQ Plus Single Quad Detector) underwent servicing and recalibration, this caused a slight change in observed mass for the untreated Fab fragment of Herceptin.

(a)

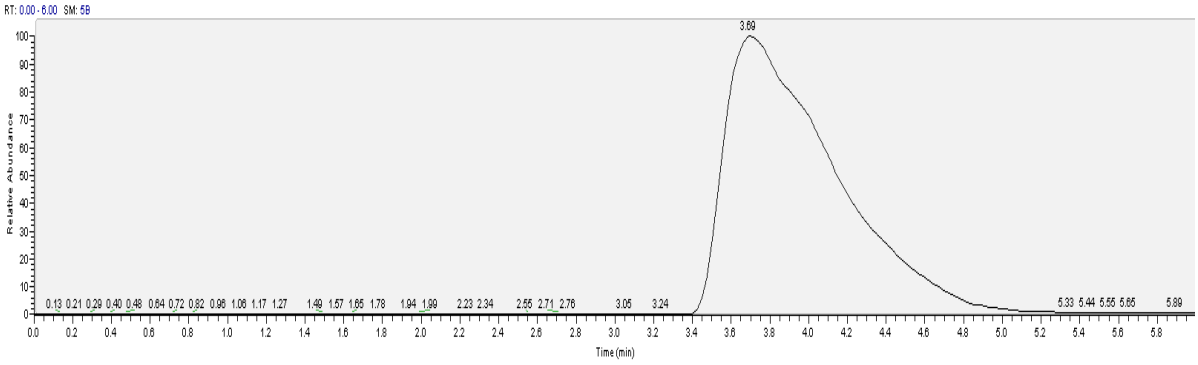

(b)

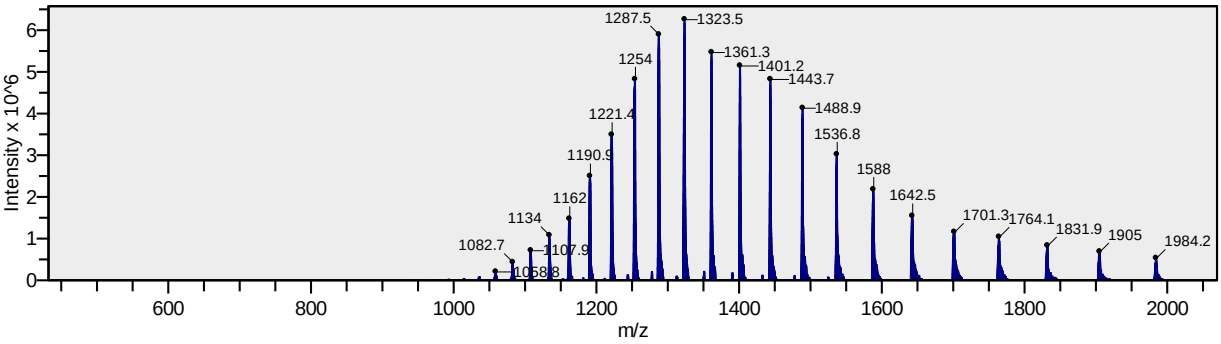

(c)

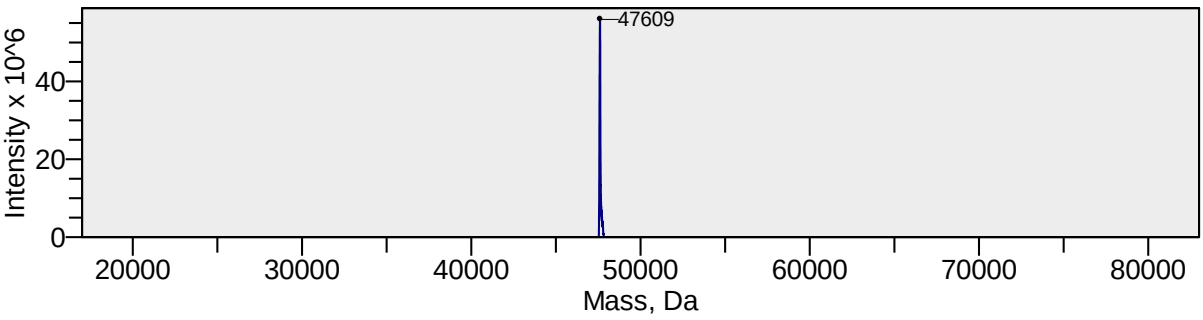

Figure **S32**. (a) TIC, (b) non-deconvoluted and (c) deconvoluted MS data for untreated Fab fragment of Herceptin for experiments using pyridazinedione **15**.

Reaction of Fab fragment of Herceptin with pyridazinedione 15 (1.25 eq) (Synthesis of bioconjugate 16)

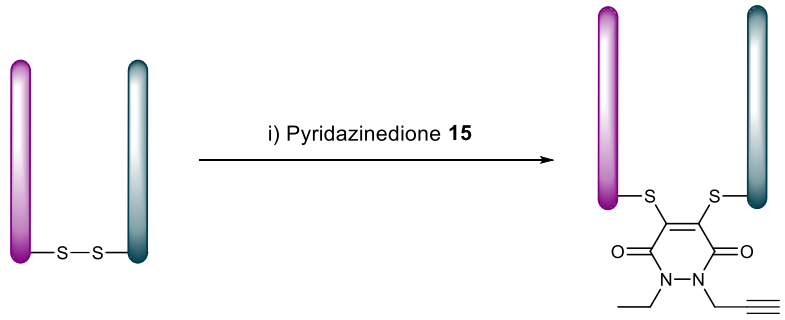

Pyridazinedione **15** (0.57 µL, 2.0 mM in DMF, 1.25 eq) was added to Fab fragment of Herceptin (30 µL, 1.4 mg/mL, 30 µM) in BBS (25 mM sodium borate, 25 mM NaCl, 0.5 mM EDTA, pH 8.0). The reaction mixture was incubated at 37 °C for 1 h. Excess reagents were removed by repeated diafiltration into deionised water using VivaSpin sample concentrators (GE Healthcare, 10,000 MWCO). The samples were analysed by LCMS. Expected mass: 47,785 Da. Observed mass: 47,787 Da.

(a)

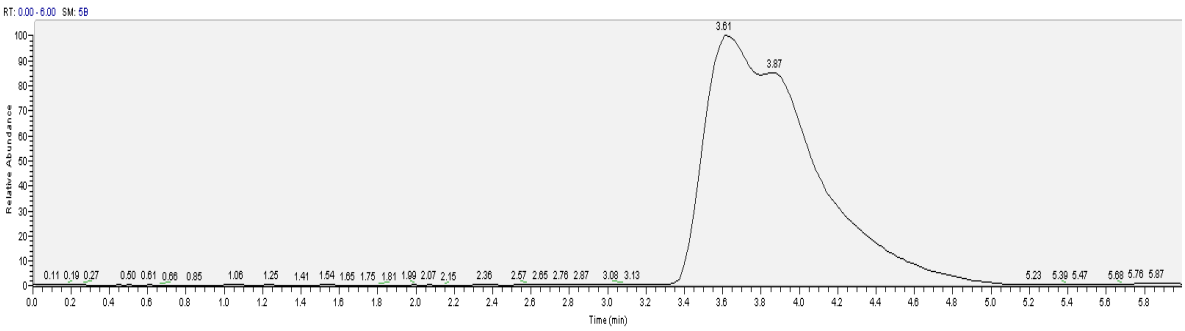

(b)

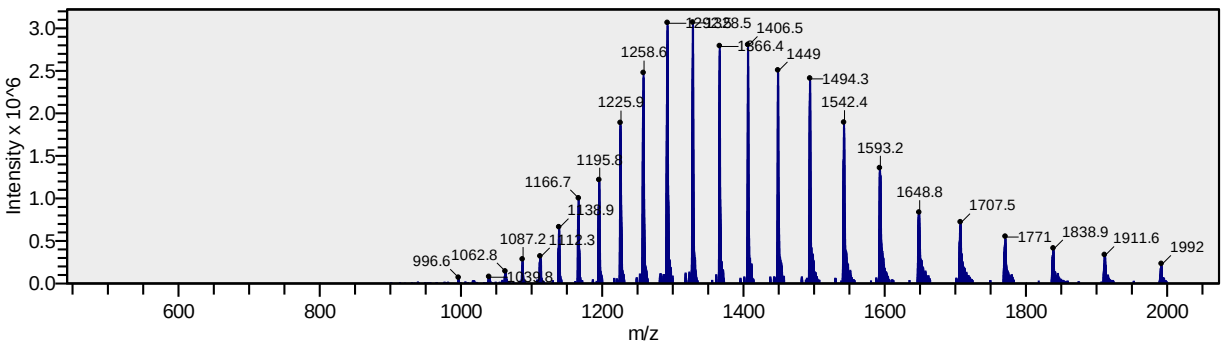

(c)

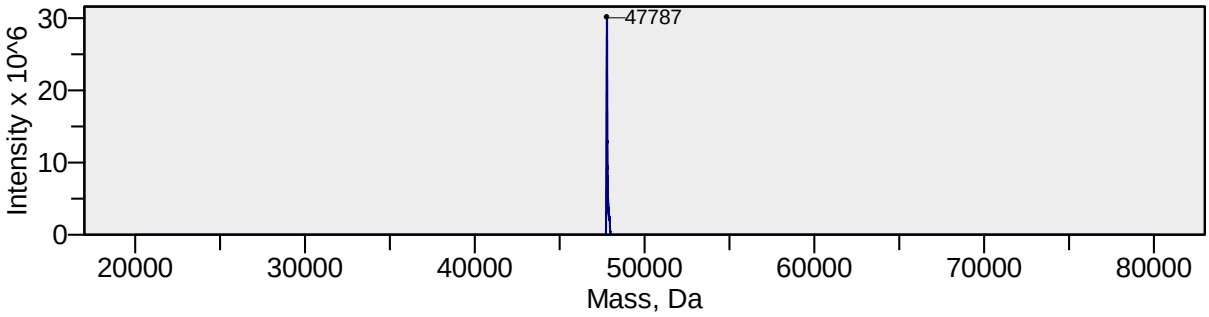

Figure **S33**. (a) TIC, (b) non-deconvoluted and (c) deconvoluted MS data for bioconjugate **16**.

Reaction of Fab-Her bioconjugate 16 with Cy5-azide (Synthesis of bioconjugate 16a)

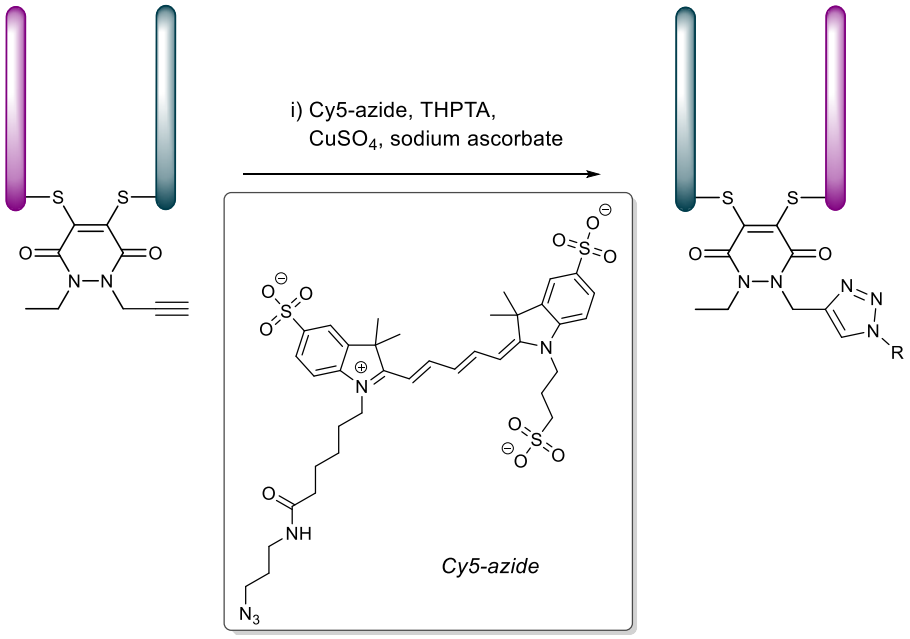

Cy5-azide (1.0 µL, 2.0 mM in water, 2 eq), $CuSO_4$ (1.0 µL, 2.0 mM in water, 2 eq), tris(3-hydroxypropyltriazolylmethyl)amine (THPTA) (1.0 µL, 10 mM in water, 10 eq) and sodium ascorbate (5.0 µL, 0.10 M in water, 500 eq) were added in series to bioconjugate **16** (20 µL, 2.4 mg/mL, 50 µM) in BBS (25 mM sodium borate, 25 mM NaCl, pH 8.0). The reaction mixture was stored at 21 °C for 1.5 h. The excess reagents were then removed by repeated diafiltration into fresh PBS with 2 mM EDTA (to remove residual copper ions) using VivaSpin sample concentrators (GE Healthcare, 10,000 MWCO). Following this, the buffer salts were removed by repeated diafiltration into deionised water using VivaSpin sample concentrators (GE Healthcare, 10,000 MWCO). The samples were then analysed by LCMS. Expected mass: 48,615 Da. Observed mass: 48,613 Da.

(a)

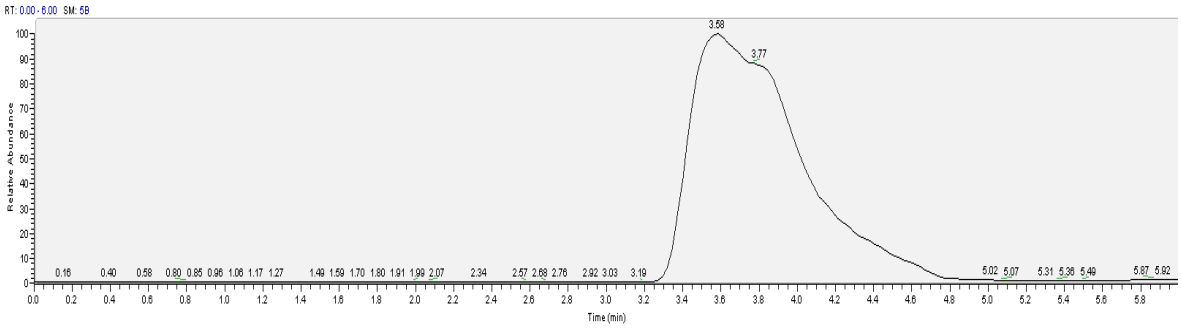

(b)

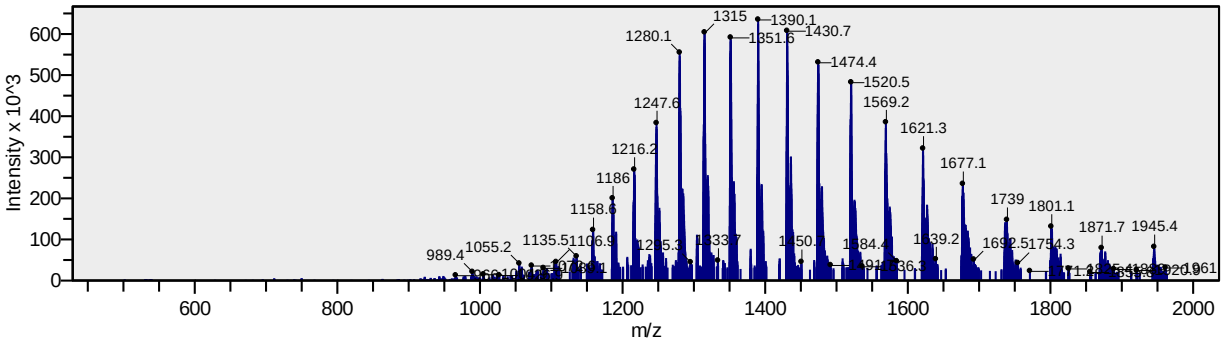

(c)

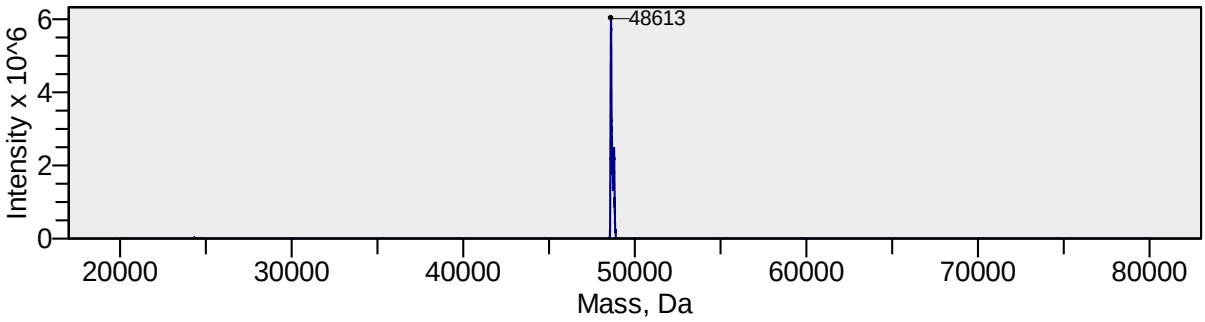

Figure **S34**. (a) TIC, (b) non-deconvoluted and (c) deconvoluted MS data for bioconjugate **16a**.

Reaction of Fab-Her bioconjugate 16 with Doxorubicin-azide[3] (Synthesis of bioconjugate 16b)

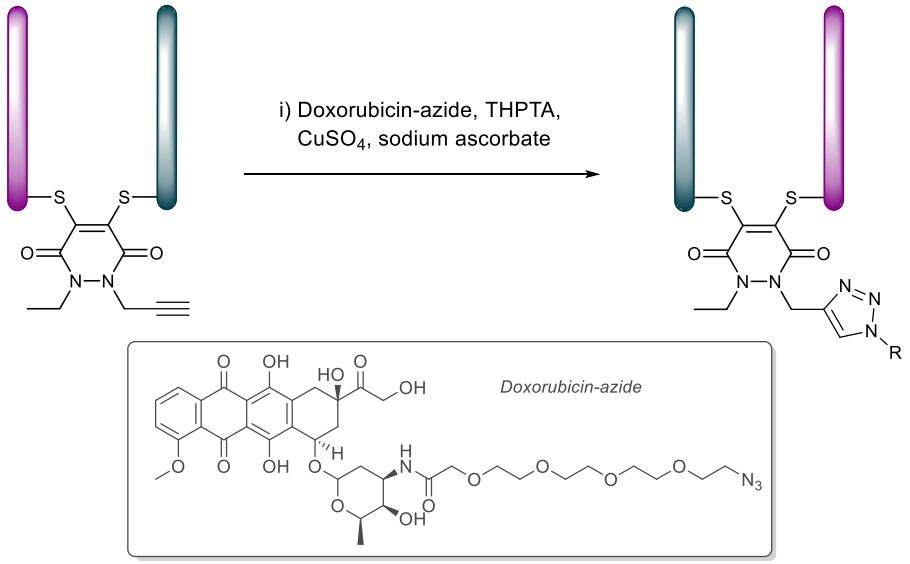

Doxorubicin-azide[3] (1.0 µL, 2.0 mM in water, 2 eq), $CuSO_4$ (1.0 µL, 2.0 mM in water, 2 eq), tris(3-hydroxypropyltriazolylmethyl)amine (THPTA) (1.0 µL, 10 mM in water, 10 eq) and sodium ascorbate (5.0 µL, 0.10 M in water, 500 eq) were added in series to bioconjugate **16** (20 µL, 2.4 mg/mL, 50 µM) in BBS (25 mM sodium borate, 25 mM NaCl, pH 8.0). The reaction mixture was stored at 21 °C for 1.5 h. The excess reagents were then removed by repeated diafiltration into fresh PBS with 2 mM EDTA (to remove residual copper ions) using VivaSpin sample concentrators (GE Healthcare, 10,000 MWCO). Following this, the buffer salts were removed by repeated diafiltration into deionised water using VivaSpin sample concentrators (GE Healthcare, 10,000 MWCO). The samples were then analysed by LCMS. Expected mass: 48,587 Da. Observed mass: 48,586 Da.

(a)

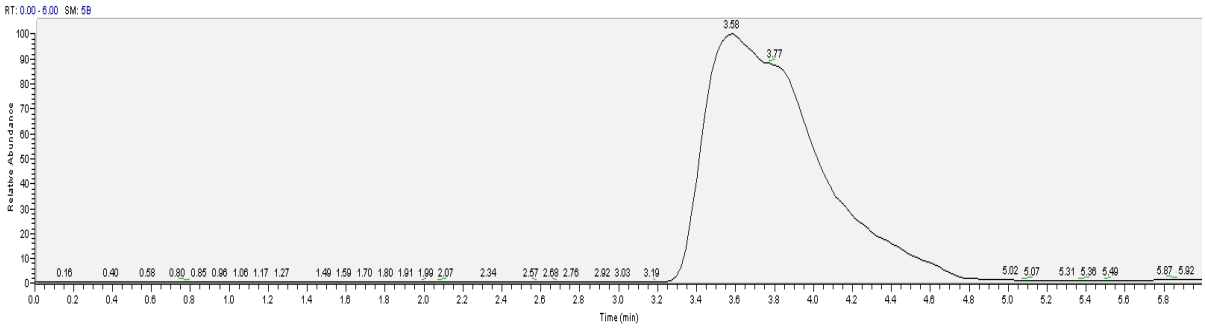

(b)

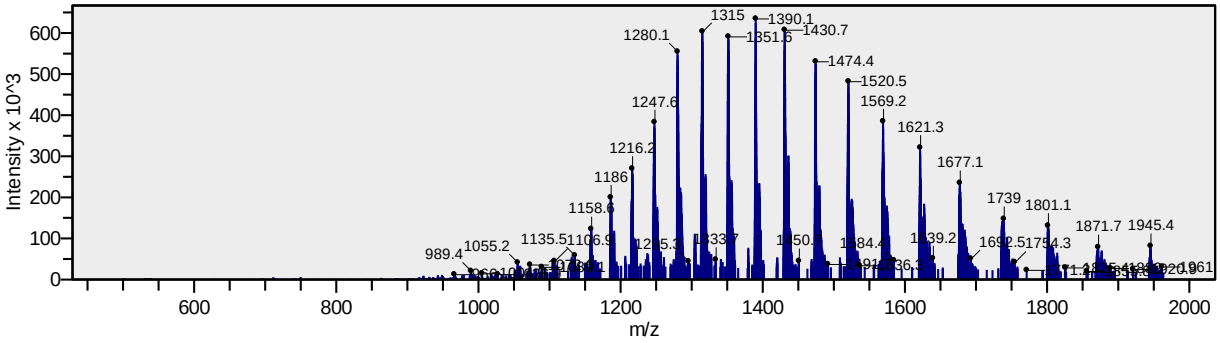

(c)

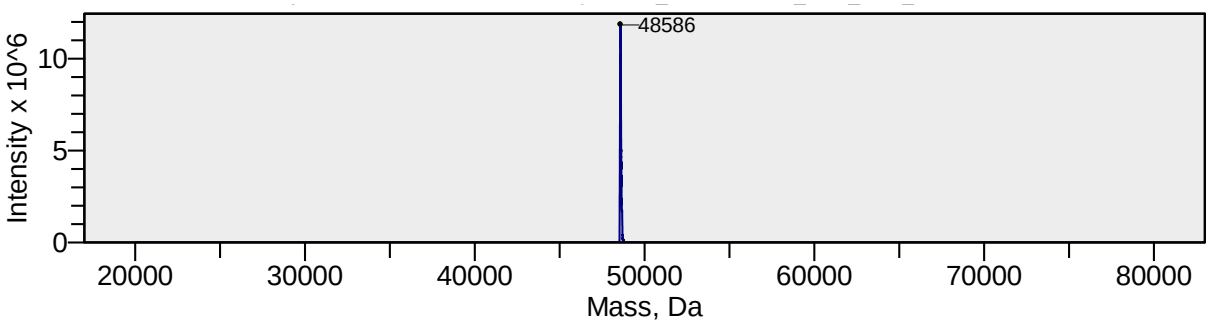

Figure **S35**. (a) TIC, (b) non-deconvoluted and (c) deconvoluted MS data for bioconjugate **16b**.

Reaction of Fab-Her bioconjugate 16 with AlexaFluor 488®-azide (Synthesis of bioconjugate 16c)

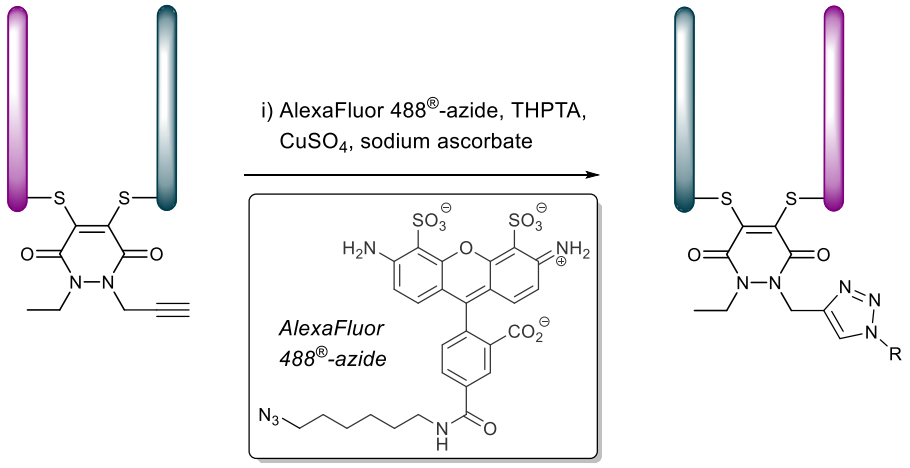

AlexaFluor 488®-azide (1.0 µL, 2.0 mM in water, 2 eq), $CuSO_4$ (1.0 µL, 2.0 mM in water, 2 eq), tris(3-hydroxypropyltriazolylmethyl)amine (THPTA) (1.0 µL, 10 mM in water, 10 eq) and sodium ascorbate (5.0 µL, 0.10 M in water, 500 eq) were added in series to bioconjugate **16** (20 µL, 2.4 mg/mL, 50 µM) in BBS (25 mM sodium borate, 25 mM NaCl, pH 8.0). The reaction mixture was stored at 21 °C for 1.5 h. The excess reagents were then removed by repeated diafiltration into fresh PBS with 2 mM EDTA (to remove residual copper ions) using VivaSpin sample concentrators (GE Healthcare, 10,000 MWCO). Following this, the buffer salts were removed by repeated diafiltration into deionised water using VivaSpin sample concentrators (GE Healthcare, 10,000 MWCO). The samples were then analysed by LCMS. Expected mass: 48,442 Da. Observed mass: 48,447 Da.

(a)

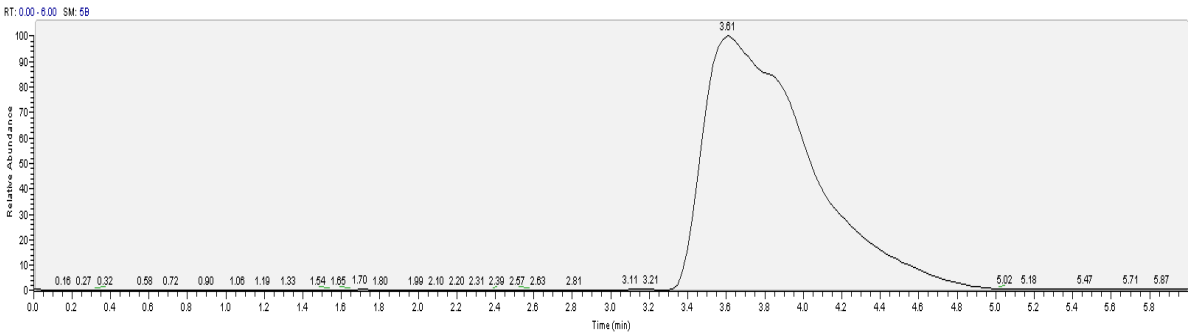

(b)

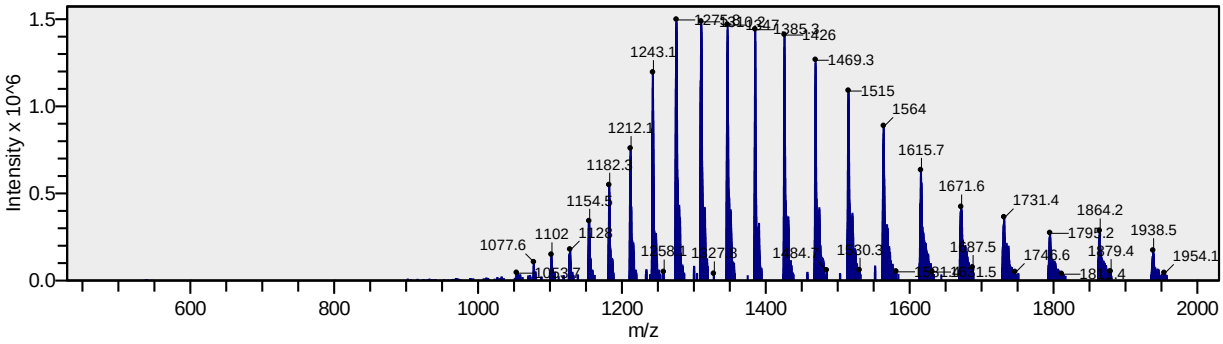

(c)

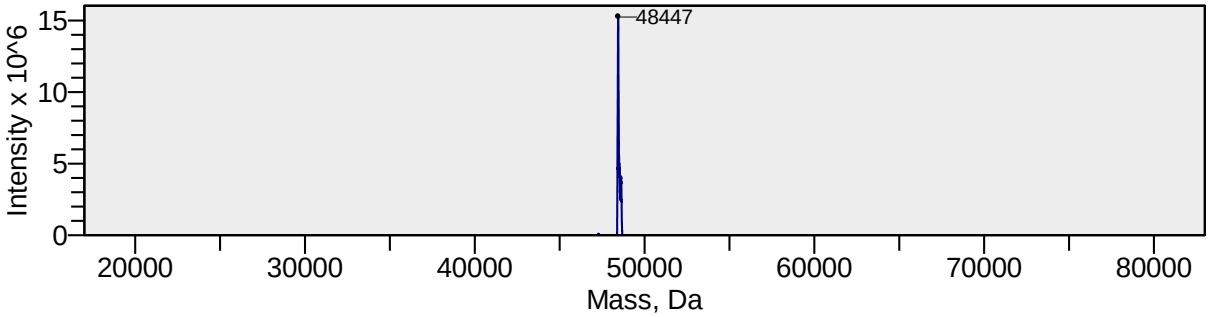

Figure **S36**. (a) TIC, (b) non-deconvoluted and (c) deconvoluted MS data for bioconjugate **16c**.

SDS-PAGE gel for Herceptin modification with pyridazinediones 4 and 7

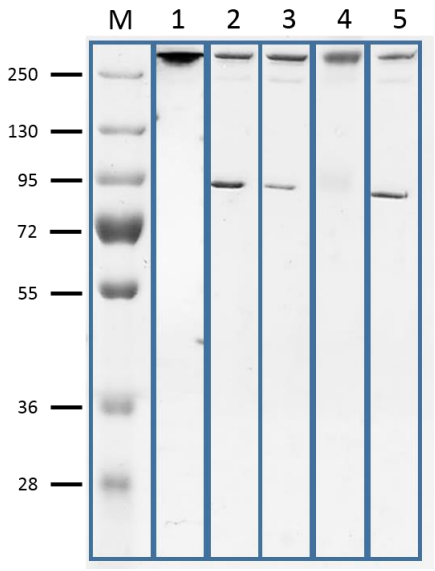

Figure **S37**. Comparison of traditional methods for Herceptin modification against the use of pyridazinedione **7**. M) Molecular weight marker. 1) Untreated Herceptin. 2) *In situ* reduction of Herceptin mAb and reaction with pyridazinedione **4** at 4 °C (25 eq.). 3) Portion-wise *in situ* reduction of Herceptin mAb and reaction with pyridazinedione **4** at 4 °C (25 eq.). 4) Reaction of Herceptin mAb with pyridazinedione **7** at 4 °C (8 eq.). 5) *In situ* reduction of Herceptin mAb and reaction with pyridazinedione **4** at 37 °C (25 eq.)

SDS-PAGE gel for Herceptin modification with pyridazinedione 3

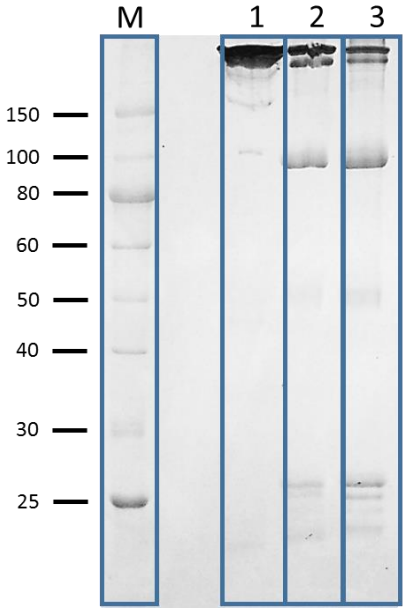

Figure **S38**. Further demonstration of traditional methods for Herceptin modification. M) Molecular weight marker. 1) Untreated Herceptin. 2) *In situ* reduction of Herceptin mAb and reaction with pyridazinedione **3** at 4 °C (25 eq.). 3) *In situ* reduction of Herceptin mAb and reaction with pyridazinedione **3** at 37 °C (25 eq.).

SDS-PAGE gel for Fab fragment of Herceptin and conjugates 16, 16a, 16b and 16c

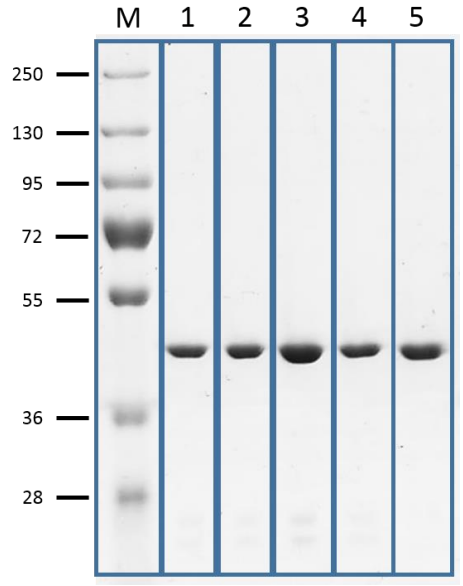

Figure **S39** Distribution of Fab-Her bioconjugates **16**, **16a**, **16b** and **16c** against unmodified Fab-Her fragment. M) Molecular weight marker. 1) Unmodified Fab-Her fragment. 2) Bioconjugate **16**. 3) Bioconjugate **16a**. 4) Bioconjugate **16b**. 5) Bioconjugate **16c**.

Activity by enzyme-linked immunosorbent assay (ELISA)[83]

Binding affinity to HER2 receptor was determined by ELISA. A 96-well plate was coated overnight at 4 °C with HER2 (100 µL of a 0.25 µg·mL^{-1} solution in PBS), including coating one row of wells with PBS only for negative controls. Next, coating solutions were removed and each well washed with PBS twice. Then, the wells were coated with a 1% BSA solution in PBS (200 µL) for 1 h at 21 °C. Then, the wells were washed with PBS three times. Solutions Fab fragment bioconjugates **16a**, **16b** and **16c** in PBS with the following dilution series: 23 nM, 7.8 nM, 2.6 nM, 0.86 nM, 0.29 nM and 0.10 nM were prepared. Wells were coated with the dilution series solutions, including a PBS only and unmodified Fab fragment at 23 nM in the absence of HER2 as negative controls, and incubated for 2 h at room temperature. Then, the solutions were removed and the wells washed with 0.1% Tween 20 in PBS twice and with PBS three times. Detection antibody (100 µL of anti-human IgG, Fab-specific-HRP solution, prepared by taking 4 µL of a 1:5000 diluted solution and further diluting with 20 mL of PBS) was added and incubated for 1 h at room temperature. Then, the solutions were removed and the wells washed with 0.1% Tween 20 in PBS twice and with PBS three times. Finally, an OPD solution (100 µL of 0.5 mg·mL^{-1} OPD in phosphate-citrate buffer with sodium perborate, prepared by dissolving 1 capsule in 100 mL water) was added to each well. After *ca.* 2 min the reaction was stopped through addition of 4 M HCl (50 µL). Absorbance was measured at 490 nm. Absorbance was corrected by subtracting average of negative controls. See Figure **S40**

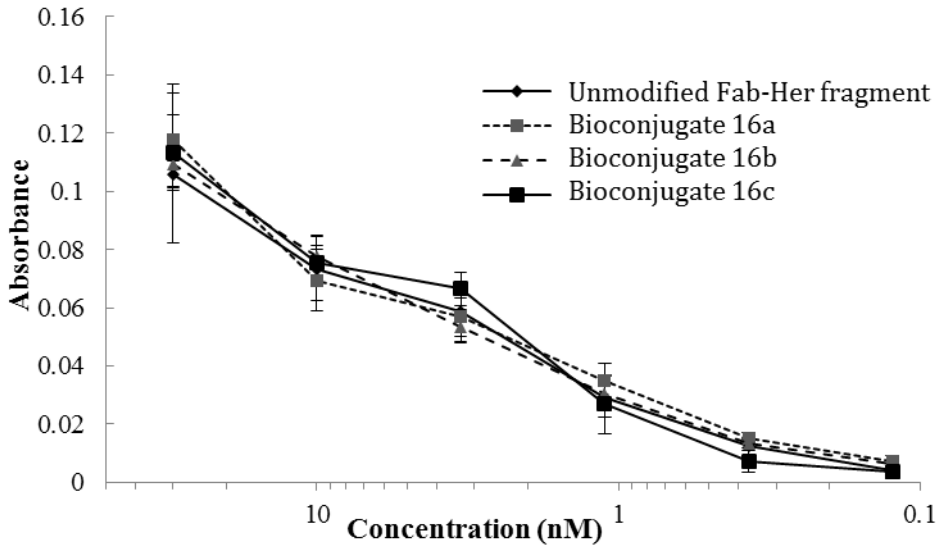

Figure **S40**. Binding activity of Fab-Her bioconjugates **16a**, **16b** and **16c** against untreated Fab fragment of Herceptin.

Reaction of Herceptin mAb with pyridazinedione 15 at 4 °C (8 eq.) for the synthesis of bioconjugate 17

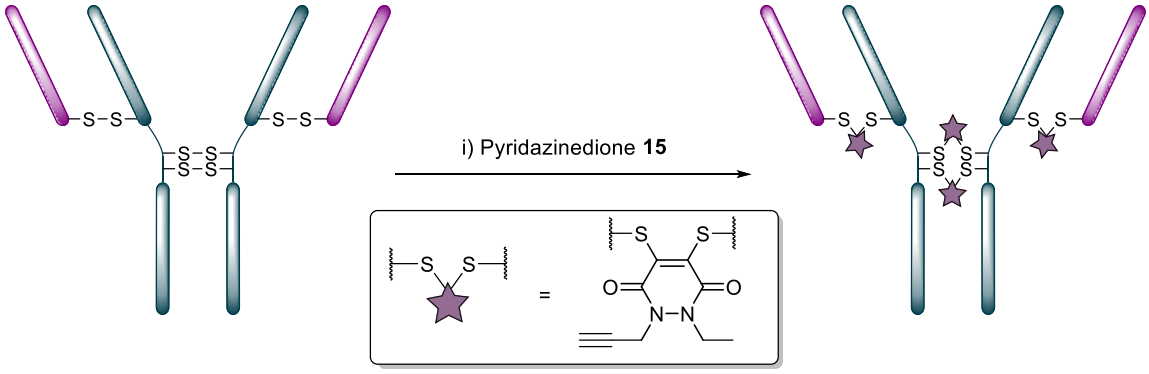

Pyridazinedione **15** (1.9 µL, 4.0 mM in DMF, 8 eq.) was added to Herceptin (30 µL, 4.4 mg/mL, 30 µM) in BBS (25 mM sodium borate, 25 mM NaCl, 0.5 mM EDTA, pH 8.0) which had been stored at 4 °C for 1 h previously. The reaction mixture was then stored at 4 °C for 16 h. Excess reagents were removed by repeated diafiltration into deionised water using VivaSpin sample concentrators (GE Healthcare, 10,000 MWCO). The samples were analysed by SDS-PAGE gel (see Figure **S43**. [lane 2]) and UV-vis spectroscopy was used to determine a PAR of 4.1. PAR was calculated according to that previously described.[3]

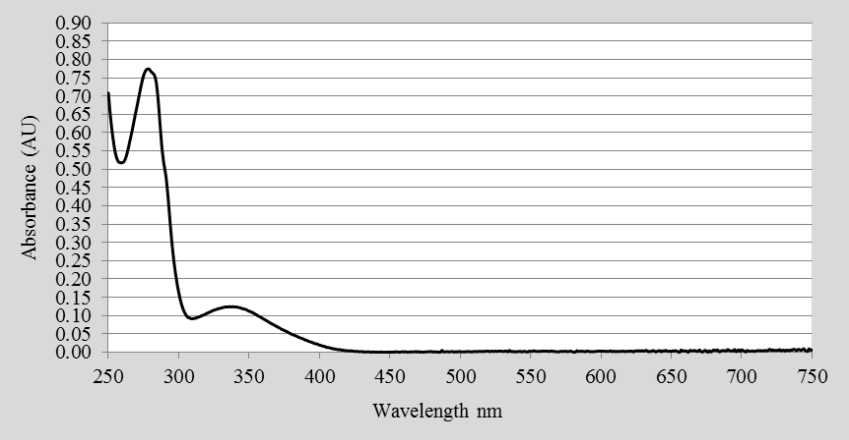

Figure **S41**. UV-vis data for Herceptin modified with pyridazinedione **15** at 4 °C.

Reaction of bioconjugate 17 with Doxorubicin-azide[83] for the synthesis of bioconjugate 18

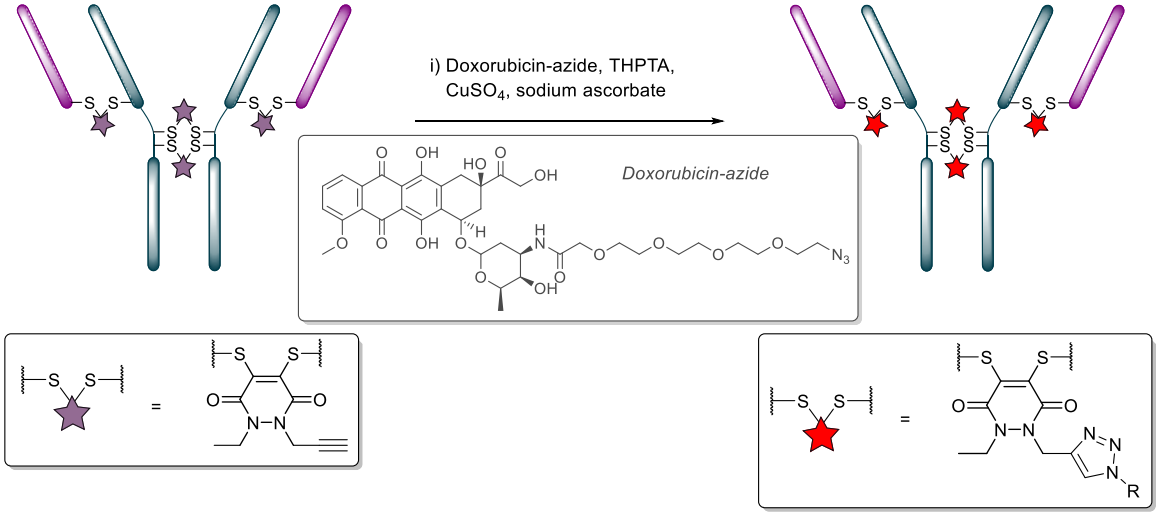

Doxorubicin-azide (1.0 µL, 2.0 mM in water, 2 eq), $CuSO_4$ (1.0 µL, 2.0 mM in water, 2 eq), tris(3-hydroxypropyltriazolylmethyl)amine (THPTA) (1.0 µL, 10 mM in water, 10 eq) and sodium ascorbate (5.0 µL, 0.10 M in water, 500 eq) were added in series to bioconjugate **17** (20 µL, 2.4 mg/mL, 50 µM) in BBS (25 mM sodium borate, 25 mM NaCl, pH 8.0). The reaction mixture was stored at 21 °C for 1.5 h. The excess reagents were then removed by repeated diafiltration into fresh PBS with 2 mM EDTA (to remove residual copper ions) using VivaSpin sample concentrators (GE Healthcare, 10,000 MWCO). Following this, the buffer salts were removed by repeated diafiltration into deionised water using VivaSpin sample concentrators (GE Healthcare, 10,000 MWCO). The samples were analysed by SDS-PAGE gel (see Figure **S43**. [lane 3]) and UV-vis spectroscopy was used to determine a PAR of 4.0. PAR was calculated according to that previously described.[84]

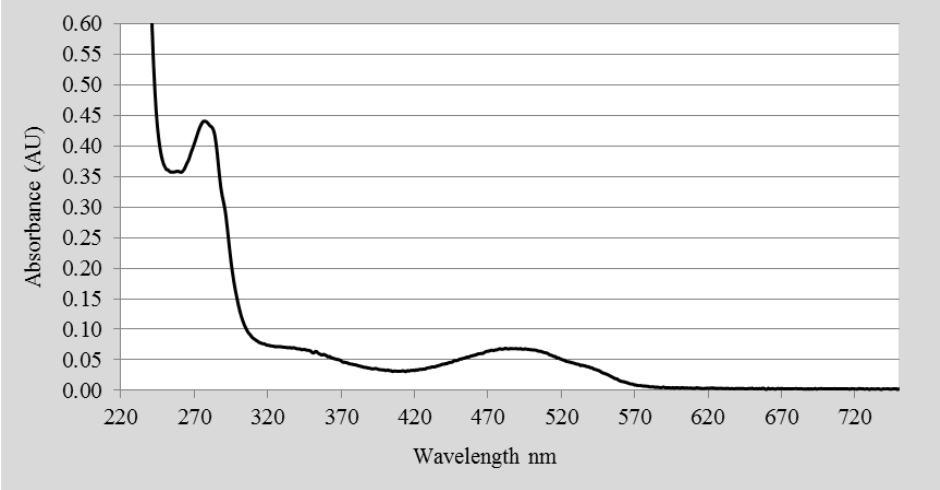

Figure **S42**. UV-vis data for bioconjugate **18**.

SDS-PAGE gel for Herceptin modification with pyridazinedione 15 and Dox-azide

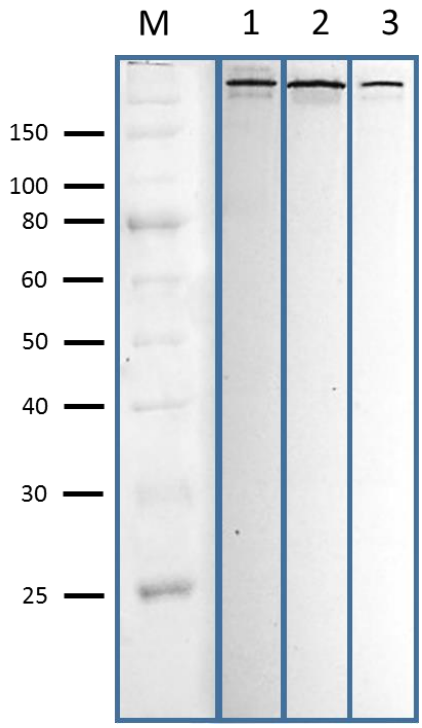

Figure **S43**. Distribution of bioconjugates **17** and **18** against unmodified native Herceptin. M) Molecular weight marker. 1) Untreated Herceptin. 2) Reaction of Herceptin mAb with pyridazinedione **15** at 4 °C (8 eq.) (*i.e.* bioconjugate **17**). 3) bioconjugate **18**.

ELISA for Her-PD7-Dox bioconjugate 18 against native Herceptin

Carried out according to procedure detailed for conjugates **16a-c**.

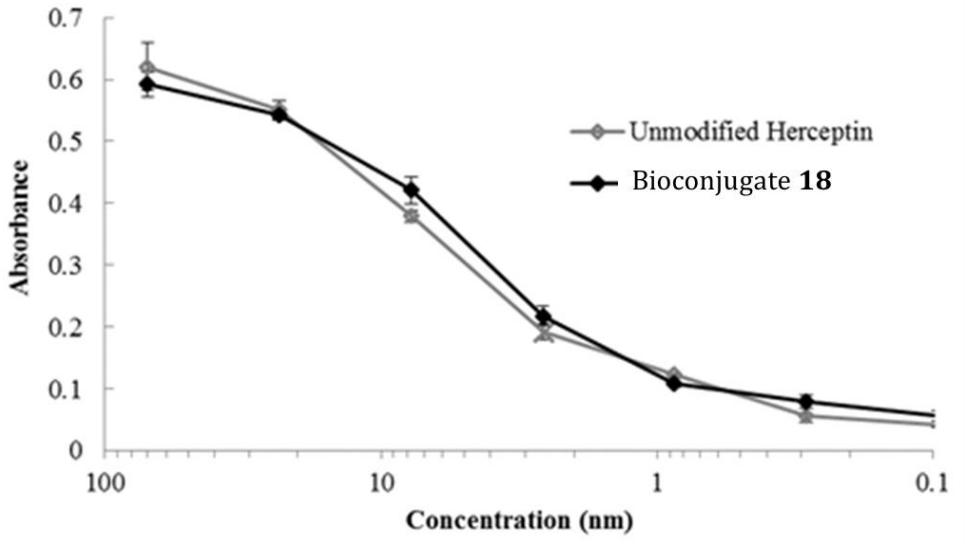

Figure **S44**. Binding activity of bioconjugate **18** against native unmodified Herceptin.

5.2 Experimental for Chapter 3

General Experimental

All reagents were purchased from Aldrich, AlfaAesar, Sino Biologial Inc or Lumiprobe and were used as received. Where described below Pet. refers to petroleum ether (40–60 °C). All reactions were monitored by thin-layer chromatography (TLC) on pre-coated SIL G/UV254 silica gel plates (254 μm) purchased from VWR. Flash column chromatography was carried out with Kiesegel 60M 0.04/0.063 mm (200–400 mesh) silica gel. ^{1}H and ^{13}C NMR spectra were recorded at ambient temperature on a Bruker Avance 300 instrument operating at a frequency of 300 MHz for ^{1}H and 75 MHz for ^{13}C, a Bruker Avance 500 instrument operating at a frequency of 500 MHz for ^{1}H and 125 MHz for ^{13}C, and a Bruker Avance 600 instrument operating at a frequency of 600 MHz for ^{1}H and 150 MHz for ^{13}C in $CDCl_3$ or CD_3OD (as indicated below). The chemical shifts (δ) for ^{1}H and ^{13}C are quoted relative to residual signals of the solvent on the ppm scale. ^{1}H NMR peaks are reported as singlet (s), doublet (d), triplet (t), quartet (q), doublet of doublets (dd), triplet of doublets (td), doublet of triplets (dt), triplet of triplets (tt) m (multiplet) and br (broad). Coupling constants (*J* values) are reported in Hertz (Hz) and are H-H coupling constants unless otherwise stated. Signal multiplicities in ^{13}C NMR were determined using the distortionless enhancement by phase transfer (DEPT) spectral editing technique. Infrared spectra were obtained on a Perkin Elmer Spectrum 100 FTIR Spectrometer operating in ATR mode with frequencies given in reciprocal centimetres (cm^{-1}). Melting points were measured with a Gallenkamp apparatus and are uncorrected. All bioconjugation reactions were carried out in triplicate.

UV-Vis spectroscopy

UV-Vis spectroscopy was used to determine protein concentrations, pyridazinedione to antibody ratios (PDAR), fluorophore to antibody ratios (FAR) and drug to antibody ratios (DAR) using a nanodrop ND-1000 spectrophotometer and a Varian Cary 100 Bio UV-Visible spectrophotometer operating at 21 °C. Sample buffer was used as blank for baseline correction with extinction coefficients; ε_{280} = 225,000 M^{-1} cm^{-1} for Herceptin™, ε_{335} = 9,100 M^{-1} cm^{-1} for pyridazinedione scaffolds, ε_{493} = 75,000 M^{-1} cm^{-1} for Alexafluor 488™ (AF488) and ε_{495} = 8,030 M^{-1} cm^{-1} for doxorubicin. The correction factors for pyridazinedione scaffolds, AF488 and doxorubicin at 280 nm are 0.25, 0.11 and 0.72, respectively. Calculations are performed according to that previously described.[84]

SDS-PAGE gels

Non-reducing glycine-SDS-PAGE at 12% acrylamide gels were performed following standard lab procedures, unless stated otherwise. A 6% stacking gel was used and a broad-range MW marker (10–250 kDa, Prestained PagerulerPlus Protein Standards, Bio-Rad) was co-run to estimate protein weights. Samples (15 μL at ~12 μM construct) were mixed with loading buffer (3 μL, composition for 6 × SDS: 1 g SDS, 3 mL glycerol, 6 mL 0.5 M Tris buffer pH 6.8, 2 mg bromophenol blue in 10 mL) and heated at 75 °C for 3 min. The gels were run at 30 mA for 50 min in 1 × SDS running buffer. The gels were stained with Coomassie dye.

Protein LC-MS

Full Herceptin™ mAb conjugate **7** and Herceptin™ mAb were prepared for analysis by repeated diafiltration into ammonium acetate buffer (50 mM ammonium acetate, pH 6.9) using VivaSpin sample concentrators (GE Healthcare, 10,000 MWCO) to a concentration of 6.6 μM (1.0 mg·ml^{-1}). Following this, PNGase F (1 μL, 15,000 units·mL^{-1}, in 20 mM Tris-HCl, 50mM NaCl, 5 mM EDTA, pH 7.5) (purchased from New England BioLabs Inc.) was added and the resultant solution was incubated at 37 °C for 16 h. After this time the solution was diluted to 0.7 μM (1.0 mg·ml^{-1}) in water and submitted to the UCL Chemistry Mass Spectrometry Facility at the Chemistry Department, UCL for analysis of antibody conjugates on the Agilent 6510 QTOF LC-MS system (Agilent, UK). 10 μL of each sample was injected onto a PLRP-S, 1000A, 8 μM, 150 mm x 2.1 mm column, which was maintained at 60 °C. The separation was achieved using mobile phase A (5% MeCN in 0.1% formic acid) and B (95% MeCN, 5% water 0.1% formic acid) using a gradient elution. The column effluent was continuously electrosprayed into capillary ESI source of the Agilent 6510 QTOF mass spectrometer and ESI mass spectra were acquired in positive electrospray ionisation (ESI) mode using the m/z range 1,000–8,000 in profile mode. The raw data was converted to zero charge mass spectra using maximum entropy deconvolution algorithm over the region 12.3 – 16.8 min with MassHunter software (version B.07.00).

5.2.1 Synthesis of compounds for Chapter 3

Tri-*tert*-butyl 2-methylhydrazine-1,1,2-tricarboxylate (22)

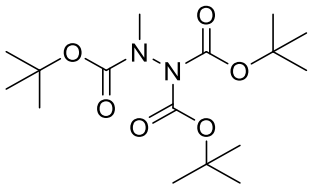

To a solution of methylhydrazine **21** (1.00 g, 1.14 mL, 21.7 mmol), NEt_3 (4.34 g, 6.04 mL, 43.4 mmol) and DMAP (260 mg, 2.17 mmol) in CH_2Cl_2 (75 mL) was added Boc_2O (18.9 g, 86.6 mmol), and the reaction mixture stirred at 20 °C for 72 h. After this time, the reaction mixture was diluted with H_2O (80 mL), extracted with EtOAc (3 × 60 mL), and the combined organic layers dried ($MgSO_4$) and concentrated *in vacuo*. The crude residue was purified by flash column chromatography (20% EtOAc/petrol) to afford tri-*tert*-butyl 2-methylhydrazine-1,1,2-tricarboxylate **22** (7.43 g, 21.5 mmol, 99%) as a yellowish oil: ^{1}H NMR (600 MHz, $CDCl_3$) (major rotamer) δ 3.05 (s, 3H), 1.51–1.43 (m, 27H); ^{13}C NMR (150 MHz, $CDCl_3$) (major rotamer) δ 154.0 (C), 150.1 (C) 83.4 (C), 81.4 (C), 35.7 (CH_3), 28.3 (CH_3), 28.1 (CH_3); LRMS (ES+) 369 (100, $[M+Na]^+$).

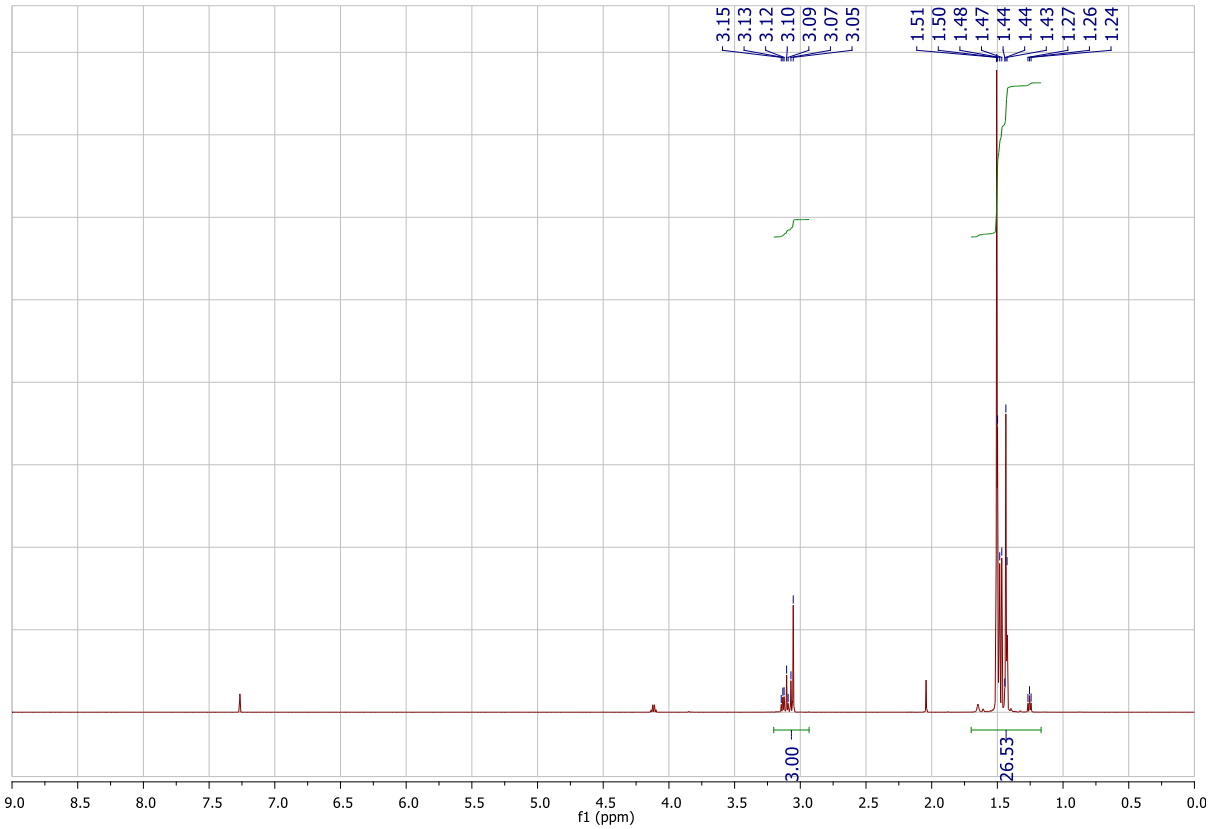

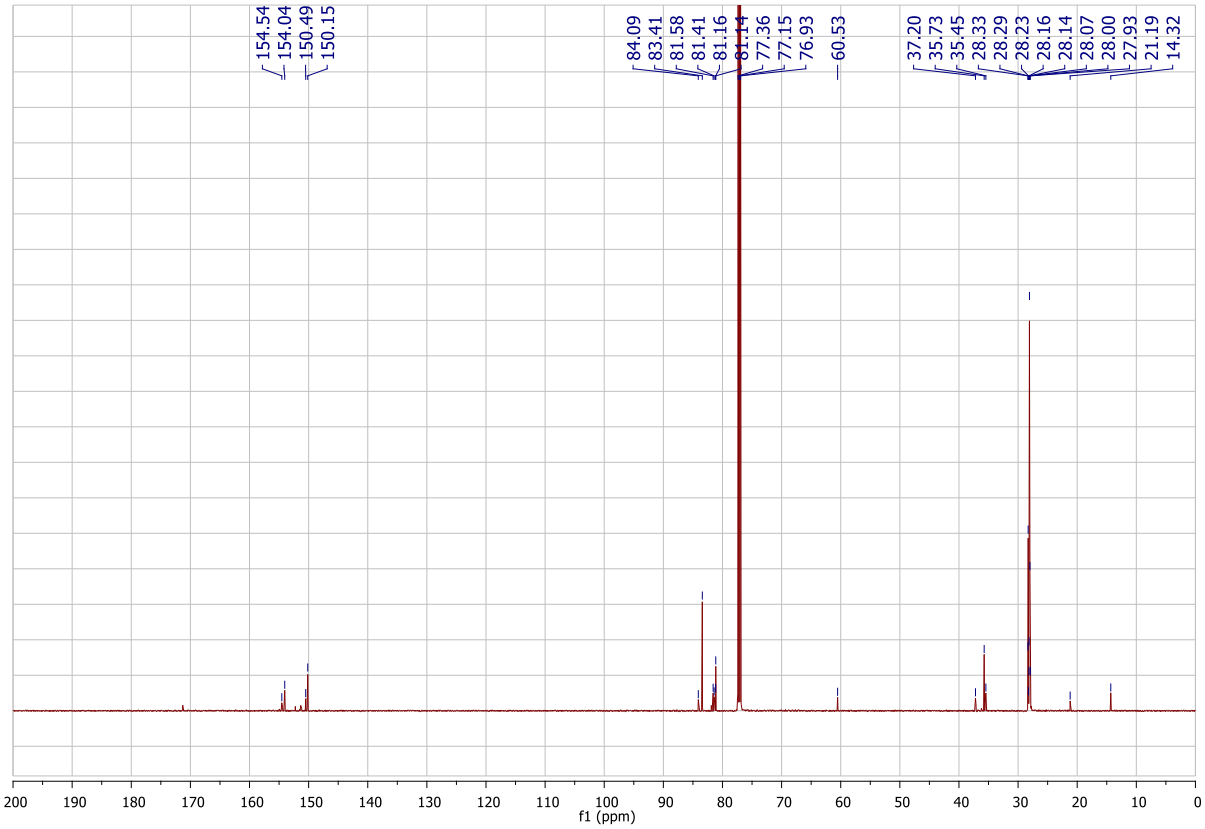

Figure **S45**. ^{1}H and ^{13}C NMR data for tri-*tert*-butyl 2-methylhydrazine-1,1,2-tricarboxylate **22**.

Di-*tert*-butyl 1-methylhydrazine-1,2-dicarboxylate (23)

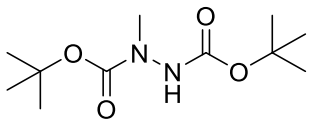

To a solution of tri-*tert*-butyl 2-methylhydrazine-1,1,2-tricarboxylate **22** (2.0 g, 5.8 mmol) in dry MeCN (15 mL) was added $Mg(ClO_4)_2$ (0.27 g, 1.21 mmol), and the reaction mixture stirred at 20 °C for 1 h. After this time, the reaction mixture was diluted with 10% aq. citric acid (20 mL) and Et_2O (15 mL), extracted with Et_2O (3 × 20 mL), and the combined organic layers were dried ($MgSO_4$) and concentrated *in vacuo*. The crude residue was purified by flash column chromatography (15% EtOAc/petrol) to afford di-*tert*-butyl 1-methylhydrazine-1,2-dicarboxylate **23** (1.3 g, 5.2 mmol, 89%) as a white solid: m.p. 54–55 °C; ^{1}H NMR (600 MHz, $CDCl_3$) (major rotamer) δ 6.40 (br. s, 1H), 3.11 (s, 3H), 1.48–1.45 (m, 18H); ^{13}C NMR (150 MHz, $CDCl_3$) (major rotamer) δ 155.9 (C), 155.3 (C) 81.3 (C), 81.1 (C), 37.6 (CH_3), 28.3 (CH_3), 28.1 (CH_3); IR (solid) 3316, 2978, 2932, 1701 cm^{-1}; LRMS (ES+) 269 (100, $[M+Na]^+$); HRMS (ES+) calcd. for $C_{11}H_{22}N_2O_4Na$ $[M+Na]^+$ 269.1477, observed 269.1476.

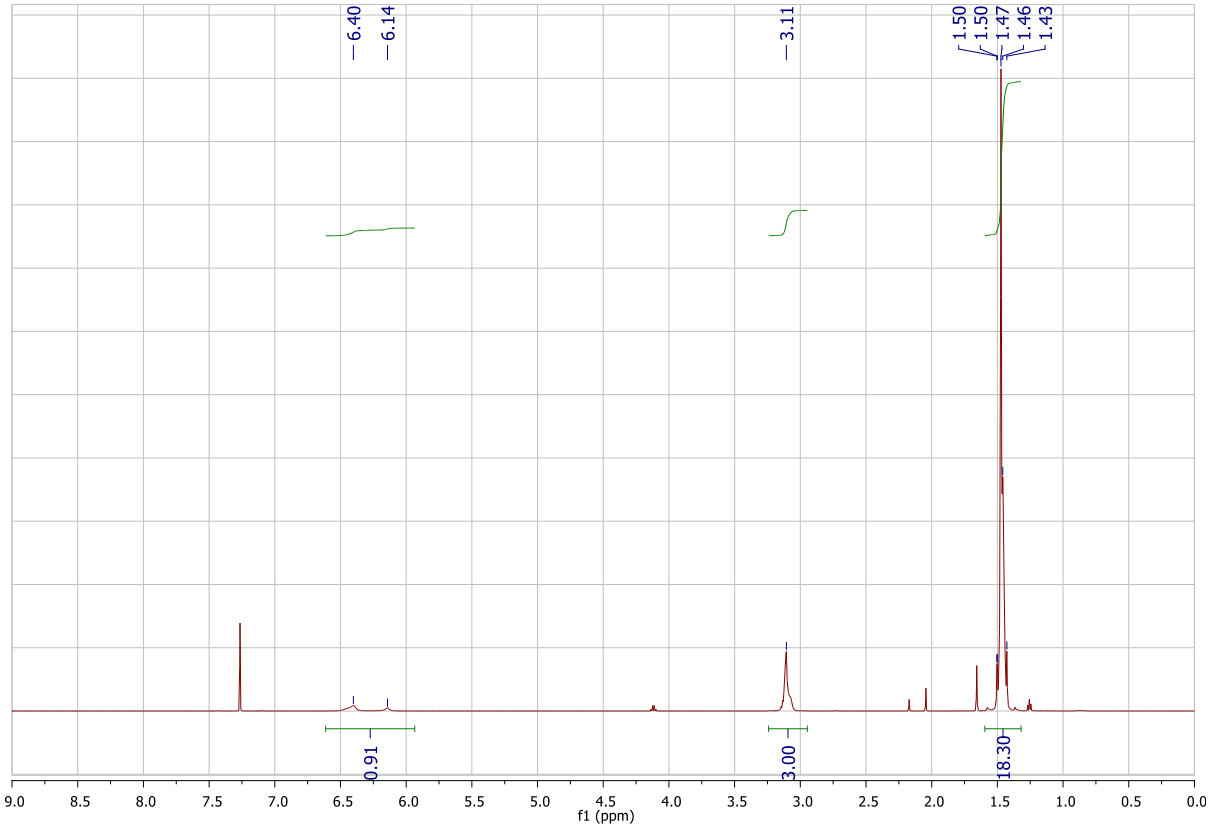

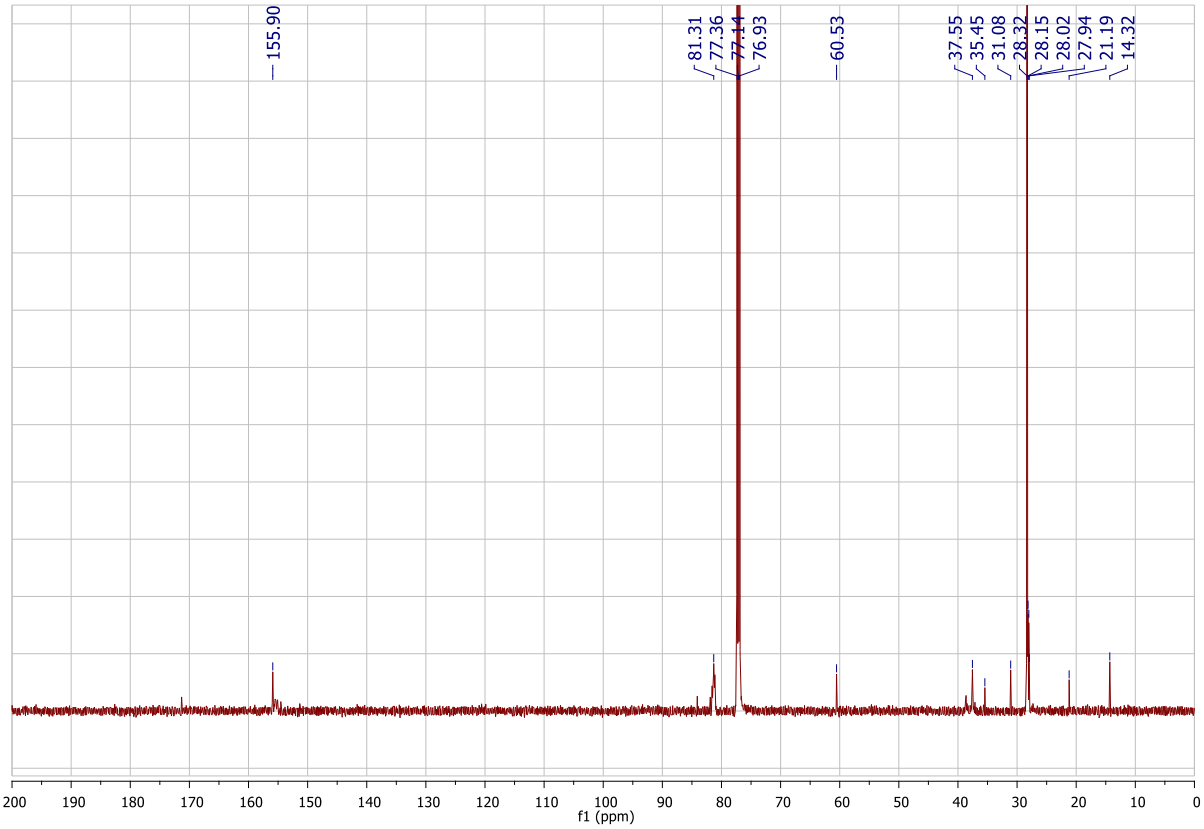

Figure **S46**. ^{1}H and ^{13}C NMR data for di-*tert*-butyl 1-methylhydrazine-1,2-dicarboxylate **23**.

Di-*tert*-butyl 1-(2-(*tert*-butoxy)-2-oxoethyl)-2-methylhydrazine-1,2-dicarboxylate (24)

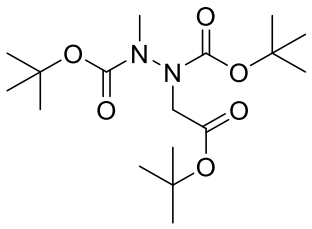

To a solution of di-*tert*-butyl 1-methylhydrazine-1,2-dicarboxylate (0.94 g, 3.8 mmol) in DMF (20 mL) was added caesium carbonate (1.86 g, 5.7 mmol) and then *tert*-butyl bromoacetate (1.1 g, 0.84 mL, 5.7 mmol), and the reaction mixture stirred at 20 °C for 16 h. After this time, the reaction mixture was diluted with H_2O (50 mL), extracted with Et_2O (4 × 50 mL), the combined organic layers washed with sat. aq. LiCl (2 × 30 mL), dried ($MgSO_4$), and concentrated *in vacuo*. Purification by flash column chromatography (10% Et_2O/petrol) yielded di-*tert*-butyl 1-(2-(*tert*-butoxy)-2-oxoethyl)- 2-methylhydrazine-1,2-dicarboxylate **24** (1.3 g, 3.7 mmol, 98%) as a colourless oil: ^{1}H NMR (600 MHz, $CDCl_3$) δ 4.73–4.04 (m, 2H), 3.68–3.10 (m, 3H), 1.54–1.39 (m, 27H); ^{13}C NMR (150 MHz, $CDCl_3$) (major rotamer) δ 169.2 (C), 155.2 (C), 81.9 (C), 81.6 (C), 81.1 (C), 52.7 (CH_2), 36.8 (CH_3), 28.4 (CH_3), 28.3 (CH_3), 28.2 (CH_3); IR (thin film) 2978, 1748 cm^{-1}; LRMS (ES+) 361 (100, $[M+H]^+$); HRMS (ES+) calcd for $C_{17}H_{33}O_6N_2$ $[M+H]^+$ 361.2339, observed 361.2333.

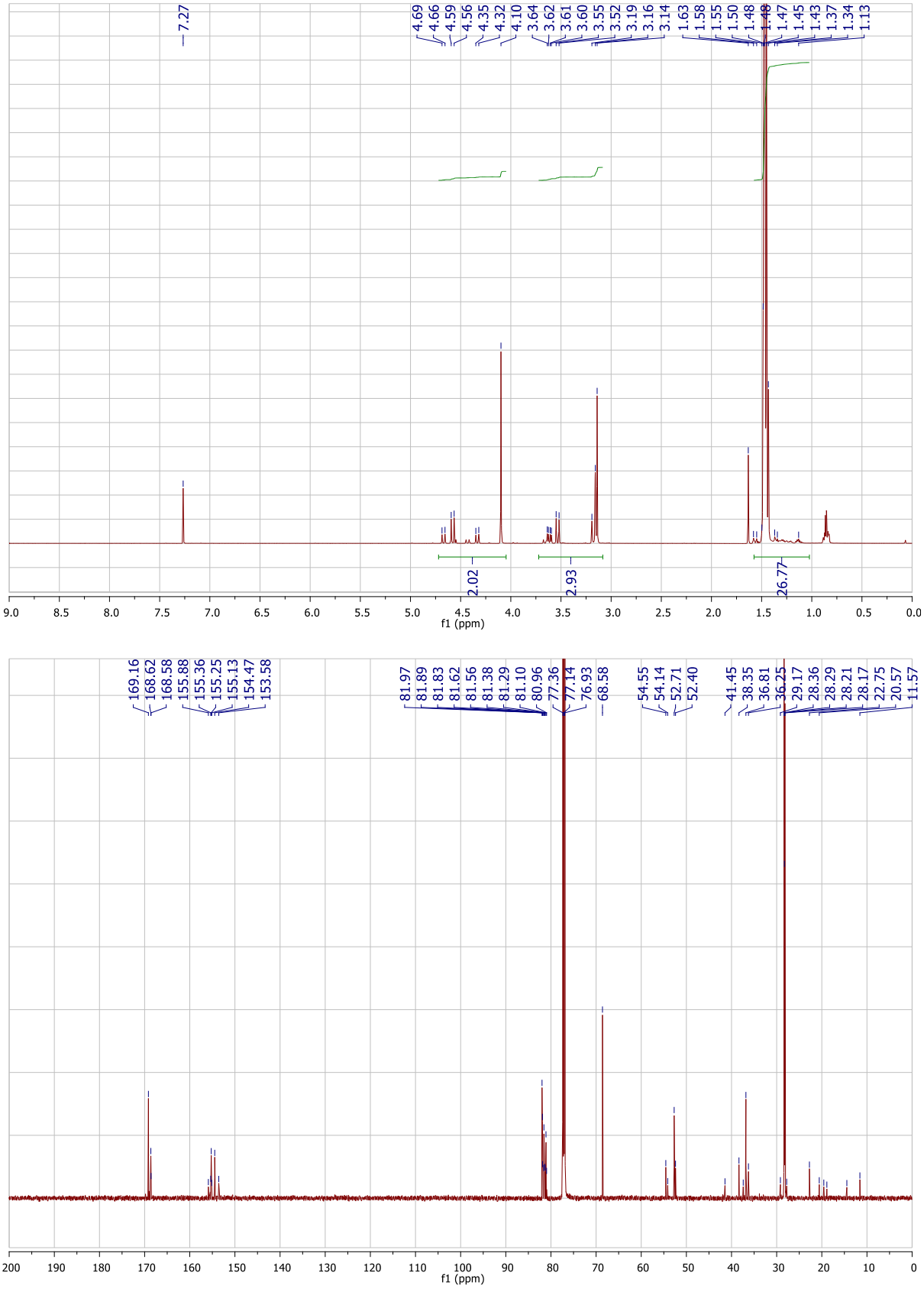

Figure **S47**. ^{1}H and ^{13}C NMR data for di-*tert*-butyl 1-(2-(*tert*-butoxy)-2-oxoethyl)-2-methylhydrazine-1,2-dicarboxylate **24**.

2-(4,5-Dibromo-2-methyl-3,6-dioxo-3,6-dihydropyridazin-1(2*H*)-yl)acetic acid (20)[84]

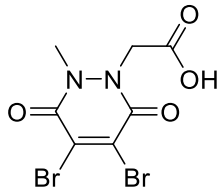

To a solution of di-*tert*-butyl 1-(2-(*tert*-butoxy)-2-oxoethyl)-2-methylhydrazine-1,2-dicarboxylate **24** (1.0 g, 2.8 mmol) in CH_2Cl_2 (10 mL) was added TFA (10 mL), and the reaction mixture stirred at 20 °C for 2 h. After this time, all volatile materials were removed *in vacuo*. The crude residue was added to a solution of 2,3-dibromomaleic anhydride (0.75 g, 2.8 mmol) in glacial AcOH (40 mL), and the reaction mixture stirred at 20 °C for 16 h before raising the temperature to 130 °C for 16 h. After this time, the reaction mixture was concentrated *in vacuo*, and purification of the crude residue by flash column chromatography (3% MeOH/CH_2Cl_2 with 1% AcOH) yielded 2-(4,5-dibromo-2-methyl-3,6-dioxo-3,6-dihydropyridazin-1(2*H*)-yl)acetic acid **20** (0.65 g, 1.9 mmol, 73%) as a white solid: m.p. 210–214 °C; ^{1}H NMR (600 MHz, MeOD) δ 4.96 (s, 2H), 3.62 (s, 3H); ^{13}C NMR (150 MHz, MeOD) δ 170.2 (C), 154.8 (C), 154.0 (C), 137.4 (C), 135.7 (C), 49.5 (CH_2), 35.0 (CH_3); IR (solid) 3023, 2969, 1731, 1662 cm^{-1}; LRMS (ES–) 341 (50, [M^{81}Br^{81}Br-H]$^-$), 339 (100, [M^{81}Br^{79}Br-H]$^-$), 337 (50, [M^{79}Br^{79}Br-H]$^-$); HRMS (ES–) calcd for $C_7H_5N_2O_4Br_2$ [M^{79}Br^{79}Br-H]$^-$ 336.8538, observed 336.8540.

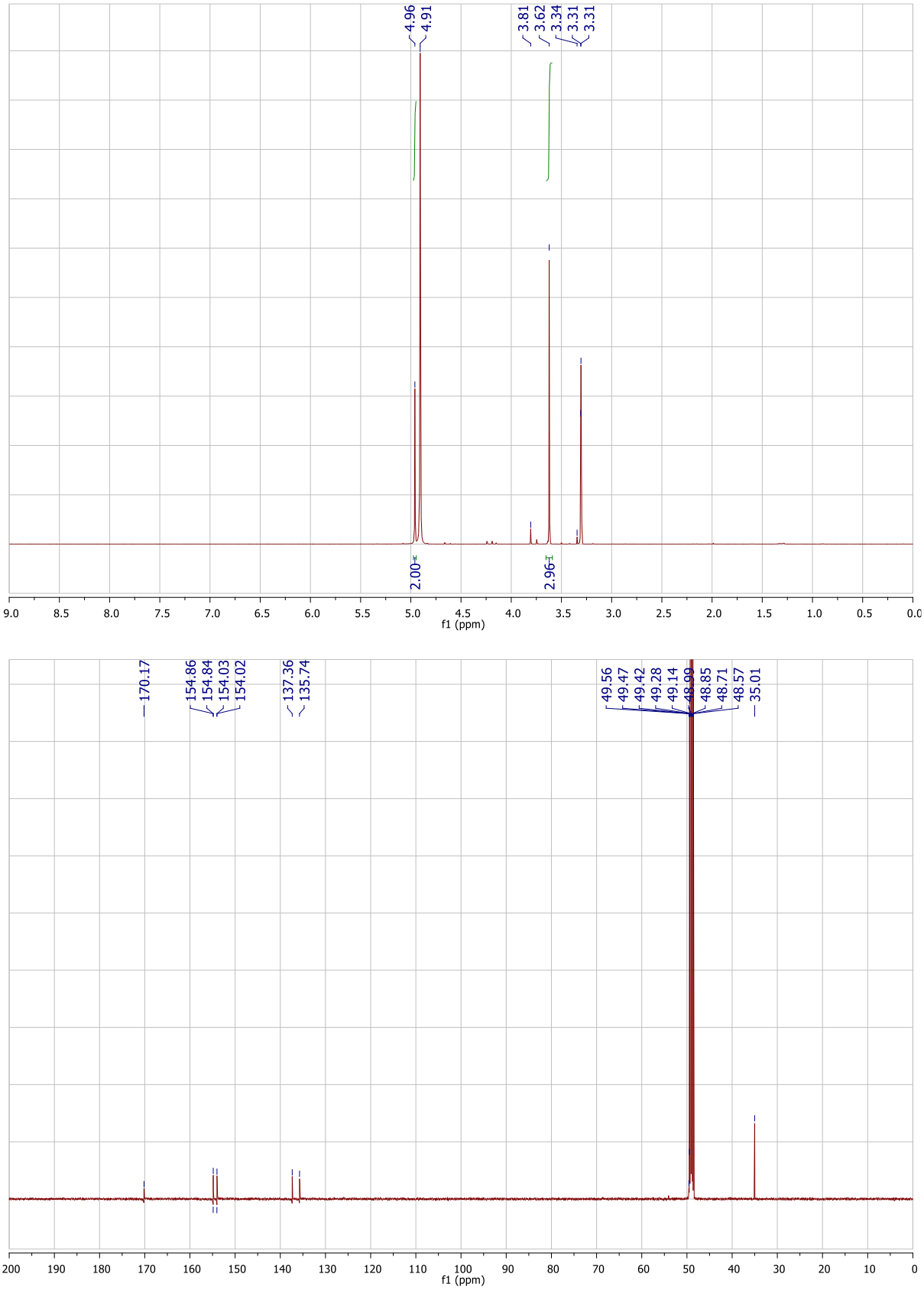

Figure **S48**. ^{1}H and ^{13}C NMR data for 2-(4,5-dibromo-2-methyl-3,6-dioxo-3,6-dihydropyridazin-1(2*H*)-yl)acetic acid **20**.

Di-*tert*-butyl-1-(prop-2-yn-1-yl)hydrazine-1,2-dicarboxylate(25)

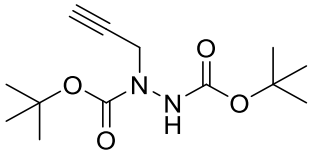

To a solution of di-*tert*-butyl hydrazine-1,2-dicarboxylate **1** (2.00 g, 8.62 mmol) in a mixture of toluene (10 mL) and 5% aq. NaOH (10 mL) were added tetra-*n*-butylammonium bromide (87 mg, 0.26 mmol) and then propargyl bromide (3.08 g, 25.86 mmol). The reaction mixture was stirred at 20 °C for 16 h. After this time, H_2O (20 mL) was added and the mixture was extracted with EtOAc (3 × 15 mL). The combined organic layers were washed with brine (15 mL), dried ($MgSO_4$), and concentrated *in vacuo*. Purification of the crude residue by flash column chromatography (20% EtOAc/petrol) yielded di-*tert*-butyl 1-(prop-2-yn- 1-yl)hydrazine-1,2-dicarboxylate **25** (1.93 g, 7.14 mmol, 83%) as a white solid: m.p. 101–103 °C; ^{1}H NMR (500 MHz, $CDCl_3$) δ 6.47 (br. s, 0.78H), 6.18 (br. s, 0.22H,), 4.27 (s, 2H), 2.24 (t, *J* = 2.4 Hz, 1H), 1.48 (s, 18H); ^{13}C NMR (150 MHz, $CDCl_3$) δ 155.0 (C), 82.2 (C), 81.7 (C), 79.0 (C), 77.7 (C), 72.5 (CH), 39.5 (CH_2), 28.5 (CH_3), 28.5 (CH_3); IR (solid) 3310, 2109, 1703 cm^{-1}.

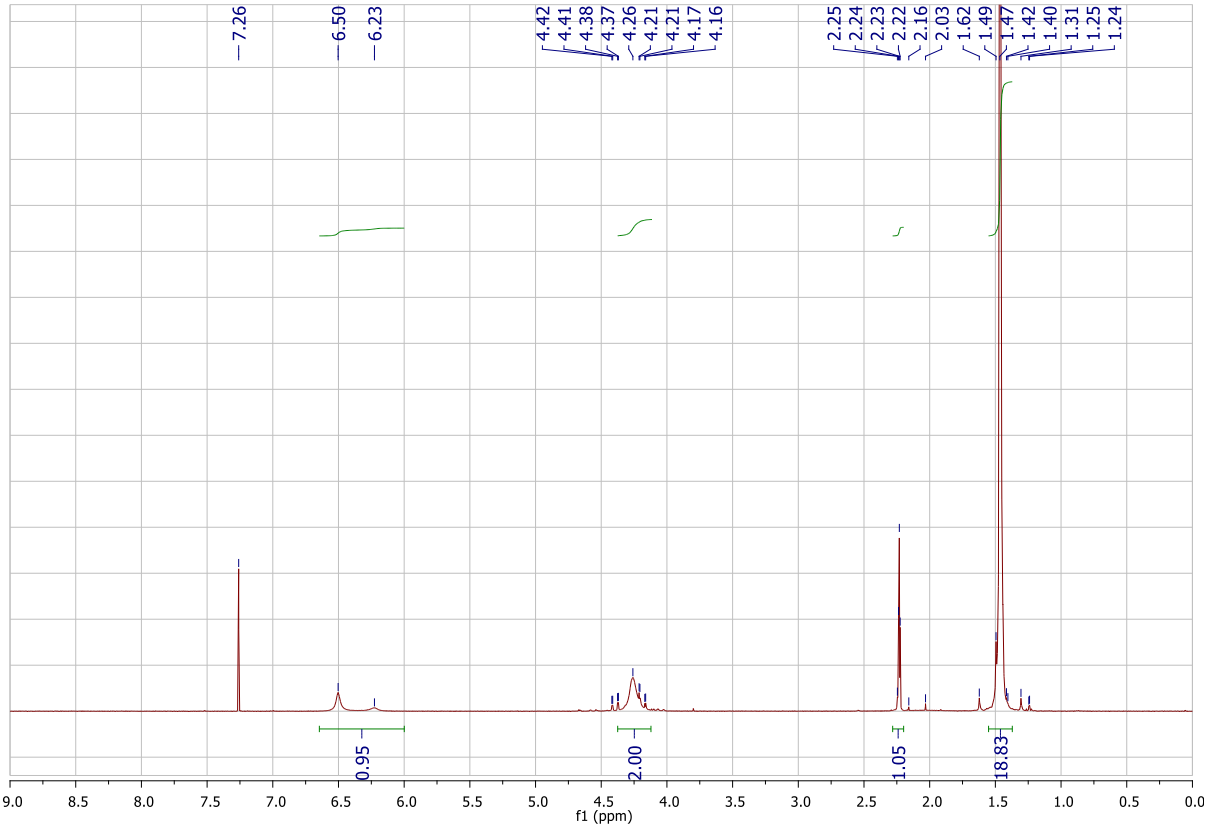

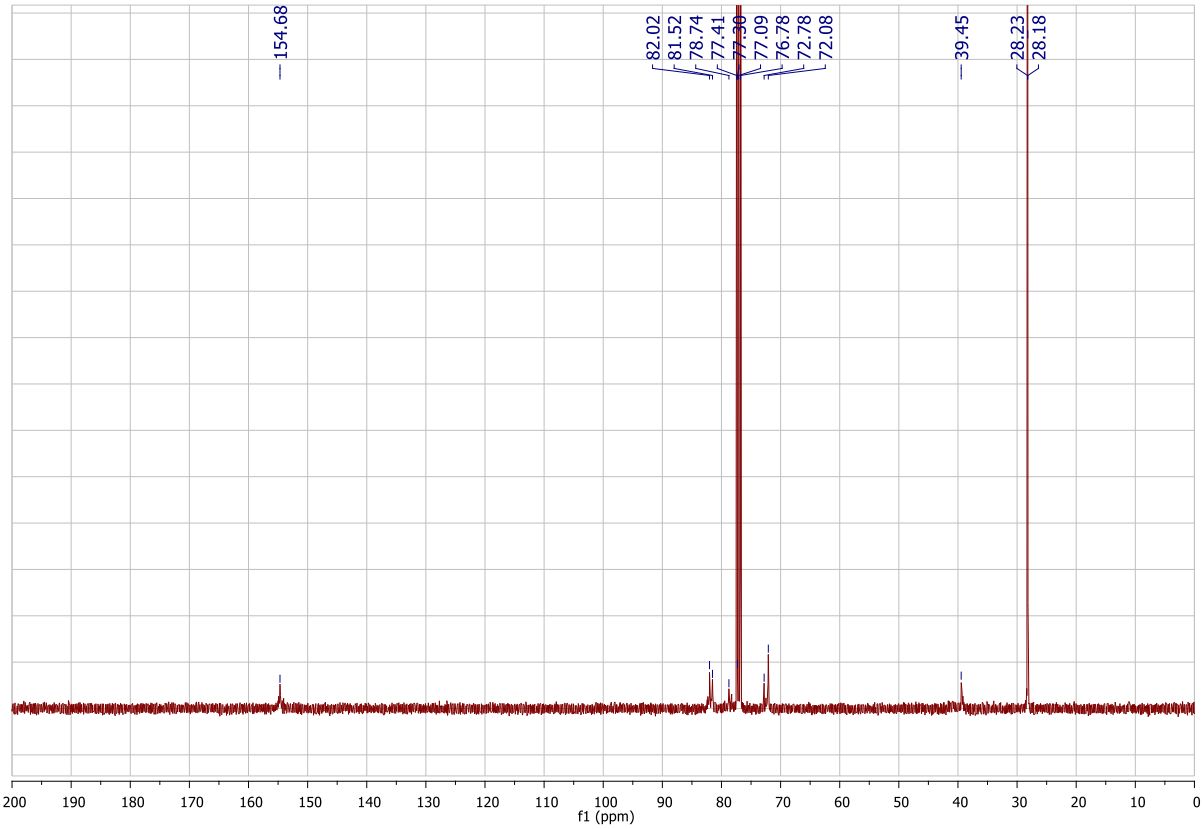

Figure **S49**. ^{1}H and ^{13}C NMR data for di-*tert*-butyl-1-(prop-2-yn-1-yl)hydrazine-1,2-dicarboxylate **25**.

Di-*tert*-butyl 1-(2-(tert-butoxy)-2-oxoethyl)-2-(prop-2-yn-1-yl)hydrazine-1,2-dicarboxylate (26)

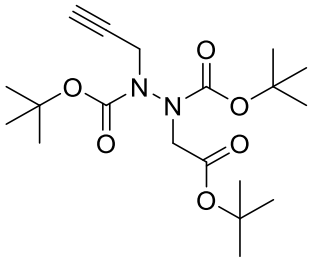

To a solution of di-*tert*-butyl 1-(prop-2-yn-1-yl)hydrazine-1,2-dicarboxylate **25** (1.45 g, 5.36 mmol) in DMF (20 mL) were added caesium carbonate (3.56 g, 10.92 mmol) and then *tert*-butyl bromoacetate (1.57 g, 2.8 mmol), and the reaction mixture stirred at 20 °C for 16 h. After this time, the reaction mixture was diluted with H_2O (50 mL), extracted with EtOAc (4 × 50 mL), the combined organic layers washed with sat. aq. LiCl (2 × 30 mL), dried ($MgSO_4$), and concentrated *in vacuo*. Purification of the crude residue by flash column chromatography (10% EtOAc/petrol) yielded di-*tert*-butyl 1-(2-(*tert*-butoxy)-2-oxoethyl)-2-(prop-2-yn-1- yl)hydrazine-1,2-dicarboxylate **26** (2.00 g, 5.20 mmol, 97%) as a colourless oil: ^{1}H NMR (600 MHz, $CDCl_3$) δ 4.58–4.35 (m, 2H), 4.16–4.01 (m, 1H), 3.67–3.64 (m, 1H), 2.18 (t, *J* = 2.3 Hz, 1H), 1.53–1.41 (m, 27H); ^{13}C NMR (150 MHz, $CDCl_3$) (major rotamer) δ 168.1 (C), 166.3 (C), 153.9 (C), 83.0 (C), 81.9 (C), 81.8 (C), 79.4 (C), 71.9 (CH), 53.5 (CH_2), 40.1 (CH_2), 28.3 (CH_3), 28.3 (CH_3), 28.1 (CH_3); IR (thin film) 3265, 2108, 1714 cm$^-$; LRMS (CI) 385 (55, $[M+H]^+$), 329 (65), 273 (100); HRMS (CI) calcd for $C_{19}H_{33}O_6N_2$ $[M+H]^+$ 385.2333, observed 385.2319.

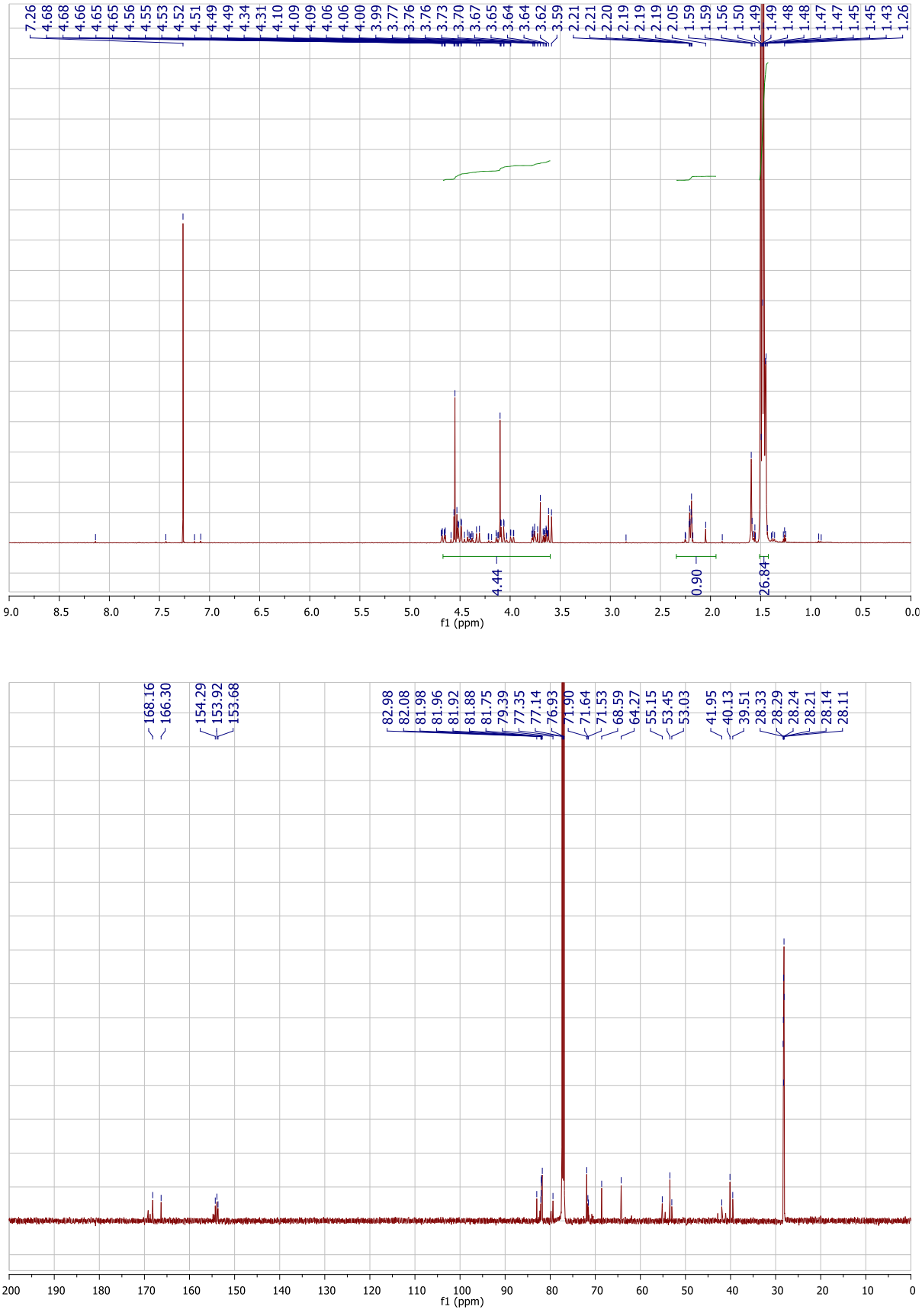

Figure **S50**. ^{1}H and ^{13}C NMR data for di-*tert*-butyl 1-(2-(*tert*-butoxy)-2-oxoethyl)-2-(prop-2-yn-1-yl)hydrazine-1,2-dicarboxylate **26**.

2-(4,5-Dibromo-3,6-dioxo-2-(prop-2-yn-1-yl)-2,3-dihydropyridazin-1(6*H*)-yl) acetic acid (27)[83]

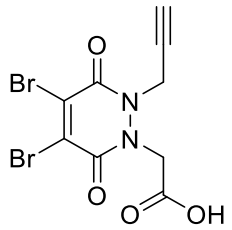

To a solution of di-*tert*-butyl 1-(2-(*tert*-butoxy)-2-oxoethyl)-2-(prop-2-yn-1-yl)hydrazine- 1,2-dicarboxylate **26** (0.50 g, 1.30 mmol) in CH_2Cl_2 (10 mL) was added TFA (10 mL), and the reaction mixture stirred at 20 °C for 2 h. After this time, all volatile materials were removed *in vacuo*. The crude residue was added to a solution of 2,3-dibromomaleic anhydride (0.40 g, 1.57 mmol) in glacial AcOH (40 mL), and the reaction mixture stirred at 20 °C for 16 h before raising the temperature to 130 °C for 2 h. Then the reaction mixture was concentrated *in vacuo*, and purification of the crude residue by flash column chromatography (3% MeOH/CH_2Cl_2 with 1% AcOH) yielded 2-(4,5-dibromo-3,6-dioxo-2-(prop-2-yn-1-yl)- 2,3-dihydropyridazin-1(6*H*)-yl)acetic acid **27** (0.31 g, 0.85 mmol, 65%) as a white solid: m.p. 108–110 °C; ^{1}H NMR (600 MHz, MeOD) δ 4.93 (s, 2H), 4.79 (d, *J* = 2.5 Hz, 2H), 2.46 (t, *J* = 2.5 Hz, 1H); ^{13}C NMR (150 MHz, $CDCl_3$) δ 168.1 (C), 153.9 (C), 152.6 (C), 136.3 (C), 135.9 (C), 77.3 (C), 75.4 (CH), 48.4 (CH_2), 37.1 (CH_2); IR (solid) 3444, 3287, 2109, 1729, 1631 cm^{-1}; LRMS (CI) 369 (50, $[M^{81}Br^{81}Br+H]^+$), 367 (100, $[M^{81}Br^{79}Br+H]^+$), 365 (50, $[M^{79}Br^{79}Br+H]^+$); HRMS (CI) calcd for $C_9H_7N_2O_4Br_2$ $[M^{79}Br^{79}Br+H]^+$ 364.8767, observed 364.8762.

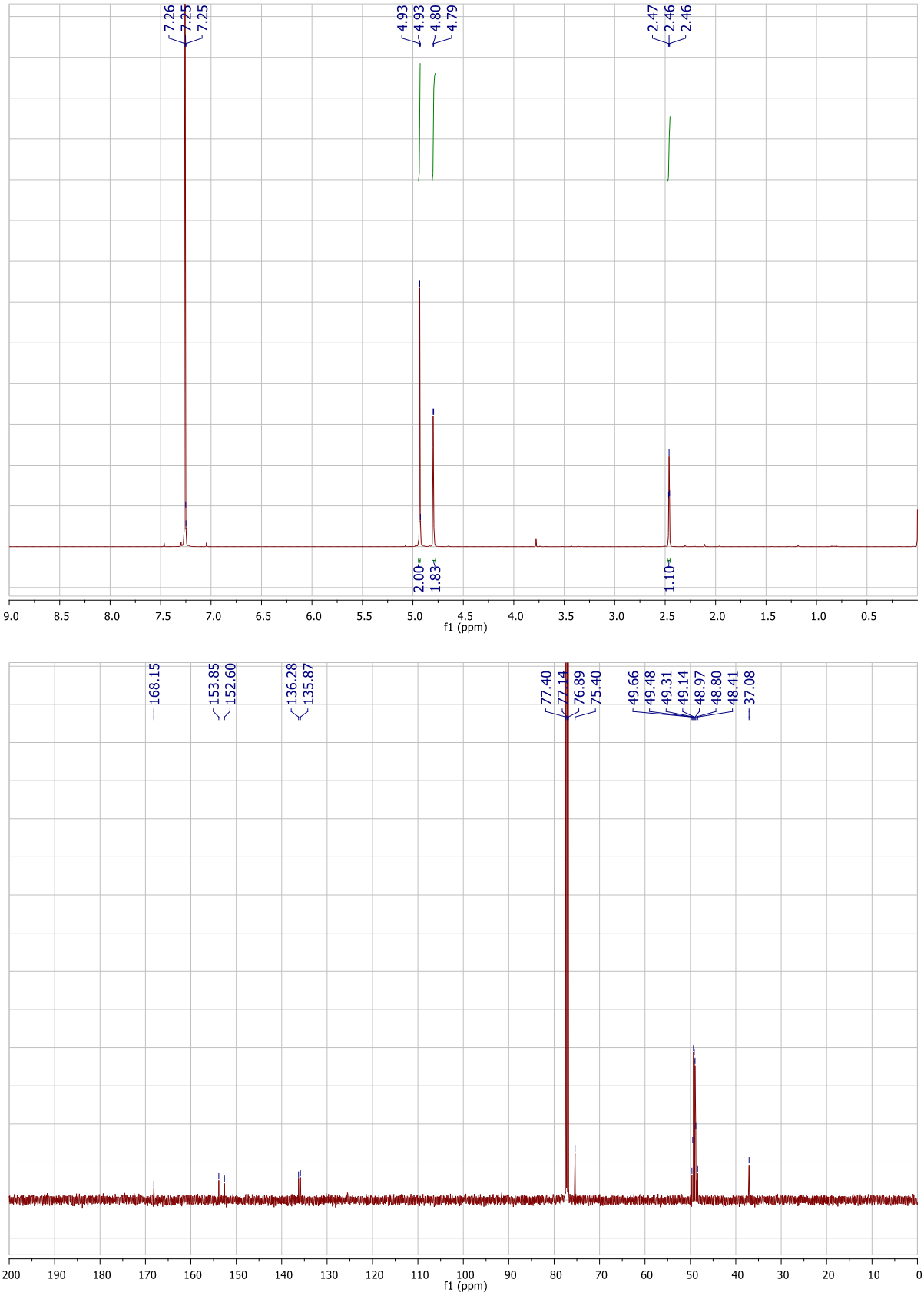

Figure **S51**. ^{1}H and ^{13}C NMR data for 2-(4,5-dibromo-3,6-dioxo-2-(prop-2-yn-1-yl)-2,3-dihydropyridazin-1(6*H*)-yl) acetic acid **27**.

***tert*-Butyl (3-(2-(2-(3-aminopropoxy)ethoxy)ethoxy)propyl)carbamate (28)**[139]

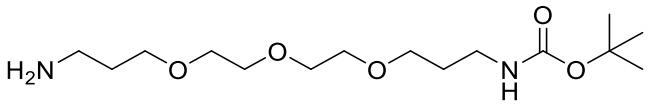

To a stirring solution of 3,3'-((oxybis(ethane-2,1-diyl))bis(oxy))bis(propan-1-amine) (8.10 g, 37.1 mmol) in 1,4-dioxane (60 mL) was added dropwise di-*tert*-butyl dicarbonate (1.00 g, 4.60 mmol, pre-dissolved in 1,4-dioxane (25 mL)) over 2 h, ensuring that the temperature did not exceed 21 °C. After this time, the reaction mixture was stirred at 21 °C for a further 30 mins. Following this, the reaction mixture was concentrated *in vacuo*, the crude residue dissolved in water (50 mL), and the organics extracted into EtOAc (5 × 30 mL). The organics were combined, dried ($MgSO_4$) and concentrated *in vacuo* to give *tert*-butyl (3-(2-(2-(3-aminopropoxy)ethoxy)ethoxy)propyl)carbamate **28** (1.1 g, 34 mmol, 75%) as a colourless oil. ^{1}H NMR (600 MHz, $CDCl_3$) δ 5.11 (br s, 1H), 4.99 (d, *J* = 1.9 Hz, 4H), 4.93 (s, 4H), 3.65-3.61 (m, 12H), 3.24-3.19 (m, 2H), 2.79 (t, *J* = 6.7 Hz, 2H), 1.72 (tt, *J* = 6.5 Hz, 4H), 1.43 (s, 9H); ^{13}C NMR 151 MHz, $CDCl_3$) δ 156.2 (C), 79.0 (C), 70.7 (CH_2), 70.7 (CH_2), 70.4 (CH_2), 70.3 (CH_2), 69.7 (CH_2), 69.6 (CH_2), 39.8 (CH_2), 38.6 (CH_2), 33.5 (CH_2), 29.7 (CH_2), 28.6 (CH_3); IR (thin film) 3360, 2928, 2865, 1696, 1521, 1102 cm^{-1}.

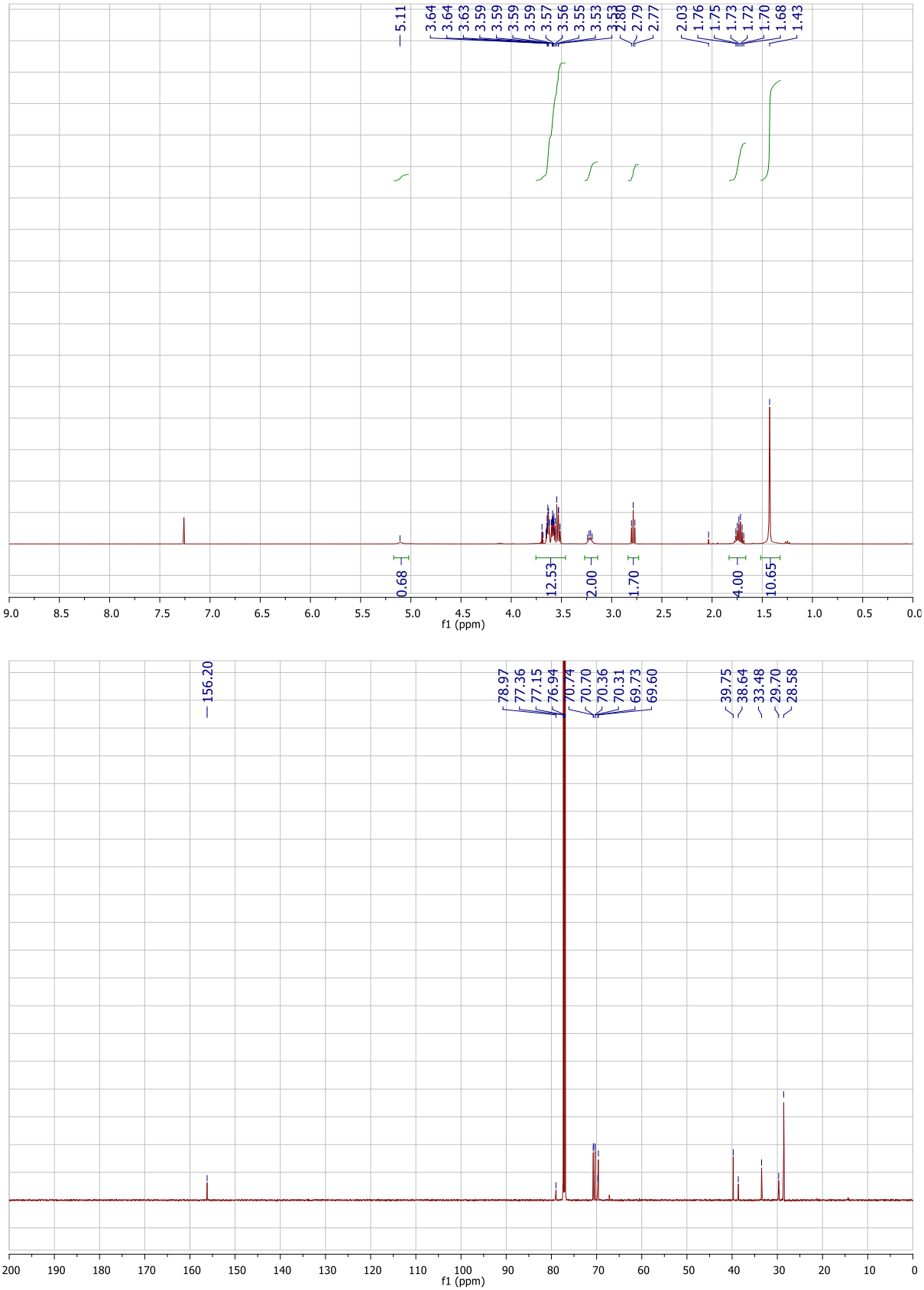

Figure **S52**. ^{1}H and ^{13}C NMR data for *tert*-butyl (3-(2-(2-(3-aminopropoxy)ethoxy)ethoxy)propyl)carbamate **28**.

***tert*-Butyl (1-(4,5-dibromo-2-methyl-3,6-dioxo-3,6-dihydropyridazin-1(2*H*)-yl)-2-oxo-7,10,13-trioxa-3-azahexadecan-16-yl) (29)**

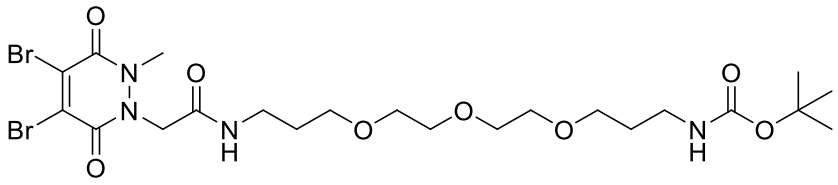

To a solution of 2-(4,5-dibromo-2-methyl-3,6-dioxo-3,6-dihydropyridazin-1(2*H*)-yl)acetic acid **20** (350 mg, 1.02 mmol) in DMF (30 mL) was added CDI (165 mg, 1.02 mmol), and the reaction mixture stirred at 21 °C for 15 mins. After this time, to the reaction mixture was added *tert*-butyl (3-(2-(2-(3-aminopropoxy)ethoxy)ethoxy)propyl)carbamate) (362 mg, 1.13 mmol), and the mixture left to stir at 21 °C for a further 12 h. The reaction mixture was then diluted with EtOAc (50 mL) and washed with saturated sodium bicarbonate solution (1 × 20 mL), deionised water (4 × 20 mL) and brine (2 × 20 mL). The organic phase was then dried ($MgSO_4$) and concentrated *in vacuo*, and the resultant crude residue purified by flash column chromatography (0-20% MeOH:EtOAc). The appropriate fractions were combined and concentrated *in vacuo* to afford *tert*-butyl (1-(4,5-dibromo-2-methyl-3,6-dioxo-3,6-dihydropyridazin-1(2*H*)-yl)-2-oxo-7,10,13-trioxa-3-azahexadecan-16-yl)carbamate **29** (50 mg, 0.08 mmol, 8%) as a yellow gum. ^{1}H NMR (600 MHz, $CDCl_3$) δ 7.12 (br. s, 1H), 4.96 (br. s, 1H), 4.74 (s, 2H), 3.69 (s, 3H), 3.66-3.58 (m, 10H), 3.53 (t, *J* = 6.1 Hz, 2H), 3.42 (dd, *J* = 11.9, 5.7, 2H), 3.22-3.19 (m, 2H), 1.82-1.78 (m, 2H), 1.76-1.72 (m, 2H), 1.43 (s, 9H); ^{13}C NMR 151 MHz, $CDCl_3$) δ 165.3 (C), 156.2 (C), 153.5 (C), 152.5 (C), 136.9 (C), 134.9 (C), 79.2 (C), 70.5 (CH_2), 70.4 (CH_2), 70.2 (CH_2), 70.2 (CH_2), 69.9 (CH_2), 69.5 (CH_2), 50.7 (CH_2), 38.9 (CH_2), 38.4 (CH_2), 34.9 (CH_3), 29.9 (CH_2), 28.6 (CH_3), 28.5 (CH_2); IR (thin film) 3347, 2921, 2866, 1685, 1634, 1282, 1054 cm^{-1}; LRMS (ES+) 647 (50, $[M^{81}Br^{81}Br+H]^+$), 645 (100, $[M^{81}Br^{79}Br+H]^+$), 643 (50, $[M^{79}Br^{79}Br+H]^+$); HRMS (ES+) calcd for $C_{22}H_{37}Br_2N_4O_8$ $[M^{81}Br^{79}Br+H]^+$ 643.0973, observed 643.0954.

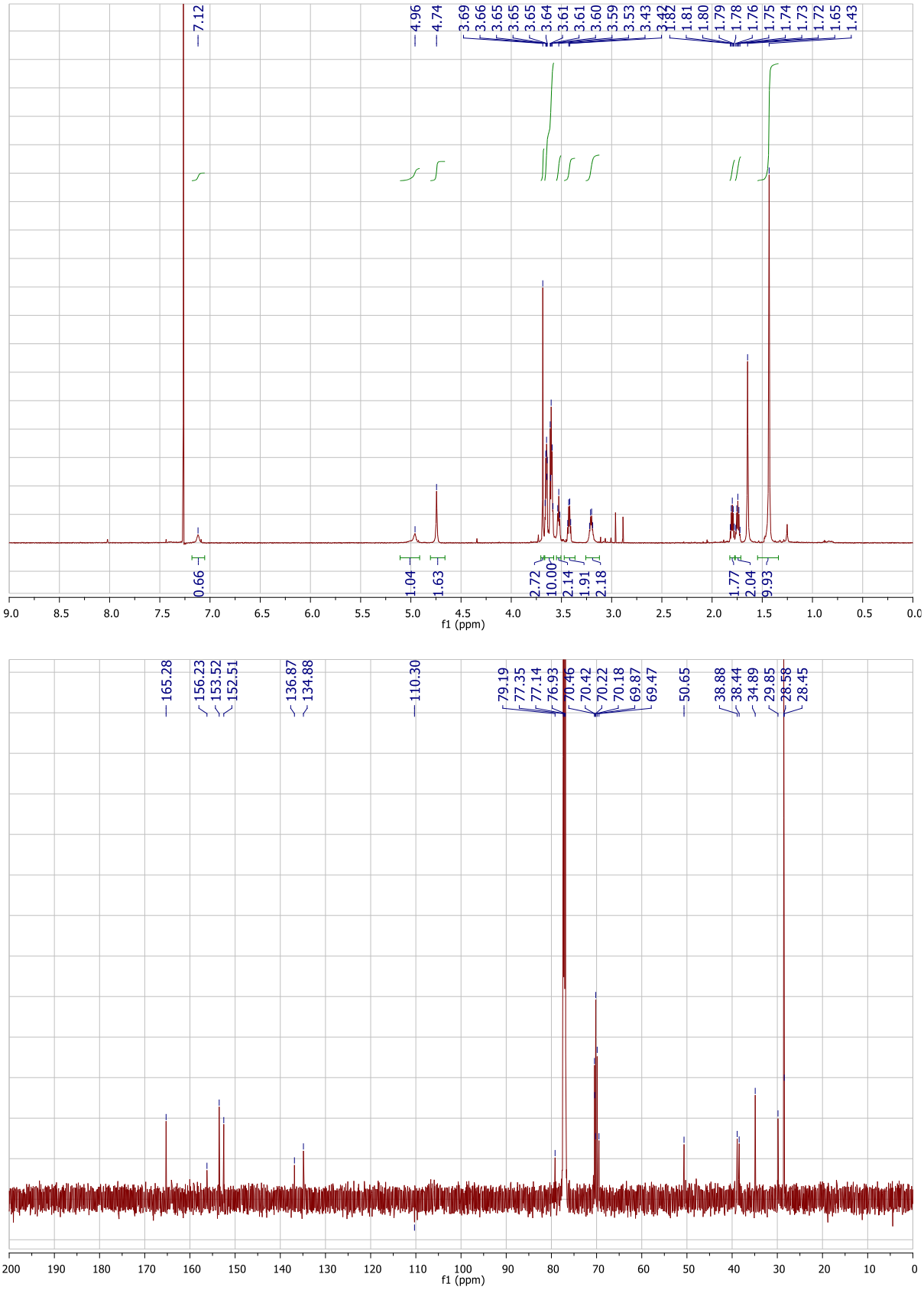

Figure **S53**. ^{1}H and ^{13}C NMR data for *tert*-butyl (1-(4,5-dibromo-2-methyl-3,6-dioxo-3,6-dihydropyridazin-1(2*H*)-yl)-2-oxo-7,10,13-trioxa-3-azahexadecan-16-yl)carbamate **29**.

2-(4,5-Dibromo-2-methyl-3,6-dioxo-3,6-dihydropyridazin-1(2*H*)-yl)-*N*-(1-(4,5-dibromo-3,6-dioxo-2-(prop-2-yn-1-yl)-3,6-dihydropyridazin-1(2*H*)-yl)-2-oxo-7,10,13-trioxa-3-azahexadecan-16-yl)acetamide (19)

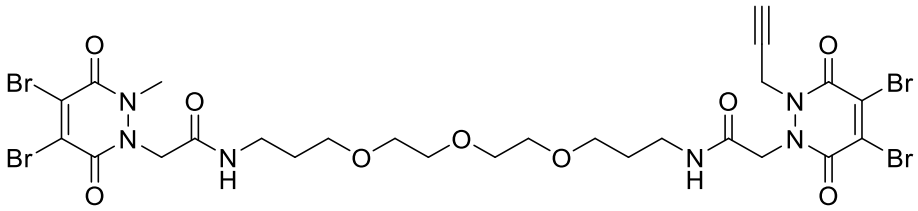

To a solution of 2-(4,5-dibromo-2-methyl-3,6-dioxo-3,6-dihydropyridazin-1(2*H*)-yl)-N-(1-(4,5-dibromo-3,6-dioxo-2-(prop-2-yn-1-yl)-3,6-dihydropyridazin-1(2*H*)-yl)-2-oxo-7,10,13-trioxa-3-azahexadecan-16-yl)acetamide **29** (50.0 mg, 0.08 mmol) in CH_2Cl_2 (5 mL) was added TFA (5 mL), and the reaction mixture stirred for 30 mins at 21 °C. After this time, the reaction mixture was concentrated *in vacuo* and the residue dissolved in CH_2Cl_2 (5 mL). The resultant solution was added to a pre-mixed (20 mins at 21 °C) solution of 2-(4,5-dibromo-3,6-dioxo-2-(prop-2-yn-1-yl)-3,6-dihydropyridazin-1(2*H*)-yl)acetic acid **27** (27.3 mg, 0.08 mmol), HATU (28.4 mg, 0.08 mmol) and *N*-ethyldiisopropylamine (21.2 mg, 0.16 mmol, 30 µL) in CH_2Cl_2 (10 mL). The reaction mixture was then stirred for 16 h at 21 °C. Following this, the reaction mixture was washed with water (3 × 10 mL) and the resultant aqueous washes extracted with CH_2Cl_2 (10 mL). The organic phases were combined, dried ($MgSO_4$) and concentrated *in vacuo*, and the crude residue purified by flash column chromatography (0-15% MeOH:EtOAc). The appropriate fractions were combined and concentrated *in vacuo* to afford 2-(4,5-dibromo-2-methyl-3,6-dioxo-3,6-dihydropyridazin-1(2*H*)-yl)-*N*-(1-(4,5-dibromo-3,6-dioxo-2-(prop-2-yn-1-yl)-3,6-dihydropyridazin-1(2*H*)-yl)-2-oxo-7,10,13-trioxa-3-azahexadecan-16-yl)acetamide **19** (20 mg, 0.02 mmol, 30%) as a yellow gum. ^{1}H NMR (600 MHz, $CDCl_3$) δ 7.25 (t, *J* = 5.4 Hz, 1H), 7.21 (t, *J* = 5.2 Hz, 1H), 4.99 (d, *J* = 2.0 Hz, 2H), 4.93 (s, 2H), 4.79 (s, 2H), 3.68 (s, 3H), 3.67-3.57 (m, 14H), 3.40 (td, *J* = 12.3, 5.9, 4H), 2.46 (t, *J* = 2.0 Hz, 1H), 1.82-1.76 (m, 4H); ^{13}C NMR 151 MHz, $CDCl_3$) δ 165.4 (C), 165.3 (C), 153.7 (C), 153.6 (C), 152.5 (C), 152.4 (C), 137.0 (C), 136.6 (C), 135.8 (C), 134.8 (C), 76.3 (C), 75.0 (CH), 70.3 (CH_2), 69.8 (CH_2), 69.7 (CH_2), 69.6 (CH_2), 69.6 (CH_2), 50.6 (CH_2), 50.5 (CH_2), 38.4 (CH_2), 38.3 (CH_2), 37.4 (CH_2), 34.9 (CH_3), 28.5 (CH_2), 28.5 (CH_2); IR (thin film) 3305, 2924,

2870, 1636, 1571, 1287 cm^{-1}; LRMS (ES+) 895 (55, $[M^{81}Br^{81}Br^{81}Br^{79}Br + H]^+$), 893 (100, $[M^{81}Br^{81}Br^{79}Br^{79}Br+H]^+$), 891 (55, $[M^{81}Br^{79}Br^{79}Br^{79}Br+H]^+$); HRMS (ES+) calcd for $C_{28}H_{32}Br_4N_6O_9$ $[M^{79}Br^{79}Br^{79}Br^{79}Br+H]^+$ 888.9037, observed 888.9039.

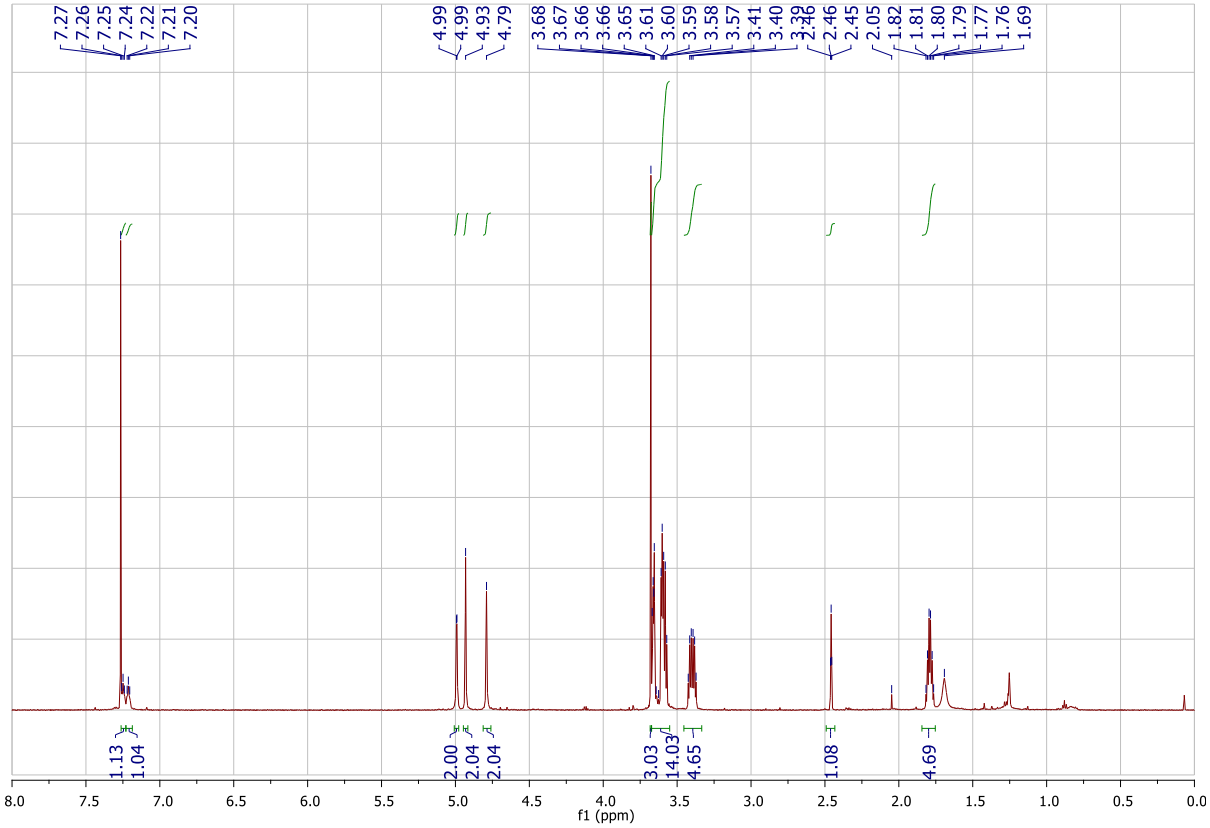

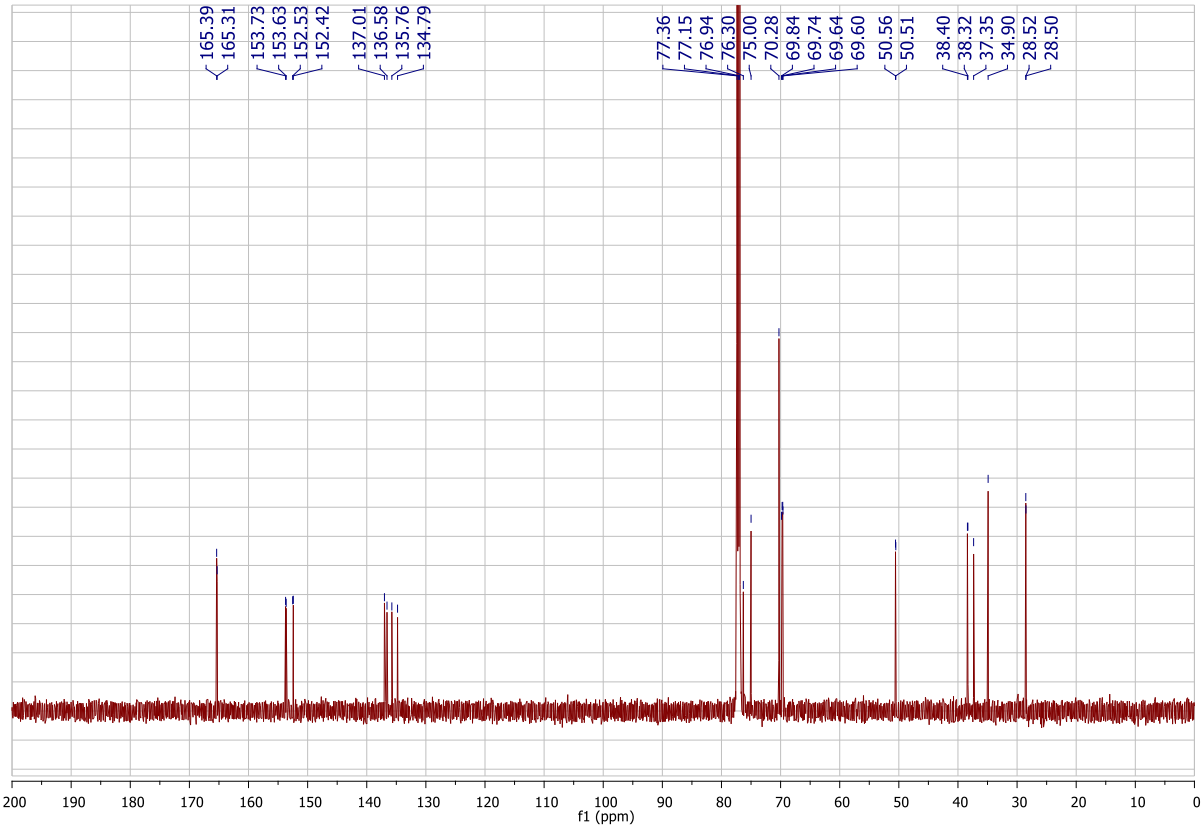

Figure **S54**. ^{1}H and ^{13}C NMR data for 2-(4,5-dibromo-2-methyl-3,6-dioxo-3,6-dihydropyridazin-1(2*H*)-yl)-*N*-(1-(4,5-dibromo-3,6-dioxo-2-(prop-2-yn-1-yl)-3,6-dihydropyridazin-1(2*H*)-yl)-2-oxo-7,10,13-trioxa-3-azahexadecan-16-yl)acetamide **19**.

***N*,*N*'-(((Oxybis(ethane-2,1-diyl))bis(oxy))bis(propane-3,1-diyl))bis(2-(4,5-dibromo-3,6-dioxo-2-(prop-2-yn-1-yl)-3,6-dihydropyridazin-1(2*H*)-yl)acetamide) (33)**

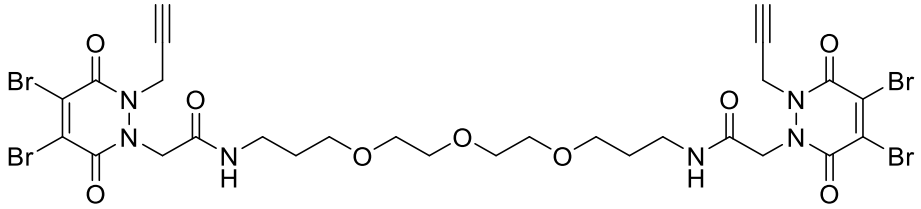

To a solution of 2-(4,5-dibromo-3,6-dioxo-2-(prop-2-yn-1-yl)-3,6-dihydropyridazin-1(2*H*)-yl)acetic acid **27** (200 mg, 0.60 mmol) in DMF (5 mL) was added DCC (120 mg, 0.58 mmol), and the reaction mixture stirred at 21 °C for 15 mins. After this time, to the reaction mixture was added 3,3'-((oxybis(ethane-2,1-diyl))bis(oxy))bis(propan-1-amine) (26 μL, 0.12 mmol), and the resultant mixture stirred at 21 °C for 12 h. After this time, the reaction mixture was diluted with EtOAc (20 mL) and washed with deionised water (4 × 10 mL) and brine (2 × 10 mL). The organic phase was then dried ($MgSO_4$), concentrated *in vacuo* and the crude residue purified by flash column chromatography (0-10% MeOH:CH_2Cl_2), which yielded *N*,*N*'-(((oxybis(ethane-2,1-diyl))bis(oxy))bis(propane-3,1-diyl))bis(2-(4,5-dibromo-3,6-dioxo-2-(prop-2-yn-1-yl)-3,6-dihydropyridazin-1(2*H*)-yl)acetamide) **33** (20 mg, 0.02 mmol, 18%) as a yellow gum. ^{1}H NMR (600 MHz, $CDCl_3$) δ 7.22 (t, *J* = 5.4 Hz, 2H), 4.99 (d, *J* = 1.9 Hz, 4H), 4.93 (s, 4H), 4.99 (d, *J* = 1.9 Hz, 4H), 3.68–3.62 (m, 4H), 3.62–3.56 (m, 8H), 3.39 (dd, *J* = 12.1, 5.9, 4H), 2.46 (t, *J* = 2.4 Hz, 2H), 1.79 (dt, *J* = 12.1, 5.9, 4H); ^{13}C NMR 151 MHz, $CDCl_3$) δ 165.4 (C), 153.8 (C), 152.4 (C), 136.5 (C), 135.8 (C), 76.3 (C), 75.0 (CH), 70.3 (CH_2), 69.8 (CH_2), 69.7 (CH_2), 50.5 (CH_2), 38.4 (CH_2), 37.3 (CH_2), 28.5 (CH_2); IR (thin film) 3299, 2928, 2052, 1643, 1285 cm^{-1}; LRMS (ES+) 917 (50, $[M^{81}Br^{81}Br^{81}Br^{79}Br+H]^+$), 915 (100, $[M^{81}Br^{81}Br^{79}Br^{79}Br+H]^+$), 913 (50, $[M^{81}Br^{79}Br\ ^{79}Br^{79}Br+H]^+$); HRMS (ES+) calcd for $C_{28}H_{32}Br_4N_6O_9$ $[M^{81}Br^{79}Br\ ^{79}Br^{79}Br+H\ ]^+$ 912.9042, observed 912.9048.

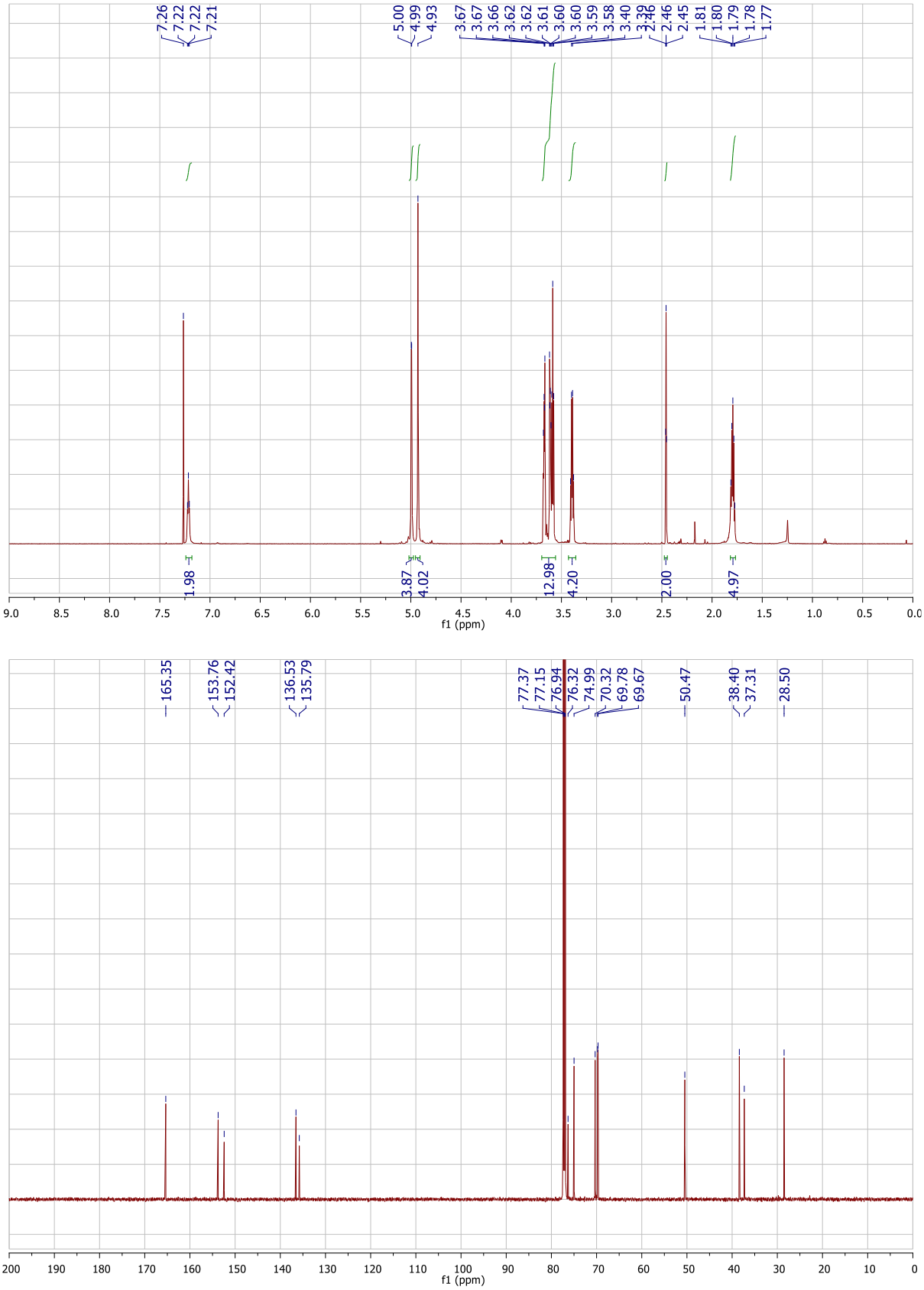

Figure **S55**. ^{1}H and ^{13}C NMR data for *N*'-(((Oxybis(ethane-2,1-diyl))bis(oxy))bis(propane-3,1-diyl))bis(2-(4,5-dibromo-3,6-dioxo-2-(prop-2-yn-1-yl)-3,6-dihydropyridazin-1(2*H*)-yl)acetamide) **9**.

5.2.2 Bioconjugation reactions for Chapter 3

***In situ* reduction of Herceptin™ mAb and reaction with bis-diBrPD 1 at 4 °C (16 eq.) for the formation of conjugate 30**

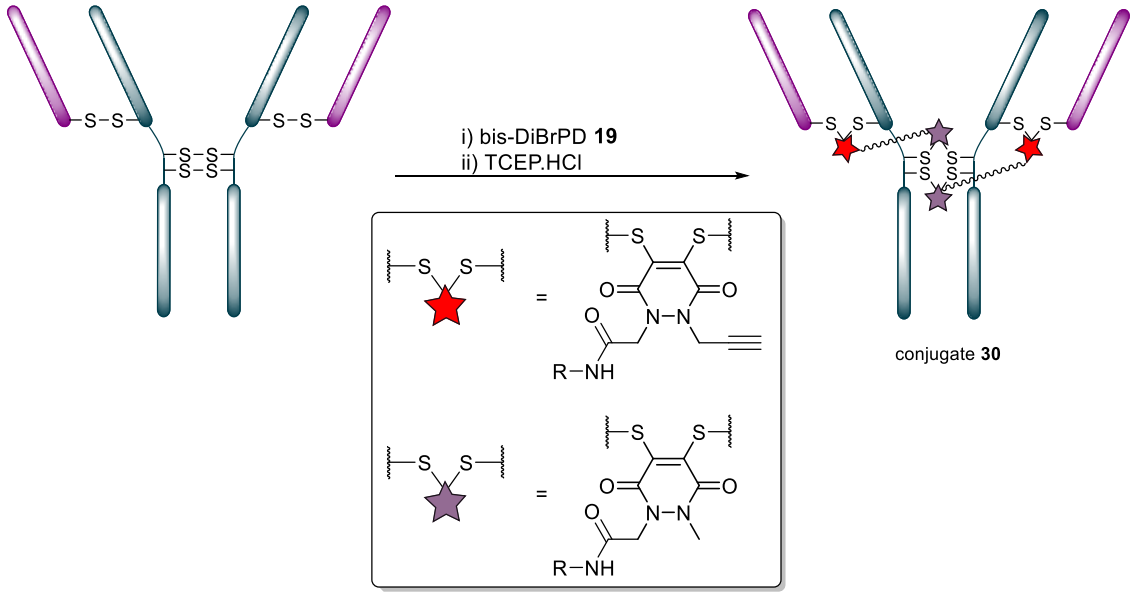

Each pair of red and purple stars per linker molecule are independently interchangeable, and other disulfide pairs (e.g. Fab-Fab, Hinge-Hinge) may be functionally re-bridged.

TCEP.HCl (10 µL, 20 mM in deionised water, 80 eq.) was added to a solution of Herceptin™ (50 µL, 7.5 mg/mL, 50 µM) in BBS (25 mM sodium borate, 25 mM NaCl, 0.5 mM EDTA, pH 8.0) which had been pre-treated with bis-diBrPD **19** (2.0 µL, 20 mM in DMSO, 16 eq.) and stored at 4 °C for 1 h previously. The reaction mixture was then stored at 4 °C for 15 h. Excess reagents were removed by repeated diafiltration into deionised water using VivaSpin sample concentrators (GE Healthcare, 10,000 MWCO). The samples were analysed by SDS-PAGE gel and UV-Vis spectroscopy, which was used to determine a PDAR of 4.0. This reaction was repeated on 7 separate occasions with remarkable reproducibility; PDARs in the range of 3.9-4.1 were observed. A TCEP reduction control was also conducted on conjugate **30**: TCEP.HCl (10 µL, 20 mM in deionised water, 80 eq.) was added to conjugate **30** (50 µL, 7.5 mg/mL, 50 µM) in BBS (25 mM sodium borate, 25 mM NaCl, 0.5 mM EDTA, pH 8.0), the reaction mixture was then incubated at 37 °C for 1 h. The sample was then analysed by LCMS. Expected mass: 146,320 Da. Observed mass: 146,328 Da. The sample was analysed further by SDS-PAGE gel (lane 3, below). As there was no fragmentation observed (going from lane 2 to lane 3) it was concluded that no accessible inter-chain disulfide bonds were present in conjugate **30** (control Herceptin™ reduction below, Figure S20). This experiment, combined with the lack of any fragments

being observed in the SDS-PAGE gel in lane 2+3 and the UV-Vis data, confirmed that all accessible disulfides bonds were functionally re-bridged with PD molecules.

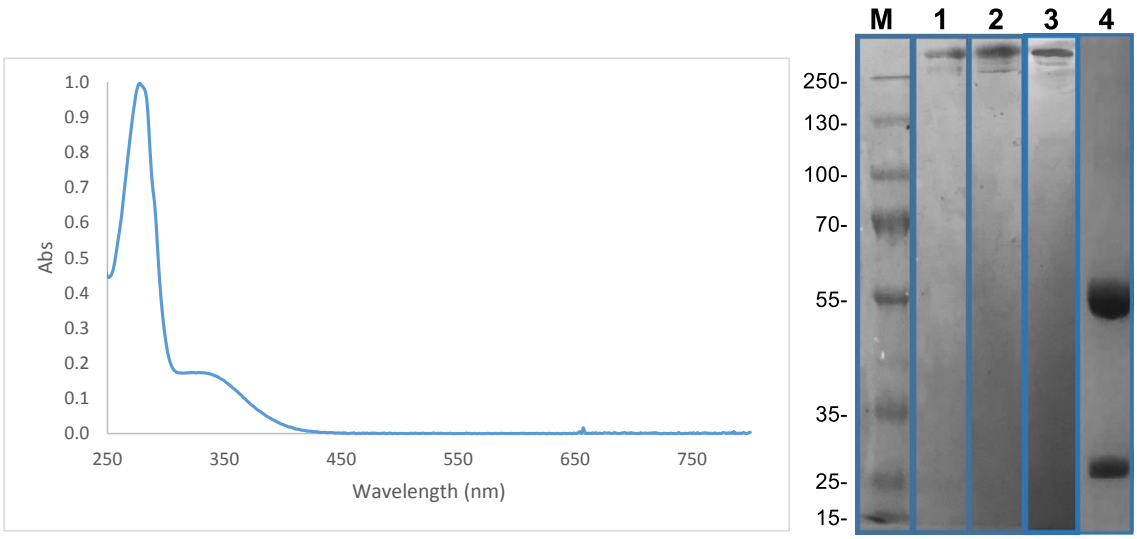

Figure **S56a**. (Left) UV-Vis data for conjugate **30**. (Right) SDS-PAGE gel; M.) Molecular weight marker; 1) Unmodified Herceptin™; 2) Conjugate **30**; 3) Conjugate **30** treated with TCEP.HCl; 4) Herceptin™ reduced with TCEP.HCl displaying heavy chain and light chain fragments.

a.)

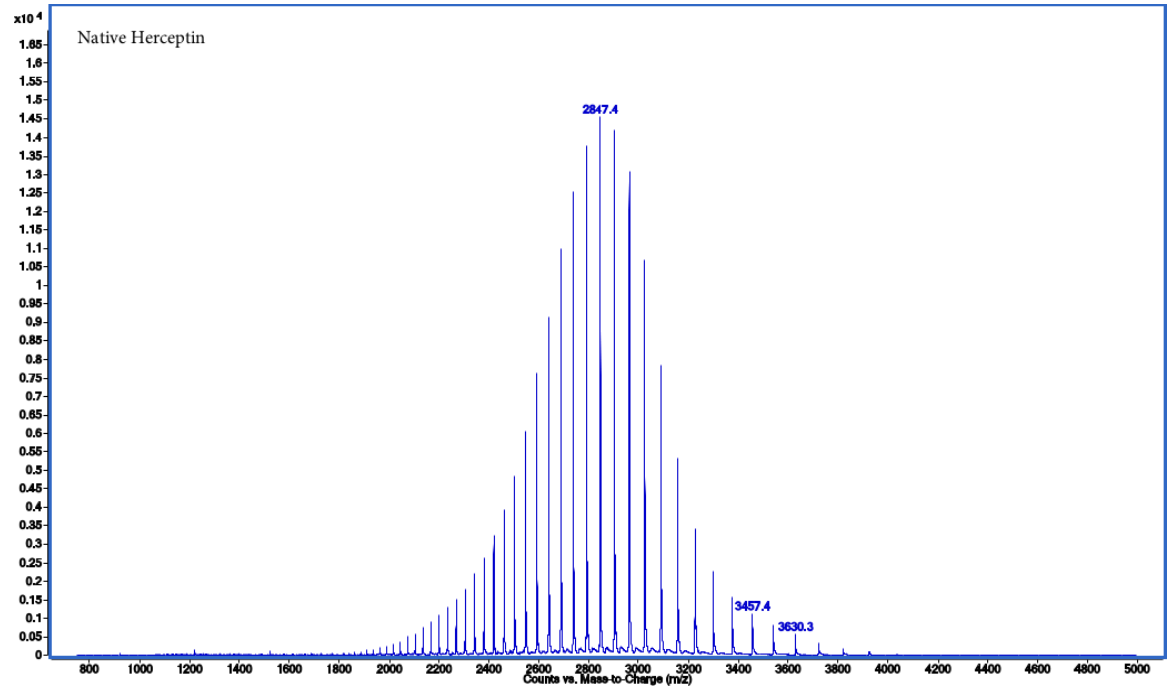

b.)

Figure **S56b**. (a) non-deconvoluted and (b) deconvoluted MS data for native Herceptin™ (deglycosylated).

a.)

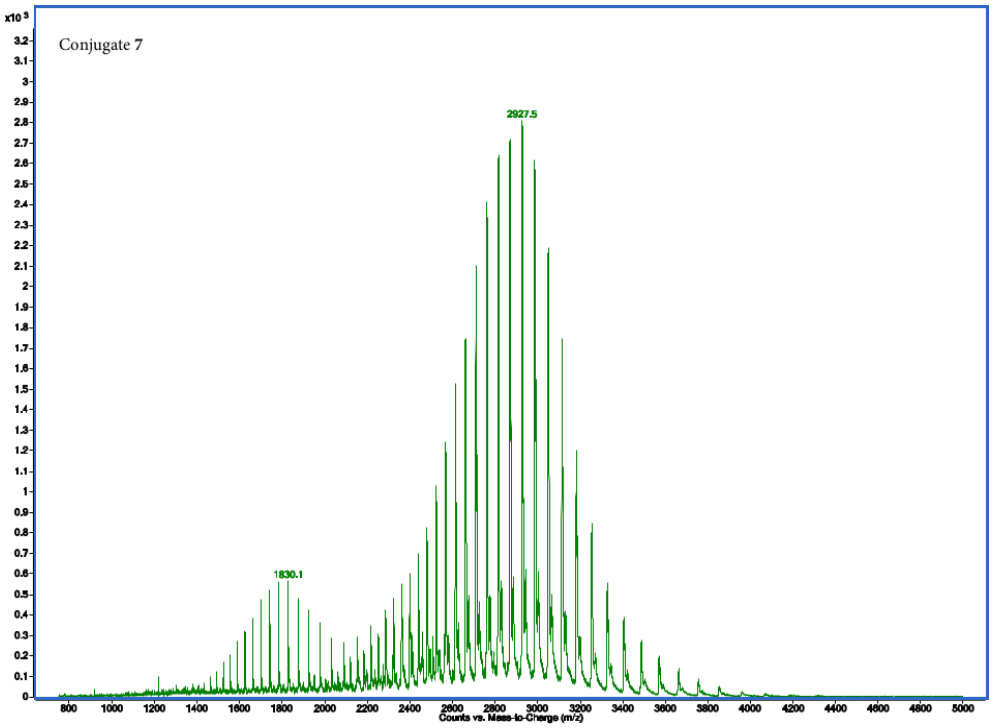

b.)

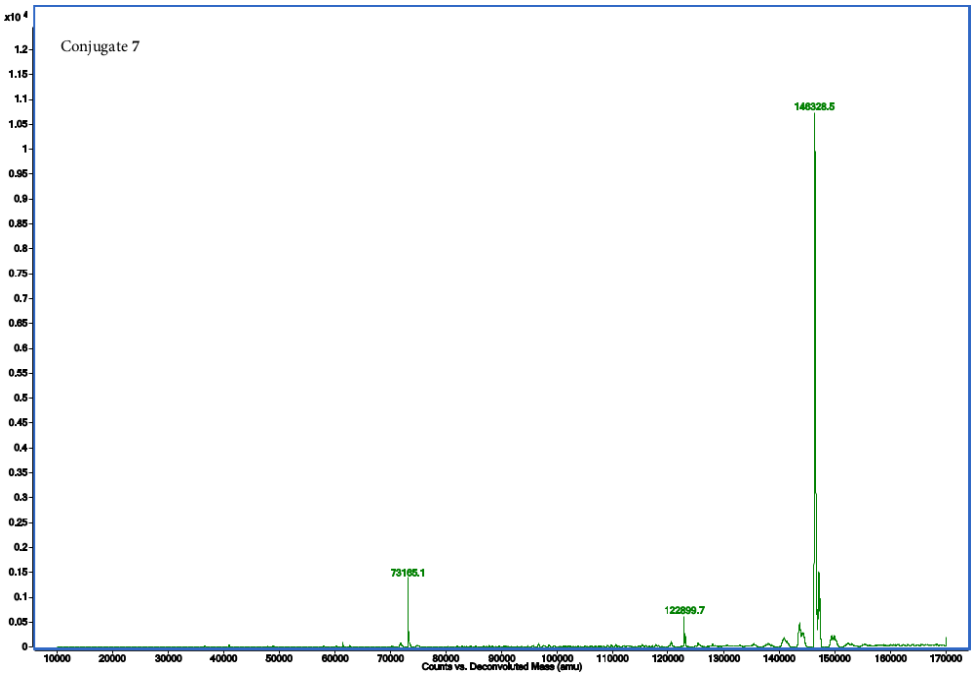

Figure **S56c**. (a) non-deconvoluted and (b) deconvoluted MS data for conjugate **30** (deglycosylated).

Reaction of conjugate 30 with AlexaFluor 488®-azide for the formation of conjugate 31

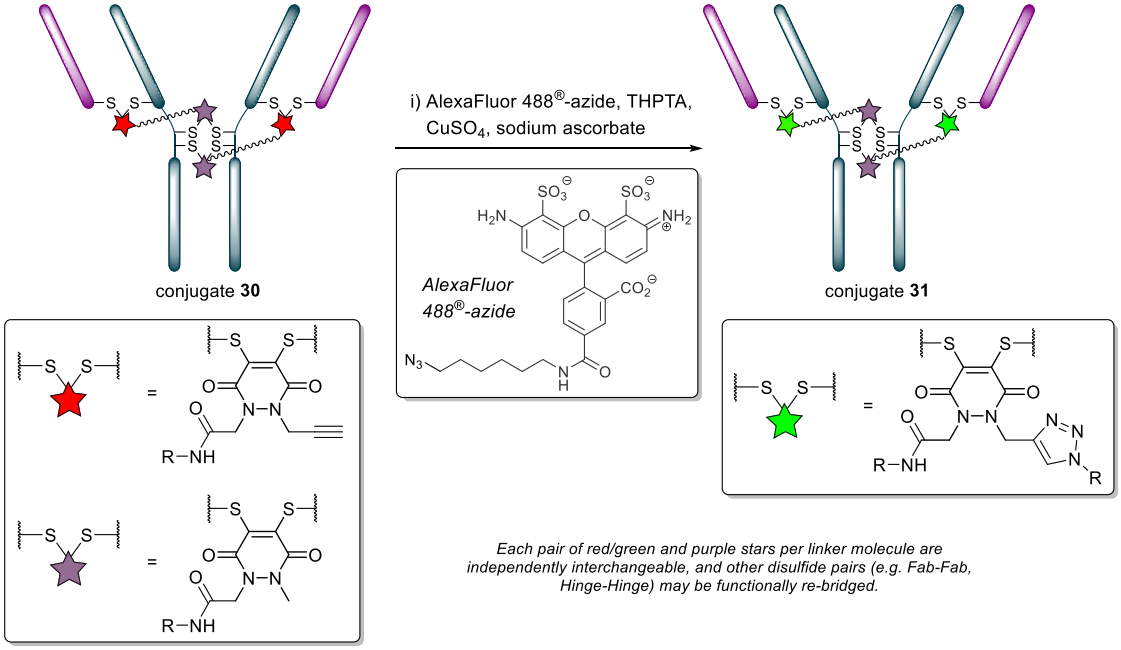

AlexaFluor 488®-azide (5.0 µL, 10.0 mM in DMSO, 20 eq.), $CuSO_4$ (1.0 µL, 20.0 mM in water, 8 eq.), tris(3-hydroxypropyltriazolylmethyl)amine (THPTA) (1.0 µL, 100 mM in water, 40 eq.) and sodium ascorbate (5.0 µL, 0.10 M in water) were added in series to conjugate **30** (50 µL, 7.5 mg/mL, 50 µM) in BBS (25 mM sodium borate, 25 mM NaCl, pH 8.0). The reaction mixture was stored at 21 °C for 1.5 h. The excess reagents were then removed by repeated diafiltration into fresh PBS with 2 mM EDTA (to remove residual copper ions) using VivaSpin sample concentrators (GE Healthcare, 10,000 MWCO). Following this, the buffer salts were removed by repeated diafiltration into deionised water using VivaSpin sample concentrators (GE Healthcare, 10,000 MWCO). The samples were analysed by SDS-PAGE gel and UV-Vis spectroscopy, which was used to determine a FAR of 2.0. This reaction was repeated on 7 separate occasions with remarkable reproducibility; FARs in the range of 1.9-2.1 were observed.

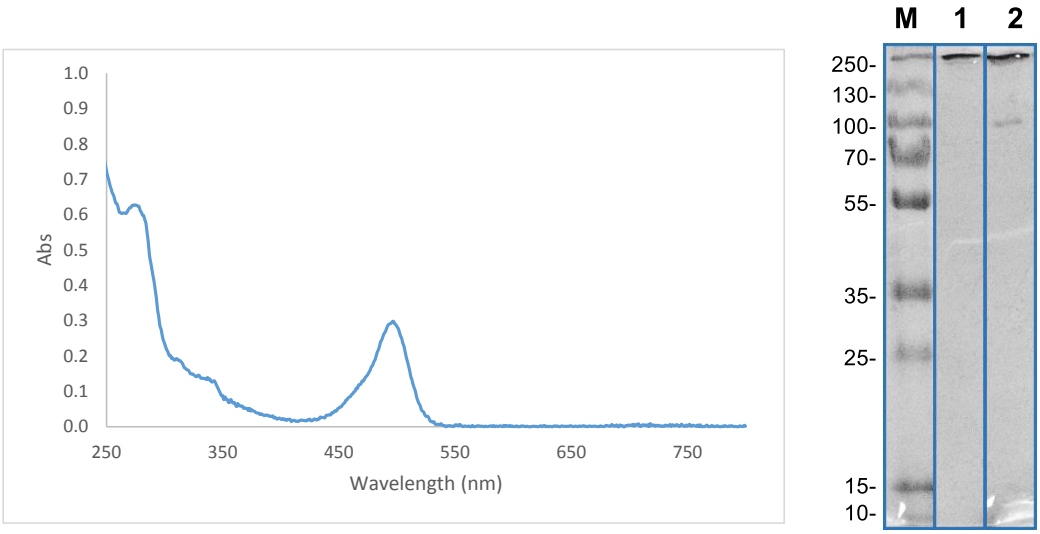

Figure **S57**. (Left) UV-Vis data for conjugate **31**. (Right) SDS-PAGE gel; M.) Molecular weight marker; 1) Unmodified Herceptin™; 2) Conjugate **31**.

Reaction of conjugate 30 with Doxorubicin-azide[83] for the formation of conjugate 32

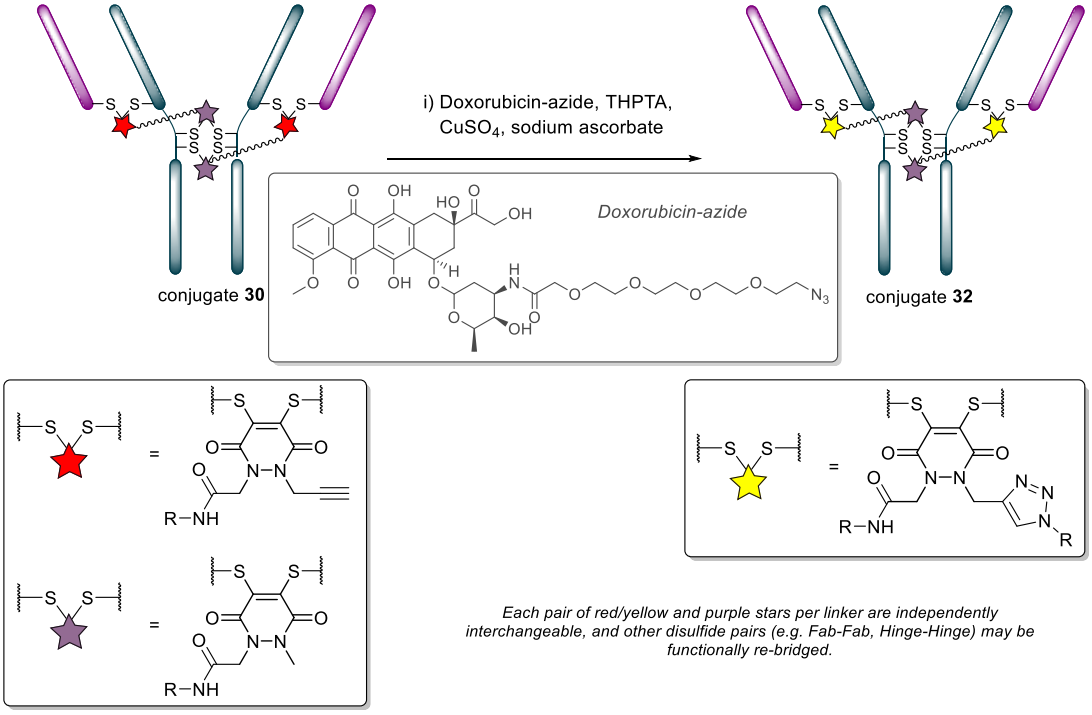

Doxorubicin-azide (5.0 µL, 10.0 mM in DMSO, 20 eq.), $CuSO_4$ (1.0 µL, 20.0 mM in water, 8 eq.), tris(3-hydroxypropyltriazolylmethyl)amine (THPTA) (1.0 µL, 100 mM in water, 40 eq.) and sodium ascorbate (5.0 µL, 0.10 M in water) were added in series to conjugate **30** (50 µL, 7.5 mg/mL, 50 µM) in BBS (25 mM sodium borate, 25 mM NaCl, pH 8.0). The reaction mixture was stored at 21 °C for 1.5 h. The excess reagents were then removed by repeated diafiltration into fresh PBS with 2 mM EDTA (to remove residual copper ions) using VivaSpin sample concentrators (GE Healthcare, 10,000 MWCO). Following this, the buffer salts were removed by repeated diafiltration into deionised water using VivaSpin sample concentrators (GE Healthcare, 10,000 MWCO). The samples were analysed by SDS-PAGE gel and UV-Vis spectroscopy was used to determine a DAR of 2.0.

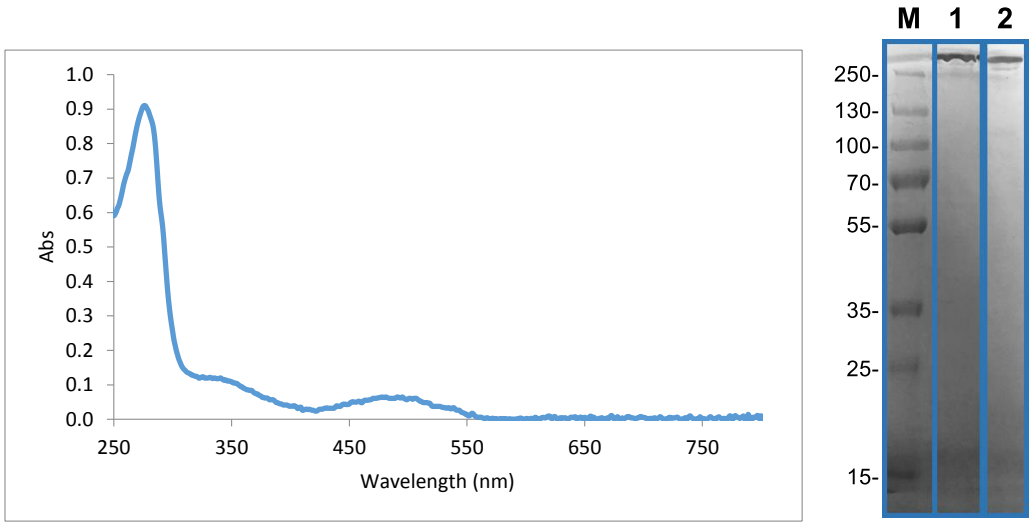

Figure **S58**. (Left) UV-Vis data for conjugate **32**. (Right) SDS-PAGE gel; M.) Molecular weight marker; 1) Unmodified Herceptin™; 2) Conjugate **32**.

***In situ* reduction of Herceptin™ mAb and reaction with bis-diBrPD 33 at 4 °C (16 eq.) for the formation of conjugate 34**

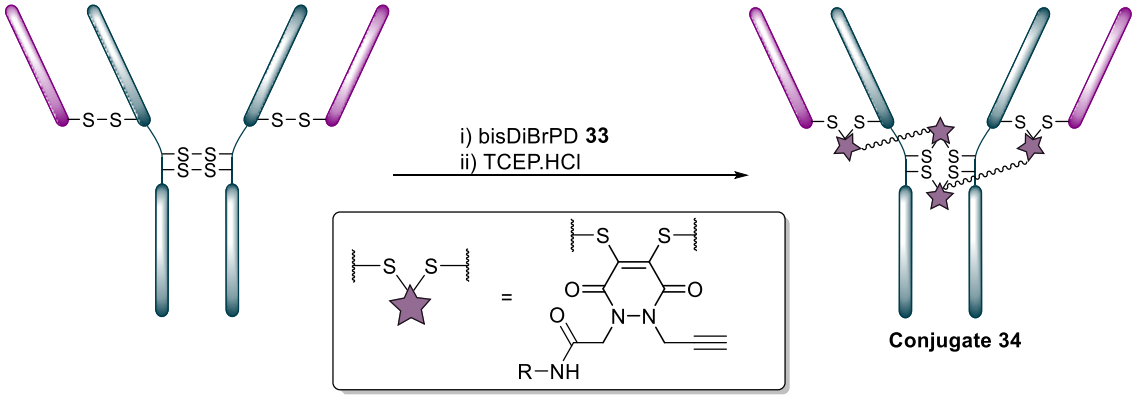

TCEP.HCl (10 µL, 20 mM in deionised water, 80 eq.) was added to a solution of Herceptin™ (50 µL, 7.5 mg/mL, 50 µM) in BBS (25 mM sodium borate, 25 mM NaCl, 0.5 mM EDTA, pH 8.0) which had been pre-treated with bis-diBrPD **33** (2.0 µL, 20 mM in DMSO, 16 eq.) and stored at 4 °C for 1 h previously. The reaction mixture was then stored at 4 °C for 15 h. Excess reagents were removed by repeated diafiltration into deionised water using VivaSpin sample concentrators (GE Healthcare, 10,000 MWCO). The samples were analysed by SDS-PAGE gel and UV-Vis spectroscopy was used to determine a PDAR of 3.9.

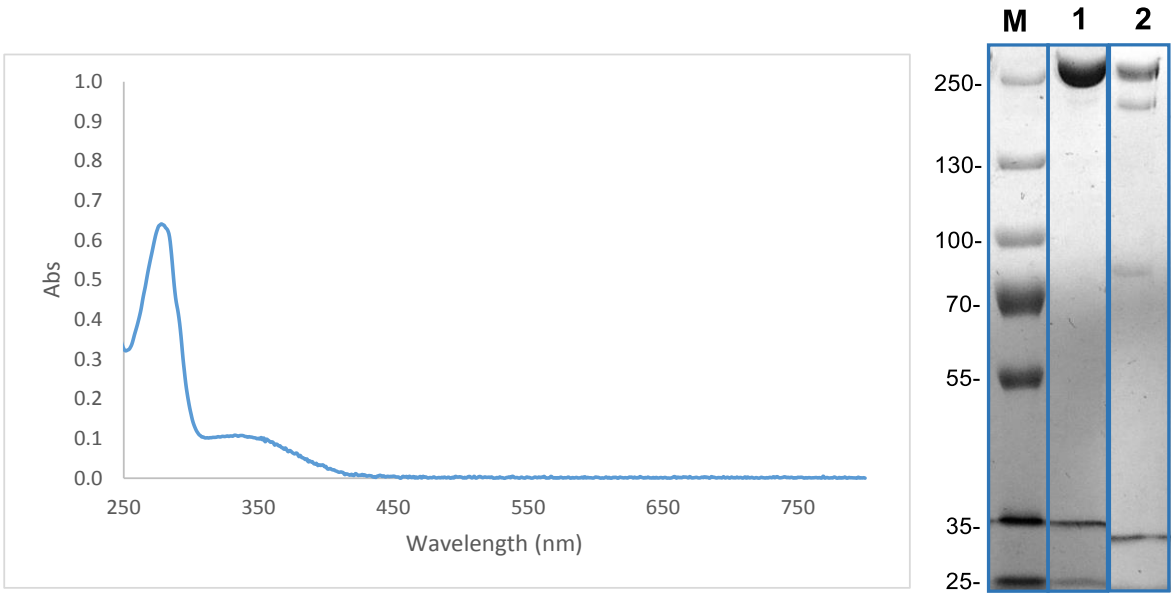

Figure **S59**. (Left) UV-Vis data for conjugate **34**. (Right) SDS-PAGE gel; M) Molecular weight marker; 1) Untreated Herceptin™; 2) Conjugate **34**. Artefact in SDS-PAGE gel observed in both samples (*ca.* 35 kDa).

Reaction of conjugate 34 with AlexaFluor 488™-azide for the formation of conjugate 35

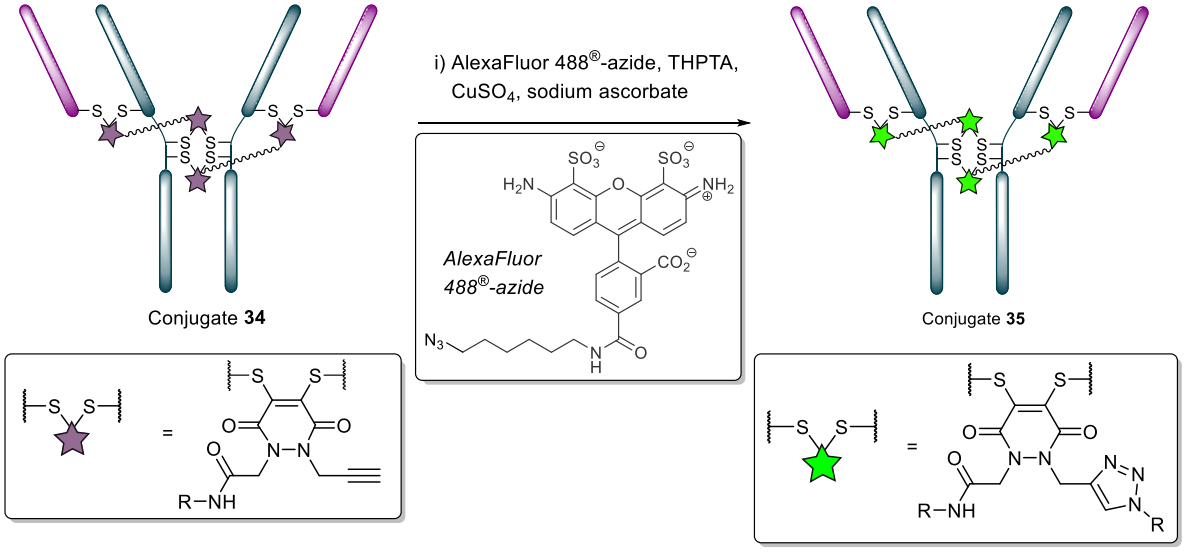

AlexaFluor 488®-azide (10.0 µL, 10.0 mM in DMSO, 40 eq.), $CuSO_4$ (1.0 µL, 20.0 mM in water, 8 eq.), tris(3-hydroxypropyltriazolylmethyl)amine (THPTA) (1.0 µL, 100 mM in water, 40 eq.) and sodium ascorbate (5.0 µL, 0.10 M in water) were added in series to conjugate **34** (50 µL, 7.5 mg/mL, 50 µM) in BBS (25 mM sodium borate, 25 mM NaCl, pH 8.0). The reaction mixture was stored at 21 °C for 1.5 h. The excess reagents were then removed by repeated diafiltration into fresh PBS with 2 mM EDTA (to remove residual copper ions) using VivaSpin sample concentrators (GE Healthcare, 10,000 MWCO).

Following this, the buffer salts were removed by repeated diafiltration into deionised water using VivaSpin sample concentrators (GE Healthcare, 10,000 MWCO). The samples were analysed by SDS-PAGE gel and UV-Vis spectroscopy was used to determine a FAR of 3.9.

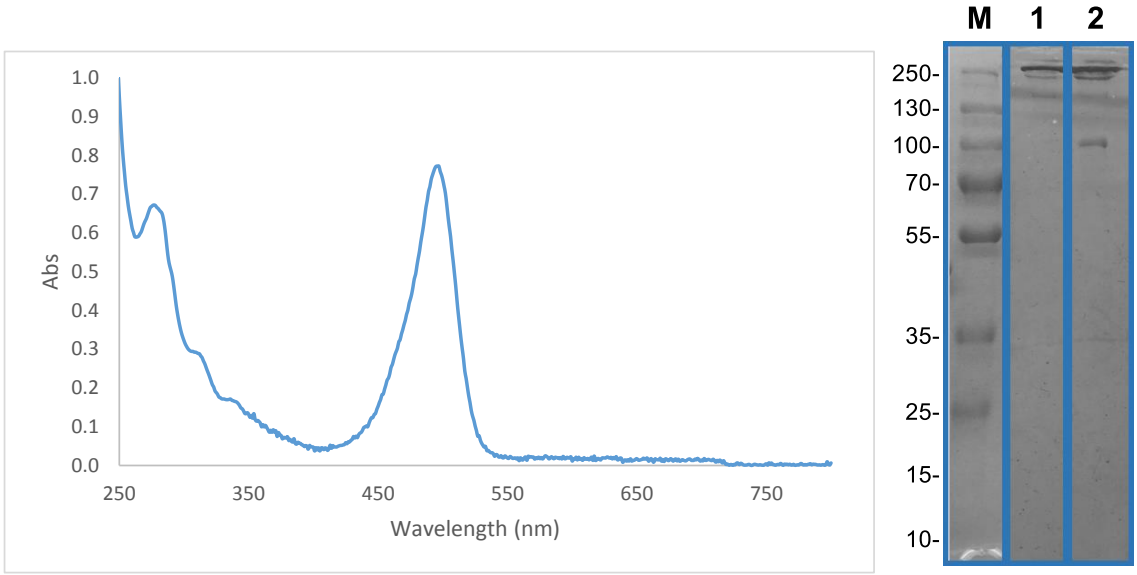

Figure **S60**. (Left) UV-Vis data for conjugate **35** modified with AlexaFluor 488™-azide. (Right) SDS-PAGE gel; M) Molecular weight marker; 1)Unmodified Herceptin™; 2) Conjugate **35**.

Reduction of Herceptin™ mAb control for elucidation of accessible disulfides

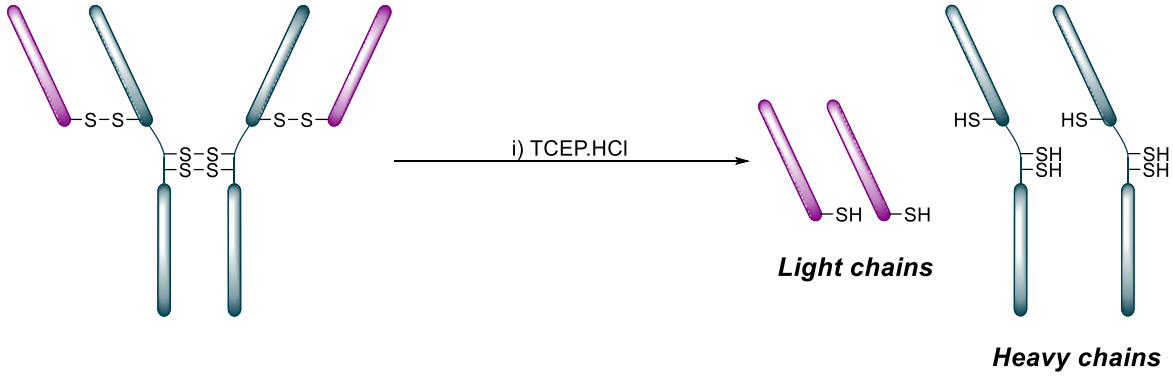

TCEP.HCl (10 µL, 20 mM in deionised water, 80 eq.) was added to Herceptin™ (50 µL, 7.5 mg/mL, 50 µM) in BBS (25 mM sodium borate, 25 mM NaCl, 0.5 mM EDTA, pH 8.0). The reaction mixture was then incubated at 37 °C for 1 h. The sample was analysed by SDS-PAGE gel revealing light chain and heavy chain fragments.

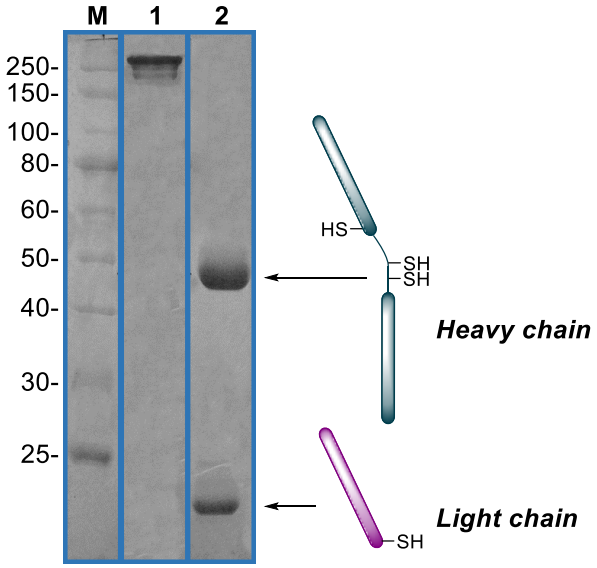

Figure **S61**. SDS-PAGE gel; M) Molecular weight marker; 1) Unmodified Herceptin™; 2) Herceptin™ reduced with TCEP.HCl displaying heavy chain and light chain fragments.

Activity of Conjugates by enzyme-linked immunosorbent assay (ELISA)

A 96-well Maxisorp plate was coated overnight at 4 °C with HER2 (0.25 µg·mL^{-1} in 50 mM sodium carbonate buffer pH = 9.6, 100 µl). As a negative control one row was coated with only buffer. The solutions were removed and each well washed (2 × PBS with 0.05% Tween). The wells were subsequently coated with a 1% BSA solution in PBS for one hour at room temperature. After this the wells were emptied and washed (4 × PBS with 0.05% Tween). Solutions of Native Herceptin™, Herceptin™ DiEt, conjugate **31,** and conjugate **35** in PBS pH = 7.4 were prepared in the following dilutions: 60.0 nM, 15.0 nM, 3.75 nM, 0.938 nM, 0.234 nM and 0.00586 nM. The dilutions were placed into the wells, each in triplicate, and incubated for two hours at room temperature. As negative controls sodium carbonate buffer only and the antibodies at 60 nM in the absence of HER2 were also subjected to the same protocol. The solutions were removed and the wells washed (4 × PBS with 0.05% Tween). Detection antibody (100 µL of anti-human IgG, Fab-specific-HRP solution, 4 µL of a 1:5000 solution diluted further in 20 ml of PBS) was added and left for one hour at room temperature. The solutions were removed and the wells washed (4 × PBS with 0.05% Tween). Finally, a TMB solution (1 × TMB Solution, eBioscience, 100 µL) was added to each well. After five minutes the reaction was stopped through addition of 0.2 M sulfuric acid (50 µL). Absorbance was measured at 450 nm and corrected by subtracting the average of negative controls. Protocol was adapted from a literature procedure.

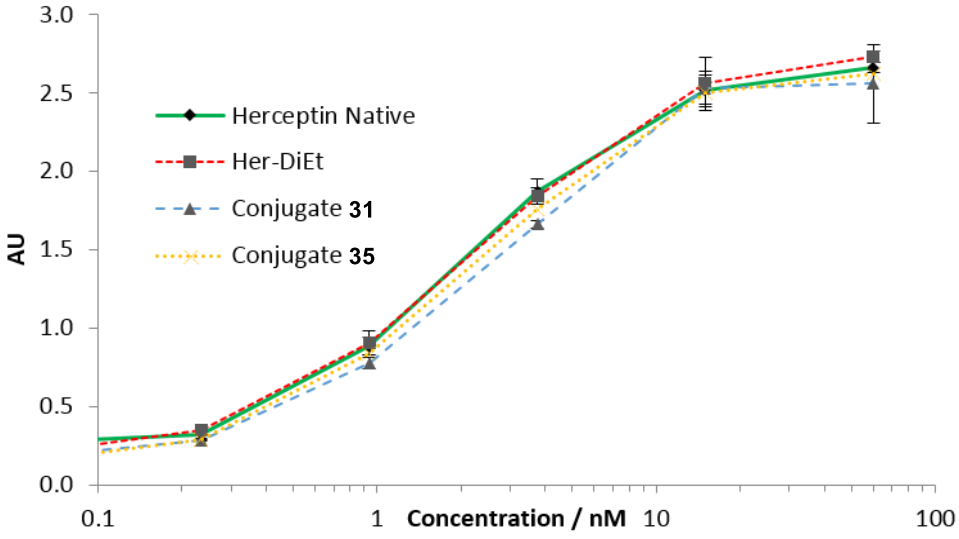

Figure **S62**. Binding activity of conjugates **31, 35** and **Her-DiEt** against unmodified Herceptin™**.**

Cell internalisation with confocal microscopy

Cells on cover slips at 70% confluency were incubated with AlexaFluor-488™-conjugated constructs at 10 µg/ml for 1 h at 4 °C. Cells were extensively washed with PBS to remove unbound antibodies and incubated at 37 °C in growth media. Internalisation was allowed for 1 h, followed by extensive washing and fixation with 4% formaldehyde for 10 min at 4 °C. Cover slips were then blocked with 5% goat serum in 0.3% Triton-X100 (Sigma). Actin was detected with phalloidin-568 (Invitrogen) and Hoechst trihydrochloride (Invitrogen) was used to stain cell nuclei. Unconjugated antibody was detected using Alexa-Fluor-488 Donkey anti-rabbit IgG. Cover slips were mounted on slides using ProLong Gold antifade (Invitrogen) and examined using a Zeiss LSM880 Confocal Plus microscope.

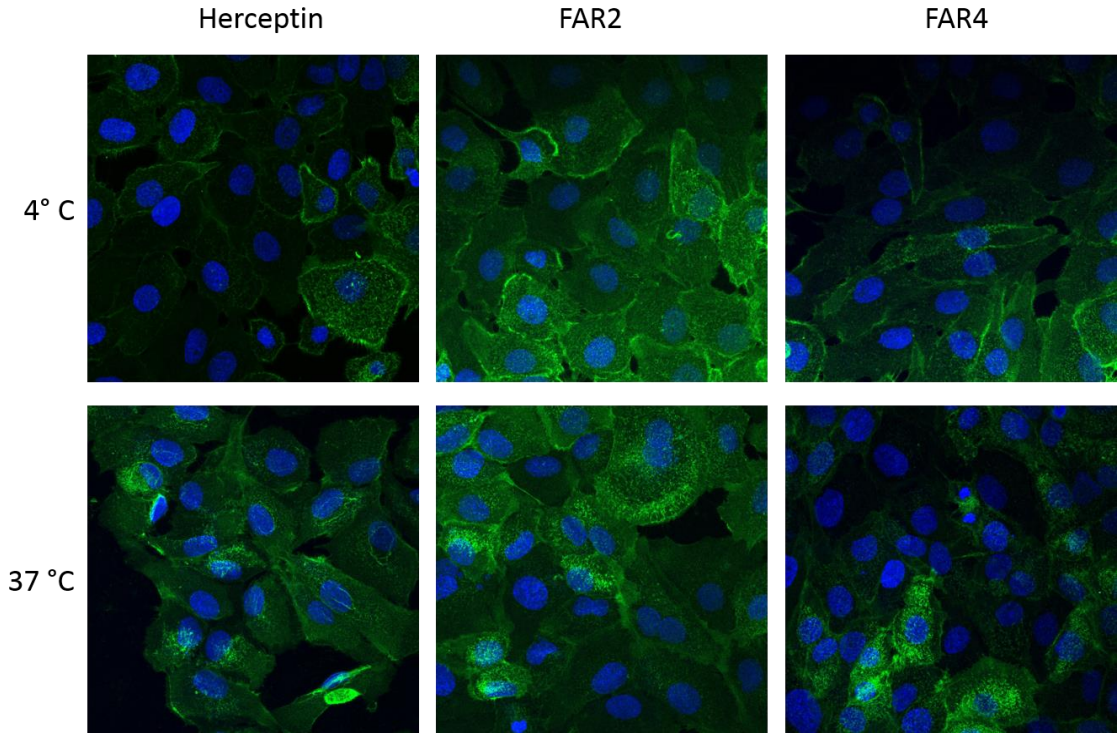

Figure **S63**. Cell inernalisation visualised with confocal microscopy of Herceptin™ bioconjugates **31** (FAR2) and **35** (FAR4) compared with Herceptin™ positive control.

References

1. C. T. Walsh, *Posttranslational Modification of Proteins: Expanding Nature's Inventory*, Roberts and Company Publishers, Colorado, 2006.
2. B. Leader, Q. J. Baca and D. E. Golan, *Nat. Rev. Drug Discov.*, 2008, **7**, 21-39.
3. M.-S. Kim, S. M. Pinto, D. Getnet, R. S. Nirujogi, S. S. Manda, R. Chaerkady, A. K. Madugundu, D. S. Kelkar, R. Isserlin, S. Jain, J. K. Thomas, B. Muthusamy, P. Leal-Rojas, P. Kumar, N. A. Sahasrabuddhe, L. Balakrishnan, J. Advani, B. George, S. Renuse, L. D. N. Selvan, A. H. Patil, V. Nanjappa, A. Radhakrishnan, S. Prasad, T. Subbannayya, R. Raju, M. Kumar, S. K. Sreenivasamurthy, A. Marimuthu, G. J. Sathe, S. Chavan, K. K. Datta, Y. Subbannayya, A. Sahu, S. D. Yelamanchi, S. Jayaram, P. Rajagopalan, J. Sharma, K. R. Murthy, N. Syed, R. Goel, A. A. Khan, S. Ahmad, G. Dey, K. Mudgal, A. Chatterjee, T.-C. Huang, J. Zhong, X. Wu, P. G. Shaw, D. Freed, M. S. Zahari, K. K. Mukherjee, S. Shankar, A. Mahadevan, H. Lam, C. J. Mitchell, S. K. Shankar, P. Satishchandra, J. T. Schroeder, R. Sirdeshmukh, A. Maitra, S. D. Leach, C. G. Drake, M. K. Halushka, T. S. K. Prasad, R. H. Hruban, C. L. Kerr, G. D. Bader, C. A. Iacobuzio-Donahue, H. Gowda and A. Pandey, *Nature*, 2014, **509**, 575-581.
4. T. Farrah, E. W. Deutsch, G. S. Omenn, Z. Sun, J. D. Watts, T. Yamamoto, D. Shteynberg, M. M. Harris and R. L. Moritz, *J. Proteome Res.*, 2014, **13**, 60-75.
5. J. Kalia and R. T. Raines, *Curr. Org. Chem.*, 2010, **14**, 138-147.
6. O. Boutureira and G. J. L. Bernardes, *Chem. Rev.*, 2015, **115**, 2174-2195.
7. R. D. Astronomo, H.-K. Lee, C. N. Scanlan, R. Pantophlet, C.-Y. Huang, I. A. Wilson, O. Blixt, R. A. Dwek, C.-H. Wong and D. R. Burton, *J. Virol.*, 2008, **82**, 6359-6368.
8. L. Schofield, M. C. Hewitt, K. Evans, M.-A. Siomos and P. H. Seeberger, *Nature*, 2002, **418**, 785-789.
9. L. M. Krug, G. Ragupathi, C. Hood, C. George, F. Hong, R. Shen, L. Abrey, H. J. Jennings, M. G. Kris and P. O. Livingston, *Cancer Immunol. Immunother.*, 2012, **61**, 9-18.
10. J. J. Day, B. V. Marquez, H. E. Beck, T. A. Aweda, P. D. Gawande and C. F. Meares, *Curr. Opin. Chem. Biol.*, 2010, **14**, 803-809.
11. P. Agarwal and C. R. Bertozzi, *Bioconjugate Chem.*, 2015, **26**, 176-192.
12. C. R. Behrens and B. Liu, *mAbs*, 2014, **6**, 46-53.
13. J. M. Chalker, G. J. L. Bernardes and B. G. Davis, *Acc. Chem. Res.*, 2011, **44**, 730-741.
14. D. M. Patterson, L. A. Nazarova and J. A. Prescher, *ACS Chem. Biol.*, 2014, **9**, 592-605.
15. J. Y. Axup, K. M. Bajjuri, M. Ritland, B. M. Hutchins, C. H. Kim, S. A. Kazane, R. Halder, J. S. Forsyth, A. F. Santidrian, K. Stafin, Y. C. Lu, H. Tran, A. J. Seller, S. L. Biroce, A. Szydlik, J. K. Pinkstaff, F. Tian, S. C. Sinha, B. Felding-Habermann, V. V. Smider and P. G. Schultz, *Proc. Natl. Acad. Sci. U. S. A.*, 2012, **109**, 16101-16106.
16. D. Rabuka, J. S. Rush, G. W. deHart, P. Wu and C. R. Bertozzi, *Nat. Protoc.*, 2012, **7**, 1052-1067.
17. T. S. Young, I. Ahmad, J. A. Yin and P. G. Schultz, *J. Mol. Biol.*, 2010, **395**, 361-374.
18. J. A. Prescher, D. H. Dube and C. R. Bertozzi, *Nature*, 2004, **430**, 873-877.

19. J. M. Chalker, C. S. C. Wood and B. G. Davis, *J. Am. Chem. Soc.*, 2009, **131**, 16346-16347.
20. Y. A. Lin, J. M. Chalker, N. Floyd, G. J. L. Bernardes and B. G. Davis, *J. Am. Chem. Soc.*, 2008, **130**, 9642-9643.
21. C. D. Spicer and B. G. Davis, *Nat. Commun.*, 2014, **5**.
22. S. H. Hong, Y.-C. Kwon and M. C. Jewett, *Front. Chem.*, 2014, **2**, 34.
23. M. J. Lajoie, A. J. Rovner, D. B. Goodman, H.-R. Aerni, A. D. Haimovich, G. Kuznetsov, J. A. Mercer, H. H. Wang, P. A. Carr, J. A. Mosberg, N. Rohland, P. G. Schultz, J. M. Jacobson, J. Rinehart, G. M. Church and F. J. Isaacs, *Science*, 2013, **342**, 357-360.
24. K. Lang, L. Davis, J. Torres-Kolbus, C. Chou, A. Deiters and J. W. Chin, *Nat. Chem.*, 2012, **4**, 298-304.
25. A. Sachdeva, K. Wang, T. Elliott and J. W. Chin, *J. Am. Chem. Soc.*, 2014, **136**, 7785-7788.
26. W. H. Schmied, S. J. Elsässer, C. Uttamapinant and J. W. Chin, *J. Am. Chem. Soc.*, 2014, **136**, 15577-15583.
27. I. S. Carrico, *Chem. Soc. Rev.*, 2008, **37**, 1423-1431.
28. D. M. Bauer, I. Ahmed, A. Vigovskaya and L. Fruk, *Bioconjugate Chem.*, 2013, **24**, 1094-1101.
29. H. Ban, J. Gavrilyuk and C. F. Barbas, *J. Am. Chem. Soc.*, 2010, **132**, 1523-1525.
30. J. M. Antos and M. B. Francis, *J. Am. Chem. Soc.*, 2004, **126**, 10256-10257.
31. M. B. Francis and I. S. Carrico, *Curr. Opin. Chem. Biol.*, 2010, **14**, 771-773.
32. N. Stephanopoulos and M. B. Francis, *Nat. Chem. Biol.*, 2011, **7**, 876-884.
33. R. Lundblad, *Chemical Reagents for Protein Modification*, CRC Press, Florida, 2005.
34. J. Tuls, L. Geren and F. Millett, *J. Biol. Chem.*, 1989, **264**, 16421-16425.
35. J. M. Hooker, A. P. Esser-Kahn and M. B. Francis, *J. Am. Chem. Soc.*, 2006, **128**, 15558-15559.
36. J. C. Gildersleeve, O. Oyelaran, J. T. Simpson and B. Allred, *Bioconjugate Chem.*, 2008, **19**, 1485-1490.
37. P. M. S. D. Cal, J. B. Vicente, E. Pires, A. V. Coelho, L. s. F. Veiros, C. Cordeiro and P. M. P. Gois, *J. Am. Chem. Soc.*, 2012, **134**, 10299-10305.
38. H. K. Erickson and J. M. Lambert, *The AAPS Journal*, 2012, **14**, 799-805.
39. A. Filntisi, D. Vlachakis, G. K. Matsopoulos and S. Kossida, *Cancer Inform.*, 2014, **13**, 179-186.
40. G. E. Means and R. E. Feeney, *Bioconjugate Chem.*, 1990, **1**, 2-12.
41. J. A. Flygare, T. H. Pillow and P. Aristoff, *Chem. Biol. Drug Des.*, 2013, **81**, 113-121.
42. L. Ducry and B. Stump, *Bioconjugate Chem.*, 2010, **21**, 5-13.
43. P. A. Trail, D. Willner, S. J. Lasch, A. J. Henderson, S. Hofstead, A. M. Casazza, R. A. Firestone, I. Hellstrom and K. E. Hellstrom, *Science*, 1993, **261**, 212-215.
44. J. R. Adair, P. W. Howard, J. A. Hartley, D. G. Williams and K. A. Chester, *Expert Opin. Biol. Ther.*, 2012, **12**, 1191-1206.
45. S. Kubetzko, C. A. Sarkar and A. Plückthun, *Mol. Pharmacol.*, 2005, **68**, 1439-1454.
46. F. M. Veronese and G. Pasut, *Drug Discovery Today*, 2005, **10**, 1451-1458.
47. X. Chen, K. Muthoosamy, A. Pfisterer, B. Neumann and T. Weil, *Bioconjugate Chem.*, 2012, **23**, 500-508.

48. V. Chudasama, A. Maruani and S. Caddick, *Nat. Chem.*, 2016, **8**, 114-119.
49. J. M. Chalker, G. J. L. Bernardes, Y. A. Lin and B. G. Davis, *Chem. Asian J.*, 2009, **4**, 630-640.
50. J. R. Junutula, H. Raab, S. Clark, S. Bhakta, D. D. Leipold, S. Weir, Y. Chen, M. Simpson, S. P. Tsai, M. S. Dennis, Y. Lu, Y. G. Meng, C. Ng, J. Yang, C. C. Lee, E. Duenas, J. Gorrell, V. Katta, A. Kim, K. McDorman, K. Flagella, R. Venook, S. Ross, S. D. Spencer, W. Lee Wong, H. B. Lowman, R. Vandlen, M. X. Sliwkowski, R. H. Scheller, P. Polakis and W. Mallet, *Nat. Biotechnol.*, 2008, **26**, 925–932.
51. C. Lind, R. Gerdes, Y. Hamnell, I. Schuppe-Koistinen, H. B. von Löwenhielm, A. Holmgren and I. A. Cotgreave, *Arch. Biochem. Biophys.*, 2002, **406**, 229-240.
52. D. J. Betting, K. Kafi, A. Abdollahi-Fard, S. A. Hurvitz and J. M. Timmerman, *The Journal of Immunology*, 2008, **181**, 4131-4140.
53. Y. Zhang, V. S. Bhatt, G. Sun, P. G. Wang and A. F. Palmer, *Bioconjugate Chem.*, 2008, **19**, 2221-2230.
54. I. Shin, H. J. Jung and M. R. Lee, *Tetrahedron Lett.*, 2001, **42**, 1325-1328.
55. M. Esmann, P. C. Sar, K. Hideg and D. March, *Anal. Biochem.*, 1993, **213**, 336-348.
56. H. H. Winkler, R. M. Daugherty and J. P. Audia, *Biochemistry (Mosc.)*, 2003, **42**, 12562-12569.
57. S. Trapp, S. Haider, P. Jones, M. S. P. Sansom and F. M. Ashcroft, *EMBO J.*, 2003, **22**, 2903-2912.
58. A. Denicola-Seoane and B. M. Anderson, *Biochim. Biophys. Acta*, 1990, **1040**, 84-88.
59. J. A. Thomas, Y. C. Chai and C. H. Jung, in *Oxygen Radicals in Biological Systems, Part C (Methods in Enzymology) – Protein S-Thiolation and Dethiolation*, Academic Press, 1994, pp. 385-395.
60. J. M. May, *J. Biol. Chem.*, 1988, **263**, 13635-13640.
61. J. M. Chalker, S. B. Gunnoo, O. Boutureira, S. C. Gerstberger, M. Fernandez-Gonzalez, G. J. L. Bernardes, L. Griffin, H. Hailu, C. J. Schofield and B. G. Davis, *Chem. Sci.*, 2011, **2**, 1666-1676.
62. L. M. Tedaldi, M. E. B. Smith, R. I. Nathani and J. R. Baker, *Chem. Commun.*, 2009, 6583-6585.
63. V. Chudasama, M. E. B. Smith, F. F. Schumacher, D. Papaioannou, G. Waksman, J. R. Baker and S. Caddick, *Chem. Commun.*, 2011, **47**, 8781-8783.
64. E. M. Sletten and C. R. Bertozzi, *Angew. Chem. Int. Ed.*, 2009, **48**, 6974-6998.
65. M. E. B. Smith, F. F. Schumacher, C. P. Ryan, L. M. Tedaldi, D. Papaioannou, G. Waksman, S. Caddick and J. R. Baker, *J. Am. Chem. Soc.*, 2010, **132**, 1960-1965.
66. G. Badescu, P. Bryant, M. Bird, K. Henseleit, J. Swierkosz, V. Parekh, R. Tommasi, E. Pawlisz, K. Jurlewicz, M. Farys, N. Camper, X. Sheng, M. Fisher, R. Grygorash, A. Kyle, A. Abhilash, M. Frigerio, J. Edwards and A. Godwin, *Bioconjugate Chem.*, 2014, **25**, 1124-1136.
67. J. P. M. Nunes, M. Morais, V. Vassileva, E. Robinson, V. S. Rajkumar, M. E. B. Smith, R. B. Pedley, S. Caddick, J. R. Baker and V. Chudasama, *Chem. Commun.*, 2015, **51**, 10624-10627.
68. S. Brocchini, S. Balan, A. Godwin, J.-W. Choi, M. Zloh and S. Shaunak, *Nat. Protocols*, 2006, **1**, 2241-2252.
69. P. D. Senter and E. L. Sievers, *Nat. Biotechnol.*, 2012, **30**, 631-637.

70. S. O. Doronina, B. E. Toki, M. Y. Torgov, B. A. Mendelsohn, C. G. Cerveny, D. F. Chace, R. L. DeBlanc, R. P. Gearing, T. D. Bovee, C. B. Siegall, J. A. Francisco, A. F. Wahl, D. L. Meyer and P. D. Senter, *Nat. Biotechnol.*, 2003, **21**, 778-784.
71. *CHMP Public Assessment Report (Adcetris)*, EMA, 2012.
72. S. L. Kuan, T. Wang and T. Weil, *Chem. Eur. J.*, 2016, **22**, 17112-17129.
73. S. Shaunak, A. Godwin, J.-W. Choi, S. Balan, E. Pedone, D. Vijayarangam, S. Heidelberger, I. Teo, M. Zloh and S. Brocchini, *Nat. Chem. Biol.*, 2006, **2**, 312-313.
74. F. F. Schumacher, J. P. M. Nunes, A. Maruani, V. Chudasama, M. E. B. Smith, K. A. Chester, J. R. Baker and S. Caddick, *Org. Biomol. Chem.*, 2014, **12**, 7261-7269.
75. M. T. W. Lee, A. Maruani, J. Baker, S. Caddick and V. Chudasama, *Chem. Sci.*, 2016, **7**, 799-802.
76. M. T. W. Lee, A. Maruani, D. A. Richards, J. R. Baker, S. Caddick and V. Chudasama, *Chem. Sci.*, 2017, **8**, 2056-2060.
77. N. Griebenow, A. M. Dilmaç, S. Greven and S. Bräse, *Bioconjugate Chem.*, 2016, **27**, 911-917.
78. F. F. Schumacher, M. Nobles, C. P. Ryan, M. E. B. Smith, A. Tinker, S. Caddick and J. R. Baker, *Bioconjugate Chem.*, 2011, **22**, 132-136.
79. D. A. Richards, S. A. Fletcher, M. Nobles, H. Kossen, L. Tedaldi, V. Chudasama, A. Tinker and J. R. Baker, *Org. Biomol. Chem.*, 2016, **14**, 455-459.
80. S. A. Fletcher, P. K. B. Sin, M. Nobles, E. Arstad, A. Tinker and J. R. Baker, *Org. Biomol. Chem.*, 2015, **13**, 9559-9563.
81. P. Moody, M. E. B. Smith, C. P. Ryan, V. Chudasama, J. R. Baker, J. Molloy and S. Caddick, *Chembiochem*, 2012, **13**, 1-1.
82. A. Maruani, S. Alom, P. Canavelli, M. T. W. Lee, R. E. Morgan, V. Chudasama and S. Caddick, *Chem. Commun.*, 2015, **51**, 5279-5282.
83. A. Maruani, M. E. B. Smith, E. Miranda, K. A. Chester, V. Chudasama and S. Caddick, *Nat. Commun.*, 2015, **6**, 6645-6654.
84. A. Maruani, H. Savoie, F. Bryden, S. Caddick, R. Boyle and V. Chudasama, *Chem. Commun.*, 2015, **51**, 15304-15307.
85. H. C. Kolb, M. G. Finn and K. B. Sharpless, *Angew. Chem. Int. Ed.*, 2001, **40**, 2004-2021.
86. R. A. Evans, *Aust. J. Chem.*, 2007, **60**, 384-395.
87. B.-Q. Shen, K. Xu, L. Liu, H. Raab, S. Bhakta, M. Kenrick, K. L. Parsons-Reponte, J. Tien, S.-F. Yu, E. Mai, D. Li, J. Tibbitts, J. Baudys, O. M. Saad, S. J. Scales, P. J. McDonald, P. E. Hass, C. Eigenbrot, T. Nguyen, W. A. Solis, R. N. Fuji, K. M. Flagella, D. Patel, S. D. Spencer, L. A. Khawli, A. Ebens, W. L. Wong, R. Vandlen, S. Kaur, M. X. Sliwkowski, R. H. Scheller, P. Polakis and J. R. Junutula, *Nat. Biotechnol.*, 2012, **30**, 184-189.
88. C. A. Janeway, P. Travers, M. Walport and M. J. Shlomchick, *Immunobiology*, Garland Science, New York, 2001.
89. P. Ehrlich, *The British Medical Journal*, 1913, **2**, 353-359.
90. G. Mathe, T. B. Loc and J. Bernard, *C. r. hebd. séances Acad. sci.*, 1958, **246**, 1626-1628.
91. T. Ghose and S. P. Nigam, *Cancer*, 1972, **29**, 1398-&.
92. G. F. Rowland, G. J. Oneill and D. A. L. Davies, *Nature*, 1975, **255**, 487-488.
93. G. A. Pietersz and K. Krauer, *J. Drug Target.*, 1994, **2**, 183-215.

94. M. L. Linenberger, T. Hong, D. Flowers, E. L. Sievers, T. A. Gooley, J. M. Bennett, M. S. Berger, L. H. Leopold, F. R. Appelbaum and I. D. Bernstein, *Blood*, 2001, **98**, 988-994.
95. A. Younes, N. L. Bartlett, J. P. Leonard, D. A. Kennedy, C. M. Lynch, E. L. Sievers and A. Forero-Torres, *N. Engl. J. Med.*, 2010, **363**, 1812-1821.
96. S. Verma, D. Miles, L. Gianni, I. E. Krop, M. Welslau, J. Baselga, M. Pegram, D. Y. Oh, V. Dieras, E. Guardino, L. Fang, M. W. Lu, S. Olsen, K. Blackwell and E. S. Grp, *N. Engl. J. Med.*, 2012, **367**, 1783-1791.
97. P. M. LoRusso, D. Weiss, E. Guardino, S. Girish and M. X. Sliwkowski, *Clin. Cancer Res.*, 2011, **17**, 6437-6447.
98. N. Diamantis and U. Banerji, *Br. J. Cancer*, 2016, **114**, 362-367.
99. J. R. Junutula, S. Bhakta, H. Raab, K. E. Ervin, C. Eigenbrot, R. Vandlen, R. H. Scheller and H. B. Lowman, *J. Immunol. Methods*, 2008, **332**, 41–52.
100. S. K. Wootton and D. Yoo, *J. Virol.*, 2003, **77**, 4546-4557.
101. S. Panowski, S. Bhakta, H. Raab, P. Polakis and J. R. Junutula, *mAbs*, 2014, **6**, 34-45.
102. B. Bernardim, P. M. S. D. Cal, M. J. Matos, B. L. Oliveira, N. Martínez-Sáez, I. S. Albuquerque, E. Perkins, F. Corzana, A. C. B. Burtoloso, G. Jiménez-Osés and G. J. L. Bernardes, *Nat. Commun.*, 2016, **7**, 13128.
103. C. S. Greenberg, P. J. Birckbichler and R. H. Rice, *FASEB J.*, 1991, **5**, 3071-3077.
104. P. Strop, S. H. Liu, M. Dorywalska, K. Delaria, R. G. Dushin, T. T. Tran, W. H. Ho, S. Farias, M. G. Casas, Y. Abdiche, D. Zhou, R. Chandrasekaran, C. Samain, C. Loo, A. Rossi, M. Rickert, S. Krimm, T. Wong, S. M. Chin, J. Yu, J. Dilley, J. Chaparro-Riggers, G. F. Filzen, C. J. O'Donnell, F. Wang, J. S. Myers, J. Pons, D. L. Shelton and A. Rajpal, *Chem. Biol.*, 2013, **20**, 161-167.
105. L. M. Hinman, P. R. Hamann, R. Wallace, A. T. Menendez, F. E. Durr and J. Upeslacis, *Cancer Res.*, 1993, **53**, 3336-3342.
106. P. R. Hamann, L. M. Hinman, C. F. Beyer, L. M. Greenberger, C. Lin, D. Lindh, A. T. Menendez, R. Wallace, F. E. Durr and J. Upeslacis, *Bioconjugate Chem.*, 2005, **16**, 346-353.
107. W. Wang, J. Vlasak, Y. Li, P. Pristatsky, Y. Fang, T. Pittman, J. Roman, Y. Wang, T. Prueksaritanont and R. Ionescu, *Mol. Immunol.*, 2011, **48**, 860-866.
108. R. Jefferis, *Biotechnol. Prog.*, 2005, **21**, 11-16.
109. M. Morais, J. P. M. Nunes, K. Karu, N. Forte, I. Benni, M. E. B. Smith, S. Caddick, V. Chudasama and J. R. Baker, *Org. Biomol. Chem.*, 2017, **15**, 2947-2952.
110. E. Robinson, J. P. M. Nunes, V. Vassileva, A. Maruani, J. C. F. Nogueira, M. E. B. Smith, R. B. Pedley, S. Caddick, J. R. Baker and V. Chudasama, *RSC Adv.*, 2017, **7**, 9073-9077.
111. F. F. Schumacher, J. P. M. Nunes, A. Maruani, V. Chudasama, M. E. B. Smith, K. A. Chester, J. R. Baker and S. Caddick, *Org. Biomol. Chem.*, 2014, **12**, 7261–7269.
112. L. Leinartaitė and A.-S. Johansson, *PLoS One*, 2013, **8**, e78060.
113. R. Arnold, M. E. Trautmann, W. Creutzfeldt, R. Benning, M. Benning, C. Neuhaus, R. Jürgensen, K. Stein, H. Schäfer, C. Bruns and H. J. Dennler, *Gut*, 1996, **38**, 430.
114. C. A. Hudis, *N. Engl. J. Med.*, 2007, **357**, 39-51.

115. S. Verma, D. Miles, L. Gianni, I. E. Krop, M. Welslau, J. Baselga, M. Pegram, D.-Y. Oh, V. Diéras, E. Guardino, L. Fang, M. W. Lu, S. Olsen and K. Blackwell, *N. Engl. J. Med.*, 2012, **367**, 1783-1791.
116. J. Mantaj, P. J. M. Jackson, K. M. Rahman and D. E. Thurston, *Angew. Chem. Int. Ed.*, 2017, **56**, 462-488.
117. J. A. Hartley, *Expert Opinion on Investigational Drugs*, 2011, **20**, 733-744.
118. M. S. Kung Sutherland, R. B. Walter, S. C. Jeffrey, P. J. Burke, C. Yu, H. Kostner, I. Stone, M. C. Ryan, D. Sussman, R. P. Lyon, W. Zeng, K. H. Harrington, K. Klussman, L. Westendorf, D. Meyer, I. D. Bernstein, P. D. Senter, D. R. Benjamin, J. G. Drachman and J. A. McEarchern, *Blood*, 2013, **122**, 1455-1463.
119. A. C. Tiberghien, J.-N. Levy, L. A. Masterson, N. V. Patel, L. R. Adams, S. Corbett, D. G. Williams, J. A. Hartley and P. W. Howard, *ACS Med. Chem. Lett.*, 2016, **7**, 983-987.
120. P. Akkapeddi, S.-A. Azizi, A. M. Freedy, P. M. S. D. Cal, P. M. P. Gois and G. J. L. Bernardes, *Chem. Sci.*, 2016, **7**, 2954-2963.
121. H. Yao, F. Jiang, A. Lu and G. Zhang, *Int. J. Mol. Sci.*, 2016, **17**, 194-220.
122. H. Bouchard, C. Viskov and C. Garcia-Echeverria, *Bioorg. Med. Chem. Lett.*, 2014, **24**, 5357-5363.
123. J. A. Hartley and D. Hochhauser, *Curr. Opin. Pharmacol.*, 2012, **12**, 398-402.
124. J. Wu, P. H. Clingen, V. J. Spanswick, M. Mellinas-Gomez, T. Meyer, I. Puzanov, D. Jodrell, D. Hochhauser and J. A. Hartley, *Clin. Cancer Res.*, 2013, **19**, 721-730.
125. L. R. Saunders, A. J. Bankovich, W. C. Anderson, M. A. Aujay, S. Bheddah, K. Black, R. Desai, P. A. Escarpe, J. Hampl, A. Laysang, D. Liu, J. Lopez-Molina, M. Milton, A. Park, M. A. Pysz, H. Shao, B. Slingerland, M. Torgov, S. A. Williams, O. Foord, P. Howard, J. Jassem, A. Badzio, P. Czapiewski, D. H. Harpole, A. Dowlati, P. P. Massion, W. D. Travis, M. C. Pietanza, J. T. Poirier, C. M. Rudin, R. A. Stull and S. J. Dylla, *Sci. Transl. Med.*, 2015, **7**, 302ra136.
126. H. Liu, C. Chumsae, G. Gaza-Bulseco, K. Hurkmans and C. H. Radziejewski, *Anal. Chem.*, 2010, **82**, 5219-5226.
127. E. V. Vinogradova, C. Zhang, A. M. Spokoyny, B. L. Pentelute and S. L. Buchwald, *Nature*, 2015, **526**, 687-691.
128. L. J. Harris, E. Skaletsky and A. McPherson, *J. Mol. Biol.*, 1998, **275**, 861-872.
129. L. K. Rasmussen, *The Journal of Organic Chemistry*, 2006, **71**, 3627-3629.
130. R. Y. C. Huang and G. Chen, *Drug Discovery Today*, 2016, **21**, 850-855.
131. C. R. Behrens, E. H. Ha, L. L. Chinn, S. Bowers, G. Probst, M. Fitch-Bruhns, J. Monteon, A. Valdiosera, A. Bermudez, S. Liao-Chan, T. Wong, J. Melnick, J.-W. Theunissen, M. R. Flory, D. Houser, K. Venstrom, Z. Levashova, P. Sauer, T.-S. Migone, E. H. van der Horst, R. L. Halcomb and D. Y. Jackson, *Mol. Pharm.*, 2015, **12**, 3986-3998.
132. S. Luisier, M. Avital-Shmilovici, M. A. Weiss and S. B. H. Kent, *Chem. Commun. (Camb.)*, 2010, **46**, 10.1039/c1030cc03141k.
133. J. Brange, Langkj\sgmaelig, L. r, S. Havelund and A. Vølund, *Pharm. Res.*, 1992, **9**, 715-726.
134. K. D. Hinds and S. W. Kim, *Advanced Drug Delivery Reviews*, 2002, **54**, 505-530.
135. K. Hinds, J. J. Koh, L. Joss, F. Liu, M. Baudyš and S. W. Kim, *Bioconjugate Chem.*, 2000, **11**, 195-201.

136. F. M. Veronese, B. Saccà, P. Polverino de Laureto, M. Sergi, P. Caliceti, O. Schiavon and P. Orsolini, *Bioconjugate Chem.*, 2001, **12**, 62-70.
137. C. Seung-Gu, C. Ki-Doo, J. Seung-Hwan and S. Hang-Cheol, *Mol. Cells*, 2003, **16**, 323-330.
138. K. Gorska, A. Manicardi, S. Barluenga and N. Winssinger, *Chem. Commun.*, 2011, **47**, 4364-4366.
139. J. C. Slootweg, S. van der Wal, H. C. Quarles van Ufford, E. Breukink, R. M. J. Liskamp and D. T. S. Rijkers, *Bioconjugate Chem.*, 2013, **24**, 2058-2066.

Appendix I – Associated publications

Attached in the following appendix are the publications authored by Maximillian Lee, including those which pertain to the work presented in the thesis.

In order:

A mild TCEP-based para-azidobenyl cleavage strategy to transform reversible cysteine thiol labelling reagents into irreversible conjugates
Maruani, A., Alom, S., Canavelli, P., Lee, M., Morgan R.E., **Chudasama, V**.*, Caddick, S.
Chem Commun, 2015, 51, 5279-5282.

Chapter 2

Next-generation disulfide stapling: Reduction and functional re-bridging all in one
Lee, M.T.W., Maruani, A., Baker, J.R., Caddick, S., **Chudasama, V.***
Chem Sci, 2016, 7, 799-802.

The use of 3,6-pyridazinediones in organic synthesis and chemical biology
Lee, M.T.W., Maruani, A., **Chudasama, V.***
J Chem Res, 2016, 40, 1-9.

A facile, one-pot procedure for the conversion of aromatic aldehydes to esters, as well as thioesters and amides, via acyl hydrazide intermediates
Maruani, A., Lee, M.T.W, Watkins, G., Akhbar, A.R., Baggs, H., Shamsabadi, A., Richards D.A., **Chudasama, V.***
RSC Adv, 2016, 6, 3372-3376.

Chapter 3

Enabling the controlled assembly of antibody conjugates with a loading of two modules without antibody engineering
Lee, M.T.W., Maruani, A., Richards, D.A., Baker, J.R., Caddick, S., **Chudasama, V.***
Chem Sci, 2017, 8, 2056-2060.

ChemComm

COMMUNICATION

View Article Online
View Journal | View Issue

Cite this: *Chem. Commun.*, 2015, **51**, 5279

Received 28th October 2014,
Accepted 12th November 2014

DOI: 10.1039/c4cc08515a

www.rsc.org/chemcomm

A mild TCEP-based *para*-azidobenzyl cleavage strategy to transform reversible cysteine thiol labelling reagents into irreversible conjugates†

Antoine Maruani, Shamim Alom, Pierre Canavelli, Maximillian T. W. Lee, Rachel E. Morgan, Vijay Chudasama* and Stephen Caddick

It has recently emerged that the succinimide linkage of a maleimide thiol addition product is fragile, which is a major issue in fields where thiol functionalisation needs to be robust. Herein we deliver a strategy that generates selective cysteine thiol labelling reagents, which are stable to hydrolysis and thiol exchange.

Advances in protein modification by chemical means have led to the development of a range of protein bioconjugation methodologies.[1] These methodologies have been successfully applied to a number of fields such as the fluorescent tagging of proteins,[2] and the development of therapeutic protein conjugates[3,4] to treat indications such as HIV,[5] cancer,[6] and malaria.[7] Chemically modified proteins are also utilised as diagnostics.[8]

The use of synthetic methodology to modify proteins has to overcome many major obstacles, the most significant of which is the need for high selectivity, *i.e.* modifying only one amino acid type by discriminating against the other natural amino acids in a protein.[9] As free cysteines are extremely rare in proteins[10] and the thiol side chain has the highest nucleophilicity of all proteinogenic groups at physiological conditions,[11] it is a very popular target for the selective and site-specific modification of proteins.[12] Moreover, with the possibility of facile cysteine introduction by site-directed mutagenesis, cysteine modification is a leading approach. The most popular strategy for labelling the thiol moiety of cysteine residues is by alkylation with maleimides to form thioether-succinimides.[12,13] However, it has recently come to light that such an appendage is sub-optimal owing to issues of hydrolysis, and thiol exchange with reactive thiols in the blood (*e.g.* albumin).[14] This has major implications for biologics that employ a maleimide motif to functionalise a protein thiol for *in vivo* applications. For example, in antibody-drug conjugates (ADCs), where an antibody delivers a toxic payload to cancerous tissue selectively, the use of maleimides to attach cytotoxic drugs to an antibody is not ideal as thiol exchange onto human serum albumin in the blood results in off-site toxicity.[14] Although recent advances have been made in this area through the use of hydrolysed maleimides and succinimides,[14,15] a strong drive to develop novel reagents for reliable, chemoselective, stable and irreversible thiol labelling remains, and particularly for the construction of ADCs.[16]

Recently, we have described a novel, reversible approach to cysteine bioconjugation through the use of bromomaleimides and bromopyridazinediones.[17] To date, our approach has provided access to complex bioconjugates in high yields, without prior activation of reagents with reliable, reversible conjugation. Owing to the demand for hydrolytically stable and thiol irreversible bioconjugates that react in a chemoselective manner, we naturally sought to explore the use of reagents that would meet these criteria. During the course of developing bromopyridazinediones for reversible cysteine bioconjugation, we became intrigued by the prospect of pyridazinediones (PDs) as irreversible cysteine functionalisation reagents. Previously we have shown that if one of the nitrogen atoms on the PD core is unsubstituted the molecule does not react with thiols at physiological pH or higher.[17a] We postulate that this is a consequence of such a structure existing as its enol tautomer, which is likely to be significantly deprotonated under physiological

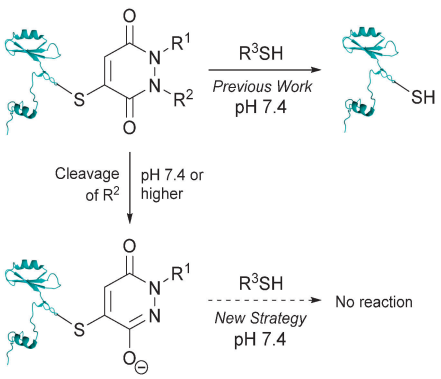

Fig. 1 A novel strategy for developing thiol-stable pyridazinedione bioconjugates.

Department of Chemistry, University College London, 20 Gordon Street, London, WC1H OAJ, UK. E-mail: v.chudasama@ucl.ac.uk; Tel: +44 (0)20 7679 2077

† Electronic supplementary information (ESI) available: LC-MS, ES-MS and deconvoluted spectra for all reactions with proteins described herein, and ^{1}H and ^{13}C NMR spectra for all small molecule constructs. See DOI: 10.1039/c4cc08515a

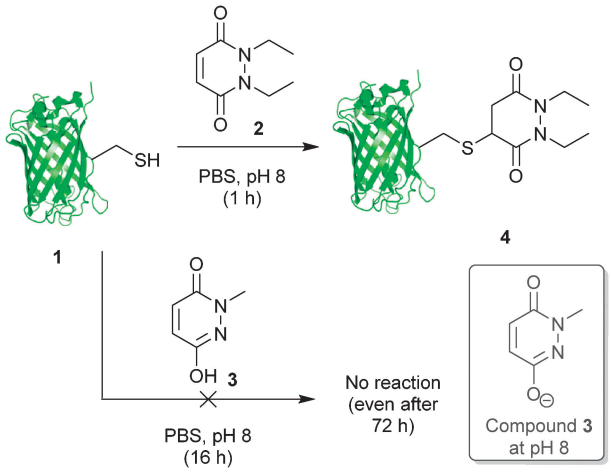

Fig. 2 Incubation of GFPS147C **1** with pyridazinediones **2** and **3**.

pH (or higher), based on the reported pK_a of 1-methyl-3,6-(1*H*,2*H*)-pyridazinedione being ~5.7 in H_2O and the calculated pK_a of its thioether analogue,‡ 1-methyl-4-(methylthio)-3,6-(1*H*,2*H*)-pyridazinedione, being ~5.9.[18] Thiol reactivity will therefore be greatly reduced as the electrophilicity of the resulting PD-core moiety will be tuned down considerably. As such, we set about developing a strategy where we could generate a mono-alkylated-PD species post-bioconjugation to a cysteine thiol to afford a thiol stable construct (see Fig. 1).

Our study began with the reaction of model protein GFP-S147C **1** with pyridazinediones **2** and **3** to confirm our previous observations when using protein Grb2-L111C (see Fig. 2).[17a] These results were consistent with our previous work and confirmed that a mono-alkylated-PD is unreactive to thiol (or other nucleophilic functional groups on amino acid side-chains).

These initial studies paved the way for us to appraise the use of a novel strategy for developing thiol-stable pyridazinedione bioconjugates (see Fig. 1). To do so, we needed to develop a selective method for cleavage of R^2 from the PD core. There are many strategies that could be applied, however, at this juncture we took the opportunity to develop a novel, mild and simple method based on an azide trigger. Our desire to use an azide-based cleavable handle originates from the bioorthogonality of the azide functional group. Taking inspiration from the well-documented work on *p*-aminobenzyloxycarbonyl (PABC) linkers,[19] we set about using a *p*-azidobenzyl cleavage strategy (see Fig. 3).

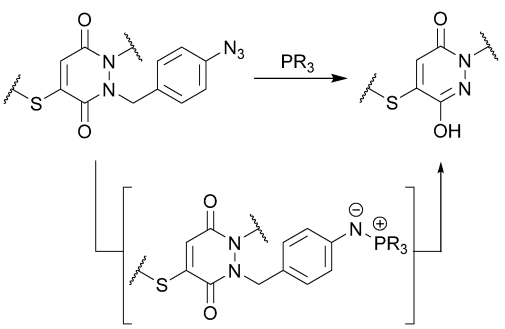

Fig. 3 Use of a *p*-azidobenzyl cleavage strategy to generate a thiol-stable pyridazinedione bioconjugate.

We initially evaluated our *p*-azidobenzyl cleavage strategy in a small molecule study through the use of cysteine derivative **6**, formed by reaction of *N*-(*tert*-butoxycarbonyl)-L-cysteine methyl ester and mono-bromo PD **5** (see ESI† for details on synthesis). The use of an alkyne handle, which would conceptually be retained post *p*-azidobenzyl cleavage, would allow for the resulting construct to be readily functionalised by a Cu(I)-catalyzed Azide-Alkyne Cycloaddition (CuAAC). To our delight, treatment of derivative **6** with TCEP led to clean conversion to derivative **7**, thus providing proof of concept for our novel cleavage strategy. Moreover, incubation of derivatives **6** and **7** with 15 equivalents of 1-hexanethiol in THF/PBS buffer (pH 7.4) only led to thiol exchange in the case of derivative **6**. This provided encouragement for our hypothesis of a mono-alkylated-PD being thiol unreactive under physiological pH or higher (Fig. 4).

Following these encouraging results on a small molecule study, we appraised our strategies on a model protein with a single cysteine mutation, GFPS147C **1**. Initially, GFPS147C **1** was incubated with mono-bromo-PD **5** in sodium phosphate buffer (pH 8.0) for 1 h at 37 °C. As expected, this proceeded with complete conversion and afforded GFP-derivative **8**. We next applied our TCEP cleavage strategy, by incubation of this derivative with 10 equivalents of TCEP in phosphate buffer at pH 8.0. Satisfyingly, clean conversion to bioconjugate **9** was observed, which is consistent with our small molecule study. It is also noteworthy that no hydrolysis occurred under these conditions, which is consistent with our previous observations on the PD core being hydrolytically stable.[17a]

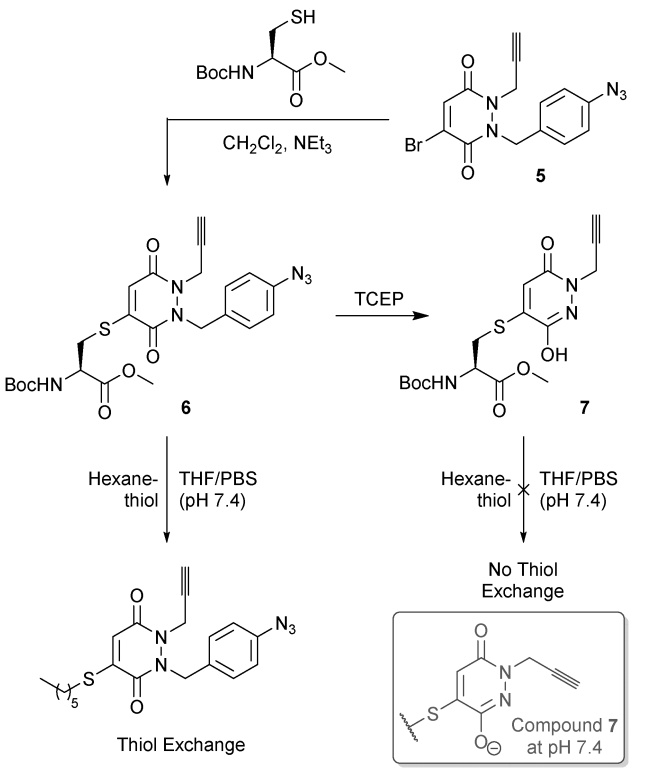

Fig. 4 Use of TCEP in our *p*-azidobenzyl cleavage strategy to generate pyridazinedione derivative **7** from derivative **6**, and the thiol stability of each construct.

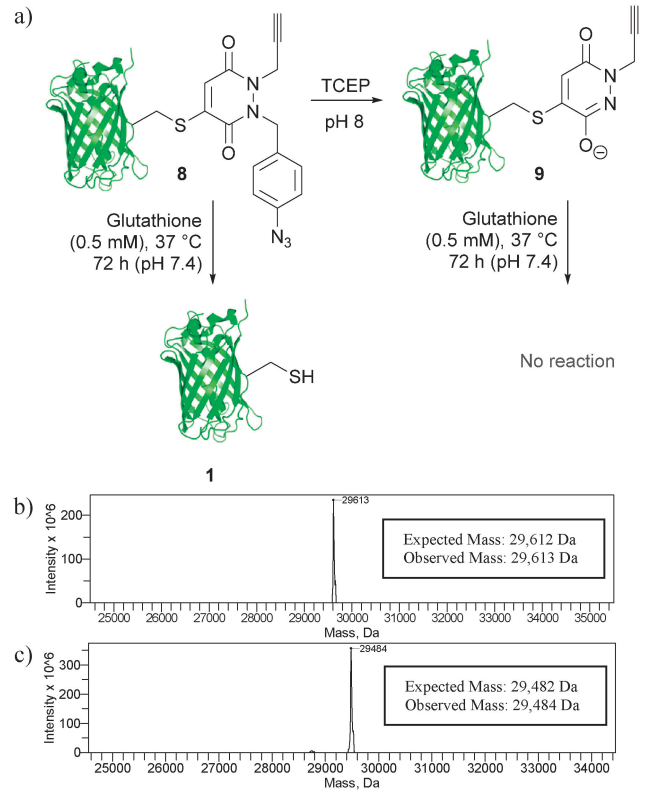

Fig. 5 (a) Translation of our thiol cleavage and thiol stability strategies onto protein bioconjugates **8** and **9**, and deconvoluted MS data for (b) bioconjugate **8** and (c) bioconjugate **9**.

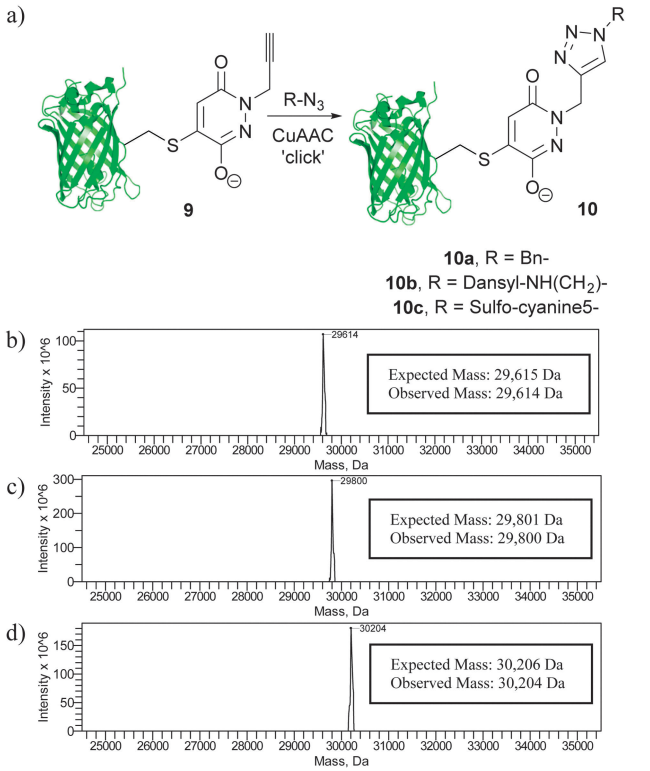

Fig. 6 (a) The use of 'click' chemistry to functionalise bioconjugate **9**, and deconvoluted MS data for (b) bioconjugate **10a**, (c) bioconjugate **10b** and (d) bioconjugate **10c**.

Having established, using mass spectrometry, that our cleavage strategy is applicable on a protein, we next compared the thiol stability of **8** and **9** by incubation with glutathione (0.5 mM) for 72 h at pH 7.4 and 37 °C. Gratifyingly, GFP-derivative **9** was completely stable under the reaction conditions, whereas derivative **8** showed complete thiol exchange with glutathione. This therefore established proof of concept for both our strategies on a model protein scaffold. Moreover, this work also highlights the versatility of the PD platform with a facile shift from reversible to irreversible constructs achieved under mild conditions (Fig. 5).

Following our work on developing a novel *p*-azidobenzyl cleavage strategy and obtaining a thiol stabile construct, we set about functionalising protein scaffold **9** by the use of 'click' chemistry. If successful, this would result in a facile method for functionalising the thiol-stable bioconjugate. A number of 'click' conditions were trialled using benzyl azide as our model azide. The most promising conditions were the use of Cu(I)Br as copper source and THPTA as ligand. These conditions gave complete conversion of starting material alkyne **9** to triazole bioconjugate **10a**. Moreover, these conditions also allowed for clean reaction of the alkyne derivative with a dansyl azide and a sulfo-cyanine5 azide to afford **10b** and **10c**, respectively (Fig. 6).

In conclusion, we have developed, *via* a novel *p*-azidobenzyl cleavage strategy, a route to thiol stable cysteine-bioconjugates that has a clear advantage over conventional maleimide chemistry. The strategy has been demonstrated on both a small molecule system and on a model protein, GFPS147C. Owing to the plethora of fields where thiol functionalisation needs to be robust and irreversible, *e.g.* in antibody-drug conjugates (ADCs), imaging and theranostics, we believe this work will find use in a variety of domains. We hope to deliver on the application of our platform in a range of contexts, including ADCs, in the near future.

The authors gratefully acknowledge the EPSRC, Ramsay Memorial Trust and UCL for support of our programme.

Notes and references

‡ MarvinSketch and its calculator plugins were used for pK_a prediction, MarvinSketch 14.11.3.0, ChemAxon (http://www.chemaxon.com).

1 C. D. Spicer and B. G. Davis, *Nat. Commun.*, 2014, **5**, 5740 and references therein.
2 S. Girouard, M. H. Houle, A. Grandbois, J. W. Keillor and S. W. Michnick, *J. Am. Chem. Soc.*, 2005, **127**, 559–566.
3 D. H. Dube and C. R. Bertozzi, *Nat. Rev. Drug Discovery*, 2005, **4**, 477–488.
4 S. Jevševar, M. Kunstelj and V. G. Porekar, *Biotechnol. J.*, 2010, **5**, 113–128.
5 R. D. Astronomo, H. K. Lee, C. N. Scanlan, R. Pantophlet, C. Y. Huang, I. A. Wilson, O. Blixt, R. A. Dwek, C. H. Wong and D. R. Burton, *J. Virol.*, 2008, **82**, 6359–6368.
6 L. M. Krug, G. Ragupathi, K. K. Ng, C. Hood, H. J. Jennings, Z. Guo, M. G. Kris, V. Miller, B. Pizzo, L. Tyson, V. Baez and P. O. Livingston, *Clin. Cancer Res.*, 2004, **10**, 916–923.
7 L. Schofield, M. C. Hewitt, K. Evans, M.-A. Siomos and P. H. Seeberger, *Nature*, 2002, **18**, 785–789.
8 J. J. Day, B. V. Marquez, H. E. Beck, T. A. Aweda, P. D. Gawande and C. F. Meares, *Curr. Opin. Chem. Biol.*, 2010, **14**, 803–809.
9 I. S. Carrico, *Chem. Soc. Rev.*, 2008, **37**, 1423–1431.

10 R. Bhattacharyya, D. Pal and P. Chakrabarti, *Protein Eng., Des. Sel.*, 2004, **17**, 795–808.
11 R. L. Lundblad, *Chemical Reagents for Protein Modification*, CRC Press, Boca Raton, FL, 3rd edn, 2005.
12 J. M. Chalker, G. J. L. Bernardes, Y. A. Lin and B. G. Davis, *Chem. – Asian J.*, 2009, **4**, 630–640 and references therein.
13 (*a*) D. J. Betting, K. Kafi, A. Abdollahi-Fard, S. A. Hurvitz and J. M. Timmerman, *J. Immunol.*, 2008, **181**, 4131–4140; (*b*) Y. Zhang, V. S. Bhatt, G. Sun, P. G. Wang and A. F. Palmer, *Bioconjugate Chem.*, 2008, **19**, 2221–2230; (*c*) I. Shin, H. J. Jung and M. R. Lee, *Tetrahedron Lett.*, 2001, **42**, 1325–1328; (*d*) C. Linda, R. Gerdesa, Y. Hamnella, I. Schuppe-Koistinenc, H. B. von Löwenhielmd, A. Holmgrene and I. A. Cotgreavea, *Arch. Biochem. Biophys.*, 2002, **406**, 229–240.
14 B.-Q. Shen, K. Xu, L. Liu, H. Raab *et al.*, *Nat. Biotechnol.*, 2012, **30**, 184–189.
15 (*a*) R. P. Lyon, J. R. Setter, T. D. Bovee, S. O. Doronina, J. H. Hunter, M. E. Anderson, C. L. Balasubramanian, S. M. Duniho, C. I. Leiske, F. Li and P. D. Senter, *Nat. Biotechnol.*, 2014, **32**, 1059–1062; (*b*) L. N. Tumey, M. Charati, T. He, E. Sousa, D. Ma, X. Han, T. Clark, J. Casavant, F. Loganzo, F. Barletta, J. Lucas and E. I. Graziani, *Bioconjugate Chem.*, 2014, **25**, 1871–1880; (*c*) C. P. Ryan, M. E. B. Smith, F. F. Schumacher, D. Grohmann, D. Papaioannou, G. Waksman, F. Werner, J. R. Baker and S. Caddick, *Chem. Commun.*, 2011, **47**, 5452–5454.
16 (*a*) P. M. S. D. Cal, G. J. L. Bernardes and P. M. P. Gois, *Angew. Chem., Int. Ed.*, 2014, **53**, 10585–10587; (*b*) R. V. J. Chari, M. L. Miller and W. C. Widdison, *Angew. Chem., Int. Ed.*, 2014, **53**, 3796–3827.
17 (*a*) V. Chudasama, M. E. B. Smith, F. F. Schumacher, D. Papaioannou, G. Waksman, J. R. Baker and S. Caddick, *Chem. Commun.*, 2011, **47**, 8781–8783; (*b*) R. I. Nathani, V. Chudasama, C. P. Ryan, P. R. Moody, R. E. Morgan, R. J. Fitzmaurice, M. E. B. Smith, J. R. Baker and S. Caddick, *Org. Biomol. Chem.*, 2013, **11**, 2408–2411; (*c*) M. E. B. Smith, F. F. Schumacher, C. P. Ryan, L. M. Tedaldi, D. Papaioannou, G. Waksman, S. Caddick and J. R. Baker, *J. Am. Chem. Soc.*, 2010, **132**, 1960–1965.
18 (*a*) N. A. Burton, D. V. S. Green, I. H. Millier, P. J. Taylor, M. A. Vincent and S. Woodcock, *J. Chem. Soc., Perkin Trans. 2*, 1993, 331–335; (*b*) H. Feuer, G. B. Silverman, H. P. Angstadt and A. R. Fauke, *J. Org. Chem.*, 1962, **27**, 2081–2084; (*c*) D. M. Miller and R. W. White, *Can. J. Chem.*, 1956, **34**, 1510–1512; (*d*) S. Du Breuil, *J. Org. Chem.*, 1961, **26**, 3382–3386.
19 P. L. Carl, P. K. Chakravarty and J. A. Katzenellenbogen, *J. Med. Chem.*, 1981, **24**, 479–480.

Chemical Science

EDGE ARTICLE

View Article Online
View Journal | View Issue

Cite this: *Chem. Sci.*, 2016, **7**, 799

Next-generation disulfide stapling: reduction and functional re-bridging all in one†

Maximillian T. W. Lee, Antoine Maruani, James R. Baker, Stephen Caddick and Vijay Chudasama*

Received 22nd July 2015
Accepted 13th September 2015

DOI: 10.1039/c5sc02666k

www.rsc.org/chemicalscience

Herein we present a significant step towards next-generation disulfide stapling reagents. A novel class of reagent has been designed to effect both disulfide reduction and functional re-bridging. The strategy has been applied to great success across various peptides and proteins. Moreover, application to a multi-disulfide system resulted in functional re-bridging without disulfide scrambling.

Advances in protein modification by chemical means have led to the development of a range of protein bioconjugation methodologies.[1] These methodologies have been successfully applied to a number of fields such as the fluorescent tagging of proteins,[2] the development of therapeutic protein conjugates[3,4] to treat indications such as HIV,[5] cancer[6] and malaria,[7] and for use as diagnostic tools.[8]

Whilst a large number of reagents and protocols have been developed to modify proteins, novel strategies for site-specific conjugation continue to attract considerable interest in view of the increasingly stringent requirements in the development of biologics.[1] Several amino acid side-chains have been targeted for site-selective modification over the past few decades, *e.g.* tryptophan, histidine, tyrosine and, in particular, lysine and cysteine. However, the modification of native disulfides through functional re-bridging, pioneered by Brocchini *et al.*, has attracted significant interest in recent years with various approaches being developed.[9–13]

Recently, Chudasama, Caddick *et al.* have shown dibromopyridazinediones to be viable candidates for disulfide stapling and that the resulting bisthioether is stable in blood plasma-mimicking conditions.[9j] Whilst this approach, as well as others, offer advances in this growing field of disulfide labelling, a common limitation is the requirement for reduction and re-bridging in distinct steps. This is mainly due to the incompatibility of the bridging and reducing agents. This introduces inefficiencies in terms of cost, time and practicality. Whilst one-pot *in situ* methods have been employed, this is only at the expense of using a vast excess of reducing and bridging agents to compensate for the reaction between the two reagents.[9j]

In view of the above, we set about designing a reagent that could incorporate both reducing and re-bridging functions (Fig. 1). During the course of our previous studies, we observed dithiophenolpyridazinediones to be unreactive towards commonly used disulfide reducing agent tris(2-carboxyethyl) phosphine (TCEP). In light of this, TCEP moieties were a logical choice for incorporation into a dithiophenolpyridazinedione. More specifically, the TCEP functional moieties were to be tethered onto the thiophenol groups of the dithiophenolpyridazinedione since these groups would be extruded post-bioconjugation with a reduced disulfide.

A suitable route to a dithioaryl(TCEP)pyridazinedione was conceived (Scheme 1). Initially, TFA cleavage of the Boc groups of di-Boc-diethylhydrazine **1**, followed by reaction with dibromomaleic anhydride under reflux in AcOH, afforded diethyl dibromopyridazinedione **2**. This dibromopyridazinedione was reacted with 4-aminothiophenol to form dithioarylpyridazinedione **3**, which was finally coupled to mono-acid TCEP derivative **4** to form target dithioaryl(TCEP)pyridazinedione **5**.

With dithioaryl(TCEP)pyridazinedione **5** in hand, we appraised its suitability as a bioconjugation reagent for both disulfide reduction and functional re-bridging. To do this,

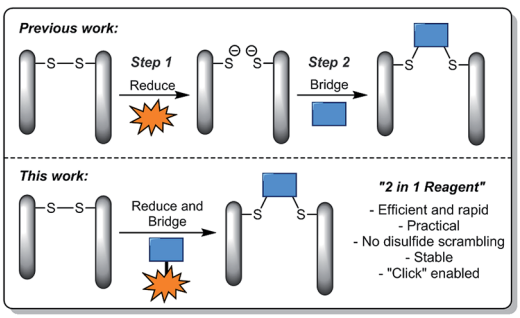

Fig. 1 Illustration highlighting previous strategies towards disulfide stapling and the novel strategy described in this manuscript.

Department of Chemistry, University College London, 20 Gordon Street, London, WC1H 0AJ, United Kingdom. E-mail: v.chudasama@ucl.ac.uk; Tel: +44207 679 2077

† Electronic supplementary information (ESI) available: ^{1}H and ^{13}C NMR spectra for all small molecules, LC-MS, SDS-PAGE gels and UV-Vis analysis (where applicable) for all bioconjugates. See DOI: 10.1039/c5sc02666k

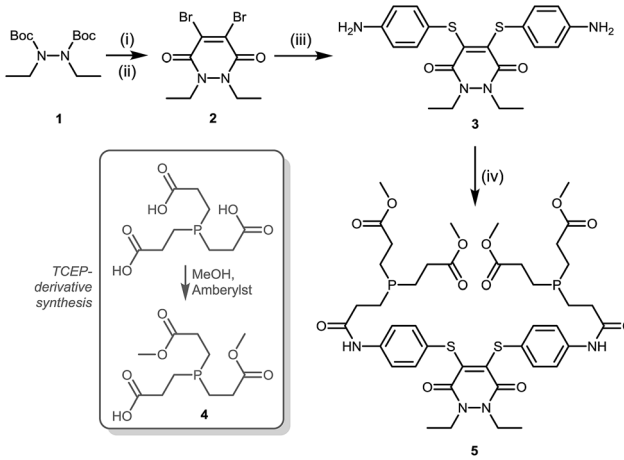

Scheme 1 Synthesis of dithioaryl(TCEP)pyridazinedione **5**. Reagents and conditions: (i) TFA, CH_2Cl_2, 21 °C, 1 h; (ii) dibromomaleic anhydride, AcOH, reflux, 2 h; (iii) 4-aminothiophenol, NEt_3, CH_2Cl_2, 21 °C, 2 h; (iv) acid **4**, DMF, HATU, DIPEA, 21 °C, 12 h.

pyridazinedione **5** was incubated with a selection of biologically relevant disulfide containing peptides and proteins, *i.e.* somatostatin, octreotide and a Fab (fragment antigen-binding) arm of Herceptin™. To our delight, in each and every case, pyridazinedione **5** was shown to reduce and functionally re-bridge the singly accessible disulfide (see Scheme 2 and ESI for further details†). Moreover, only a small excess of "2-in-1" reagent **5**, 1.25 equivalents, was required to effect complete conversion. Another favourable property of pyridazinedione **5** is that it is a solid which can be stored with complete stability over a protracted period at −18 °C under argon.

At this stage we rationalised that a molecule with both reducing and re-bridging functions would minimise the residency time of the cysteines liberated from disulfide reduction. This is especially in view of no reduced protein being observed upon incubation of the above peptides and proteins with reagent **5** (see ESI for details†). To appraise this further, we incubated the Fab fragment of Herceptin™ with 1, 2 and 5 equivalents of dipropyl-pyridazinedione **6** prior to incubation with 2 equivalents of diethylpyridazinedione **5** (Scheme 3). Validating our hypothesis, re-bridging was only observed with the TCEP-bearing diethylpyridazinedione. The control reaction of reducing the Fab prior to adding a mixture of

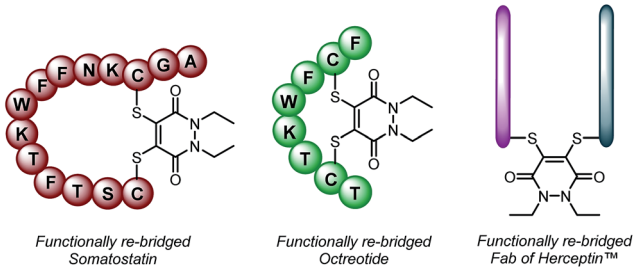

Scheme 2 Functionally re-bridged somatostatin, octreotide and a Fab of Herceptin™ using dithioaryl(TCEP)pyridazinedione **5**.

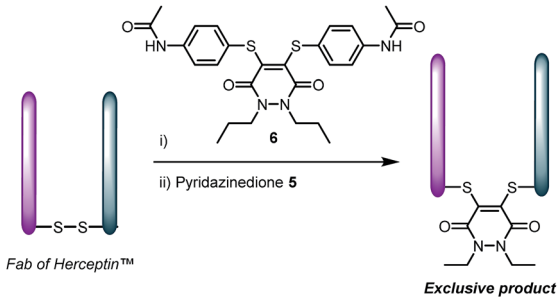

Scheme 3 Pre-incubation of Fab fragment of Herceptin™ with pyridazinedione **6**, followed by addition of **5** affords product derived from reagent **5** only.

pyridazinedione **5** and **6** afforded a mixture of bioconjugates (see ESI for details†).

With the knowledge of the use of dithioaryl(TCEP)pyridazinedione **5** resulting in a high local concentration of the specific pyridazinedione incorporated into the "2-in-1" scaffold, we appraised the use of the reagent in the context of a multi-disulfide system. To do this, we chose to use Herceptin™ – an antibody comprising four disulfide bonds – whose disulfide bonds can be scrambled on attempted functional disulfide re-bridging.[9h] Although this scrambling can be minimised, the leading strategy is reagent specific.[9j] We rationalised that the use of pyridazinedione **5** would ensure minimisation of

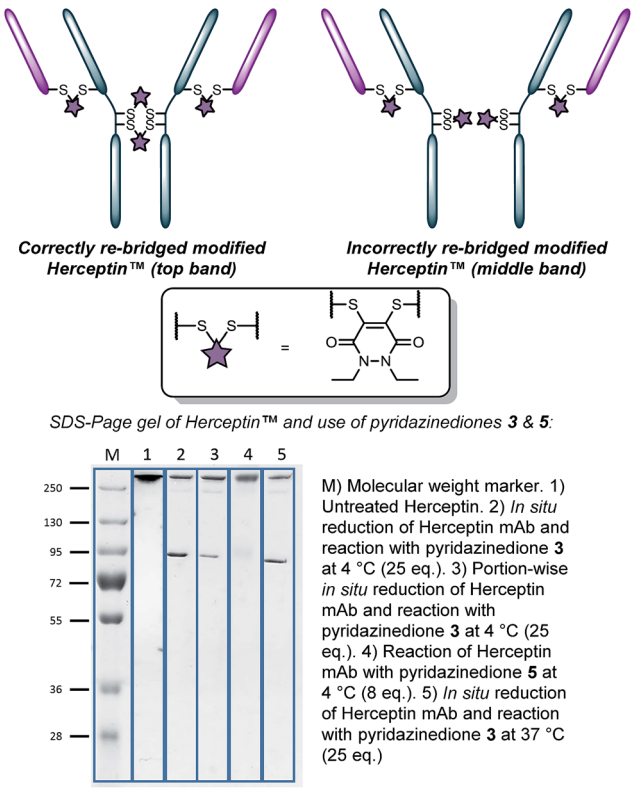

Fig. 2 Appraisal of the use of pyridazinediones **3** (*in situ* 4 °C (pre-reduced, portion-wise reduction), 37 °C) and **5** for functional re-bridging of Herceptin™.

disulfide scrambling in a general sense. To this end, pyridazinediones **3** (with no internal reducing agent function) and **5** (with reducing agent function) were reacted with Herceptin™ under the appropriate reaction conditions, *i.e.* reaction with pyridazinedione **3** required reduction of Herceptin™ with TCEP. Gratifyingly, no disulfide scrambling was observed by SDS-PAGE for reagent **5**, with complete re-bridging of all disulfides confirmed by UV-Vis (Fig. 2, lane 4). Analogous reagent **3**, with no inherent reducing capability, afforded a disulfide scrambled product (Fig. 2, lane 2). Even when dithiopyridazinedione **3** was used in excess and TCEP was added in small portions multiple times (6 × 0.33 eq per disulfide every 30 min), *i.e.* to minimise the number of open disulfides at any given time, disulfide scrambling was still observed (Fig. 2, lane 3). Although scrambling was far less pronounced, the reaction protocol is highly cumbersome and inefficient. Reaction of dithiopyridazinedione **3** at 37 °C also afforded a mixture of products (Fig. 2, lane 5). Furthermore, reaction of pyridazinedione **2** at 4 °C and 37 °C also afforded a mixture of correctly and incorrectly re-bridged modified Herceptin™ conjugates (see ESI for details†).

Providing a reagent that can functionally re-bridge the disulfide bonds of Herceptin™ without disulfide scrambling is a major contribution in view of the desire to create homogenous conjugates in the field of antibody–drug conjugates.[14] Use of Herceptin™, in view of its clinical validation alone and as the antibody component of FDA-approved ADC Kadcyla™,[15] provides direct applicability of the chemistry to this exciting area of targeted therapy.

To make this approach modular and expand its scope, we synthesised an analogue of pyridazinedione **5**, which contained an alkyne handle for "click" functionalisation, in alkyne-pyridazinedione **7** (see Scheme 4). An analogous route to that described in Scheme 1 was followed (see ESI for further details†). The appraisal of this molecule was carried on the Fab fragment of Herceptin™ as this would allow extensive analysis by UV-Vis, MS, SDS-PAGE and ELISA (for binding). The optimised conditions for the insertion of dithioaryl(TCEP)pyridazinedione **5**, was applied to the alkyne bearing analogue for the functional re-bridging of the Fab fragment of Herceptin™ to form conjugate **8**. The efficiency of reduction and re-bridging was translated cleanly from reagent **5** to alkyne analogue **7** by MS, SDS-PAGE and UV-Vis (see Scheme 4 and ESI for further details†).

Finally, conjugate **8** was functionalised by "click" modification using doxorubicin, AlexaFluor488™ and sulfo-cyanine5 azides (see Scheme 4). In all cases, complete conversion was observed to afford functionalised conjugates **9a–c**, thus demonstrating how the platform may be used for efficient introduction of functional modalities as well as reduction and re-bridging. Moreover, the binding of the Fab protein was not compromised, by ELISA analysis (see ESI for details†), through the chemistry applied. Pyridazinedione **7** was also shown to successfully re-bridge the full antibody system of Herceptin™ and be amenable to "click" functionalisation with doxorubicin azide (see ESI for details†).

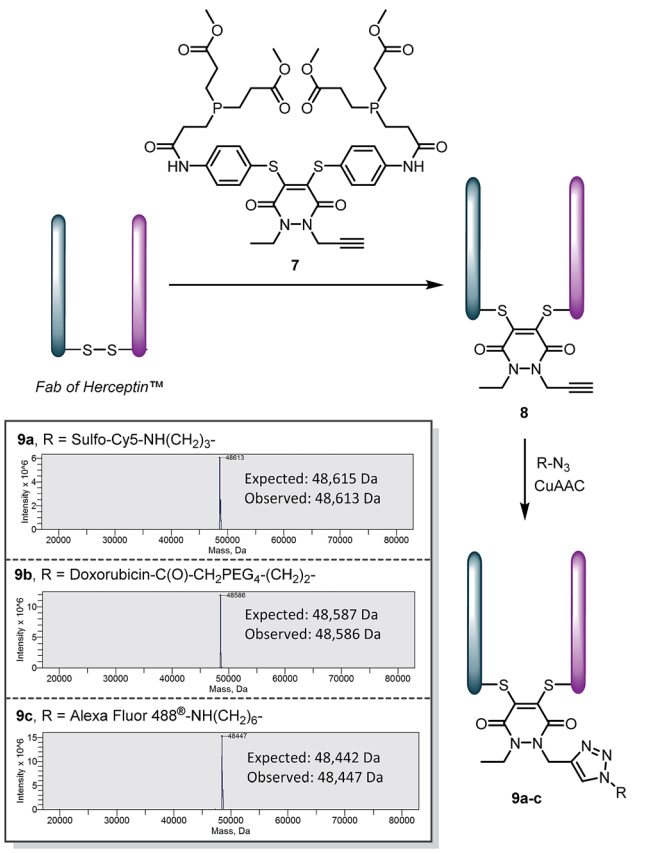

Scheme 4 Application of alkyne bearing pyridazinedione **7** for disulfide reduction and re-bridging as well as "click" functionalisation of the product with various azides to form bioconjugates **9a–c**.

Conclusions

In conclusion, we have provided an important step towards delivering on next-generation disulfide stapling. This first-in class technology allows for reduction and functional re-bridging by the use of a single reagent. Moreover, this strategy has been shown to result in a high local concentration of bridging agent, which has been exploited for the functional re-bridging of a multi-disulfide system (*i.e.* Herceptin™) without disulfide scrambling. Finally, facile "click" functionalisation and retention of binding affinity, using our strategy, has been demonstrated on a Fab of Herceptin™.

Acknowledgements

The authors gratefully acknowledge the EPSRC and UCL for funding. MTWL and AM funded by EPSRC (164255). VC funded by UCL Excellence Fellowship.

Notes and references

1 (*a*) C. D. Spicer and B. G. Davis, *Nat. Commun.*, 2014, **5**, 5740 and references therein; (*b*) O. Boutureira and G. J. L. Bernardes, *Chem. Rev.*, 2015, **115**, 2174 and

references therein; (*c*) O. Konieva and A. Wagner, *Chem. Soc. Rev.*, 2015, **44**, 5495.

2 S. Girouard, M. H. Houle, A. Grandbois, J. W. Keillor and S. W. Michnick, *J. Am. Chem. Soc.*, 2005, **127**, 559.

3 D. H. Dube and C. R. Bertozzi, *Nat. Rev. Drug Discovery*, 2005, **4**, 477.

4 S. Jevševar, M. Kunstelj and V. G. Porekar, *Biotechnol. J.*, 2010, **5**, 113.

5 R. D. Astronomo, H. K. Lee, C. N. Scanlan, R. Pantophlet, C. Y. Huang, I. A. Wilson, O. Blixt, R. A. Dwek, C. H. Wong and D. R. Burton, *J. Virol.*, 2008, **82**, 6359.

6 L. M. Krug, G. Ragupathi, K. K. Ng, C. Hood, H. J. Jennings, Z. Guo, M. G. Kris, V. Miller, B. Pizzo, L. Tyson, V. Baez and P. O. Livingston, *Clin. Cancer Res.*, 2004, **10**, 916.

7 L. Schofield, M. C. Hewitt, K. Evans, M. A. Siomos and P. H. Seeberger, *Nature*, 2002, **18**, 785.

8 J. J. Day, B. V. Marquez, H. E. Beck, T. A. Aweda, P. D. Gawande and C. F. Meares, *Curr. Opin. Chem. Biol.*, 2010, **14**, 803.

9 (*a*) F. F. Schumacher, V. A. Sanchania, B. Tolner, Z. V. F. Wright, C. P. Ryan, M. E. B. Smith, J. M. Ward, S. Caddick, C. W. M. Kay, G. Aeppli, K. A. Chester and J. R. Baker, *Sci. Rep.*, 2013, **3**, 1525; (*b*) C. P. Ryan, M. E. B. Smith, F. F. Schumacher, D. Grohmann, D. Papaioannou, G. Waksman, F. Werner, J. R. Baker and S. Caddick, *Chem. Commun.*, 2011, **47**, 5452; (*c*) F. F. Schumacher, M. Nobles, C. P. Ryan, M. E. B. Smith, A. Tinker, S. Caddick and J. R. Baker, *Bioconjugate Chem.*, 2011, **22**, 132; (*d*) M. E. B. Smith, F. F. Schumacher, C. P. Ryan, L. M. Tedaldi, D. Papaioannou, G. Waksman, S. Caddick and J. R. Baker, *J. Am. Chem. Soc.*, 2010, **132**, 1960; (*e*) L. Castañeda, A. Maruani, F. F. Schumacher, E. Miranda, V. Chudasama, K. A. Chester, J. R. Baker, M. E. B. Smith and S. Caddick, *Chem. Commun.*, 2013, **49**, 8187; (*f*) V. Chudasama, M. E. B. Smith, F. F. Schumacher, D. Papaioannou, G. Waksman, J. R. Baker and S. Caddick, *Chem. Commun.*, 2011, **47**, 8781; (*g*) F. Bryden, A. Maruani, H. Savoie, V. Chudasama, M. E. B. Smith, S. Caddick and R. W. Boyle, *Bioconjugate Chem.*, 2014, **25**, 611; (*h*) F. F. Schumacher, J. P. M. Nunes, A. Maruani, V. Chudasama, M. E. B. Smith, K. A. Chester, J. R. Baker and S. Caddick, *Org. Biomol. Chem.*, 2014, **12**, 7261; (*i*) A. Maruani, S. Alom, P. Canavelli, M. T. W. Lee, R. E. Morgan, V. Chudasama and S. Caddick, *Chem. Commun.*, 2015, **51**, 5279; (*j*) A. Maruani, M. E. B. Smith, E. Miranda, K. A. Chester, V. Chudasama and S. Caddick, *Nat. Commun.*, 2015, **6**, 6645; (*k*) J. P. M. Nunes, M. Morais, V. Vassileva, E. Robinson, V. Rajkumar, M. E. B. Smith, B. R. Pedley, S. Caddick, J. R. Baker and V. Chudasama, *Chem. Commun.*, 2015, **51**, 10624–10627; (*l*) A. Maruani, H. Savoie, F. Bryden, S. Caddick, R. W. Boyle and V. Chudasama, *Chem. Commun*, 2015, DOI: 10.1039/C5CC06985H.

10 N. Assem, D. J. Ferreira, D. W. Wolan and P. E. Dawson, *Angew. Chem., Int. Ed.*, 2015, **54**, 8665.

11 (*a*) S. P. Brown and A. B. Smith, *J. Am. Chem. Soc.*, 2015, **137**, 4034; (*b*) M. J. Tucker, J. R. Courter, J. Chen, O. Atasoylu, A. B. Smith and R. M. Hochstrasser, *Angew. Chem., Int. Ed.*, 2010, **49**, 3612.

12 (*a*) S. Shaunak, A. Godwin, J.-W. Choi, S. Balan, E. Pedone, D. Vijayarangam, S. Heidelberger, I. Teo, M. Zloh and S. Brocchini, *Nat. Chem. Biol.*, 2006, **2**, 312; (*b*) S. Balan, J.-W. Choi, A. Godwin, I. Teo, C. M. Laborde, S. Heidelberger, M. Zloh, S. Shaunak and S. Brocchini, *Bioconjugate Chem.*, 2007, **18**, 61; (*c*) S. Brocchini, A. Godwin, S. Balan, J.-W. Choi, M. Zloh and S. Shaunak, *Adv. Drug Delivery Rev.*, 2008, **60**, 3; (*d*) H. Khalili, A. Godwin, J.-W. Choi, R. Lever and S. Brocchini, *Bioconjugate Chem.*, 2012, **23**, 2262; (*e*) A. Lewis, Y. Tang, S. Brocchini, J.-W. Choi and A. Godwin, *Bioconjugate Chem.*, 2008, **19**, 2144.

13 P. Wilson, A. Anastasaki, M. R. Owen, K. Kempe, D. M. Haddleton, S. K. Mann, A. P. R. Johnston, J. F. Quinn, M. R. Whittaker, P. J. Hogg and T. P. Davis, *J. Am. Chem. Soc.*, 2015, **137**, 4215.

14 P. Agarwal and C. R. Bertozzi, *Bioconjugate Chem.*, 2015, **26**, 176 and references therein.

15 (*a*) C. A. Hudis, *N. Engl. J. Med.*, 2007, **357**, 39; (*b*) S. Verma, D. Miles, L. Gianni, I. E. Krop, M. Welslau, J. Baselga, M. Pegram, D. Y. Oh, V. Diéras, E. Guardino, L. Fang, M. W. Lu, S. Olsen and K. Blackwell, *N. Engl. J. Med.*, 2012, **367**, 1783.

Chemical Science

EDGE ARTICLE

View Article Online
View Journal | View Issue

Cite this: *Chem. Sci.*, 2017, **8**, 2056

Enabling the controlled assembly of antibody conjugates with a loading of two modules without antibody engineering†

Maximillian T. W. Lee, Antoine Maruani, Daniel A. Richards, James R. Baker, Stephen Caddick and Vijay Chudasama*

Received 15th August 2016
Accepted 24th November 2016

DOI: 10.1039/c6sc03655d

www.rsc.org/chemicalscience

The generation of antibody conjugates with a loading of two modules is desirable for a host of reasons. Whilst certain antibody engineering approaches have been useful in the preparation of such constructs, a reliable method based on a native antibody scaffold without the use of enzymes or harsh oxidative conditions has hitherto not been achieved. The use of native antibodies has several advantages in terms of cost, practicality, accessibility, time and overall efficiency. Herein we present a novel, reliable method of furnishing antibody conjugates with a loading of two modules starting from a native antibody scaffold.

Antibody conjugates play an important role in a variety of applications, particularly in the field of diagnostics and therapeutics.[1,2] In recent years, there has been significant interest in the area of antibody-drug conjugates (ADCs).[2] ADCs comprise antibodies covalently attached to highly potent drugs using a linker conjugation technology.[2] As therapeutics, they conceptually combine the specificity of antibodies, *i.e.* enabling discrimination between healthy and diseased tissue, with the cell-killing ability of cytotoxic drugs. This powerful and exciting class of targeted therapy has shown considerable promise in the treatment of various cancers with two US Food and Drug Administration approved ADCs currently on the market (Adcetris™ and Kadcyla™)[3,4] and approximately 40 currently undergoing clinical evaluation.[5] However, most of these ADCs exist as heterogeneous mixtures, which can result in a narrow therapeutic window and have major pharmacokinetic implications.[2,6] In order for ADCs to achieve their full potential, sophisticated site-specific conjugation technologies to connect the drug to the antibody are increasingly being developed.[2]

Whilst a large number of reagents and strategies have been developed to create these next generation ADCs, novel strategies for site-specific conjugation continue to attract considerable interest.[2] This is especially important as it is coming to light that specific requirements are essential for each particular ADC to operate at its optimum.[2] Whilst engineered antibodies have worked well in meeting the demand for these tailor-made antibody conjugates, *e.g.* by using engineered cysteine residues, unnatural amino acids, selenocysteine or enzymatic conjugation,[7] there is a requirement for methods that are based on native antibody modification. This is to ensure that technologies to make these "designer" ADCs are more accessible and cost-effective; engineered approaches often require significant optimisation on each antibody scaffold they are applied, as well not being accessible to a broad range of scientists.

It has recently come to light that in various tailor-made ADCs one of the most desirable ratios of drugs to antibody is two. The reason for this is that for certain hydrophobic drugs, *e.g.* pyrrolobenzodiazepines (PBDs), a loading of two is preferable as it provides a good balance between efficacy and pharmacokinetic profile (higher payload loading tends to result in too rapid clearance and lower loadings reduce efficacy). This argument is supported by the PBD-based ADCs that are currently in clinical trials.[2,8] Whilst this particular challenge has to some extent been addressed by antibody engineering approaches, *e.g.* THIOMAbs for homogeneous DAR 2 conjugates, they are not readily accessible and there are issues associated with the methodology (*e.g.* potential for disulfide scrambling and the inefficiency of having to reduce, carefully re-oxidise and then conjugate).[2] Thus, there is a need for a reliable method of constructing antibody conjugates with a loading of two entities starting from a native antibody construct. This is especially in the context of: (i) the rapid progression in the development of further hydrophobic drugs being used and developed in the field;[8a,b,9] and (ii) the major attempts on native antibodies (*i.e.* based on the selective reduction of the Fab or hinge disulfides of an IgG1)[10g,11] proving to lack broad applicability, as evidenced by the lack of uptake in the field, or having to employ harsh oxidation conditions or enzymes under specific conditions.[12] Herein we detail the realisation of a reliable and reproducible strategy to make antibody conjugates with a loading of two starting from a native scaffold. It has significant advantages in terms of

Department of Chemistry, University College London, 20 Gordon Street, London, WC1H 0AJ, UK. E-mail: v.chudasama@ucl.ac.uk; Tel: +44 (0)207 679 2077

† Electronic supplementary information (ESI) available: ^{1}H and ^{13}C NMR spectra for all small molecules, ELISA, SDS-PAGE gels and UV-vis analysis (where applicable) for all bioconjugates. See DOI: 10.1039/c6sc03655d

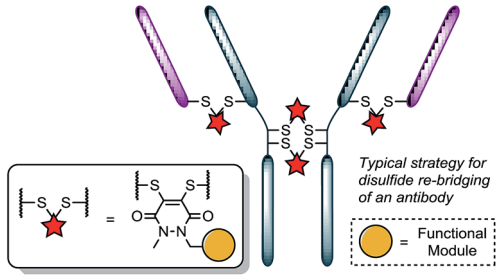

Fig. 1 Illustration detailing the typical approach to functional disulfide re-bridging conjugates.

cost, practicality, accessibility, time and overall efficiency when compared to existing methods.

Recently, we have shown dibromopyridazinediones (diBrPDs) and dibromo/dithio-maleimides to be excellent candidates for the functional re-bridging of inter-chain disulfides in antibodies (Fig. 1). Moreover, the resulting bisthioether conjugates have been shown to be stable in blood plasma-mimicking conditions and retain activity plus selectivity *in vitro*.[10] The dibromomaleimide platform has also been shown to be effective *in vivo* by Jackson and co-workers.[13] Whilst this approach, as well as others,[10,13,14] offer advances in terms of providing homogeneous DAR 4 conjugates starting from a non-engineered antibody scaffold, there has as yet been no translation of the technologies to form controlled DAR 2 conjugates. Nonetheless, we set out to explore if we could exploit the efficient functional re-bridging of disulfides with diBrPDs as a conduit to realise the goal of controlled DAR 2 conjugate formation starting from a native antibody scaffold. We envisaged that conjugation of two bis-dibromopyridazinediones (containing a single functional modality) with an appropriate linker length could "tie up" two pairs of the 4 disulfides on an IgG1 to allow the formation of a conjugate with an overall loading of two functional modules (see Fig. 2).

Our study began with the synthesis of an appropriate spaced bis-dibromopyridazinedione, bis-diBrPD **1**. As we were aiming to react a pair of disulfides using bis-diBrPD **1** it was rationalised from the outset that the linker length would be key. If too short, the bis-PD could not react with a pair of disulfides as it could not span the appropriate length; too long and it would increase the likelihood of undesirable intermolecular reaction(s) by losing the high local concentration effect – thus resulting in inefficient bridging of bis-diBrPD **1** across a pair of disulfides. In an effort to avoid these issues we designed a linker based on the spacing of the disulfides on an IgG1 for which a crystal structure has been obtained (~16.7 Å = maximum linear distance).[14,‡] To ensure flexibility, and improve water solubility of the bis-dibromopyridazinedione, a PEG spacer was used to link together the PD bioconjugation sites. We installed a single alkyne on the bis-PD scaffold so as to eventually allow a loading of two modules, through the use of click chemistry, post-conjugation of bis-diBrPD **1** on a full antibody. The click handle was also positioned by design to be close to a PD-disulfide bridging site to minimise exposure of the clicked entity.

Compound **1** was synthesised by the route described in Scheme 1; in view of the maximum linear distance between inter-chain disulfides being ~16.7 Å in the crystal structure of the IgG1, ~25 Å was anticipated to be a suitable separation between the bridging sites when taking into account the resolution of the measurement,[15] the flexibility of this region of the antibody and the PEG chain not being structurally linear. Initially, protected hydrazine **2** was formed *via* alkylation of diboc-hydrazine (see ESI for further details†). This species was then deprotected using TFA, and reacted with dibromomaleic anhydride under reflux in AcOH to afford methyl-PD **3**. Amide coupling of this PD with a mono-boc protected bis-amine resulted in the formation of PD linker reagent **4**. Finally, this species was deprotected and reacted with alkyne-PD **6** (prepared in an analogous manner to methyl-PD **3**) to afford target compound bis-diBrPD **1**. Whilst the overall yield for the

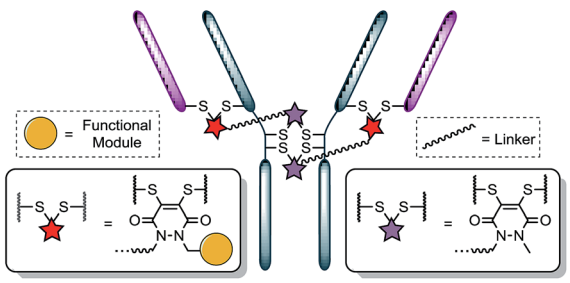

Fig. 2 Illustration detailing a novel approach to achieving antibody conjugate with a loading of two. Each pair of red and purple stars per linker molecule are independently interchangeable, and other disulfide pairs (*e.g.* Fab–Fab, hinge–hinge) may be functionally re-bridged.

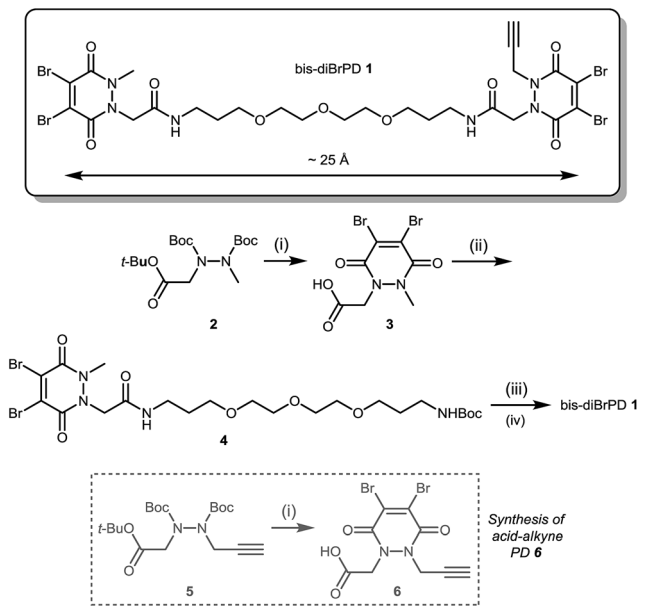

Scheme 1 Synthesis of bis-diBrPD **1**. Reagents and conditions: (i) TFA, CH_2Cl_2, 21 °C, 1 h; dibromomaleic anhydride, AcOH, reflux, 2 h; (ii) *tert*-butyl (3-(2-(2-(3-aminopropoxy)ethoxy)ethoxy)propyl)carbamate, CDI, DMF, 21 °C, 12 h; (iii) TFA/DCM, 21 °C, 30 min; (iv) HATU, DIPEA, DMF, acid-alkyne PD **6** 21 °C, 16 h.

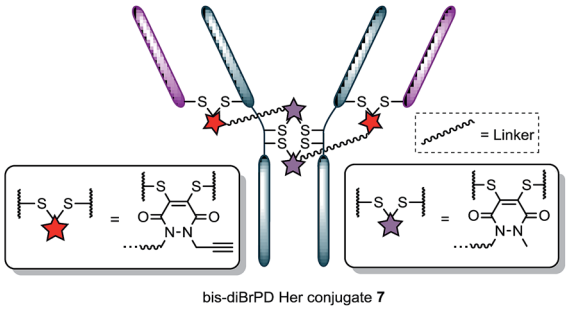

Fig. 3 Illustration of bis-diBrPD her conjugate 7. Each pair of red and purple stars per linker molecule are independently interchangeable, and other disulfide pairs (*e.g.* Fab–Fab, hinge–hinge) may be functionally re-bridged.

synthesis was low (<5%) we do highlight that the chemistry is straightforward to carry out and that none of the steps were optimised as we were more interested in exploring the novel chemical biology methodology.

Following the successful synthesis, the conjugation of **1** on a full antibody was appraised on Herceptin™, a clinically improved immunoglobulin used for the treatment of breast cancer and the antibody component of FDA-approved ADC Kadcyla™.[4] On account of pyridazinediones having a significant extinction coefficient at a distinct wavelength to other entities in the corresponding antibody conjugate, UV-vis was considered to be an appropriate method to analyse PD loading on the antibody. To our delight, after minimal optimisation, reaction of Herceptin™ with bis-diBrPD **1** gave a pyridazinedione-to-antibody ratio (PDAR) of 4.0 with complete functional re-bridging confirmed by SDS-PAGE (including under TCEP reducing conditions). This result supported our hypothesis, as it suggested each bis-diBrPD had re-bridged two disulfides; *i.e.* only such a result could have yielded the observed SDS-PAGE profile and PDAR. Despite the challenges of using mass spec for characterisation of antibody conjugates,[16] especially for disulfide modified conjugates,[13] we obtained mass spec data for conjugate 7 (see ESI for details†), which further verified our observation; *i.e.* we observed two additions of bis-diBrPD **1** to Herceptin™ (see representation in Fig. 3).

With conjugate 7 in hand, we next appraised what the loading would be if we were to click on a fluorophore-azide. Owing to its favourable optical properties and our previous experience with the azide,[10i] we chose to click on Alexa Fluor® 488 azide. To ensure that all available pendant alkynes on conjugate 7 would be reacted, an excess of Alexa Fluor® 488 azide was used in the click reaction (20 eq.). Gratifyingly, these conditions resulted in the formation of a conjugate where the loading of the Alexa Fluor® 488 dye on the antibody conjugate was 2.0. Furthermore, the result was highly reproducible with the click reaction not affecting PDAR or promoting antibody degradation by SDS-PAGE. In addition to this, pre-click modification (*i.e.* carrying out the click reaction prior to bioconjugation) afforded similar results (see ESI for details†).

It is also noteworthy that the final conjugate retained binding activity by ELISA (Fig. 4), even when compared to

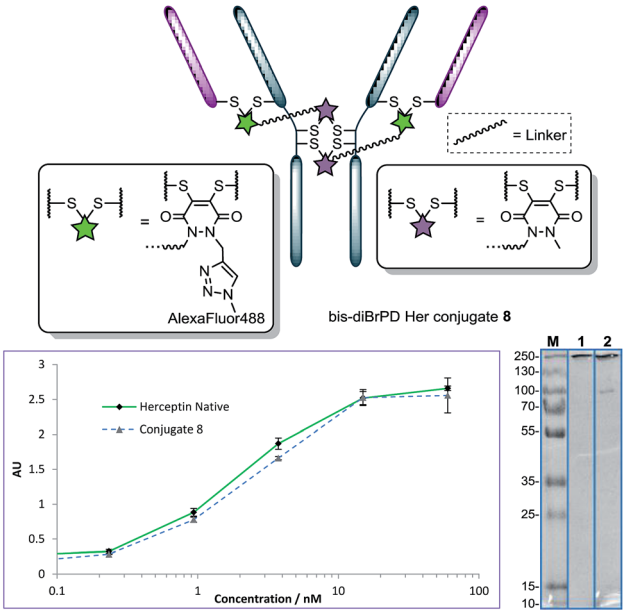

Fig. 4 Structure of conjugate **8** (each pair of green and purple stars per linker molecule are independently interchangeable, and other disulfide pairs (*e.g.* Fab–Fab, hinge–hinge) may be functionally re-bridged); ELISA and SDS-PAGE gel (M: molecular weight marker; **1**: native Herceptin™; **2**: conjugate **8**) of conjugate **8** with native Herceptin™ control.

classical diBrPD conjugation (see ESI for details†).[10c,i] More than this, the reactions were highly reproducible, with as many as seven attempts showing PDARs in the range of 3.9–4.1 and Alexa Fluor® 488 loadings in the range of 1.9–2.1. Finally, an ADC with a DAR of 2.0, based on the "click" conjugation of an azide functionalised doxorubicin[10i] to conjugate 7, was prepared in a facile manner owing to the modular nature of the chemistry. These results thus provide the first examples of forming a conjugate with a controlled loading of 2.0 on a native antibody scaffold in a facile and reliable manner.

Not content with providing conjugates with a controlled loading of two modules, we next turned our attention to the synthesis of an antibody conjugate with a loading of four to showcase the flexibility of our strategy. This would also serve as further proof of our disulfide pair functional re-bridging hypothesis as well as provide a novel conjugation strategy for making antibody conjugates with a loading of four. To this end,

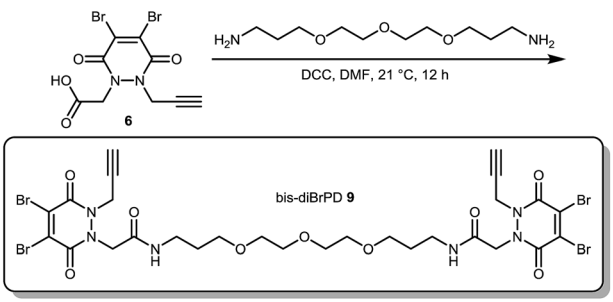

Scheme 2 Synthesis of bis-diBrPD **9**.

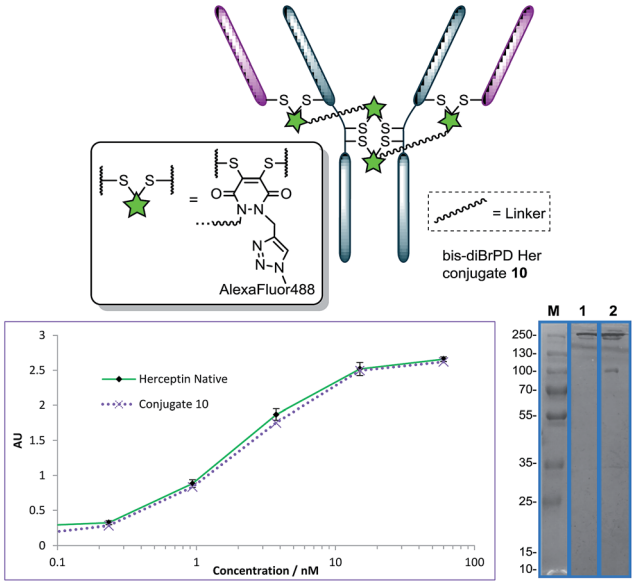

Fig. 5 Structure of conjugate **10** (other disulfide pairs (*e.g.* Fab–Fab, hinge–hinge) may be functionally re-bridged); ELISA and SDS-PAGE gel (M: molecular weight marker; **1**: native Herceptin™; **2**: conjugate **10**) of conjugate **10** with native Herceptin™ control.

we synthesised bis-diBrPD **9** in a similar manner to which bis-diBrPD **1** was formed (see Scheme 2).

Pleasingly, application of the optimised conditions for functional re-bridging, in the formation conjugate **7**, to reagent **9** on Herceptin™ afforded a conjugate with a PDAR 3.9 with all disulfides of the antibody functionalised (Fig. 5, see ESI for further details†). Moreover, reaction with an excess of Alexa Fluor® 488 azide resulted in a fluorophore loading of 3.9 (Fig. 5, see ESI for details†). This, in combination with the SDS-PAGE data, further verifies the bridging mode of these first-in-class reagents, and ELISA data again showed binding to be unaffected by the strategy. Moreover, it showcases how this novel class of reagent can act as a branch point for the construction of antibody conjugates with distinct and controlled module loadings of two and four.

Conclusions

In conclusion, we have provided a first-in-class strategy for enabling the controlled, reproducible loading of two modules onto a native antibody scaffold. This was enabled by the successful synthesis and application of an entity, containing one "click" handle, which functionally re-bridges two pairs of disulfide bonds on an IgG1. Subsequent reaction of the formed conjugate with an azide-fluorophore and azide-drug showed that the controlled loading of two modules was feasible and reproducible. The strategy, starting from the same branch point, was also readily adapted for the formation of a conjugate with a loading of four modules. Furthermore, all final conjugates were shown to retain binding by ELISA and antibody-PD conjugates have previously been shown to be biologically functional and stable.[10i–k] We believe this simple yet elegant approach to facilitate the loading of two modules starting from a native antibody scaffold will find application in multiple fields where the controlled loading of lower than four entities is desirable (*e.g.* antibody conjugates bearing highly hydrophobic modules) and especially in laboratories where antibody engineering techniques are not accessible, too expensive or not practical.

Acknowledgements

We gratefully acknowledge the EPSRC (EP/M01792X/1) and i-sense EPSRC IRC in Early Warning Sensing Systems for Infectious Diseases (EP/K031953/1) for funding AM and DAR, respectively. We also acknowledge the UCL Chemistry Mass Spectrometry Facility (Dr Kersti Karu) for assistance in mass spec and LCMS, and Dr Eleanor Gray (LCN) for assistance with the ELISAs, and the EPSRC UK National Mass Spectrometry Facility at Swansea University.

Notes and references

‡ Linear distance between disulfides determined by use of PyMol software.

1 (*a*) J. J. Day, B. V. Marquez, H. E. Beck, T. A. Aweda, P. D. Gawande and C. F. Meares, *Curr. Opin. Chem. Biol.*, 2010, **14**, 803; (*b*) A. L. Nelson and J. M. Reichert, *Nat. Biotechnol.*, 2009, **27**, 331; (*c*) A. C. Freise and A. M. Wu, *Mol. Immunol.*, 2015, **67**, 142.

2 (*a*) V. Chudasama, A. Maruani and S. Caddick, *Nat. Chem.*, 2016, **8**, 114, and references therein; (*b*) P. Akkapeddi, S.-A. Azizi, A. M. Freedy, P. M. S. D. Cal, P. M. P. Gois and G. J. L. Bernardes, *Chem. Sci.*, 2016, **7**, 2954, and references therein; (*c*) H. Yao, F. Jiang, A. Lu and G. Zhang, *Int. J. Mol. Sci.*, 2016, **17**, 194, and references therein; (*d*) N. Diamantis and U. Banerji, *Br. J. Cancer*, 2016, **114**, 362, and references therein.

3 (*a*) A. Younes, *et al.*, *N. Engl. J. Med.*, 2010, **363**, 1812; (*b*) P. D. Senter and E. L. Sievers, *Nat. Biotechnol.*, 2012, **30**, 631.

4 (*a*) S. Verma, *et al.*, *N. Engl. J. Med.*, 2012, **367**, 1783; (*b*) P. M. LoRusso, D. Weiss, E. Guardino, S. Girish and M. X. Sliwkowski, *Clin. Cancer Res.*, 2011, **17**, 6437.

5 A. Mullard, *Nat. Rev. Drug Discovery*, 2013, **12**, 329.

6 (*a*) K. J. Hamblett, *et al.*, *Clin. Cancer Res.*, 2004, **10**, 7063; (*b*) P. Strop, *et al.*, *Chem. Biol.*, 2013, **20**, 161.

7 (*a*) A. Lyons, *et al.*, *Protein Eng.*, 1990, **3**, 703; (*b*) J. R. Junutula, *et al.*, *Nat. Biotechnol.*, 2008, **26**, 925; (*c*) M. Sunbul and J. Yin, *Org. Biomol. Chem.*, 2009, **7**, 3361; (*d*) T. S. Young, I. Ahmad, J. A. Yin and P. G. Schultz, *J. Mol. Biol.*, 2010, **395**, 361; (*e*) D. Rabuka, J. S. Rush, G. W. deHart, P. Wu and C. R. Bertozzi, *Nat. Protoc.*, 2012, **7**, 1052; (*f*) J. Y. Axup, *et al.*, *Proc. Natl. Acad. Sci. U. S. A.*, 2012, **109**, 16101.

8 (*a*) M. S. K. Sutherland, *et al.*, *Blood*, 2013, **122**, 1455; (*b*) H. Bouchard, C. Viskov and C. Garcia-Echeverria, *Bioorg. Med. Chem. Lett.*, 2014, **24**, 5357; (*c*) A. C. Tiberghien, J.-N. Levy, L. A. Masterson, N. V. Patel, L. R. Adams, S. Corbett, D. G. Williams, J. A. Hartley and P. W. Howard, *ACS Med. Chem. Lett.*, 2016, **7**, 983; (*d*) N. Jain, S. W. Smith,

S. Ghone and B. Tomczuk, *Pharm. Res.*, 2015, **32**, 3526; (*e*) D. Antonow and D. E. Thurston, *Chem. Rev.*, 2011, **111**, 2815.

9 (*a*) J. A. Hartley and D. Hochhauser, *Curr. Opin. Pharmacol.*, 2012, **12**, 398; (*b*) J. Wu, P. H. Clingen, V. J. Spanswick, M. Mellinas-Gomez, T. Meyer, I. Puzanov, D. Jodrell, D. Hochhauser and J. A. Hartley, *Clin. Cancer Res.*, 2013, **19**, 721; (*c*) J. A. Hartley, *Expert Opin. Invest. Drugs*, 2011, **20**, 733; (*d*) L. R. Saunders, *et al.*, *Sci. Transl. Med.*, 2015, **7**, 302ra136.

10 (*a*) F. F. Schumacher, V. A. Sanchania, B. Tolner, Z. V. F. Wright, C. P. Ryan, M. E. B. Smith, J. M. Ward, S. Caddick, C. W. M. Kay, G. Aeppli, K. A. Chester and J. R. Baker, *Sci. Rep.*, 2013, **3**, 1525; (*b*) C. P. Ryan, M. E. B. Smith, F. F. Schumacher, D. Grohmann, D. Papaioannou, G. Waksman, F. Werner, J. R. Baker and S. Caddick, *Chem. Commun.*, 2011, **47**, 5452; (*c*) M. T. W. Lee, A. Maruani, J. R. Baker, S. Caddick and V. Chudasama, *Chem. Sci.*, 2016, **7**, 799–802; (*d*) L. Castañeda, A. Maruani, F. F. Schumacher, E. Miranda, V. Chudasama, K. A. Chester, J. R. Baker, M. E. B. Smith and S. Caddick, *Chem. Commun.*, 2013, **49**, 8187; (*e*) V. Chudasama, M. E. B. Smith, F. F. Schumacher, D. Papaioannou, G. Waksman, J. R. Baker and S. Caddick, *Chem. Commun.*, 2011, **47**, 8781; (*f*) F. Bryden, A. Maruani, H. Savoie, V. Chudasama, M. E. B. Smith, S. Caddick and R. W. Boyle, *Bioconjugate Chem.*, 2014, **25**, 611; (*g*) F. F. Schumacher, J. P. M. Nunes, A. Maruani, V. Chudasama, M. E. B. Smith, K. A. Chester, J. R. Baker and S. Caddick, *Org. Biomol. Chem.*, 2014, **12**, 7261; (*h*) A. Maruani, S. Alom, P. Canavelli, M. T. W. Lee, R. E. Morgan, V. Chudasama and S. Caddick, *Chem. Commun.*, 2015, **51**, 5279; (*i*) A. Maruani, M. E. B. Smith, E. Miranda, K. A. Chester, V. Chudasama and S. Caddick, *Nat. Commun.*, 2015, **6**, 6645; (*j*) J. P. M. Nunes, M. Morais, V. Vassileva, E. Robinson, V. Rajkumar, M. E. B. Smith, B. R. Pedley, S. Caddick, J. R. Baker and V. Chudasama, *Chem. Commun.*, 2015, **51**, 10624–10627; (*k*) A. Maruani, H. Savoie, F. Bryden, S. Caddick, R. W. Boyle and V. Chudasama, *Chem. Commun.*, 2015, **51**, 15304; (*l*) M. T. W. Lee, A. Maruani and V. Chudasama, *J. Chem. Res.*, 2016, **40**, 1.

11 (*a*) H. Liu, C. Chumsae, G. Gaza-Bulseco, K. Hurkmans and C. H. Radziejewski, *Anal. Chem.*, 2010, **82**, 5219; (*b*) M. M. C. Sun, K. S. Beam, C. G. Cerveny, K. J. Hamblett, R. S. Blackmore, M. Y. Torgov, F. G. M. Handley, N. C. Ihle, P. D. Senter and S. C. Alley, *Bioconjugate Chem.*, 2005, **16**, 1282; (*c*) https://www.tools.thermofisher.com/content/sfs/manuals/MAN0011182_2Mercaptoethylamine_HCl_UG.pdf.

12 (*a*) L. M. Hinman, P. R. Hamann, R. Wallace, A. T. Menendez, F. E. Durr and J. Upeslacis, *Cancer Res.*, 1993, **53**, 3336; (*b*) P. R. Hamann, L. M. Hinman, C. F. Beyer, L. M. Greenberger, C. Lin, D. Lindh, A. T. Menendez, R. Wallace, F. E. Durr and J. Upeslacis, *Bioconjugate Chem.*, 2005, **16**, 346; (*c*) Q. Zhou, *et al.*, *Bioconjugate Chem.*, 2014, **25**, 510; (*d*) R. van Geel, M. A. Wijdeven, R. Heesbeen, J. M. M. Verkade, A. A. Wasiel, S. S. van Berkel and F. L. van Delft, *Bioconjugate Chem.*, 2015, **26**, 2233.

13 C. R. Behrens, *et al.*, *Mol. Pharmaceutics*, 2015, **12**, 3986.

14 G. Badescu, *et al.*, *Bioconjugate Chem.*, 2014, **25**, 112.

15 L. J. Harris, E. Skaletsky and A. McPherson, *J. Mol. Biol.*, 1998, **275**, 861–872.

16 R. Y.-C. Huang and G. Chen, *Drug Discovery Today*, 2016, **21**, 850.

